UNIVERSITEIT VAN PRETORIA
UNIVERSITY OF PRETORIA
YUNIBESITHI YA PRETORIA

System Dynamics Modelling for Sensitivity Analysis Evaluation of Driving Factors on Decoupled Aquaponic Systems in South-Africa.

by

Adriaan J.G. Roux (13012470)

A dissertation submitted in partial fulfilment of the requirements for the degree

Master of Engineering (Industrial Engineering)

in the

Department of Industrial and Systems Engineering

Faculty of Engineering, Built Environment and Information Technology

October 2021

Acknowledgements

During my research, I have received immense support and advice which aided in the successful completion of this dissertation.

Firstly, I would like to thank my supervisor, Dr Michael K. Ayomoh. The expertise you provided was invaluable in formulating the research questions and methodology. The feedback I received from you helped to sharpen my thinking and carry my work to new levels.

I would like to thank my wife, family and friends for their support and advice during my research. Not only did they keep me motivated during the whole process, but they also greatly assisted with advice on formatting, technical aspects, and general proofreading.

Abstract

The growing impact of climate change on human society which has continuously resulted in environmental degradation and the death of several aquatic species has heightened research for the design and development of controlled and regulated artificial systems for the safe cultivation and growth of diverse aquatic species such as fish via closed controlled dynamic energy systems. It is in the light of the above that this research has presented a decoupled aquaponics system design for energy efficiency. A decoupled aquaponics system is one that separates the recirculating aquaculture system (RAS) from the hydroponic (HP) unit, hence creating a detached ecosystem with inherent advantages for both the plants and housed aquatic species. Standardised models drawn from the literature covering lighting, aeration, circulation pumps, ultraviolet disinfection, oxygen generation, environmental control, heat loss/gains and internal heat flux, amongst others, were utilised for an effective design outcome of the aquaponic system. The various models were built into a system dynamics network of models and used to investigate and evaluate a range of parameters including energy and water usage. The variability and sensitivity analysis premised on system dynamics modelling was applied to a wide range of selected countries with the potential for aquaponics research based on supportive environmental conditions. Weather data for the respective locations served as input to the system dynamics model. Causal loop diagrams were developed and presented after which stock and flow diagrams were developed. The governing differential equations were derived and employed in conformance with the literature. The time response plots illustrating the stock variables that were location dependent and location independent were presented and discussed.

The results that were obtained revealed that Floresta Brazil was the most energy efficient country in which to operate such a system with a peak energy demand of 12.6 MW and a total yearly energy usage of 4239 MW. Furthermore, the city of Abuja in Nigeria in Africa was the second-best performing region with a peak energy demand of 13.1 MW and a total yearly energy usage of 4330 MW; 2.1% more than the Brazil region. The third-best performing region, Alor Setar in Malaysia, had a peak energy demand of 13.1 MW and a total yearly energy usage of 4372 MW; 3.1% more than the Brazil region. The top three energy performing locations have hot humid climates where minimal heating was required during the year. Durban was the best performing region in South Africa with a peak energy demand of 18.4 MW and a total yearly energy usage of 4550 MW. Durban had a 7.3% higher cumulative energy compared to the identified best performing region on the globe. Even though the energy usage was higher throughout the year, Durban was considered to be a good performing region.

The cooling demand during summer was comparable with the top three performing countries. The region had a peak cooling load of 13.3 MW and contributed 72.3% to the total energy usage in the system. Given the humid and hot climate in the Durban region, the results showed that Durban offers favourable climatic conditions when compared to global operations. Other regions in South Africa could still be suitable for operating aquaponic systems on a large scale; however, they might be less energy efficient.

The recommendation made with respect to the South African situation is that the city of Durban has a suitable climate regarding both energy and water efficiency. Furthermore, it was concluded that the continuous use of energy sources dependent on fossil fuel would lead to a rise in energy consumption due to an increase in energy demand created by a rise in global temperature.

Keywords: *System dynamics modelling, decoupled aquaponics, energy modelling, water efficiency, biosystems engineering, controlled environments.*

List of Figures

List of Tables

List of Nomenclature

Parameter	Description	Units
Abbreviations		
AHU	Air Handling Unit	–
HP	Hydroponic System	–
$HVAC$	Heating, Ventilation and Air-conditioning	–
RAS	Recirculating Aquaculture System	–
General Symbols		
AC	Air changes	$1/hr$
A_{cHP}	Outer surface area of hydroponic greenhouse	m^2
A_{fHP}	Floor area of hydroponic greenhouse	m^2
A_{fRAS}	Floor area of RAS facility	m^2
$A_{s\ RAS}$	Outer surface area of RAS facility	m^2
$A_{s\ tanks}$	Outer surface area of RAS tanks	m^2
$A_{s\ water}$	Water surface area	m^2
b	Seasonal correction for solar time constant	–
$C_{p,air}$	Specific heat of air	J/kgK
$C_{p,water}$	Specific heat of water	J/kgK
CO_2P	Carbon dioxide production rate	kg_{CO_2}/kg_{O_2}
COP_{HP}	Coefficient of performance of heat pump for hydroponic greenhouse heating	–
$COP_{RAS,chiller}$	Coefficient of performance of chiller for cooling of RAS facility	–
$COP_{RAS,heatpump}$	Coefficient of performance of heat pump for cooling of RAS facility	–
D_{CO_2}	Daily Carbon Dioxide production by biomass	kg_{CO_2}/day
D_{H_2O-air}	Mass diffusivity of water vapour in air	m^2/s
D_l	Daylight intensity	lux
D_{O_2}	Daily Oxygen consumption by biomass	kg_{O_2}/day
D_v	Daylight value	$binary$

Parameter	Description	Units
d	Stocking density	kg_{fish}/m^3
d_{gc}	Growth cycle to harvest	$days$
d_r	Inverse relative distance Earth to Sun	$radians$
ET_o	Reference evapotranspiration rate	$kg_{H_2O}/m^2.s$
ET	Evapotranspiration rate	$kg_{H_2O}/m^2.s$
e^o	Environmental saturation vapour pressure	kPa
e^a	Actual environmental vapour pressure	kPa
FCR	Feed conversion rate	kg_{feed}/kg_{fish}
$Feed_d$	Daily feed	kg_{feed}/day
FR_d	Daily feed rate	$kg_{feed}/kg_{fish}/day$
Gr	Grashof number	$-$
G_f	Annual fish production goal	kg
G_{hr}	Hourly soil heat flux density	$MJ/m^2/hr$
G_{sc}	Solar constant	$MJ/m^2/min$
g	Gravitational acceleration	m/s^2
$H_{HP,pump}$	Pump head for HP heating pump	m
$H_{RAS,circ\ pump}$	Pump head for RAS circulation pumps	m
$H_{RAS,HVAC\ pump\ cool}$	Pump head for RAS HVAC cooling pumps	m
$H_{RAS,HVAC\ pump\ heat}$	Pump head for RAS HVAC heating pumps	m
$H_{RAS,O_2\ comp}$	Pressure drop for RAS Oxygen compressors	Pa
HRT	Hydraulic retention time	s
h_{fg}	Latent heat flux of evaporation	kJ/kg
h_{HP}	Height of greenhouse	m
h_{mass}	Mass transfer coefficient	m/s

Parameter	Description	Units
h_n	Enthalpy of water-air vapour at condition point "n"	kJ/kg
h_{RAS}	RAS facility height	m
h_t	Tank height	m
$\tilde{I}_{sr}$	Hourly incoming solar radiation, time variant parameter. Data input	W/m^2
J	Day of the year	$-$
K_c	Crop coefficient, time variant parameter. Data input	$-$
K_o	Initial fish weight at day 0	kg
K_n	Estimated fish weight after n days	kg
k	Heat capacity ratio of Oxygen	$-$
L_c	Critical length	m
L_m	Longitude of the measurement site	$Degrees$
L_x	Length of crop at a certain crop growth stage, where x is defined by the subscripts	mm
L_z	Longitude of the centre of the local time zone	$Degrees$
m_{bio}	RAS system biomass	kg
$\dot{m}_{ex}$	Mass flow rate of make-up water	kg/s
$\dot{m}_{HVAC\ pump\ cool}$	Mass flow rate of HVAC cooling pump	kg/s
$\dot{m}_{HVAC\ pump\ heat}$	Mass flow rate of HVAC heating pump	kg/s
$\dot{m}_{OA}$	Outside air mass flow rate for RAS facility (Ventilation mass flow rate)	kg/s
$\dot{m}_{RA}$	Return air mass flow rate for RAS facility	kg/s
$\dot{m}_{SA}$	Supply air mass flow rate for RAS facility	kg/s
$\dot{m}_w$	Mass flow rate of tank water vapour to RAS environment	kg/s
$\dot{m}_{w\ cond}$	Mass flow rate of water condensation on HVAC coils	kg/s
N_{Occ}	Number of occupants	$-$
n	Number of days	$-$

Parameter	Description	Units
O_2C	Oxygen consumption rate	kg_{O_2}/kg_{feed}
P_{atm}	Pressure at standard atmospheric conditions	Pa
$P_{HP,light}$	Light power rating for hydroponic greenhouse	W/m^2
$P_{O_2,1}$	Pressure at Oxygen compressor inlet	Pa
$P_{O_2,2}$	Pressure at Oxygen compressor outlet	Pa
$\widetilde{P}_o$	Local atmospheric pressure, location variant parameter. Data input	Pa
$P_{RAS,light}$	Light power rating for RAS facility	W/m^2
$P_{RAS,tot}$	Total pressure in RAS facility	Pa
$P_{RAS,UV}$	UV light power rating for RAS facility	W/m^2
$P_{sat\ @\ T_\infty}$	Saturation pressure at RAS facility temperature	Pa
$P_{v,w}$	Vapour saturation pressure at tank water surface	Pa
$P_{v,\infty}$	Vapour saturation pressure away from tank water surface	Pa
$Prod_d$	Daily fish production	kg_{fish}/day
p	Tank perimeter	m
Q_{lat}	Latent heat produced by an occupant based on medium work	$W/person$
Q_{sens}	Sensible heat produced by an occupant based on medium work	$W/person$
$\dot{Q}_{HP,cd}$	Heat transfer due to conduction and convection (HP)	W
$\dot{Q}_{HP,cool}$	Heat transfer required to cool greenhouse to setpoint	W
$\dot{Q}_{HP,ET}$	Heat transfer due to plant evapotranspiration (HP)	W
$\dot{Q}_{HP,heat}$	Heat transfer required to heat greenhouse to setpoint	W
$\dot{Q}_{HP,infil}$	Heat transfer due to air infiltration	W
$\dot{Q}_{HP,tot}$	Total heat transfer in hydroponic greenhouse	W
$\dot{Q}_{HP,rad}$	Heat transfer due to thermal radiation (HP)	W
$\dot{Q}_{HP,sr}$	Heat transfer due to solar radiation (HP)	W

Parameter	Description	Units
$\dot{Q}_{HP,v}$	Heat transfer due to ventilation (HP)	W
$\dot{Q}_{RAS,cond\ tanks}$	Heat transfer from tanks to RAS facility through tank wall due to conduction	W
$\dot{Q}_{RAS,conv\ tanks}$	Heat transfer from tanks to RAS facility due to convection	W
$\dot{Q}_{RAS,evap\ tanks}$	Heat transfer from tanks to RAS facility due to evaporation	W
$\dot{Q}_{RAS,e\ cond}$	Heat transfer from/to RAS facility due to conduction	W
$\dot{Q}_{RAS,e\ conv}$	Heat transfer from/to RAS facility due to convection	W
$\dot{Q}_{RAS,e\ rad}$	Heat transfer from RAS facility due to thermal radiation	W
$\dot{Q}_{RAS,e\ srad}$	Heat transfer to RAS facility due to solar radiation	W
$\dot{Q}_{RAS,external}$	Heat transfer to the external environment	W
$\dot{Q}_{RAS,HVAC}$	Heat transfer by RAS HVAC system to reach setpoint	W
$\dot{Q}_{RAS,internal}$	Heat transfer between internal RAS systems	W
$\dot{Q}_{RAS,i\ equip}$	Heat transfer due to internal RAS facility equipment	W
$\dot{Q}_{RAS,i\ lighting}$	Heat transfer due to internal RAS facility lighting	W
$\dot{Q}_{RAS,i\ occ\ lat}$	Heat transfer due to internal latent heat by occupants	W
$\dot{Q}_{RAS,i\ occ\ sens}$	Heat transfer due to internal sensible heat by occupants	W
$\dot{Q}_{RAS,loss\ tanks}$	Heat transfer losses from the tanks to the RAS facility	W
$\dot{Q}_{RAS,rad\ tanks}$	Heat transfer from tanks to RAS facility due to radiation	W
$\dot{Q}_{RAS,room\ sens}$	Heat transfer due to the room sensible heat in the RAS facility	W
$\dot{Q}_{RAS,room\ tot}$	Heat transfer due to the room total heat in the RAS facility	W
$\dot{Q}_{RAS,tot}$	Total heat transfer in RAS facility	W
$\dot{Q}_{RAS,vent}$	Heat transfer due to the ventilation system	W
$\dot{Q}_{RAS,v\ lat}$	Heat transfer due to latent heat component of ventilation	W
$\dot{Q}_{RAS,v\ sens}$	Heat transfer due to sensible heat component of ventilation	W
R_a	Extra-terrestrial radiation	$MJ/m^2/hr$

Parameter	Description	Units
R_{air}	Gas constant of air	$J/mol/K$
R_{O_2}	Gas constant of Oxygen	$J/mol/K$
R_{cond}	Thermal resistance of material due to conduction	m^2K/W
R_{conv}	Thermal resistance of material due to convection	m^2K/W
R_n	Net radiation present in greenhouse	$MJ/m^2/hr$
R_{nl}	Long wave radiation	$MJ/m^2/hr$
R_{ns}	Short wave radiation	$MJ/m^2/hr$
R_{tot}	Total thermal resistance of material	m^2K/W
R_{so}	Clear sky radiation	$MJ/m^2/hr$
R_v	Gas constant of water vapour	$J/mol/K$
r	Fish growth rate	%
r_t	Tank radius	m
SC	Shading coefficient of hydroponic greenhouse cover	–
Sh	Sherwood Number	–
Sc	Schmidt Number	–
S_c	Seasonal correction for solar time	hr
T_{ave}	Average temperature between water and RAS facility	K
T_{dbn}	Dry bulb temperature at condition point “n”	℃
T_{dewn}	Dew point at condition point “n”	℃
$T_{Hw,in}$	Hot water return temperature (HP)	℃
$T_{Hw,out}$	Hot water supply temperature (HP)	℃
T_{iHP}	Inside temperature of hydroponic greenhouse	℃
T_n	Temperature at condition point “n”	℃
$T_{O_2,1}$	Compressor inlet temperature	K

Parameter	Description	Units
$\widetilde{T}_o$	Hourly outside temperature, time variant parameter. Data input	℃
$T_{RAS,i}$	RAS internal temperature	℃
T_{sky}	Extra-terrestrial sky temperature	K
$T_{s\,tank}$	Tank surface temperature	K
$T_{s\,RAS}$	RAS facility surface temperature	K
T_w	Tank water temperature	℃
T_{wbn}	Wet bulb temperature at condition point "n"	℃
T_∞	Temperature of internal RAS environment	K
t_m	Standard clock time at the midpoint of the period	hr
U_{HP}	Overall heat transfer coefficient of hydroponic greenhouse material	W/m^2K
U_{RAS}	Overall heat transfer coefficient of RAS facility material	W/m^2K
$U_{RAS,tanks}$	Overall heat transfer coefficient of RAS tank material	W/m^2K
u_2	Average hourly windspeed, time variant parameter. Data input	m/s
Vol_{HP}	Hydroponic greenhouse volume	m^3
Vol_{RAS}	RAS facility volume	m^3
$\dot{V}_{HP,circ}$	Volumetric flow rate for hydroponic greenhouse circulation pump	m^3/s
$\dot{V}_{HP,pump}$	Volumetric flow rate for hydroponic greenhouse heating pump	m^3/s
$\dot{V}_{HP,v}$	Ventilation volumetric flow rate for hydroponic greenhouse	m^3/s
$\dot{V}_{RAS,circ}$	Volumetric flow rate for RAS circulation pump	m^3/s
$\dot{V}_{RAS,CO_2}$	Volumetric flow rate for Carbon Dioxide stripping	m^3/s
$\dot{V}_{RAS,HVAC\ AHU\ cool}$	Volumetric flow rate for AHU cooling fans	m^3/s
$\dot{V}_{RAS,HVAC\ AHU\ heat}$	Volumetric flow rate for AHU heating fans	m^3/s
$\dot{V}_{RAS,HVAC\ pump\ cool}$	Volumetric flow rate for HVAC cooling pumps	m^3/s
$\dot{V}_{RAS,HVAC\ pump\ heat}$	Volumetric flow rate for HVAC heating pumps	m^3/s

Parameter	Description	Units
$\dot{V}_{RAS,O_2}$	Volumetric flow rate for RAS Oxygen compressor	m^3/s
$\dot{W}_{HP,circ\ pump}$	Power required by circulation pumps for the hydroponic greenhouse	W
$\dot{W}_{HP,cool}$	Power required to cool hydroponic greenhouse to setpoint	W
$\dot{W}_{HP,heat\ pump}$	Power required by the heat pump to heat hydroponic greenhouse to setpoint	W
$\dot{W}_{HP,lighting}$	Power required to power lighting in hydroponic greenhouse	W
$\dot{W}_{HP,p\ heat}$	Power required by the pump to heat hydroponic greenhouse to setpoint	W
$\dot{W}_{HP,tot\ heat}$	Power required to heat hydroponic greenhouse to setpoint	W
$\dot{W}_{HP,v\ heat}$	Power required by the ventilation fans to heat hydroponic greenhouse to setpoint	W
$\dot{W}_{RAS,circ\ pump}$	Power required to power circulation pumps for the RAS facility	W
$\dot{W}_{RAS,CO_2\ fan}$	Power required to power CO_2 degassing fans	W
$\dot{W}_{RAS,HVAC\ AHU\ cool}$	Power required by RAS cooling AHU	W
$\dot{W}_{RAS,HVAC\ AHU\ heat}$	Power required by RAS heating AHU	W
$\dot{W}_{RAS,HVAC\ Chiller}$	Power required by RAS chiller	W
$\dot{W}_{RAS,HVAC\ cool\ tot}$	Total power required for RAS cooling	W
$\dot{W}_{RAS,HVAC\ Heat\ pump}$	Power required by RAS Heat pump	W
$\dot{W}_{RAS,HVAC\ heat\ tot}$	Total power required for RAS heating	W
$\dot{W}_{RAS,HVAC\ pump\ cool}$	Power required by RAS HVAC cooling pumps	W
$\dot{W}_{RAS,HVAC\ pump\ heat}$	Power required by RAS HVAC heating pumps	W
$\dot{W}_{RAS,light}$	Power required by lighting in RAS facility	W
$\dot{W}_{RAS,O_2\ comp}$	Power required by Oxygen compressors for the RAS facility	W
$\dot{W}_{RAS,UV}$	Power required for UV-disinfection of RAS facility	W
$\dot{W}_{RAS,water\ heat}$	Power required to keep water at set point	W
Z	Elevation above sea level	m
Z_c	Compressibility factor of Oxygen	$-$

Parameter	Description	Units
Greek symbols		
$\boldsymbol{\alpha}$	Albedo	–
$\boldsymbol{\alpha_{RAS}}$	Absorptivity of RAS facility walls	–
$\boldsymbol{\gamma}$	Psychrometric constant	$kPa/℃$
Δ	Saturation slope	$kPa/℃$
$\boldsymbol{\Delta P_{HP,fan}}$	Pressure drop in HP system, that the fan needs to overcome	Pa
$\boldsymbol{\Delta P_{RAS,AHU\ Cool}}$	Pressure drop in RAS AHU system	Pa
$\boldsymbol{\Delta P_{RAS,AHU\ Heat}}$	Pressure drop in RAS AHU system	Pa
$\boldsymbol{\Delta P_{RAS,CO_2\ fan}}$	Pressure drop in RAS CO_2 degassing system	Pa
$\boldsymbol{\Delta T_{cool}}$	Temperature difference for cooling system	℃
$\boldsymbol{\Delta T_{heat}}$	Temperature difference for heating system	℃
$\boldsymbol{\delta}$	Solar declination	$Radians$
$\boldsymbol{\varepsilon_{iHP}}$	Emissivity of interior hydroponic greenhouse surface	–
$\boldsymbol{\varepsilon_{RAS}}$	Emissivity of RAS facility	–
$\boldsymbol{\varepsilon_{sky}}$	Emissivity of extra-terrestrial sky	–
$\boldsymbol{\varepsilon_{tank}}$	Emissivity of tank material	–
$\boldsymbol{\eta_{HP,f}}$	Hydroponic system ventilation fan efficiency	%
$\boldsymbol{\eta_{HP,p}}$	Hydroponic system heating pump efficiency	%
$\boldsymbol{\eta_{RAS,AHU\ cool\ fan}}$	RAS facility AHU cooling fans efficiency	%
$\boldsymbol{\eta_{RAS,AHU\ heat\ fan}}$	RAS facility AHU heating fans efficiency	%
$\boldsymbol{\eta_{RAS,CO_2\ fan}}$	RAS facility CO_2 fans efficiency	%
$\boldsymbol{\eta_{RAS,cp}}$	RAS facility circulation pump efficiency	%
$\boldsymbol{\eta_{RAS,HVAC\ cool\ p}}$	RAS facility HVAC cooling pump efficiency	%
$\boldsymbol{\eta_{RAS,HVAC\ heat\ p}}$	RAS facility HVAC heating pump efficiency	%
$\boldsymbol{\eta_{RAS,O_2\ comp}}$	RAS facility Oxygen compressors efficiency	%

Parameter	Description	Units
$\boldsymbol{\lambda}$	Latent heat of vaporization for water transpiration	kJ/kg
$\boldsymbol{v_{air}}$	Kinematic viscosity of air	m^2/s
$\boldsymbol{\pi}$	Pi	$-$
$\boldsymbol{\rho_{air}}$	Density of air	kg/m^3
$\boldsymbol{\rho_{ave}}$	Average water vapour density in the RAS facility	kg/m^3
$\boldsymbol{\rho_{a,w}}$	Density of dry air away at tank water surface	kg/m^3
$\boldsymbol{\rho_{a,\infty}}$	Density of dry air away from tank water surface	kg/m^3
$\boldsymbol{\rho_{O_2}}$	Density of Oxygen	kg/m^3
$\boldsymbol{\rho_{v,w}}$	Density of water vapour at tank water surface	kg/m^3
$\boldsymbol{\rho_{v,\infty}}$	Density of water vapour away from tank water surface	kg/m^3
$\boldsymbol{\rho_{water}}$	Density of water	kg/m^3
$\boldsymbol{\rho_w}$	Density of water vapour mixture at tank water surface	kg/m^3
$\boldsymbol{\rho_\infty}$	Density of water vapour mixture in RAS facility	kg/m^3
$\widetilde{\emptyset}$	Hourly outside relative humidity, time variant parameter. Data input	%
$\emptyset_{\boldsymbol{n}}$	Relative humidity at condition point "n"	%
$\emptyset_{\boldsymbol{RAS}}$	Hourly relative humidity in the RAS facility	%
$\boldsymbol{\varphi}$	Latitude	$radians$
$\boldsymbol{\sigma}$	Stefan-Boltzmann constant	W/m^2K^4
$\boldsymbol{\tau_c}$	Transmissivity of hydroponic greenhouse material	$-$
$\boldsymbol{\tau_{os}}$	Transmissivity of hydroponic outside shading	$-$
$\boldsymbol{\tau_{tc}}$	Transmissivity of hydroponic thermal cover	$-$
$\boldsymbol{\omega_i}$	Solar time angle at beginning of period	$radians$
$\boldsymbol{\omega_m}$	Solar time angle at midpoint of the period	$radians$
$\boldsymbol{\omega_n}$	Humidity ratio of water-air vapour at condition point "n"	kg_{H_2O}/kg_{air}

Parameter	Description	Units
$\boldsymbol{\omega_e}$	Solar time angle at end of period	$radians$
Subscripts		
$\boldsymbol{a}$	Crop growth stage between initial and developing growth stage	–
$\boldsymbol{b}$	Crop growth stage between developing and middle growth stage	–
$\boldsymbol{ini}$	Initial crop growth stage	–
$\boldsymbol{dev}$	Developing crop growth stage	–
$\boldsymbol{mid}$	Middle crop growth stage	–
$\boldsymbol{end}$	End crop growth stage	–
$\mathbf{1}$	Outside air conditions	–
$\mathbf{2}$	Mixed air conditions (on coil conditions)	–
$\mathbf{3}\boldsymbol{a}$	Off-coil conditions (cooling)	–
$\mathbf{3}\boldsymbol{b}$	Off-coil conditions (heating)	–
$\mathbf{4}$	Return air conditions	–

Table of Contents

CHAPTER ONE

Introduction

1.1 Background Information

Decoupled aquaponic systems design and sensitivity analysis, premised on systems thinking and dynamics, are beginning to gain significant attention in the literature on biosystems engineering and systems modelling (Goddek et al., 2016; Goddek & Körner, 2019). When conditions of a recirculating aquaculture system (RAS) and hydroponic (HP) systems deviate from optimal operating conditions, lower production efficiency can be expected. Instead of accounting for trade-offs between those component parts, the objective should be to provide the best practicable conditions for each component and combination of species (Goddek, et al., 2016). Even though similar growth performances between aquaponics and hydroponics have been observed, optimising the respective conditions could lead to enhanced fish and plant growth (Jijakli et al., 2016). If the subsystems are controlled and run independently from one another, these optimal conditions could be achieved. Decoupled multi-loop aquaponics systems separate the RAS and HP units from each other, creating detached ecosystems with inherent advantages for both plants and fish. This gives the advantage of improved crop and fish cultivation in combination with using the minimum resource input (Goddek & Körner, 2019).

Recent research has investigated and discussed energy efficiency based on regional climate. The investigations were conducted on an actual aquaponic system. It is reported that aquaponics systems are fairly new to countries in Africa and the Middle East as evident in an international survey conducted in 2014 where only a single response was received from each Ghana, Oman and South Africa (Alkhalidi et al., 2020). A 2016 survey that yielded 44 responses from aquaponics farmers, helped shed light on the status of aquaponics in South Africa. Eighty-two percent of raised fish is tilapia and 75% of the farmed plants are leafy vegetables. The study classified the aquaponics farming stage in South Africa as an emerging practice (Mchunu et al., 2018).

System dynamics modelling offers a powerful approach to system simulation in order to capture the complex dynamic interactions within the systems (Bala et al., 2017). System dynamic modelling is applied to complex biological systems such as aquaponic systems across the world.

Aquaponic systems grow both fish and plants in a single system where the fish water fertilises the plants, which in turn helps remove some of the nitrogen and other nutrients from the water

(Davison, 2018). Aquaponics is not a novel concept, but it is underutilised and underdeveloped in numerous countries. System dynamic modelling approaches can be implemented to properly plan sustainable policies and to ensure success in countries where local challenges may act as a deterrent against implementing aquaponic systems. It can be used as a tool to manage energy usage, reduce waste whilst maximising yield, drive job creation, and food security as well as efficiently stimulate sustainable fishing and agriculture.

1.2 Problem Statement

The world continues to face widespread food insecurity and achieving food security for all is increasingly complicated (Chakona & Shackleton, 2019). There are a variety of factors that contribute to an increase in food security, for example climate change, an increase in population and a decline in resources (Andersen & Lorch, 1998; Bremner, 2012; FAO, 2010).

Almost 20% of South African households had inadequate or severely inadequate access to food in 2017 (Africa, 2017). The majority of households in South African informal settlements were moderately or severely food insecure owing to a lack of access to food, which was directly related to income (Battersby, 2011). An increase in population is placing an increasing strain on natural resources and the ability of the country to feed its people.

Food sovereignty through aquaponics has great potential to address food and nutrition insecurity in South Africa (Mchunu et al., 2017). If aquaponic systems can be modelled by means of system dynamic simulations, some complexities can be easily analysed. Parameters such as yield potential, optimal fish to plant arrangements and energy usage can be simulated in order to observe how the system is affected. Ultimately, these models can be integrated with the food security of a country in order to evaluate the advantages and disadvantages of such systems.

Systems can be observed to identify the influencing factors, their interactions and impacts in order to find the root causes of these problems and to arrive at viable policy options (Bala et al., 2017).

1.3 Project Rationale and Motivation

In a country where resources are limited, development and economic growth are difficult. Aquaponics holds the potential to create jobs, reduce the load on the environment and contribute to food security. Within an already struggling economy, simulation and modelling will play an imperative role in ensuring proper planning and decision making.

To ensure a positive outcome during the conceptualisation phases of projects and or policy design, the research will aid all involved parties in coming to the best solution without expensive experimentation and trial and error methodologies.

Furthermore, the models research will serve as a tool to determine how different factors influence an aquaponic system and how the system will react when changing certain parameters. This will have positive effects during the entire project life cycle and affected supply chains should these types of systems be used on a large commercial scale.

The motivation for the research was to contribute to a sector that is not sufficiently explored in a country that possesses ample opportunity. If correctly implemented, aquaculture and aquaponics could offer major financial and environmental advantages. Efforts should be invested in research in order to make this a viable endeavour.

1.4 Aim and Research Objectives

1.4.1 Aim

The researcher aimed to achieve a working system dynamics model of a generic reference decoupled aquaponics system in order to investigate and evaluate a range of parameters such as energy and water usage. The reference model was used to compare and evaluate a series of different locations and the climatic effects on certain stock variables. The model will serve as a decision-making tool for proper sustainable policy development with regard to aquaponics systems in South Africa, a field that is currently unexplored for large commercial applications. Further, the researcher aimed to explore socio-economic factors such as agricultural and aqua-cultural sustainability with regard to energy and water resources.

1.4.2 Research Objectives

The following research objectives were identified.

1. To conceptualise and model a generic reference decoupled aquaponic system using a systems thinking and systems modelling approach.
2. To capture the effects of local climatic factors and system stock variables such as system energy consumption and system water consumption and based on this, to investigate the suitability of aquaponics in a diverse South African climate.
3. To carry out a sensitivity analysis of different system dynamics modelling variables via parameter variation.

1.5 Research Questions

The following research questions were identified for this research.

1. How can a system dynamic modelling and systems thinking methodology be applied to represent a generic notional decoupled aquaponic system?
2. What effects do local climatic factors have on system stock variables such as water and energy usage?
3. How feasible could a large commercial aquaponic system operation be in the South African context and how does it compare to other locations around the world?
4. Where in South Africa could a large commercial aquaponic system be located to provide the most optimal conditions with regard to water and energy usage?
5. How does global climate change affect certain system parameters and what effect will it have on resource usage and sustainability?

1.6 Scope of the Research

The scope of the research includes the development of system dynamic models to further understand the system dynamics of aquaponics systems considering local conditions experienced in South-Africa. The scope includes the investigation of how a predefined reference model is affected given variational changes in the external environment, that is, weather conditions and location.

Locations around South Africa where commercial aquaponic systems could be achievable were identified. The locations were identified based on economic and infrastructural factors. The

climate and geographical aspects of the locations were discussed and summarised. International locations where aquaculture and aquaponic systems are operated were identified and discussed. International locations served as reference regions against which the domestic locations could be compared. The comparison provides an indication of how viable a similar operation could be in South Africa. The domestic regions were also compared locally in order to determine where the best location would be if aquaponics is considered for commercial purposes. The weather data of each location aided in the understanding of the effects of local conditions on the energy and water usage of an aquaponic system.

A generic decoupled aquaponic system was conceptualised, described and modelled using system dynamics modelling. A generic system was presented and all the physical components and parameters that describe the system were presented and discussed. Equations that describe the dynamics of the system were also thoroughly presented and discussed. The equations that are presented serve as an input to the system dynamics model and were derived in the differential equation form.

The research focuses primarily on two important stock variables, namely total system energy usage and total system water consumption. These two parameters, which are an indication of the viability and sustainability of the system, are important factors to consider. Other factors that contribute to the energy usage of the system were presented but not emphasised.

Causal loop diagrams that illustrate the cause-and-effect relationships between the system variables were constructed. The balancing and reinforcing closed loops were identified and indicated in a series of causal loop diagrams. Stock and flow diagrams were constructed and presented which illustrate the ‘cumulating’ and ‘rate’ parameters of the system. Both the causal loop diagram and stock-flow diagrams are visual representations of the system. Python programming language was used to simulate the model by incorporating the derived differential equations and by simulating the weather conditions of each location on a time series plot. The time interval of the simulation was considered in days. The effects of climate change were observed by extending the simulation period to the year 2100 (roughly 80 years). This is based on the current projections as per the Representative Concentration Pathway (RCP) projections as discussed in section 4.4.5.

The results were presented as several time series response plots. The plots were used to extract valuable information regarding the validity of operating large scale aquaponic systems in South Africa. The system energy usage and system water usage were compared with similar systems across the world and the effects of local climate were observed. Conclusions were

drawn based on the extracted data. A recommendation was made at the end of the research to comment on the viability of aquaponics in South Africa and how it could contribute to a sustainable, food secure and thriving economy.

The model should become a useful and valuable tool to make predictions on complex aquaponic systems and how these systems could aid in sustainable farming and food security in South Africa.

1.7 Limitations of the Research

An unfortunate limitation to this research is the access to free, up-to-date weather data. Weather data can be accessed via certain free databases; however, this data can be outdated which could create a misrepresentation of the most recent observed climatic conditions. As far as possible, the most recent data were used.

The modelling software AnyLogic was used to represent the models to illustrate the use of system dynamics theory. However, the actual simulations were executed using Python programming which required coding from first principles. Commercial software packages are more robust and sophisticated. Their packages contain a variety of optimisation and additional functions. The manually coded solver does not include any additional functionality.

1.8 Delimitations of the Research

Internationally selected locations were limited to two locations per continent for comparison. A variety of locations around the world were considered and simulated. Only the best performing countries regarding energy and water usage were used for the comparison in order to better visualise the data.

Infrastructural development played a major role in the selection of domestic locations. Locations that were excluded from the selection may well be situated in regions that perform better with regard to energy and water usage compared with the current selection. This may lead to an oversight of better suited regions owing to economic factors.

The same reference model was applied for all international and domestic locations. This assumption may cause inaccuracies due to regional building codes and practices. Buildings are built to cater specifically for the local climate and to optimise energy usage.

There are numerous methods that can be incorporated to optimise energy usage in buildings and greenhouses. Methods such as thermal storage and the use of waste process heat to heat buildings are implemented to optimise energy efficiency. Energy optimisation methods

were not considered to be part of this research. This could cause the results to be considerably higher and more conservative.

Assumptions, as mentioned in the research, were made to simplify the system to a certain extent. There will be deviations from how the system will operate in reality. More complex modelling, testing and experimentation will be required to accurately predict the system dynamics. For the purposes of this research, which is comparative, the assumptions are valid.

It was assumed that each country has a stable electrical distribution network and that energy costs are comparable. This is not necessarily the case given the use of alternative energy generation such as solar and wind power. This could affect the comparability of the locations.

This research does not provide any guarantee that a certain location will or will not be suitable for aquaponics. It serves as a guideline and a tool that should be used to explore how a modelled system could react given local conditions. The models are only as good as the input data and should be used in a comparative sense. Further research, accurate data and, most importantly, testing and experimentation are required to conclusively prescribe a certain location.

1.9 Organisation of the Dissertation

The following basic structure was followed during the compilation of this research dissertation.

- Chapter One is an introductory chapter which addresses the project background, problem statement, project rationale and motivation, aim and objectives, research questions, scope and limitations.
- Chapter Two comprises a detailed literature review with specific sub-headings. The sub-headings depict advances, depth and width of research in the problem domain.
- Chapter Three describes the methodology and development of the proposed model and system. It explains how theory was used to develop the solution approach and how the system is represented in terms of system dynamics modelling theory.
- Chapter Four includes the results and data of the developed model in the form of tables, graphs and diagrams. It includes a detailed discussion of the results.
- Chapter Five contains a detailed conclusion and any relevant recommendations drawn from the preceding chapters.

CHAPTER TWO
Literature Review

2.1 Chapter Overview

The following section contains an overview of relevant literature regarding system dynamics (SD) applied to aquaponic systems. For purposes of this research, the focus will be aimed at recirculating aquaculture systems (RAS) decoupled from the hydroponic systems (HP) to analyse the dynamics of the system. A few areas of research that were referenced include predictions of the composition of nutrients using SD, definitions of RAS and HP: modelling of fish population and decoupled aquaponic systems using a system dynamics design approach.

2.2 Literature Study

2.2.1 Climatic Factors

A big driver for the dynamic behaviour in the models presented in this research comprises climatic factors. Regional climatic factors such as temperature, humidity and solar radiation play a major role in how the system behaves. Numerous papers on the effects of climate and climate change on energy usage have been published. These papers are mostly applicable to the built environment sector such as residential and commercial office heating and cooling. The theory can still be made applicable to industrial operations such as aquaponic systems. The dynamics of heat transfer will differ and were considered in this research.

ASHRAE Climate Zones

The American Society of Heating, Refrigerating and Air Conditioning Engineers (ASHRAE) Standard 169-2013, Climatic Data for Building Design Standards, serves as a comprehensive source of climate data for use in building design. Additionally, it provides a variety of climatic information for designing, planning, and sizing building energy systems and equipment. Information such as dry-bulb, wet-bulb, dewpoint temperatures, humidity ration, enthalpy, solar irradiation, wind conditions, latitude, longitude, and location specific elevation are provided by the standard. Statistical data such as mean temperatures, daily ranges, degree hours, and seasonal percentages within ranges of temperatures are also provided by the standard. ASHRAE (2013) defines eight climate zones that design engineers use to determine the thermal envelope in building heating and cooling systems.

The Köppen Climate Classification

The Köppen climate classification is a vegetation-based, empirical climate classification system. The classification system aimed to develop formulas that would define climatic boundaries to correspond with those of the vegetation zones (biomes). Other climatologists have modified portions of Köppen's procedure on the basis of their experience in various parts of the world (Arnfield, 2020).

These classification systems make it easier to generalise areas that experience similar climates. These classifications play an important role in identifying general weather trends in a country like South Africa where there is such a diverse climate. The different climate classifications specific to a certain area are discussed in Chapter Three. The classification of the climate of each region will aid the comparative study.

Impact of Climatic Factors on Energy Consumption

Hong et al. (2013) reported how weather can play a significant role and that weather directly affects thermal loads on buildings and by extension the energy performance. The researcher employed large-scale building simulation which studied the impact that weather exerted on peak electricity demand and energy use over a 30-year (1980 to 2009) period. "Actual Meteorological Year" weather data for three types of office buildings and at two design efficiency levels were considered and the simulations were executed across all 17 ASHRAE climate zones. Two important findings were noted. Firstly, the weather impact was greater for buildings in colder climates compared to warmer climates. Secondly, the simulated energy savings and peak demand reduction, by means of energy conservation measures, can be significantly under- or overestimated. It was emphasised that it is crucial to execute multi-decade simulations with Actual Meteorological Year weather data to fully evaluate the impact of weather on the long-term performance of buildings.

Global and regional climate changes produced a significant effect on energy production and consumption, particularly on heating and air conditioning across residential, commercial, and industrial applications as investigated by Ginzburg et al. (2016). The dynamics of duration and temperature of a heating season were analysed. This was carried out for a variety of regions in Russia in a published comparative study of heat energy consumption. They found that the projected climate warming for the Moscow region, laterally with the energy conservation measures, will encourage a significant reduction in energy consumption in winter.

Clarke et al. (2018) explored potential future consequences of climate change on building energy usage around the globe. The analysis was conducted using a model of the global building sector within the GCAM integrated assessment model. The results indicate that changes in the net expenses were not constant across the globe. The net expenditure decreased in regions where heating demands dominated and it increased the most in areas with a smaller demand for space heating and a greater demand for space cooling. In a similar study conducted by Li et al. (2020), 16 cities from four major climate zones of China were selected. The heating and cooling loads of an office building were simulated during 1961–2017. The effects of climate change on extreme loads were analysed. The results indicated that the days of peak heat loads significantly decreased in nearly all the simulated cities. Furthermore, there were no significant changes in the days of peak cooling loads. The simulations showed that the daily peak cooling load was closely related to multiple climate factors. These factors included temperature, relative humidity, and solar irradiation. The publication showed that the effect of temperature on peak cooling loads decreased for cold climate zones compared to hot climate zones. However, the impacts of relative humidity and solar irradiation gradually increased.

Additionally, the results showed that a combination of multiple climate factors should be considered when implementing improved operating efficiency of air-conditioning system rather than the single temperature. Furthermore, the different responses of peak cooling energy consumption are sensitive to climate change in different climate zones.

Energy Efficient Aquaponics Facilities Based on Regional Climate

Alkhalidi et al. (2020) discussed energy efficiency based on regional climate which was conducted on an actual aquaponic system. The paper reported that aquaponic systems are starting to emerge in countries in Africa and the Middle East. Although aquaponics is not a novel concept, it is considered uncharted territory for certain countries and regions as evident in an international survey conducted in 2014. Only a single response was received from Ghana, Oman and South Africa respectively. Alkhalidi et al. (2020) mentioned that a 2016 survey, conducted and published by Mchunu et al. (2018), which yielded 44 responses from a variety of aquaponics farmers helped to indicate the status of aquaponics in South Africa. Tilapia accounted for 82% of raised fish and 75% of the farmed plants are leafy vegetables. The study classified South Africa as an emerging country with regard to aquaponics farming. Although Europe's research concerning aquaponics is quite recent, the region is classified as an emerging practice. Although the region has only a few commercial facilities, it is considered to be more

advanced compared to the rest of the world. Due to climatic differences between the Middle East and other leading aquaponic locations, such as America and Europe, the same practices cannot always be utilised and requires different approaches.

It may turn out that this is the same case for the South African climate given its vast regional diversity. Developing countries are facing problems that cause them to fall behind in energy efficiency in buildings and greenhouses. Issues such as the lack of consistent data, poor documentation, or the absence of documentation altogether render research and development more difficult. It was predicted that by 2050 the international agricultural sector will have to double the amount of water used to feed the world as discussed by Pahl-Wostl et al. (2008). Aquaponics uses 90% less water than conventional farming (Nichols & Savidov, 2012). Therefore, there is a strong case from a sustainability perspective and it should be seriously considered since it is a practice that could draw the attention of investors. Proper management of natural resources, particularly water, is vital. In hot climates cultivating crops is not easy and improper freshwater management jeopardises food independence.

2.2.2 Recirculating Aquaculture Systems

Recirculating aquaculture systems is defined as an aquaculture system that has a water exchange rate of 10% or less of the total system water volume per day (Davison, 2018). A RAS system takes the inputs of water, electricity and feed and outputs protein for consumption. Some advantages of these systems include the relatively low space and water requirements, effective treatment, and collection and recycling of waste streams, as well as isolation of the fish population which excludes predators and allows close control and monitoring of the environment and diseases.

Ultimately RAS facilities can serve as a protein alternative that alleviates the strain on the natural resources. The start-up costs for these systems are quite high and skilled staff are required to operate these systems, thus contributing to high overhead costs.

Motivation for Recirculating Aquaculture Systems

Aquaculture systems like earthen ponds and concrete tanks are encountering undesirable sustainability problems (El-Sayed & Kawanna, 2008). These systems may cause environmental problems such as the ejection of effluent into the local environment, a shortage of freshwater, an increase in land costs and climatic changes. Recirculating systems pose an alternative solution that could possibly replace such land-based systems which could address the issue of especially fresh water shortages and extreme climatic conditions.

A recent paper published by Ahmed and Turchini (2021) further supports and recommends the use of RAS systems. Adopting "Recirculating Aquaculture Systems (RAS)" strategies could assist in environmentally sustainable practices and address the vulnerability of the effects of climate change on fish production. An RAS, which is a highly productive intensive farming system and utilises a minimum amount of water, is considered eco-friendly. Environmental impacts are kept to a minimum since habitat destruction and other ecological effects are limited by these systems. Water pollution and eutrophication could be limited and controlled in an effective manner and local biodiversity is protected due to fish being kept in a controlled environment reducing the risk of introducing invasive species into the environment. Disease and parasite transmissions can also be closely monitored and controlled.

The RAS systems can be operated in extreme climates and external conditions since RAS operate in indoor controlled environments. Extreme climate conditions such as rainfall variation, floods, droughts and global warming will not influence the production of fish. However, maintaining the internal conditions for optimal production is an energy intensive endeavour. Another concern is greenhouse gas emissions. Even though RASs hold great potential, it has not been widely utilised and implemented. This is especially true for developing countries. Since these systems are complex and costly to design, they remain a topic of research and have not been widely implemented. It is important that research continues investigate new technologies that are cost effective and produce systems that are energy efficient, reduce greenhouse gas emissions and will be adaptive to climate change.

This research focuses on investigating the sustainability of RASs especially with regard to energy use. An RAS is energy intensive which is undesirable since high energy usage increases operational costs and the potential dependence on fossil fuels. Although energy use in an RAS has been studied or mentioned in other publications, its importance and impacts have not been studied (Badiola et al., 2018). This is therefore the focal point of this research.

Energy Consuming Components in Recirculating Aquaculture Systems

The design and production parameters of an RAS will determine the overall energy consumption. The energy-intensive nature hampers its sustainability and cost-effectiveness (Badiola et al., 2017). During the study conducted by Badiola et al. (2017), energy consumption of an RAS unit was observed. Each energy consuming component of the system was monitored independently and the energy usage was measured. The experiment showed that the main consumers of energy were the heat pump and the pumps of the system. The study further explains that the electricity produced by fossil fuel was the most environmentally unfriendly

input. Temperature variations in the water temperature were the reason for the high energy use since the heat pump had to maintain the water at the setpoint.

Poor design will ultimately lead to the failure of an RAS. There is no universal solution, and each system has its own factors to consider. Many systems are modified after previous approaches which may not be suitable for that specific system. Poor management owing to a lack of skills is a major problem. With the increasing use of RASs, it will be crucial to develop skills and technology that is system specific. Research on a commercial scale and experimentation with the best combinations of components for each situation are key priorities (Badiola et al., 2012).

Socio-Economic Considerations of Aquaponics

Water scarce regions are facing a threat to food security. It is an increasing local and global challenge. Therefore, it is important to find new innovative ways to increase sustainable agricultural production (Yogev et al., 2016). An alternative to traditional monoculture is the advancement of aquaponics which produces vegetables and fish. This method offers quite a few advantages.

Aquaponic systems are nearly closed systems which means that there is almost no water loss except for evaporative loss (Jensen, 2001). Water is used more sustainably and the overall volume of water required for the yield of both fish and vegetables (Resources, 2008; Rakocy et al., 2006) is minimised when compared to conventional agriculture (Effendi, et al., 2015).

Since the biomass from the aquaculture system is used as crop fertilizers, no additional nutrients are required to produce the vegetables in the hydroponic system (Goddek, et al., 2015; Graber & Junge, 2009). A large benefit of aquaponics is that it does not require fertile land. Systems can operate in the harshest conditions around the world even in deserts and urban areas (Rothwell et al., 2015).

Aquaponics could be a great way to ensure food security, especially in poor rural areas around the world. Smallholder farmers and people who live in rural areas comprise a significant percentage of the population in developing economies. This group also has the highest percentage with deficiency malnutrition due to a lack of vitamins and protein in their diet. This often leads to high infant mortality rates (Fanzo, 2012). Aquaponics can provide these poor communities with an easy and sustainable solution for the lack of food security.

Optimal Water Conditions

Rakocy (1990) explained that the geographical range for rearing tilapia in outdoor tanks depends on the water temperature. The temperature range for optimum tilapia growth is reported to be 27.8 °C to 30 °C. Rakocy (1990) found that growth is significantly reduced at temperatures below 20 °C and mortality will occur below temperatures of 10 °C. Tilapia will lose their resistance to disease and are subject to infections at temperatures below 12.2 °C.

Depending on location, tilapia can be held in tanks for 5 to 12 months a year in the southern regions of the USA. Hot and humid areas such as Texas and Florida are the only areas where tilapia survive outdoors year-round. Tilapia must be overwintered in heated water at other locations. Mechanical or electrical failure poses a risk for tank culture systems since they rely on continuous aeration or water pumping. If a failure occurs, this could lead to disastrous fish mortality.

One of the most important factors affecting the physiology, growth, reproduction, and metabolism of tilapia is water temperature (El-Sayed & Kawanna, 2008). The study focused on temperate and subtropical regions which experience seasonal variations in water temperature. The optimum temperature range for normal development, reproduction and growth of tilapia was stated to fall between 25°C and 32°C. The range depended on the fish species (Chervinski, 1982), the size (Hofer & Watts, 2002) and genetic variations (Cnaani et al., 2000). The study found that the growth of the fish reared at 28 °C was almost double the growth at 24 °C and 32 °C. The best feed conversion rate (FCR) was observed at water temperatures of 28 °C. This was slightly better than temperatures at 26 °C and 30 °C. The poorest FCR was obtained at 24 °C and 32 °C respectively. The reference water temperature, which will be maintained in this study, will be assumed to be 28 °C.

2.2.3 Hydroponics and Greenhouse Environments

Greenhouse Sustainability and the Environment

Greenhouse systems are widely used to improve growing conditions of vegetable, fruit and ornamental crops. Greenhouses not only protect plants from external factors, which could have a negative impact on plant growth, but also creates crop specific microclimates. Such microclimates create optimal conditions which will maximise crop yields and lengthen the market availability of products and thus improve the quality. Greenhouses make optimal use of space and yield a higher production per unit area compared to conventional practices.

However, these facilities require a large energy input to operate the facility and they produce large amounts of waste which require disposal. Certain energy reducing strategies and optimal climate control are discussed by Vox et al. (2010). Having proper control strategies for equipment and using the correct materials can have a major effect on the energy use of the system. Alternative energy sources and technologies can be incorporated to reduce the dependence on fossil fuels required for climate control. Renewable energy sources such as solar thermal and photovoltaic systems should be considered.

Cultivating in open fields can be very water intensive. It largely depends on location and season. Each location has its own weather conditions and soil characteristics that ultimately determine the factors around irrigation. Limited sources of water are determined by the groundwater system or the amount of precipitation in the area. Countries in the Middle East and North Africa are forced to rely on desalination of seawater for agricultural practices, due to water scarcity. Greenhouse agriculture can be utilised to ensure proper use of water resources and to reduce waste. This is achieved since the water can be captured and controlled within the system. As discussed by Akrami et al. (2020) the reduction of the rate of exchange between the outside environment and internal air could create optimal conditions for crops to thrive. The temperature will rise by trapping incoming thermal radiation through transparent covers, thus influencing the internal microclimate and by extension, the crop growth.

To reduce energy consumption and biocide within a greenhouse dynamic greenhouse, climate control should be utilised. This is achieved by using computerised model-based regimes. Models were designed and applied to a simple deterministic microclimate model for dynamic greenhouse climate control concepts (Körner et al., 2007). The model was used to determine crop temperature and the latent heat of evaporation at various vertical levels of a dense canopy of potted plants. The result of their simulations indicated that energy can be conserved by controlling the greenhouse temperature according to the predicted crop temperature opposed to the air temperature.

Dynamic Simulations of Internal Conditions

Both external and internal factors influence the complex dynamic nature of greenhouses. External factors could include weather and control elements such as ventilation, exhausts, and heaters. Internal factors include crop and internal components. Fitz-Rodriguez et al. (2010) state that better greenhouse design can be achieved when the physics of the greenhouse environment is understood. This will ultimately improve the chances of a successful operation.

Greenhouses take on many forms, structures and designs to overcome location specific climate conditions. Each crop has different requirements and the greenhouse needs to be designed to cater for these needs. Fitz-Rodriguez et al. (2010) explained that greenhouse designs vary in structural shape, size, glazing materials, and the various types of equipment required to achieve the desired environmental conditions. The core parameters that are controlled in a greenhouse to achieve the desired environment are air temperature, humidity levels, carbon dioxide concentration and plant specific lighting levels.

Greenhouses often contain exhaust fans and motorised ventilation openings which can introduce outside air. This will maintain the above-mentioned parameters such as internal temperature, humidity and carbon dioxide concentration at the optimum conditions. Evaporative cooling techniques and fog systems are sometimes used in warmer climates to ensure favourable air temperatures inside the greenhouse. These methods provide more efficient cooling compared to traditional air-conditioning methods. In colder climates, heating may be required, and the greenhouse is equipped with hot air, root zone heating or hot water pipes. These are some of the strategies to achieve optimal conditions (von Zabeltitz, 1999). Energy and mass balance models and equations are often used to describe the physics within a greenhouse (von Zabeltitz, 1999). The models can be classified as static or dynamic models.

Complex systems, including multiple state variables that describe the system status over time, are often coupled with drop dynamics (Jones et al., 1988; Jones et al., 1990; Takakura et al., 1971). Specific phenomena such as natural ventilation are discussed by Al-Helal (1998), Boulard and Draoui (1995), Boulard et al. (1999), de Jong (1990), and Dayan et al. (2004). Forced ventilation is described by Arbel et al. (2003) and Willits (2003) and evaporative cooling is discussed by Abdel-Ghany and Kozai (2006), Baille et al. (1994), Boulard and Baille (1993), and Boulard and Wang (2000). Heating systems are presented and discussed by Bartzanas (2005) and Kempkes et al. (2000).

Hydroponic Water Management

Since hydroponic systems efficiently make use of resources and produce quality food, hydroponic cultivation is gaining popularity throughout the world (Sharma et al., 2018). External factors such as urbanisation, natural disaster, climate change, use of chemicals and pesticides that are affecting the fertility of the land, are causing soil-based agriculture to be questioned. Hydroponics has been successfully used on a commercial scale across the world to produce crops with up to 90% water savings. To ensure successful implementation of commercial controlled environment technology, low-cost techniques are important.

Technology that is easy to operate and maintain, requires less labour with an overall lower setup and operational costs.

2.2.4 Global Aquaponic Operations

Goddek et al. (2019) discuss a few challenges concerning aquaponic operations around the world. Several key issues still need to be fully addressed. The development of energy-efficient systems with optimised nutrient recycling and suitable pathogen controls are a few. Another issue is achieving profitability, which includes effective value chains and efficient supply chain management. Legislation, licensing and policy as well issues regarding education and research are also key to the future success of aquaponics. The paper presented a graph indicating that RAS is vastly researched and that much information is available on RAS. While hydroponics is less researched by an order of magnitude of 10 times, aquaponic systems have the least research and information available and is an upcoming field of research (Goddek et al., 2019).

A limited number of countries currently implement aquaponics systems on a large scale. To identify locations where commercial aquaponics systems can be viable, aquaculture and greenhouse farming were researched. With an abundance of literature available for aquaculture operations, the locations where such operations exist were identified. If fish can be reared and harvested in certain climates it should be viable to extend such operations to include a hydroponic sub-systems in order to grow crops.

The identified locations were therefore included in this research and were used to compare local and international locations on a global scale. The comparison can then illustrate how countries with different climates compare with regard to energy and water usage.

Fitzsimmons (2006) published an extensive paper discussing the current and upcoming suppliers of Nile Tilapia to meet global demand. The publication is somewhat outdated, but the projections made in the paper are still valid and will be used and referenced in this research. Development agencies introduced the use of tilapia farming as an industry in an attempt to feed the rural poor. This industry has currently grown to a highly domesticated livestock product with sales exceeding two billion dollars a year.

The Food and Agriculture Organization of the United Nations (FAO, 2020) reported that world production of farmed tilapia came close to 1.5 metric tons (mt) in 2002. It is reported that China is the world's major producer and consumer of tilapia. The mainland provinces produced more than 700,000 mt in 2002 and Taiwan produced another 90,000 mt. Other Asian

countries produced around 325,000 mt. In 2002 the USA imported a value of $174,000,000 in tilapia making them the world's major importer of tilapia (FAO, 2020).

Global Aquaponic Operations: Africa

Small-holder farms contribute the most to tilapia production in Egypt. The farms consist of fish grown in conjunction with rice. There are a few large-scale production operations; most notable is the government supported farm at Maryut (Fitzsimmons, 2006).

Aquaculture in Uganda produces fish from stocked community water reservoirs and minor lakes. Small-scale fish farmers and emerging commercial farmers contribute to the market. It is estimated to be around 20,000 ponds across the country. The production of tilapia ranges from 1,500 kg per hectare per year for subsistence farmers to 15,000 kg per hectare per year for emerging commercial farmers.

Nigeria has a very strong domestic market for tilapia and few tilapia products are exported for international trade. The fish produced is consumed by local markets. The production trends for the various African countries are presented in Table 2.1.

Table 2.1: *Top fish producing countries in Africa in annual million tonnes (FAO, 2020)*

Country	1980s	1990s	2000s	2015	2016	2017	2018
Egypt	0.12	0.23	0.27	0.24	0.23	0.26	0.27
Nigeria	0.10	0.10	0.21	0.34	0.38	0.42	0.39
Uganda	0.19	0.22	0.33	0.40	0.39	0.39	0.44

Global Aquaponic Operations: Asia

The economy of Bangladesh is heavily influenced by aquaculture. The practice contributes to the food security of the nation, the livelihoods and income of its citizens and earnings from exports. Fish accounts for 60% of the nationwide protein consumption. According to Rahman et al., 2021, fish exports contribute to 3.5% of the country's GDP and 25.7% of the total agricultural GDP.

China has been the top fish producer in the world for many years. The country contributes nearly 70% of the global aquaculture production (FAO, 2020). China produced 65.2 million tonnes of food fish in 2015. Aquaculture accounted for 73% of the total fishing sector with the other 27% from caught captured fish. Since China is the world leader in aquaculture, it also has the most diverse systems, methods and species.

The production of fish in Indonesia reached an approximated 8.9 million tonnes in 2012. The marine catch accounted for about 5.8 million tonnes where aquaculture accounted for 3.1 million tonnes. Indonesia also produced 6.5 million tonnes of seaweed. From a food security point of view, aquaculture plays an important role since nearly 95% of the fish produced is for subsistence farming. An estimated 6.4 million people were engaged in inland and marine fishing in 2012 (FAO, 2020).

The total fish produced in Myanmar was reported to be 3.2 million tonnes in 2017. About 1.1 million tonnes of the fish produced was from aquaculture. Aquaculture is an important industry in Myanmar since the sector provided direct employment to 2.3 million people (FAO, 2020). Seven percent is attributed to the aquaculture sector. Since the early 1990s, aquaculture production in Myanmar has enjoyed significant growth in the sector with an annual average growth rate of 23% during the last few decades (FAO, 2020). A rise in demand for export has led to a spike in growth.

Aquaculture in the Philippines contributed around 25% of the total fish produced in the country. Much of its production is consumed locally. Aquaculture plays an important role in the economy of the country with the industry providing jobs for more than 1 million people (FAO, 2020). Furthermore, the industry contributes nearly 1.8% to the country's GDP. It was estimated that in 2013, exports of fish and fishery products were valued at USD 1.2 billion.

It is reported that over the last twenty years the annual aquaculture production in Thailand was about one million tons per year, on average. Aquaculture production in Thailand's yield increased from around 553,600 tons in 1995 to 928,500 tons in 2015 (FAO, 2020). The aquacultural sector of Thailand has rapidly developed during the last few decades. The development has been accompanied by tangible socio-economic development. The country was ranked among the top twenty-five countries in terms of fisheries production in 2018 (Sampantamit et al., 2020).

The culture systems in Vietnam are diversified according to national geographical and climatic conditions. Regions in the North are dominated by freshwater fishponds, rice-cum-fish, and marine cage culture. Regions in the centre of the country concentrate on the intensive culture of giant tiger prawn and the marine cage culture of finfish or lobster. The Southern regions of the country have the most diversified farming activities. These activities include pond, fence and cage culture of catfish as well as several indigenous species. Further, there is a variety of intensification levels of giant tiger prawn culture and integrated culture. The production trends for the various Asian countries are presented in Table 2.2.

Table 2.2: *Top Fish producing countries in Asia in annual million tonnes (FAO, 2020)*

Country	1980s	1990s	2000s	2015	2016	2017	2018
Bangladesh	0.44	0.50	0.86	1.02	1.05	1.16	1.22
China	0.54	1.46	2.11	1.99	2.00	2.18	1.96
Indonesia	0.27	0.31	0.31	0.47	0.43	0.43	0.51
Myanmar	0.14	0.15	0.48	0.86	0.89	0.89	0.89
Philippines	0.26	0.19	0.15	0.20	0.16	0.16	0.16
Thailand	0.10	0.18	0.21	0.18	0.19	0.19	0.20
Vietnam	0.11	0.14	0.21	0.15	0.15	0.16	0.16

Global Aquaponic Operations: Europe

The European Union was the largest fish importing market in terms of value in 2018 (FAO, 2020). The sector provides jobs for nearly 70,000 people and mostly consists of small businesses in rural coastal regions. Growth in this region seems to be stable compared to that of other countries which have shown steady growth over the last few decades. The leading countries in fish production are Spain, France, Italy and Greece (European Commission, 2021). The production trend for Europe is presented in Table 2.3.

Table 2.3: *Fish production in Europe in annual million tonnes (FAO, 2020)*

Region	1980s	1990s	2000s	2015	2016	2017	2018
Europe	0.28	0.43	0.36	0.43	0.44	0.41	0.41

Global Aquaponic Operations: Americas

The environmental conditions of Brazil make it very suitable for aquaculture operations. A popular species of fish that is currently being cultured is Tilapia. Tilapia is not only used for protein, but other products are made from their skins. Nearly all the fish produced is consumed domestically. The country produced nearly 250,000 tonnes of aquacultural products in 2002. Pond culture methods are practised in the northeast regions and caged farming, raceway and round tank farming methods are utilised in the southern regions (Fitzsimmons, 2000).

The FAO (2020) reports that freshwater aquaculture took off in Honduras in 1936 when the first fish culture station was built. The first species that were cultivated were introduced from Guatemala. In an attempt to improve the nutritional level of the rural population, aquaculture practices were implemented. Fitzsimmons (2000) mentioned that the first

commercial farms began in the early 1990s. The technology was based on existing production systems in Jamaica. The method of intensive pond culture using paddlewheel aeration together with daily water exchange was implemented.

The climate in Colombia, which can be described as tropical accompanied by stable temperatures, makes it a suitable location for aquaculture. The abundance of water further makes it well suited. The aquaculture sector has shown a fast development rate with higher profitability than traditional agricultural activities (FAO, 2020). Due to rising input costs and a stable selling price, returns have declined. Unsustainable practices such as over-fishing and habitat degradation have placed strain on natural resources. Aquaculture is serving as a more sustainable solution that could alleviate the burden.

The FAO (2020) reports that more than 95% of Ecuadorian aquaculture is attributed to marine shrimp, followed by tilapia. Tilapia has enjoyed tangible growth over the last few years. Shrimp farms are typically rotated with Tilapia farming since it is believed that crop rotation can reduce diseases in shrimp (Fitzsimmons, 2000).

Over the last 35 years, the aquaculture industry has become well developed in the United States of America. Despite the development, the USA still faces substantial challenges to maintain constant growth. It is estimated that 924 million dollars were generated by an aquaculture production of nearly 500,000 tonnes in 2008. Production is relatively stable averaging about 24,000 tonnes in the decade from 1998 to 2008. The production trend for the Americas is illustrated in Table 2.4.

Table 2.4: *Fish production in the Americas in annual million tonnes (FAO, 2020)*

Region	1980s	1990s	2000s	2015	2016	2017	2018
Americas	0.56	0.54	0.58	0.57	0.60	0.58	0.63

Asian countries and countries in Latin American are currently leading regions for aquaculture operations. European and North American countries are still competing and have well developed expertise and technologies with regard to aquaculture, particularly inland operations. It is reported that most African countries are still trailing the rest of the world despite ambitious projections at the regional and national levels. It is recommended that in order to promote marine aquaculture in Africa, there is an urgent requirement for proper policies and planning. Additionally, development in infrastructure and technical expertise are required.

2.2.5 Aquaponics in South Africa

The environmental conditions of South Africa make it a very suitable location for aquaculture on commercial scale for a variety of cultured species. It is reported that the local aquaculture sector is underperforming well below its potential. The sector is a minor contributor to national fishery products and to the GDP of the country. In recent times, this sector has been further explored and there is an attempt to identify the limitations and constraints which have limited the development of this sector. Some of the major issues which cause limited development of the practice are access to water and land, proper access to technology, extreme transactional costs and a lack of supporting policies and legislation. It was reported that the total marine aquaculture production in 2011 was 1,883 tonnes, with an estimated value of 379 million Rands. The total freshwater aquaculture production was 2,921 tonnes for 2011. Trout contributed 49% of the total production (FAO, 2020).

Mchunu et al. (2018) conducted a survey in 2016 to collect information about the types of systems used, and the management and distribution of aquaponics in South Africa. They concluded that most of the current aquaponics practitioners have limited knowledge about aquaponics production. Attention should be paid to raising awareness about the potential of aquaponics. Furthermore, the technological knowledge of aquaponic operators should be raised to increase the number of aquaponics operations and to increase the total amount of food produced with aquaponics.

With a lack of research, particularly in the South African context, this research will hopefully provide valuable insights to where operations may be most optimal with regard to energy and water usage. These are important factors since South Africa is a water scarce country with a burdened energy generation and distribution system. Therefore, there is limited room for error and for aquaponic systems to be successful in South Africa, proper planning and research are required.

The findings of the survey will be presented in this research given the limited information available regarding aquaponics in South Africa. The survey conducted by Mchunu et al. (2018) revealed that KwaZulu-Natal (KZN) was the most dominant province in South Africa with regard to aquaponic activity. The survey revealed that 32% of the respondents stemmed from KZN followed by Gauteng Province (GP) with 20%, and Eastern Cape (EC) and Western Cape (WC) with 16% each. The remaining provinces revealed to have fewer operations with the Free State (FS) reporting only 7%, the North West (NW) 5%, with Mpumalanga (MP) and Northern Cape (NC), 2% each. KZN had the most hobby scale systems

while commercial systems were being operated in GP and WC. Subsistence scale operations were evenly distributed among all the provinces (Mchunu et al., 2018).

Additionally, 71% of the respondents indicated that they constructed their own aquaponics system. Systems that were constructed by a service provider accounted for 27% of the respondents. This figure indicates that there is a lack of professional services which cater for aquaponic system design at a local level. The remaining 2% of the respondents indicated that their aquaponics system was set up by the Department of Agriculture (DoA). This figure indicates a lack of support and buy in at a government level. It is evident that aquaponics is not practised on a large commercial scale in South Africa with only 25% of the respondents indicating commercial production. The 39% of the respondents indicated that they practise on a hobby scale, followed by subsistence production (36%). With regard to the system configuration, 80% used tunnel environments for aquaponics production. Open field production, greenhouse, and closed field production accounts for 11%, 5% and 4% respectively (Mchunu et al., 2018). The high percentage of farmers who use a tunnel environment compared to greenhouses and fields suggests that aquaponics requires further climatic adjustment or control in order to operate in South Africa (Mchunu et al., 2018).

The study made no mention of energy and operating costs of aquaponic systems. The survey revealed that aquaponics in South Africa remains underdeveloped due to a lack of knowledge, expensive cost due to lack of local support and not enough support from the government to make aquaponics financially successful.

This study aims to provide some assistance and insights into future expansion and planning of this promising practice.

2.2.6 System Dynamics Applications in Aquaponics

Balancing Conditions for Multi-Species Growth in Complex Systems

Lastiri et al., (2018) suggested that the main challenge in aquaponics exists in finding the optimal conditions for the growth of multiple species. This often leads to a dynamic system with high complexity. Mathematical models can be used to capture the complex dynamics in systems such as aquaponics. These models are used to support the development of efficient systems.

Water and nutrient management strategies to produce Nile tilapia (Oreochromis niloticus) and tomato (Solanum lycopersicum) were developed which aimed to improve water and nutrient efficiency. Therefore, a system-level mathematical model and simulation were

developed. The results indicated that water and fertiliser consumption can be reduced by providing more nutrient-rich water from the fish to the crops. By transferring the water, an excess concentration of nutrients could occur which could exert negative impacts on both commodities. A system level approach was used to develop the model which was based on an existing aquaponic system. The study recommends that further investigations are required to provide the model with greater flexibility for the analysis of other systems. Other areas of interest which particularly relate to modularity were discussed. By using a detailed dynamic approach, the modularity of each component could be improved. Ultimately, reliability in the simulations could be maintained by changing the overall system configuration. It was suggested to model components such as mixing dynamics, particle size distribution effect on solids removal, effects of water quality on fish and crops, and possible reactions outside of the nitrification biofilter in order to improve modularity.

Aquaponic System Dynamics Modelling

Giaglaras et al. (1998) presented a dynamic model for the prediction of the composition of the nutrient solution from climate variables. A first order derivation approach was presented using mass and energy balances. They concluded that evapotranspiration of crops and concentration of Calcium are predicted to satisfactory precision. The tool is mostly useful for research and monitoring purposes.

In Chapter 9 of Bala et al. (2017) a detailed discussion is provided on the construction of a system dynamics model. The model was intended to simulate the sustainable development and planning of Hilsa fish production. The model is used to predict long-term trends in the Hilsa fish population over several decades. The outputs are used to analyse and assess how the harvesting of juveniles and spawning adults are impacted. The simulation results indicated that when harvesting of the adult and juvenile fish entering the rivers increased, the population in the Hilsa fish gradually declined. It indicated that at current harvesting rates, the valuable resource might disappear within a short period. This model stressed the importance of sustainable fishing. The method described by Bala et al., (2017) is designed to determine the dynamic hypothesis, construct the causal loop diagram, then the stock-flow diagram, discuss the model validation, and lastly, to present the simulation and policy analysis. Several other studies also reported on the modelling of population dynamics of fish, for example, Robadue and Simanek (2007) and Tian et al., (2004).

Karimanzira (2016) used dynamic modelling techniques applied to the production of Nile tilapia and tomatoes to analyse aquaponics systems. The study is a good example of how

dynamic models, which are based on differential equations, can be used in diverse aquaponic processes. It can be used to model aspects such as crop and fish growth, waste production and microclimates. The system dynamics and how the systems integrate with each other can be easily modelled, visualised and adjusted. By simulating various aquaponic system configurations, management strategies can be defined that will increase the chances of success for future large-scale production and to ensure environmentally sustainable practices.

Decoupled Aquaponic Systems: A System Dynamics Design Approach

Goddek et al. (2016) published a system dynamics model of a decoupled aquaponic system. It was the objective of the said study to develop a theoretical concept of a decoupled aquaponic system. The model would be able to predict water, nutrient, fish, sludge, and plant levels. To achieve this, the aquaponic system was modelled using a system dynamics modelling approach. The results of the model indicated that the water quality of the aquaculture system is dependent on the evapotranspiration rate of the hydroponic system. The study determined that certain nutrients are the limiting factor in sizing the hydroponic system since nutrients such as Phosphorus is an exhaustible resource. The study concluded that it is important to investigate additional geographically dependent aspects in future research.

Goddek (2019) presented a fully integrated simulation model of multi-loop aquaponics. The model considers the RAS and HP units separately from one another. This creates a detached ecosystem with inherent advantages for both crops and fish. Different system configurations and the associated time responses of these systems were considered in order to obtain the best fit between RAS and HP units. Aquaponic sizing simulators were created using deterministic mathematics together with detailed plant energy and growth models. The models were applied to three different types of climatic zones to test the robustness for sizing HP systems. Economic evaluations of multi-loop systems should be considered in future studies for a variety of regions across the world.

System Dynamics on Food Security

A similar methodology, as described in section 2.2.6, was followed to model food security in Malaysia. The model was investigated as a case study and the application of system dynamics (Bala et al., 2017). It was noted that to improve productivity, a gradual transition to bio-fertiliser is required. Furthermore, funding for research and the development of high-yielding hybrid rice and an increased cropping intensity were recommended.

Further studies have been reported to identify the determinants of food security at the household level using logistics models (Babatunde, 2007; Faridi and Wadood, 2010; Maharjan, 2011; Sikwela, 2008).

2.3 Alternative Solutions

Alternative solutions may be applied to certain systems including solutions such as energy modelling and simulations using a variety of software applications. Energy modelling is very popular in the built environment sector and is used in the designing of building services. These models can offer satisfying results for a single location and system.

Using system dynamics modelling offers a solution to properly capture the dynamic components of a large and complex system. It will allow for multiple iterations of simulations to truly observe the effects of parameter variations.

2.4 Preferred Solution

Goddek (2019), Goddek et al. (2016) and Karimanzira (2016) proposed very appropriate and fitting solutions when considering a full system dynamics approach to aquaponics. Methods presented in these publications were chosen in order to be progressed to develop a model which contains local geographic parameters. New model parameters were added to simulate the effects of the parameters and how system variables such as total system energy and total system water usage were affected.

The systems thinking and system dynamics modelling mythology approach described by Bala et al. (2017) was adopted and followed closely during this research. The text clearly defines steps that should be followed when constructing models and how to successfully execute the simulations. The text and the methodologies explained were closely followed and used during this research to identify the problem properly, formulate the dynamic hypothesis, construct causal loop diagrams followed by stock-and-flow diagrams, and finally, to apply a sensitivity analysis for policy making.

The theory described by Cengel and Ghajar (2014) was used to derive the differential equations which represented the heat and mass flow of the proposed system. These equations played an important role in the system dynamics model and the theory discussed in the text was closely followed and adapted to this research.

With limited research available describing the system dynamics of energy and water usage in large commercial systems, the theory of Bala et al. (2017), and Cengel and Ghajar (2014)

played an important role in deriving critical elements of the models from first principles. Solutions presented by Goddek et al. (2016), Goddek (2019), and Karimanzira (2016) were used as a basis to identify the system boundaries and basic system dynamic components which play an important role in a bigger system. These existing models could be supplemented with new parameters and additional theories to be made applicable to the proposed research questions and objectives.

2.5 Concluding Remarks

This chapter presented a detailed literature review covering both the ecosphere and biosphere of aquaponics including their respective influence on the practice of aquaponics in different countries randomly selected across the globe. Furthermore, recent studies conducted in the field of aquaponics including how existing theories will be applied to the given problems and research questions, as discussed in Chapter One, sections 1.1 and section 1.2 of this dissertation, were presented. Lastly, the adaptation of the system dynamics modelling approach to aquaponic systems was explored and presented.

CHAPTER THREE

Method and System Description

3.1 Chapter Overview

This chapter presents a description of the physical components of the notional decoupled aquaponic system used in the simulations. The system dynamics method was developed, derived and illustrated via the applicable system thinking methodology as discussed by Bala et al. (2017). Locations, domestic and international, were identified where aquaponic systems could possibly thrive. The model was applied to the various locations. Weather data of the respective locations served as input to the model. Causal loop diagrams were developed and presented, after which stock and flow diagrams were developed. The differential equations governing the system were derived and presented. The differential equations are used in the model to mathematically simulate the various stocks and flows of the system. Finally, the chapter is summarised and concluded.

3.2 System Description

The generic input model is based on a decoupled aquaponic system. The system consists of two sub-systems namely a recirculating aquaculture facility and a hydroponic system contained in a greenhouse. Both systems are subjected to environmental control in order to maintain optimal conditions for fish and crop production. Energy is required to ensure that these optimal levels are kept constant. Figure 3.1 is a process flow diagram illustrating the configuration of the decoupled system and all the physical components thereof. It describes the water flow of the system and the components that will require external energy input.

In describing and developing the system model, the system boundary has to be identified. As discussed by Bala et al. (2017), to best describe the model boundaries, the entire system that is responsible for causing the problem and which originates internally from the feedback structure of the stated complete system, should be considered. It is advised that the system boundary should focus on that portion of the whole system which addresses the most relevant variables of the system in order to address the problem and the purpose of policy analysis and design. The process flow diagram serves to achieve this purpose.

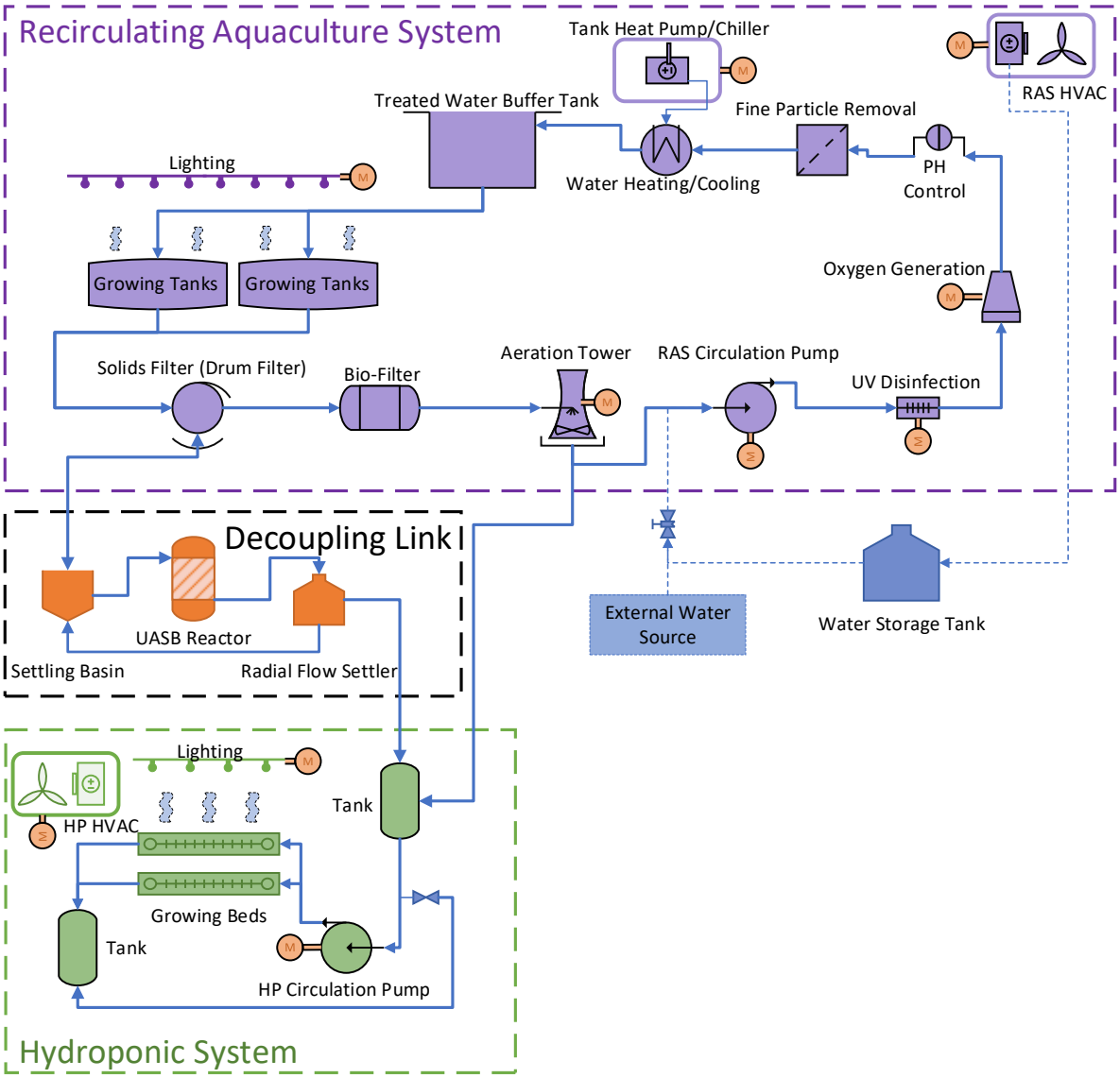

Figure 3.1: *Decoupled aquaponic system schematic. System components and flow are illustrated.*

The interactions of the various system components are illustrated in arrow diagram format (Figure 3.2). The aquaculture facility is decoupled from the hydroponic greenhouse. This is achieved by means of the decoupling link that maintains the mineral and nutrient levels for the respective systems without favouring a single system. This will achieve optimal levels for both systems and will ensure maximal yields. Each component is discussed in the following sections. Ultimately the aquaculture system will provide the necessary nutrients to the growing beds and the excess amount of biowaste will be treated or repurposed. The hydroponic system will assist in stripping the recirculated water from nutrients that could become toxic to the fish. The nutrient balance will be corrected and maintained by the decoupler, thus providing optimal conditions for both crops and fish.

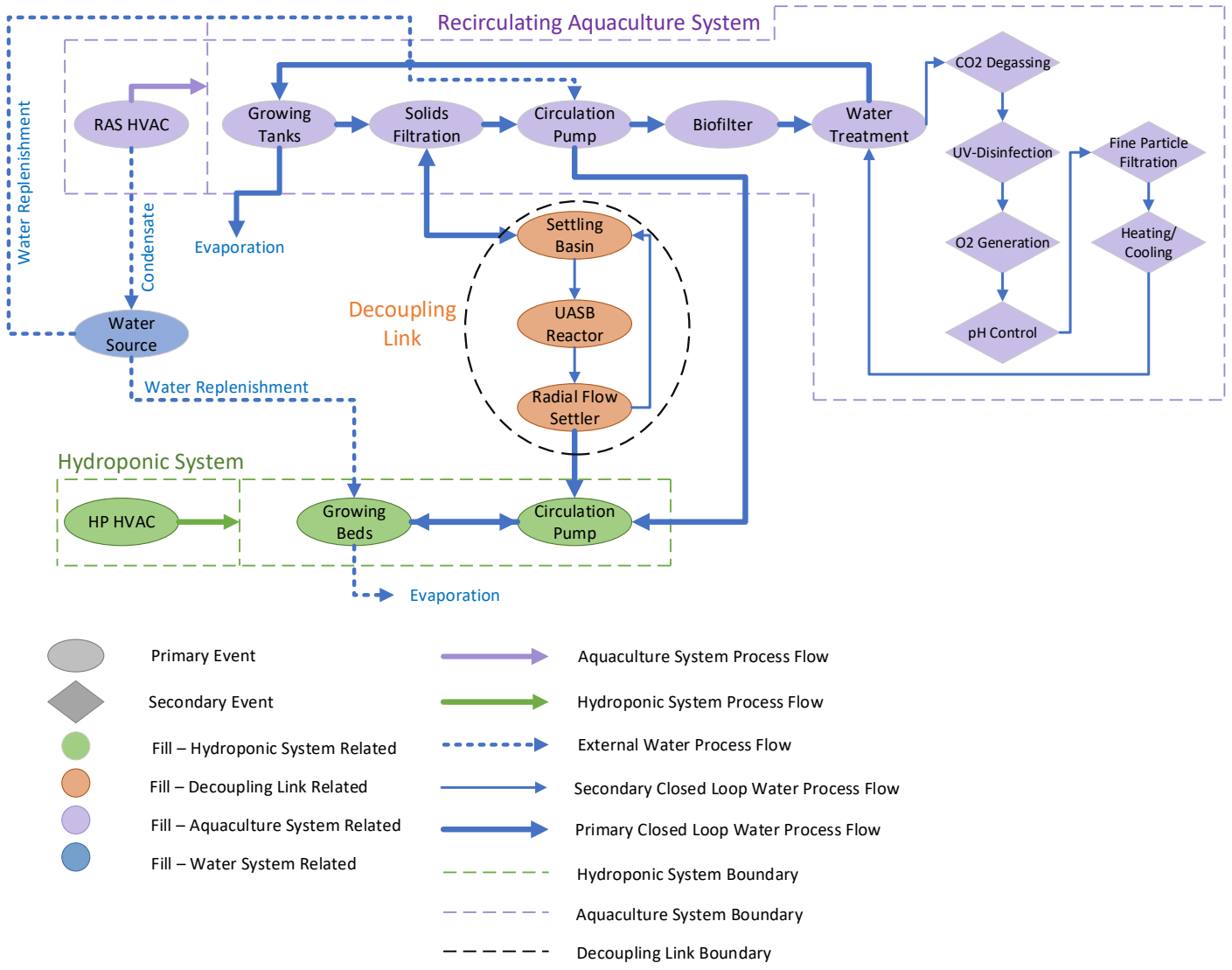

Figure 3.2: *Arrow diagram illustrating the decoupled systems.*

3.2.1 Recirculating Aquaculture System Energy Loop

Each component in the aquaculture facility (Figure 3.1) is required to maintain a favourable environment and quality of water to ensure optimal fish production. The aquaculture facility consists of the following components.

- RAS facility structure
- Growing tanks
- Solid's filtration
- Biofilter (which is supplemented by the Hydroponic System)
- Aeration towers
- Circulation pump
- UV Disinfection
- Oxygen generation cones
- pH Control
- Fine particle removal
- Water heating and cooling
- Treated water buffer tank
- RAS facility lighting
- Environmental control system (HVAC system)

Each component serves a certain purpose to ensure a successful system and to minimise fish mortality that will ensure maximum profit. The specific purpose of each component was not discussed in this research since this is not the primary focus. It was more important to identify which of these components required energy input and how the system was affected by surrounding climatic factors.

Each component in Figure 3.1 was identified and discussed with regard to energy usage. The equations derived to describe the system mathematically and that served as input to the system dynamics model were presented. The differential equations that are based on the derived equations were presented in the following sections. The following components contribute to the stock variables of "Total system energy usage" measured in Watts.

Lighting in the Aquaculture Facility

Lighting is required to extend the duration of time at which fish could feed and be active. This increases the feed rate and by extension, the growth rate. This ensures a swift harvest cycle. Lighting requires energy and emits heat to the environment.

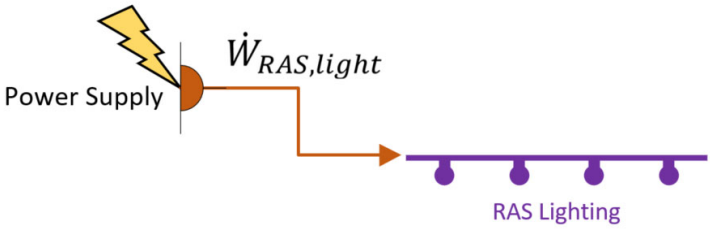

Figure 3.3: *Power supply required to provide energy to the lighting of the RAS facility.*

The power drawn by the lighting in the facility (Eq. (1)) is the area of the facility times the light power wattage per square meter, where D_v is defined as 1 or 0 depending on the daily lighting schedule. It was assumed that lighting was present in the system for 18 hours a day (Veras et al., 2013). Lighting can be supplied for 24 hours a day which will optimise fish activity and therefore fish growth and yield. The time is reduced to 18 hours in order to conserve the energy required for the lighting whilst still maximising the lighting stimuli to the fish.

$$\dot{W}_{RAS,light} = D_v A_{f\ RAS} P_{RAS,light} \tag{1}$$

Aeration Towers

Aeration towers are used to strip the water of the CO_2 that is produced by the biomass in the system. Energy is used by the fans to force air over the water so that the CO_2 can diffuse out of the water into the air stream (Figure 3.4).

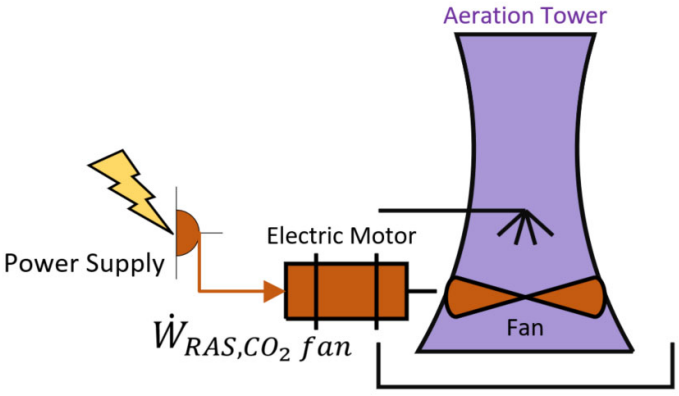

Figure 3.4: *Power supply required to provide energy to the fans for Carbon Dioxide stripping*

The energy consumed by the fans was determined using Eq. (2):

$$\dot{W}_{RAS,CO_2\ fan} = \frac{\dot{V}_{RAS,CO_2}\ \Delta P_{RAS,CO_2\ fan}}{\eta_{RAS,CO_2\ fan}} \tag{2}$$

where the flow rate of the fan was determined using the model discussed by Davison (2018) as presented in Eq. (3):

$$\dot{V}_{RAS,CO_2} = \frac{10 D_{O_2}}{d\ HRT\ FR_d\ O_2C\ O_2C} \tag{3}$$

Aquaculture Facility Circulation Pumps

Circulation pumps (Figure 3.5) are important since they maintain the water quality in the system. The pumps drive the water through the entire system and ensure that system pressure is maintained. Multiple pumps can be configured in parallel in order to maintain a certain system pressure.

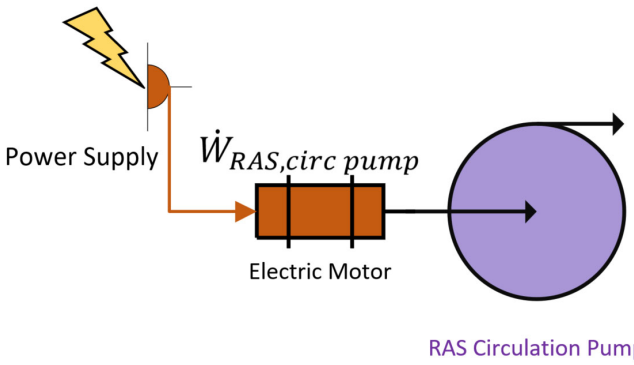

Figure 3.5: *Power supply required to provide energy to the circulation pumps of the RAS facility.*

It was assumed that the pumps are fitted with variable speed drives to ramp up and down during the life cycle of the fish. The smaller the biomass the less flow is required and therefore energy can be saved. The energy usage of the pump was determined using Eq. (4):

$$\dot{W}_{RAS,circ\ pump} = \frac{\rho_{water} g \dot{V}_{RAS,circ} H_{RAS,circ\ pump}}{\eta_{RAS,cp}} \tag{4}$$

The parameters in Eq. (4) are defined as follows. The volumetric flow rate of the system, $\dot{V}_{RAS,circ}$, was determined using Eq. (5):

$$\dot{V}_{RAS,circ} = \frac{Vol_{RAS}}{HRT} \tag{5}$$

where the hydraulic retention time, HRT is a constant and the system volume, Vol_{RAS}, was determined using Eq. (6):

$$Vol_{RAS} = \frac{m_{bio}}{d} \tag{6}$$

The stocking density, d was kept as high as possible in order to keep the fish growth rate as high as possible without causing an increase in mortality rate. The system biomass, m_{bio}, was determined using Eq. (7):

$$m_{bio} = \frac{Feed_d}{FR_d} \tag{7}$$

The daily feed required, $Feed_d$, is the daily produced fish mass multiplied by the feed conversion rate (Eq. (8)):

$$Feed_d = Prod_d \times FCR \tag{8}$$

The daily feed rate, FR_d, was determined as the multiplication of the fish growth rate, r, and the feed conversion rate, FCR (Eq. (9)):

$$FR_d = rFCR \tag{9}$$

The fish growth rates and feed conversion rates are highly dependent on the water temperature. The two parameters are also dependent on the growth stage. A piecewise function was constructed which was used to determine r and FCR for a given time during the growth cycle of the fish. Table 3.1 includes the information used to construct the piecewise function (El-Sayed, 2013).

Table 3.1: *Fish weight, growth rate and feed conversion rate parameters for the different growth stages*

Day	Stage	r	Ideal Weight	FCR
1-15	Fry	8%	6	1.8
16-31	Fry	7%	25	1.8
32-46	Mid-Start	6%	36	1.5
47-61	Mid	5%	50	1.5
62-76	Mid	4%	72	1.5
77-91	Mid	3%	100	1.5
92-105	End	3%	121	1.2
106-120	End	2%	150	1.2

The piece-wise function was used by the model to substitute the correct parameter value at the various growth stages. The weight of the fish was determined by Eq. (10):

$$K_n = K_o(1 + r)^n \tag{10}$$

The fish weight determined the end of the growth cycle and when the population can be harvested and be replaced by new fingerlings.

Eq. (4), which describes the RAS circulation pump energy consumption, is dependent on a single input, namely the annual production goal, G_f. The daily production required to reach the annual goal is given by Eq. (11):

$$Prod_d = \frac{G_f}{365} \tag{11}$$

The annual production goal determined the size of the operation, including the facility area required and the energy required to maintain favourable conditions.

Ultra-Violet Disinfection

Ultra-Violet (UV) lighting, Figure 3.6, is required to remove possible harmful pathogens that can have a disastrous mortality effect on an operation.

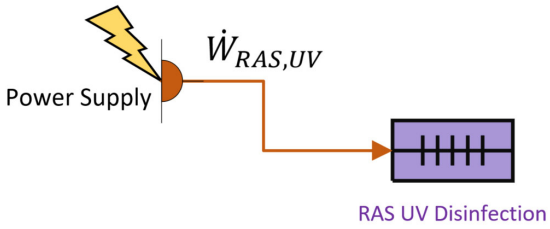

Figure 3.6: *Power supply required to provide energy to the UV disinfection lighting of the RAS facility.*

The power drawn by the UV lighting in the facility is the area of the facility times the UV light power rating per square meter. The energy was required 24 hours a day since the operation is continuous. The energy was given by Eq. (12):

$$\dot{W}_{RAS,UV} = A_{f\ RAS} P_{RAS,UV} \tag{12}$$

Oxygen Generation

Sufficient dissolved oxygen is required in the water to ensure optimal conditions for fish growth and to limit mortality. Oxygen is introduced via an oxygen cone (Figure 3.7) that diffuses high pressure oxygen into the water.

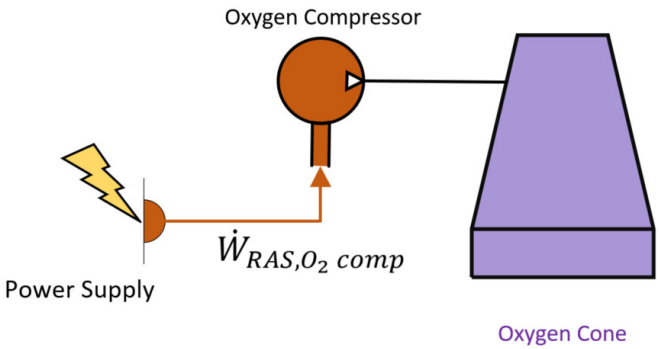

Figure 3.7: *Power supply required to provide energy to the Oxygen compressor of the RAS facility.*

A compressor is required which will keep the oxygen at a pressure to ensure that it is introduced into the water stream. The energy required by the compressor was determined using Eq. (13):

$$\dot{W}_{RAS,O_2\ comp} = \frac{\dot{V}_{RAS,O_2} H_{RAS,O_2\ comp}}{\eta_{RAS,O_2\ comp}} \tag{13}$$

The volumetric flow rate, $\dot{V}_{RAS,O_2}$ was determined by the daily oxygen consumption of the biomass, D_{O_2} shown in Eq. (14).

$$\dot{V}_{RAS,O_2} = \frac{D_{O_2}}{86400\rho_{O_2}} \tag{14}$$

D_{O_2} was determined using Eq. (15):

$$D_{O_2} = Feed_d \times O_2C \tag{15}$$

The system pressure head which the compressor needs to overcome, was described by Eq. (16):

$$H_{RAS,O_2\ comp} = \frac{Z_c R_{O_2} T_{O_2,1}}{(k-1)/k}\left[\left(\frac{P_{O_2,2}}{P_{O_2,1}}\right)^{k-1/k} - 1\right] \tag{16}$$

The internal temperature of the facility was controlled and kept at a fixed temperature throughout the operation. Therefore, the pressure head in the compressor system, $H_{RAS,O_2\ comp}$, remained constant throughout the operation.

Environmental Control in the Aquaculture Facility

To ensure optimal conditions for fish, their environment needs to be controlled and regulated. Optimal conditions will ensure that fish experience the least amount of stress, which will ensure better growth and product quality. This is very desirable from a commercial point of view.

Creating and maintaining such an environment can be an energy intensive endeavour and it is important to be as efficient as possible. If the system is not closely monitored with regard to energy usage, the running cost could outweigh the profitability of an operation.

Heating, ventilation and air conditioning (HVAC) systems are designed to create optimal environmental conditions by controlling and regulating factors such as temperature, humidity, CO_2 levels and fresh air specified by law. External climatic factors heavily influence the design, operation and efficiency of HVAC systems. Operating a RAS system in a certain climate may prove to be more or less efficient, based on its location. Hot humid climates tend to have a smaller variation in conditions such as temperature and humidity throughout the year compared to arid and semi-arid regions. This will cause the HVAC system to be more efficient in hot humid regions since the gradients between high and low temperatures are smaller compared to regions where summer and winter experience large temperature variations.

In order to size equipment, which was identified to be power consumers, the energy and mass flow of the system had to be analysed by considering the system as a controlled volume and by applying a mass and energy balance. A system diagram indicating the different modes of heat transfer experienced in a typical system is illustrated in Figure 3.8. An energy balance model was applied in order to determine the amount of heat required to heat or cool the RAS facility and to maintain it at a defined optimal condition.

For purposes of this research, an optimal internal temperature was maintained within the RAS facility and is denoted by $T_{RAS,i}$ with a value of 26 ℃. This temperature was selected since it remained close to the optimal water temperature of $28\ °C$. This meant energy loss from the tank water to the environment was limited. The temperature ensured that reasonable thermal comfort for the workers and occupants was maintained. The optimal water temperature of $28\ °C$ was based on the work of El-Sayed and Kawanna (2008) who observed that the Nile Tilapia growth rate is most optimal at this water temperature. Equations presented in the following section were based on the theory described by Cengel and Ghajar (2014).

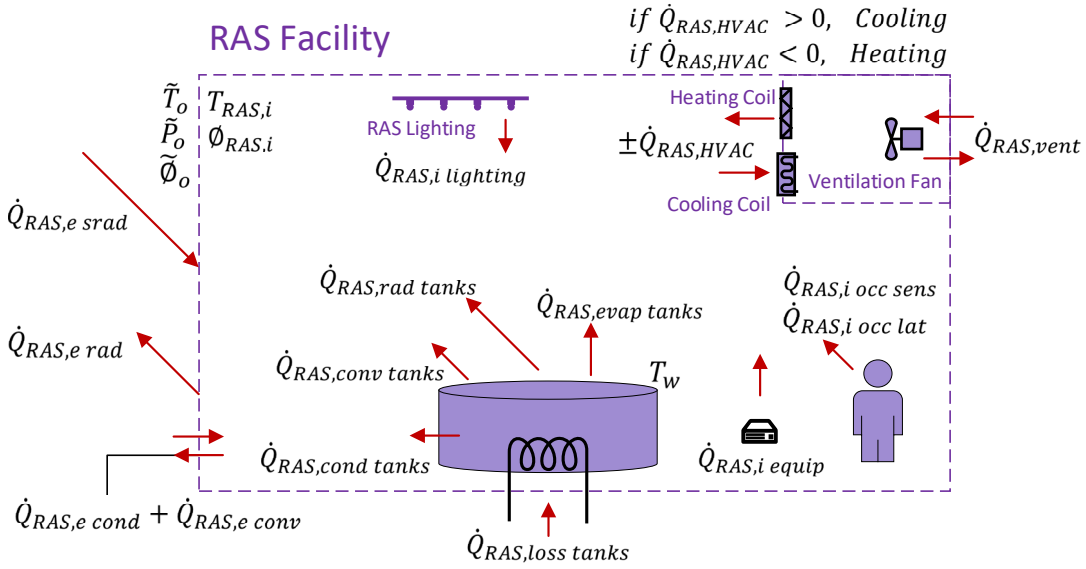

Figure 3.8: *Heat transfer modes that occur in the RAS facility*

The inside and outside condition parameters were defined as:

$T_{RAS,i}$ - Internal regulated temperature inside the RAS facility.

$\emptyset_{RAS,i}$ - Internal relative humidity inside the RAS facility, which was not actively controlled.

$\tilde{P}_o$ - External, location specific, hourly air pressure.

$\tilde{T}_o$ - External, location specific, hourly air temperature.

$\tilde{\emptyset}_o$ - External, location specific, hourly relative humidity.

The "~" sign indicates that the parameter was a time varying data input and was based on physical measurements, which were captured in a weather file for that location.

By applying an energy balance model, and considering the 1st law of thermodynamics, the system yielded the following heat balance equations (Eq. (19)):

$$\sum \dot{Q}_{RAS,tot} = 0$$

$$\dot{Q}_{RAS,loss\ tanks} + \dot{Q}_{RAS,internal} \pm \dot{Q}_{RAS,external} \pm \dot{Q}_{RAS,vent} \pm \dot{Q}_{RAS,HVAC} = 0$$

$$\pm\dot{Q}_{RAS,HVAC} = \dot{Q}_{RAS,loss\ tanks} + \dot{Q}_{RAS,internal} \pm \dot{Q}_{RAS,external} \pm \dot{Q}_{RAS,vent} \qquad (19)$$

$$if\ \dot{Q}_{RAS,HVAC} > 0,\ \ The\ system\ requires\ cooling\ and$$
$$if\ \dot{Q}_{RAS,HVAC} < 0,\ \ The\ system\ requires\ heating$$

$\dot{Q}_{RAS,HVAC}$ was the term that determined the size of the HVAC equipment. It also determined the energy required to power the equipment. If $\dot{Q}_{RAS,HVAC}$ was greater than zero, there was excess heat in the system and cooling was required in order to remove the heat. If $\dot{Q}_{RAS,HVAC}$ was less than zero, heat was required in the system in order to maintain equilibrium. If $\dot{Q}_{RAS,HVAC}$ was zero, there was thermal equilibrium, and no heat was required to be added or removed.

Each term in Eq. (19) was further defined in order to illustrate how the heat flow in the system was influenced by external climate conditions.

Heat Loss by Growing Tanks

Since the water temperature was always kept at a higher temperature than the internal environment, heat will flow from the tanks to the RAS facility. The heat loss was determined by using Eq. (20):

$$\dot{Q}_{RAS,loss\ tanks} = \dot{Q}_{RAS,cond\ tanks} + \dot{Q}_{RAS,conv\ tanks} + \dot{Q}_{RAS,rad\ tanks} + \dot{Q}_{RAS,evap\ tanks} \quad (20)$$

Heat flows from the tanks to the environment by means of conduction, convection, long wave radiation and water evaporation. Each term in Eq. (20) is defined by Eq. (21), Eq. (23) and Eq. (24) respectively.

The combined heat loss due to conduction and convection was defined by Eq. (21):

$$\dot{Q}_{RAS,cond\ tanks} + \dot{Q}_{RAS,conv\ tanks} = U_{RAS,tanks} A_{s\ tanks}[T_w - T_{RAS,i}] \quad (21)$$

These terms were combined by means of the combined heat transfer coefficient $U_{RAS,tanks}$. The coefficient was determined by using the thermal resistive properties of the material of the tanks as shown in Eq. (22):

$$U_{RAS,tanks} = \frac{1}{R_{tot}} = \frac{1}{R_{cond}} + \frac{1}{R_{conv}} \quad (22)$$

Heat loss due to thermal radiation between the tank surface to the environment was defined by Eq. (23):

$$\dot{Q}_{RAS,rad\ tanks} = \sigma \varepsilon_{tank} A_{s\ tanks}[T^4_{s\ tank} - T^4_{\infty}] \quad (23)$$

The heat loss due to water evaporation is a complex process involving a variety of variables. The complexity was incorporated for purposes of this research since relative humidity inside

the RAS facility and the water evaporation rates played important roles in the stock and flow of the systems. Heat loss due to evaporation was defined by Eq. (24):

$$\dot{Q}_{RAS,evap\ tanks} = \dot{m}_w h_{fg} \tag{24}$$

$\dot{Q}_{RAS,evap\ tanks}$ is a latent heat component since it involves the phase change of water. h_{fg} is the heat of vaporisation of water and $\dot{m}_w$ is the water evaporation rate. The water evaporation rate, Eq. (25), was determined by applying the mass flow analogy of convective heat transfer described by Cengel and Ghajar (2014).

$$\dot{m}_w = h_{mass} A_{s\ water} \left(\rho_{v,w} - \rho_{v,\infty}\right) \tag{25}$$

$A_{s\ water}$ is the water surface area determined by the annual production goal. h_{mass} was the mass transfer coefficient and $\rho_{v,w}$, $\rho_{v,\infty}$ were the density of air water vapour mixture at the tank water surface and in the surrounding environment respectively. Given the lengthy calculation to determine the mass transfer coefficient and the density of water vapour at the respective locations, only the expressions and calculation procedure are shown. Detailed descriptions of each term are stated in the table of nomenclature.

The mass transfer coefficient was calculated using Eq. (26):

$$h_{mass} = \frac{Sh D_{H_2O-air}}{L_c} \tag{26}$$

The Sherwood number, mass diffusivity of water vapour in air, and critical length were defined using Eq. (27), Eq. (30) and Eq. (33) respectively:

$$Sh = 0.15(GrSc)^{\frac{1}{3}} \tag{27}$$

With the Grashof number, Eq. (28) and Schmidt number, Eq. (29) is defined as:

$$Gr = \frac{g(\rho_\infty - \rho_w)L_c^3}{\rho_{ave}\nu_{air}^2} \tag{28}$$

$$Sc = \frac{\nu_{air}}{D_{H_2O-air}} \tag{29}$$

and ν_{air} is the kinematic viscosity of air.

$$D_{H_2O-air} = 1.87 \times 10^{-10} \frac{T_{ave}^{2.072}}{P_{RAS,tot}} \tag{30}$$

with

$$P_{RAS,tot} = \frac{\tilde{P}_o}{P_{atm}} \tag{31}$$

and

$$T_{ave} = \frac{T_w - T_{RAS,i}}{2} \tag{32}$$

$$L_c = \frac{A_{s\,water}}{p} \tag{33}$$

The density terms in the Grashof number Eq. (28) were defined by the following set of equations. Firstly, the average air-water vapour density:

$$\rho_{ave} = \frac{(\rho_\infty + \rho_w)}{2} \tag{34}$$

The density of water vapour mixture in the RAS facility, ρ_∞ was determined using Eq. (35):

$$\rho_\infty = \rho_{v,\infty} + \rho_{a,\infty} \tag{35}$$

The density of water vapour away from the water surface, $\rho_{v,\infty}$ was determined using Eq. (36):

$$\rho_{v,\infty} = \frac{P_{v,\infty}}{R_v T_\infty} \tag{36}$$

Where $T_\infty = T_{RAS,i}$, R_v was the gas constant of water vapour and the vapour saturation pressure away from the water surface, $P_{v,\infty}$ was determined with Eq. (37):

$$P_{v,\infty} = \emptyset_{RAS} P_{sat\,@\,T_\infty} \tag{37}$$

$\emptyset_{RAS}$ is a stock variable and $P_{sat\,@\,T_\infty}$ is a tabulated thermodynamic property of water vapour mixture at T_∞.

The density of dry air away from the water surface, $\rho_{a,\infty}$ was determined with Eq. (38):

$$\rho_{a,\infty} = \frac{(\tilde{P}_o - P_{v,\infty})}{R_{air} T_\infty} \tag{38}$$

$\tilde{P}_o$ is the location specific air pressure, R_{air} is the gas constant of air and $P_{v,\infty}$ is calculated as defined by Eq. (37).

The density of water vapour mixture at the water surface ρ_w, was calculated using Eq. (39):

$$\rho_w = \rho_{v,w} + \rho_{a,w} \tag{39}$$

The density of water vapour at the water surface $\rho_{v,w}$, was determined with Eq. (40):

$$\rho_{v,w} = \frac{P_{v,w}}{R_v T_w} \tag{40}$$

With the vapour saturation pressure at water surface defined using Eq. (41):

$$P_{v,w} = P_{sat\ @\ T_\infty} \tag{41}$$

And R_v is the gas constant of saturated water vapour.

The density of dry air away from the water surface $\rho_{a,w}$, was defined using Eq. (42):

$$\rho_{a,w} = \frac{(\tilde{P}_o - P_{v,w})}{R_{air} T_w} \tag{42}$$

With h_{mass}, $\rho_{v,w}$ and $\rho_{v,\infty}$ calculated, the mass flow rate of water evaporation, $\dot{m}_w$ could be calculated. This value played a role in determining the water usage of the system as explained in the upcoming sections.

Internal System Heat Gains

Certain components within the RAS facility caused internal heat gains. Activities such as the usage of equipment, lighting and physical work by occupants generate heat. The $\dot{Q}_{RAS,internal}$ component of Eq. (20) consists of the following heat flux components:

$$\dot{Q}_{RAS,internal} = \dot{Q}_{RAS,i\ lighting} + \dot{Q}_{RAS,i\ equip} + \dot{Q}_{RAS,i\ occ\ sens} + \dot{Q}_{RAS,i\ occ\ lat} \tag{43}$$

The sensible heat generated by the lighting was the light power rating per unit area multiplied by the RAS floor area. The lighting heat flux (Eq. (44)) was subjected to a lighting schedule.

$$\dot{Q}_{RAS,i\ lighting} = \dot{W}_{RAS,light} D_v A_{fRAS} \tag{44}$$

The general equipment contributes to a generation of sensible heat (Eq. (45)) and can be expressed as a constant value since the RAS facility was assumed to run 24 hours a day.

$$\dot{Q}_{RAS,i\ equip} = Constant \tag{45}$$

Human activity in the form of physical work generated sensible (Eq. (46)) and latent heat (Eq. (47)). The ASHRAE (2013) provides typical heat values for the occupants of a space based on the level of activity. For this research, moderate work activity was assumed.

The heat generated by the occupants was expressed as:

$$\dot{Q}_{RAS,i\ occ\ sens} = N_{Occ} \times Q_{sens} \tag{46}$$

$$\dot{Q}_{RAS,i\ occ\ lat} = N_{Occ} \times Q_{lat} \tag{47}$$

N_{Occ} is the number of occupants. Q_{sens} and Q_{lat} are the sensible and latent heat components generated by a single occupant.

External System Heat Flux

The external source of heat flux (Eq. (48)) is an important component of the system dynamics model. This component was driven by the variation of external climatic conditions, namely incoming solar radiation and external air temperature. The temperature gradients between the inside and outside of the facility ultimately determined whether the system required cooling or heating. The external heat flux component, $\dot{Q}_{RAS,external}$, in Eq. (20) consisted of the following modes of heat transfer and are defined in Eq. (48), Eq. (49), Eq. (50) and Eq. (51) respectively.

$$\dot{Q}_{RAS,external} = \dot{Q}_{RAS,e\ cond} + \dot{Q}_{RAS,e\ conv} + \dot{Q}_{RAS,e\ rad} + \dot{Q}_{RAS,e\ srad} \tag{48}$$

The thermal heat transfer due to conduction and convection was expressed using Eq. (49):

$$\dot{Q}_{RAS,e\ cond} + \dot{Q}_{RAS,e\ conv} = U_{RAS} A_{s\ RAS} \left[T_{RAS,i} - \tilde{T}_o\right] \tag{49}$$

The terms were combined given the overall heat transfer coefficient, which was determined by using the resistive material properties of the RAS facility shown in Eq. (50):

$$U_{RAS} = \frac{1}{R_{tot}} = \frac{1}{R_{cond}} + \frac{1}{R_{conv}} \tag{50}$$

The thermal radiation emitted to the atmosphere was described by Eq. (51):

$$\dot{Q}_{RAS,e\ rad} = \sigma \varepsilon_{RAS} A_{s\ RAS} \left[T^4_{s\ RAS} - T^4_{sky}\right] \tag{51}$$

Finally, the instantaneous thermal radiation absorbed by the RAS facility (Eq. (52)) was determined using the hourly incoming solar radiation measured and captured in the location specific weather file:

$$\dot{Q}_{RAS,e\ srad} = \alpha_{RAS} A_{s\ RAS} \tilde{I}_{sr} \tag{52}$$

To minimise the external heat gain into the facility the effects of fenestration was omitted by assuming that the facility does not contain any windows. In reality, materials will absorb heat over time and gradually release the heat into the environment. The peak heat flux experienced will not occur when the incoming radiation is at its highest but rather at a delayed period in

time when the surroundings have reached a point where more heat is lost than gained. In order to simplify the model, this effect was not considered, and the net heat flux of the system was assumed to be an instantaneous term rather than a secondary time influenced parameter.

Ventilation Heat Flux

Outside air was introduced into the system by means of ventilation. Ventilation was required to maintain low levels of carbon dioxide and to ensure adequate fresh air for the occupants. It is common for ventilation to be a requirement set forth by national and international codes and standards. Compliance with these standards is often a legal requirement to ensure the health and safety of the occupants.

A portion of conditioned air was recirculated and mixed with outside air. The outside air quantity was determined by the operation in the facility. It was expressed as the volume of air required to be replaced each hour. This quantity was defined as air changes per hour and is denoted by AC. The mass flow rate of the outside air was determined using Eq. (53):

$$\dot{m}_{OA} = \frac{\rho_{air} Vol_{RAS} AC}{3600} \tag{53}$$

The outside air was introduced into the system at external conditions that may be above or below the desired set point within the system. The air may require conditioning (heating, cooling, humidification, or dehumidification) in order to match internal conditions. This heat was the final term as described in Eq. (20). Since there is moisture in the external air the cooling process contains a latent and sensible heat component. If the air requires heating, this is a purely sensible process. The total heat flux of the ventilation air was given by Eq. (54):

$$\dot{Q}_{RAS,vent} = \dot{Q}_{RAS,v\ sens} + \dot{Q}_{RAS,v\ lat} \tag{54}$$

The total ventilation heat flux can also be determined by using the psychrometric chart. The difference in the enthalpy between the outside conditions and the off-coil conditions of the HVAC system will yield the total heat for ventilation (Eq. (55)):

$$\dot{Q}_{RAS,vent} = \dot{m}_{OA}\left(\tilde{h}_1 - h_3\right) \tag{55}$$

Off-coil conditions are fixed during the operation of the system and were based on common engineering practices. The sensible ventilation heat component $\dot{Q}_{RAS,v\ sens}$ was determined by Eq. (56).

$$\dot{Q}_{RAS,v\ sens} = \dot{m}_{OA} C_{p,air}[\tilde{T}_o - T_3] \tag{56}$$

Resulting in the latent component to be determined using Eq. (57):

$$\dot{Q}_{RAS,v\ lat} = \dot{Q}_{RAS,vent} - \dot{Q}_{RAS,v\ sens} \tag{57}$$

The latent and sensible loads were also used in the following section.

Energy Consuming Components for Aquaculture Facility Environmental Control

The HVAC system had three major components that required energy to maintain a constant environment (Figure 3.9). These components included:

- Chillers and or heat pumps for cooling and heating the system.
- Pumps for circulating the hot and cold water to the conditioning coils.
- Fans that will introduce the conditioned air into the system.

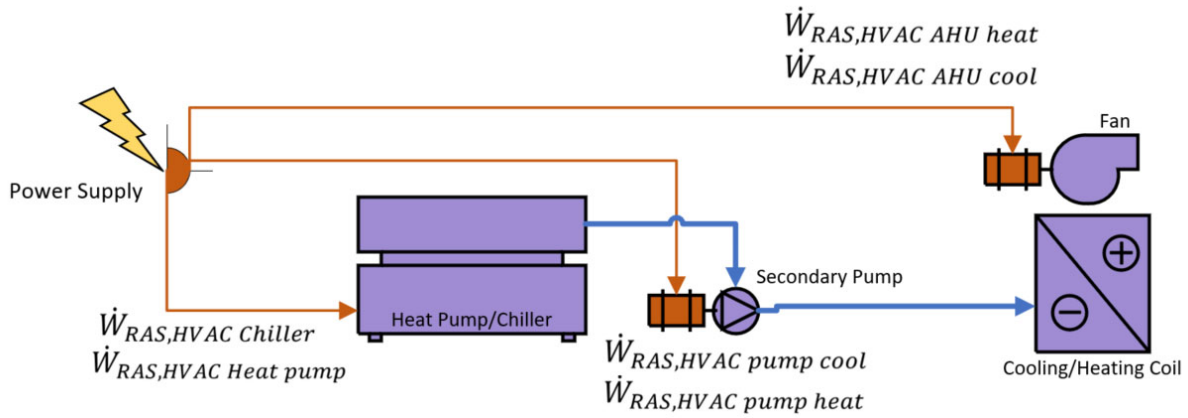

Figure 3.9: *Power supply required to provide energy to the HVAC components of the RAS facility.*

The work required by each component was determined by the energy balance in Eq. (19). The components were discussed by considering two possible cases, cooling mode and heating mode.

Aquaculture Facility in Cooling Mode

The system was in cooling mode if $\dot{Q}_{RAS,HVAC}$ was greater than zero. The work or energy required by the chiller, Eq. (58), to remove heat from the system is the amount of HVAC heat divided by the coefficient of performance (COP) of the chiller:

$$\dot{W}_{RAS,HVAC\ Chiller} = \frac{\dot{Q}_{RAS,HVAC}}{COP_{RAS,chiller}} \tag{58}$$

The pump, which circulates the cold water to the cooling coils, consumed energy based on Eq. (59):

$$\dot{W}_{RAS,HVAC\ pump\ cool} = \frac{\rho_{water} g \dot{V}_{RAS,HVAC\ pump\ cool} H_{RAS,HVAC\ pump\ cool}}{\eta_{RAS,HVAC\ cool\ p}} \tag{59}$$

Where ρ_{water}, g, $H_{RAS,HVAC\ pump\ cool}$ and the pump efficiency $\eta_{RAS,HVAC\ cool\ p}$ were constant defined parameters. The volumetric flow rate of the cooling water (Eq. (61)) was determined by calculating the mass flow rate (Eq. (60)) required to achieve a temperature gradient of $\Delta T_{cool} = 6℃$:

$$\dot{m}_{HVAC\ pump\ cool} = \frac{\dot{Q}_{RAS,HVAC}}{C_{p,water} \Delta T_{cool}} \tag{60}$$

and:

$$\dot{V}_{RAS,HVAC\ pump\ cool} = \frac{\dot{m}_{HVAC\ pump\ cool}}{\rho_{water}} \tag{61}$$

The last component was the energy required by the fan to achieve the desired heat transfer (Eq. (64)). An air handling unit (AHU) contains the cooling and heating coils together with a fan. The unit forces air through the coils for heat transfer to take place. The mass flow rate of the fan (Eq. (62)) was determined by using the room sensible heat. The latent heat component of the system was absorbed by the coil.

$$\dot{m}_{SA} = \frac{\dot{Q}_{RAS,room\ sens}}{C_{p,air}\left[T_{RAS,i} - T_3\right]} \tag{62}$$

Eq. (62) is the mass flow rate required to remove heat in order to achieve a temperature difference from the off-coil temperature, T_3, to the set point, $T_{RAS,i}$.

$\dot{Q}_{RAS,room\ sens}$ was the sum of the sensible heat flux components in the system as shown in Eq. (63):

$$\begin{aligned} \dot{Q}_{RAS,room\ sens} = {} & \dot{Q}_{RAS,cond\ tanks} + \dot{Q}_{RAS,conv\ tanks} + \dot{Q}_{RAS,rad\ tanks} + \dot{Q}_{RAS,i\ lighting} \\ & + \dot{Q}_{RAS,i\ equip} + \dot{Q}_{RAS,i\ occ\ sens} + \dot{Q}_{RAS,e\ cond} + \dot{Q}_{RAS,e\ conv} \\ & + \dot{Q}_{RAS,e\ rad} + \dot{Q}_{RAS,e\ srad} \end{aligned} \tag{63}$$

Therefore, the work or energy required by the AHU fans was determined using Eq. (64):

$$\dot{W}_{RAS,HVAC\ AHU\ cool} = \frac{\dot{V}_{RAS,HVAC\ AHU\ cool} \Delta P_{RAS,AHU\ Cool}}{\eta_{RAS,AHU\ cool\ fan}} \tag{64}$$

where

$$\dot{V}_{RAS,HVAC\ AHU\ cool} = \frac{\dot{m}_{SA}}{\rho_{air}} \tag{65}$$

$\Delta P_{RAS,AHU\ Cool}$ and $\eta_{RAS,AHU\ cool\ fan}$ were constant parameters based on the system configuration.

Aquaculture Facility in Heating Mode

The system was in heating mode if $\dot{Q}_{RAS,HVAC}$ was less than zero. Similar to Eq. (58), the work required by the heat pump, Eq. (66) is the amount of heat required by the system to reach set point divided by the COP of the heat pump.

$$\dot{W}_{RAS,HVAC\ Heat\ pump} = \frac{\dot{Q}_{RAS,HVAC}}{COP_{RAS,heatpump}} \tag{66}$$

The pump consumed energy based on Eq. (67):

$$\dot{W}_{RAS,HVAC\ pump\ heat} = \frac{\rho_{water} g \dot{V}_{RAS,HVAC\ pump\ heat} H_{RAS,HVAC\ pump\ heat}}{\eta_{RAS,HVAC\ heat\ p}} \tag{67}$$

where

$$\dot{V}_{RAS,HVAC\ pump\ heat} = \frac{\dot{m}_{HVAC\ pump\ heat}}{\rho_{water}} \tag{68}$$

and

$$\dot{m}_{HVAC\ pump\ heat} = \frac{\dot{Q}_{RAS,HVAC}}{C_{p,water} \Delta T_{heat}} \tag{69}$$

The energy required by the heating fans was determined using Eq. (70):

$$\dot{W}_{RAS,HVAC\ AHU\ heat} = \frac{\dot{V}_{RAS,HVAC\ AHU\ heat} \Delta P_{RAS,AHU\ heat}}{\eta_{RAS,AHU\ heat\ fan}} \tag{70}$$

where

$$\dot{V}_{RAS,HVAC\ AHU\ heat} = \frac{\dot{m}_{SA}}{\rho_{air}} \tag{71}$$

$\dot{m}_{SA}$ was determined with Eq. (62)

3.2.2 Hydroponic Greenhouse Energy Loop

The hydroponic system was contained in a greenhouse. The greenhouse was subjected to environmental control to ensure favourable conditions were maintained throughout the year. Crops can be grown and harvested throughout the year in order to maximise yield. The hydroponic system consisted of the following components:

- Greenhouse structure.
- Growing beds (which serves as a biofilter for the RAS facility).
- Lighting.
- Circulation pump.
- HVAC system.
- Water tanks.

The remaining components in Figure 3.1 were related to the hydroponic subsystem. All energy consuming components were identified and discussed.

Lighting in the Hydroponic Greenhouse

The hydroponic greenhouse was fitted with lighting (Figure 3.10). Lighting extended the period at which plants can go through growth cycles and biochemical processes. Lighting required energy and released heat into the surroundings.

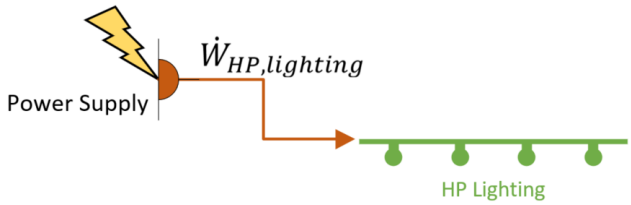

Figure 3.10: *Power supply required to provide energy to the lighting of the HP greenhouse.*

Equivalent to Eq. (1), the power required by the lighting was determined by Eq. (72):

$$\dot{W}_{HP,lighting} = D_v P_{HP,light} A_{fHP} \tag{72}$$

The power consumed is the lighting power rating per square meter times the floor area of the greenhouse. The lighting was subjected to a lighting schedule and was controlled by the parameter D_v.

Hydroponic Greenhouse Circulation pumps

Under normal operation, the circulation pumps, Figure 3.11, ran continuously at a constant flow rate. Given the hourly water loss due to evapotranspiration processes the pump ramped up and down in order to maintain system pressure.

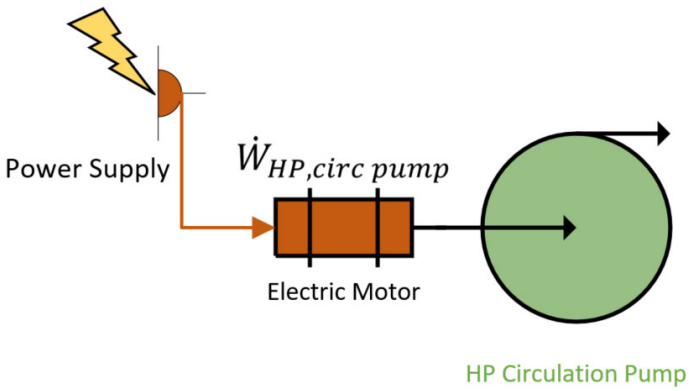

Figure 3.11: *Power supply required to provide energy to the circulation pumps of the HP greenhouse*

The power requirement of the pump was time dependent given the change in hourly evapotranspiration rates. The pump power was defined using Eq. (73):

$$\dot{W}_{HP,circ\ pump} = \frac{\rho_{water} g \dot{V}_{HP,circ} H_{HP,pump}}{\eta_{HP,p}} \tag{73}$$

Water density ρ_{water}, gravitational acceleration g, pump head $H_{HP,pump}$, and pump efficiency $\eta_{HP,p}$ are defined in Table 4.8. The volumetric flow rate was defined by Eq. (74):

$$\dot{V}_{HP,circ} = \frac{ET}{\rho_{water}} \tag{74}$$

The evapotranspiration rate ET, in kg/s, is a complex variable that is time and location dependent and was discussed in the upcoming sections.

Environmental Control in the Hydroponic Greenhouse

The remaining component that required energy was the environmental control of the greenhouse. An HVAC system is required to maintain favourable conditions for crop cultivation throughout the year. An approach and assumptions defined by Idso (1981), Kindelan (1980), and Walker (1965) and was followed in analysing the energy and mass balance within the greenhouse. Given the high latent heat component, caused by the crops, air-conditioning for purposes of cooling becomes impractical and expensive. Therefore, the greenhouse was cooled only by means of ventilation and not a cooling coil. Heating was

achieved by means of a heat pump, which produces hot water provided to radiators and a ducted AHU system.

The greenhouse was maintained at a set point of $26\ ℃ \pm 2\ ℃$ during the day and $20\ ℃ \pm 2\ ℃$ during the night. In order to size the equipment, an energy balance had to be applied to the system. The modes of heat transfer of the hydroponic system within the greenhouse are illustrated in Figure 3.12.

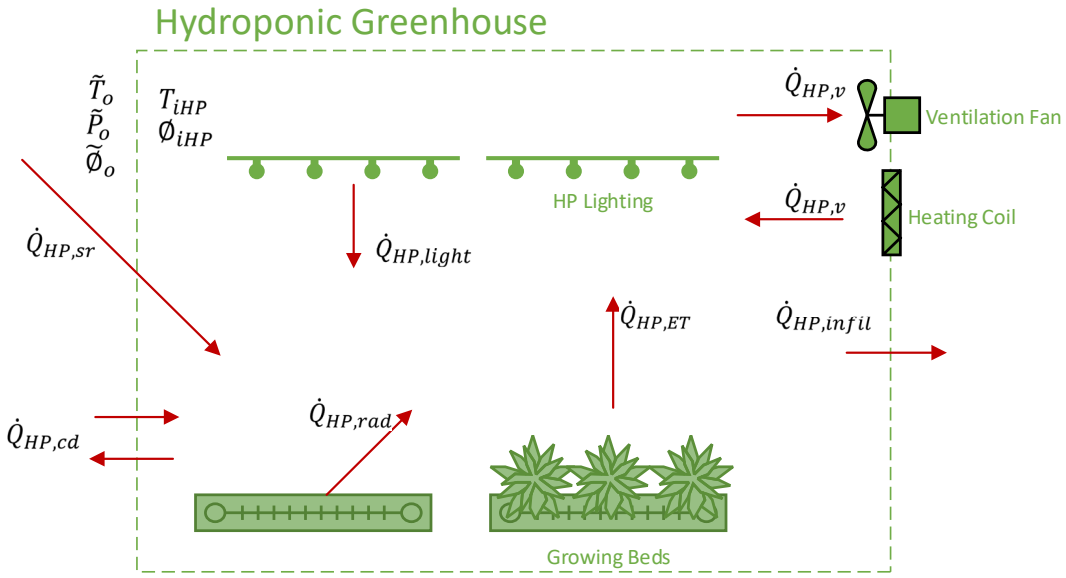

Figure 3.12: *Heat transfer modes that occur in the HP greenhouse*

The inside and outside condition parameters were defined as:

- T_{iHP} - Internal regulated temperature inside the hydroponic greenhouse.
- $\emptyset_{iHP}$ - Internal relative humidity inside the hydroponic greenhouse, which was not actively controlled.
- $\tilde{P}_o$ - External, location specific, hourly air pressure.
- $\tilde{T}_o$ - External, location specific, hourly air temperature.
- $\tilde{\emptyset}_o$ - External, location specific, hourly relative humidity.

Applying an energy balance to the controlled volume, and considering the 1st law of thermodynamics, the system yielded Eq. (75):

$$\sum \dot{Q}_{HP,tot} = 0$$

$$\dot{Q}_{HP,sr} - \dot{Q}_{HP,ET} \pm \dot{Q}_{HP,cd} \pm \dot{Q}_{HP,v} - \dot{Q}_{HP,rad} - \dot{Q}_{HP,infil} = 0$$

$$\pm\dot{Q}_{HP,v} = \dot{Q}_{HP,sr} - \dot{Q}_{HP,ET} \pm \dot{Q}_{HP,cd} - \dot{Q}_{HP,rad} - \dot{Q}_{HP,infil} \quad (75)$$

$\dot{Q}_{HP,v}$ is the term that determined whether heat was required or in surplus. If the term was positive, there was an excess amount of heat and cooling was required Eq. (76).

$$\dot{Q}_{HP,v} = \dot{Q}_{HP,cool}, \qquad if\ \dot{Q}_{HP,v} > 0, \tag{76}$$

If the term was negative, heat was required to satisfy the energy balance and achieve the set point as in Eq. (77):

$$\dot{Q}_{HP,v} = \dot{Q}_{HP,heat}\ , \qquad if\ \dot{Q}_{HP,v} < 0, \tag{77}$$

Each term in Eq. (75) was further defined to illustrate how the heat flow in the system was influenced by external climate conditions.

Incoming Solar Radiation Heat Flux in the Greenhouse

External heat was introduced into the greenhouse by solar radiation through the greenhouse material. The heat flux in the greenhouse caused by the solar radiation was given by Eq. (78):

$$\dot{Q}_{HP,sr} = \tau_c SC \tilde{I}_{sr} A_{fHP} \tag{78}$$

The hourly incoming solar radiation, $\tilde{I}_{sr}$, is a measured quantity contained in the location specific weather file and serves as a time variant input to the system dynamic model. The shading coefficient SC, and the transmissivity, τ_c were material specific parameters that were predefined and remained constant during the simulations. The floor area of the hydroponic system, A_{fHP} was determined by the yearly production goal (Eq. (11)).

Conductive and Convective Heat Flux in the Greenhouse

The incoming or outgoing heat flux due to conduction and convection was combined using the resistive properties of the greenhouse and by calculating the overall heat transfer coefficient, U_{HP}. The heat flux term was determined using Eq. (79):

$$\dot{Q}_{HP,cd} = U_{HP} A_{cHP} [T_{iHP} - \tilde{T}_o] \tag{79}$$

The external air temperature determined the magnitude of the conduction-convection heat flux. A positive temperature difference indicated that heat was flowing away from the greenhouse and a negative value indicated that heat was flowing into the greenhouse.

Radiative Heat Flux in the Greenhouse

Heat was transferred to the external environment by means of radiation, Eq. (80). The radiation heat loss was affected by the area of the greenhouse A_{fHP}, the transmissivity of the inside and outside thermal covers τ_{tc}, τ_{os}, the emissivity of the greenhouse material and the extra-terrestrial sky. The equation was given as:

$$\dot{Q}_{HP,rad} = \sigma A_{fHP} \tau_{tc} \tau_{os} (\varepsilon_{iHP} T_{iHP}^4 - \varepsilon_{sky} T_{sky}^4) \tag{80}$$

where the temperature of the sky, Eq. (81) was a function of the outside temperature:

$$T_{sky} = 0.0552 \tilde{T}_o^{\,1.5} \tag{81}$$

and the emissivity of the sky, Eq. (82), was a function of the actual local air pressure and outside air temperature:

$$\varepsilon_{sky} = 0.7 + 5.95 \times 10^{-3} e^{a} e^{1500/\tilde{T}_o} \tag{82}$$

Latent and Sensible Heat Due to Evapotranspiration

The latent and sensible heat components of the crops were determined by Eq. (83):

$$\dot{Q}_{HP,ET} = ET \lambda A_{fHP} \tag{83}$$

The evapotranspiration rate, ET, is a complex variable that is influenced by a wide variety of climatic and location specific variables. Since local climatic factors play an important role in this research, the way in which ET was determined will be fully explained.

The method for determining the evapotranspiration rate, ET was discussed in detail by Allen et al. (1998). The applicable equations and theory were presented in the following section. In determining the water usage of the system, ET played a critical role since it determined how much water was being lost by evapotranspiration. Water loss translates into the amount of water required to replace the water in the system for the duration of operation. Certain climates cause a higher rate of evapotranspiration and therefore greater water usage. Other hotter more humid climates have a lower evapotranspiration rate and therefore less water usage.

The actual evapotranspiration rate (Eq. (84)) was dependent on the reference evapotranspiration rate ET_o (Eq. (86)) and the crop specific coefficient K_c (Eq. (85)). K_c was influenced by the crop growth stage, which means, K_c was time variant. The relationship was expressed using Eq. (84):

$$ET = 0.7 K_c(t) ET_o \tag{84}$$

Lettuce was used as the crop being grown and harvested within the greenhouse. Table 3.2 includes the crop coefficient and crop height measured in mm for the various growth stages of lettuce.

Table 3.2: *Crop coefficient and crop length at various growth stages of lettuce*

	Growth Stage crop coefficient			**Crop length in mm at various growth stages**				
Crop	**$K_{c\ ini}$**	**$K_{c\ mid}$**	**$K_{c\ end}$**	**L_{ini}**	**L_{dev}**	**L_{mid}**	**L_{end}**	**Total**
Lettuce	**0.7**	1	0.95	25	35	30	10	100

A variety of crops could be used in the model to observe what effect a specific crop may have on the system. Lettuce was specifically used in this research given its growth suitability in a hydroponic environment. Table 3.2 was used to construct a piece-wise function that served as input to the model. The piece-wise function ensured that the correct crop coefficient will be used during the specific growth stage. The information is based on the work of Allen et al. (1998).

The piece-wise function was defined by the following set of equations and conditions:

$$K_c(t) = \begin{cases} K_{c,ini}, & 0 \le t \le L_{ini} \\ K_{c,a}, & L_{ini} < t \le L_{ini} + L_{dev} \\ K_{c,end}, & L_{ini} + L_{dev} < t \le L_{ini} + L_{dev} + L_{mid} \\ K_{c,b}, & L_{ini} + L_{dev} + L_{mid} < t \le L_{ini} + L_{dev} + L_{mid} + L_{end} \end{cases} \tag{85}$$

with:

$$K_{c,a} = \frac{K_{c,mid} - K_{c,ini}}{L_{dev}} t + K_{c,ini} - \frac{L_{ini}(K_{c,mid} - K_{c,ini})}{L_{dev}}$$

$$K_{c,b} = \frac{K_{c,end} - K_{c,mid}}{L_{end}} t + K_{c,end} - \frac{\sum L\,(K_{c,end} - K_{c,mid})}{L_{end}}$$

$$\sum L = L_{ini} + L_{dev} + L_{mid} + L_{end}$$

The reference evapotranspiration rate, ET_o was location dependent and was influenced by a wide variety of parameters. ET_o was defined using Eq. (86):

$$ET_o = \frac{0.408\Delta[R_n - G_{hr}] + \gamma\left(\frac{37}{\tilde{T}_o}\right)u_2[e^o - e^a]}{\Delta + \gamma(1 + 0.34u_2)} \tag{86}$$

The saturation slope Δ was determined using Eq. (87):

$$\Delta = \frac{4098e^o}{[\tilde{T}_o + 273]^2} \tag{87}$$

where the environmental saturation pressure, e^o (Eq. (88)) was determined by using the hourly external air temperature $\tilde{T}_o$:

$$e^o = 0.6108e^{\left[\frac{17.27\tilde{T}_o}{\tilde{T}_o+273.3}\right]} \tag{88}$$

The actual environmental pressure, e^a (Eq. (89)) was determined as:

$$e^a = e^o\tilde{\emptyset} \tag{89}$$

With the hourly external relative humidity $\tilde{\emptyset}$, as an input from the location specific weather file. The hourly sol heat flux density G_{hr} was given by Eq. (90):

$$G_{hr} = \begin{cases} 0.1R_n, & Day \\ 0.5R_n, & Night \end{cases} \tag{90}$$

The net radiation, R_n in Eq. (91) was the difference in short and long wave radiation:

$$R_n = R_{ns} - R_{nl} \tag{91}$$

The short-wave radiation, R_{ns} in Eq. (92) was dependent on the incoming hourly solar radiation, $\tilde{I}_{sr}$:

$$R_{ns} = (1-\alpha)\tilde{I}_{sr} \tag{92}$$

where α is the albedo.

The long-wave radiation R_{nl} was defined by Eq. (93):

$$R_{nl} = \sigma\tilde{T}_o^4\left[0.34 - 0.14\sqrt{e^a}\right]\left[\frac{1.35\tilde{I}_{sr}}{R_{so}} - 0.35\right] \tag{93}$$

The clear sky radiation, R_{so} in Eq. (94) is dependent on the location's elevation, Z and the incoming extra-terrestrial radiation R_a:

$$R_{so} = (0.75 + 2\times10^{-5}Z)R_a \tag{94}$$

The extra-terrestrial radiation R_a defined by Eq. (95):

$$R_a = \frac{(12)(60)}{\pi}G_{sc}d_r[(\omega_e-\omega_i)\sin(\varphi)\sin(\delta) + \cos(\varphi)\cos\delta\{\sin(\omega_e)-\sin(\omega_i)\}] \tag{95}$$

G_{sc} is the solar constant. d_r is the inverse relative distance of the earth to the sun and is determined using Eq. (96):

$$d_r = 1 + 0.033\cos\left(\frac{2\pi}{365}J\right) \tag{96}$$

where J is the day number of the year between 1 and 365.

The latitude was defined by Eq. (97):

$$\varphi = \frac{\pi}{180} \tag{97}$$

The solar declination was given by Eq. (98):

$$\delta = 0.409 \sin\left(\frac{2\pi}{365}J - 1.39\right) \tag{98}$$

ω_i in Eq. (99) and ω_e in Eq. (100) were the solar time angles at the beginning and end of each hour of the simulation run time.

$$\omega_i = \omega_m - \frac{\pi}{24} \tag{99}$$

and

$$\omega_e = \omega_m + \frac{\pi}{24} \tag{100}$$

The solar angle at the midpoint of the time period, ω_m was determined using Eq. (101):

$$\omega_m = \frac{\pi}{12}[t_m + 0.06667(L_z - L_m) + S_c - 12] \tag{101}$$

t_m was the standard clock time at the midpoint of the period. L_z and L_m were the longitude of the centre of the local time zone and longitude of the measurement site, respectively.

The seasonal correction for solar time S_c was determined using Eq. (102):

$$S_c = 0.1645 \sin(2b) - 0.1255 \cos(b) - 0.025 \sin(b) \tag{102}$$

where the seasonal correction for solar time constant was determined by Eq. (103):

$$b = \frac{2\pi(J - 81)}{364} \tag{103}$$

The remaining parameters in Eq. (86) γ and u_2 were the psychrometric constant and average ground windspeed, respectively. γ is a function of the hourly measured air pressure at the location and is determined using Eq. (104):

$$\gamma = 0.665 \times 10^{-3} \tilde{P}_o \tag{104}$$

Solving all the equations and substituting all variables and locational data the evapotranspiration rate ET in Eq. (84) can be determined and heat flux by crop latent and sensible heat, in Eq. (83), could be determined.

Heat Flux due to Infiltration

During colder months cold air could infiltrate and replace the treated hot air inside the greenhouse. To account for this an infiltration term was defined in Eq. (75). The infiltration term was defined using Eq. (105):

$$\dot{Q}_{HP,infil} = 0.5 Vol_{HP}\left(T_{iHP} - \tilde{T}_o\right) \tag{105}$$

This equation was referenced from the ASHRAE manual, Standard ASHRAE (1973).

Energy Consuming Components for Environmental Control in the Hydroponic Greenhouse

The HVAC system (Figure 3.13) had three major components that required energy in order to maintain a constant environment. These components included:

1. Heat pumps for heating the system.
2. Pumps for circulating the hot water to the conditioning coils.
3. Fans that introduced the heated air into the system and cooled the system by means of ventilation only.

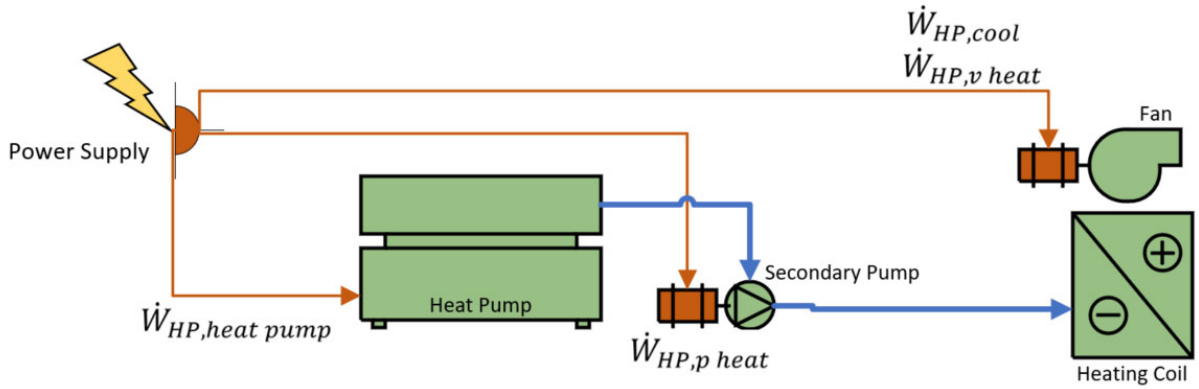

Figure 3.13: *Power supply required to provide energy to the HVAC components of the HP greenhouse.*

The work required by each component was determined by the energy balance in Eq. (75). The components are discussed by considering a cooling mode and a heating mode.

Hydroponic Greenhouse in Cooling Mode

If $\dot{Q}_{HP,v}$ in Eq. (75) was positive, it means that there was an excess amount of heat in the system and heat should be removed by means of ventilation.

The cooling heat flux was determined by Eq. (106):

$$if\ \dot{Q}_{HP,v} > 0,\quad \dot{Q}_{HP,v} = \dot{Q}_{HP,cool} \tag{106}$$

Applying the energy balance, $\dot{Q}_{HP,cool}$ becomes:

$$\dot{Q}_{HP,cool} = \rho_{air}\dot{V}_{HP,v}C_{p,air}[T_{iHP} - \tilde{T}_o] \tag{107}$$

In Eq. (107), the volumetric flow rate of the ventilation fans required to achieve the energy equilibrium can be written as Eq. (108):

$$\dot{V}_{HP,v} = \frac{\dot{Q}_{HP,cool}}{\rho_{air}C_{p,air} \times [T_{iHP} - \tilde{T}_o]} \tag{108}$$

The work input required by the fans to cool the greenhouse to set point was determined using Eq. (109):

$$\dot{W}_{HP,cool} = \frac{\dot{V}_{HP,v}\Delta P_{HP,fan}}{\eta_{HP,f}} \tag{109}$$

$\Delta P_{HP,fan}$ is the pressure drop across the HVAC system, which the fans need to overcome. $\eta_{HP,f}$ is the fan efficiency. The constant parameters are shown in Figure 3.17.

Hydroponic Greenhouse in Heating Mode

If $\dot{Q}_{HP,v}$ in Eq. (107) was negative, there was a shortage of heat in the system and heat should be added by means of a heat pump and hot water coil. The heating heat flux was determined using Eq. (110):

$$if\ \dot{Q}_{HP,v} < 0,\quad \dot{Q}_{HP,v} = \dot{Q}_{HP,heat} \tag{110}$$

The work input required by the heat pump to generate hot water for heating the system was determined using Eq. (111):

$$\dot{W}_{HP,heat\ pump} = \frac{\dot{Q}_{HP,heat}}{COP_{HP}} \tag{111}$$

COP_{HP} is the coefficient of performance of the heat pump.

The hot water circulation pump's input work was defined using Eq. (112):

$$\dot{W}_{HP,p\,heat} = \frac{\rho_{water} g \dot{V}_{HP,pump} H_{HP,pump}}{\eta_{HP,p}} \tag{112}$$

The volumetric flow rate of the pump in Eq. (113) was determined by a constant temperature difference and the heat required to achieve set point.

$$\dot{V}_{HP,pump} = \frac{\rho_{water} C_{p,water} \left[T_{Hw,in} - T_{Hw,out}\right]}{\dot{Q}_{HP,heat}} \tag{113}$$

The energy consumed by the AHU fans was determined using Eq. (114):

$$\dot{W}_{HP,v\,heat} = \frac{\dot{V}_{HP,v} \Delta P_{HP,fan}}{\eta_{HP,f}} \tag{114}$$

The volumetric flow rate of the fans was calculated using Eq. (115):

$$\dot{V}_{HP,v} = \frac{\dot{Q}_{HP,heat}}{\rho_{air} C_{p,air} \times [T_{iHP} - \tilde{T}_o]} \tag{115}$$

3.2.3 Water Loop and Psychrometry

The water flow and water usage of the system are illustrated in Figure 3.14. Water was lost through evapotranspiration in the hydroponic system due to the biochemical processes of the crops. Water was also lost due to evaporation in the aquaculture facility driven by a temperature and humidity gradient within the facility. Water was regained by the condensate water that forms on the cooling coils during the cooling process. Water condensed on the cooling coils when the air temperature was lower than the dew point at the coil condition.

Water that was lost in the hydroponic and aquaculture systems was replenished from a water storage tank. Water could be replaced directly via a mass balance between the water loss via evaporation and the water that was regained via the condensation. If the water gained from condensation was less than the water that was being lost, the water needed to be replenished via an external water supply. The external water supply was the measurement of water consumption in the system.

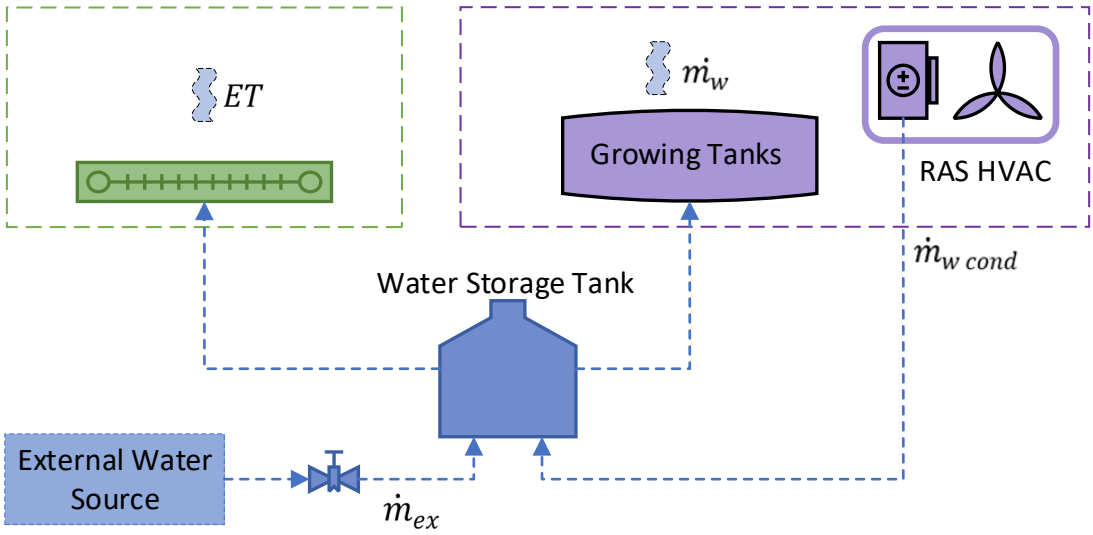

Figure 3.14: *Water mass balance in the decoupled aquaponic system*

Applying a mass balance to the system (Figure 3.14), Eq. (116) was derived:

$$\sum \dot{m}_{sys} = 0$$

$$\dot{m}_{in} - \dot{m}_{out} = 0$$

$$\dot{m}_{ex} + \dot{m}_{w\,cond} - \dot{m}_w - ET = 0$$

$$\therefore \dot{m}_{ex} = \dot{m}_w + ET - \dot{m}_{w\,cond} \qquad (116)$$

If $\dot{m}_{ex} < 0$, there was a surplus in water and the water was stored in the storage tank. The water was then available for future use.

The calculation of the terms $\dot{m}_w$ and ET have been discussed in previous sections. The remaining term, $\dot{m}_{w\,cond}$ was determined by analysing the psychrometric processes within the RAS facility.

A line diagram of the HVAC system is Illustrated in Figure 3.15. The various air vapour condition points are indicated in the diagram. Each condition point varied each hour as the conditions of the outside and inside air changed. The outside conditions changed based on the hourly measured data from the location specific weather data file. The inside conditions changed due to variations in relative humidity, caused by latent processes such as water evaporation and metabolic processes.

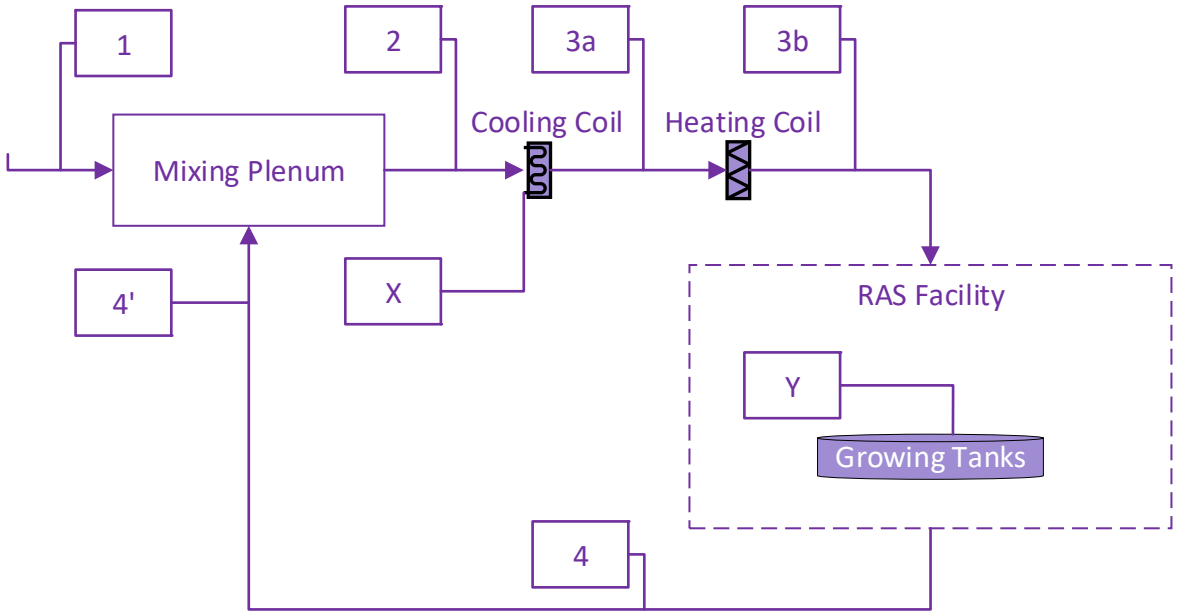

Figure 3.15: *Condition line diagram of the system psychrometry.*

Provided in Table 3.3 is an explanation of each condition point:

Table 3.3: *Psychrometric condition descriptions*

Condition point	Condition description
1	Outside air conditions. This varied on an hourly basis based on the location specific weather data.
2	On-coil conditions or mixed conditions. This was determined by the mixing of outside ventilation air (1) and the recirculated return air (4').
3a	Off-coil conditions of the cooling coil. This referred to a predefined constant value based on good engineering practices. It was the supply air conditions introduced into the space. The cool air was heated by means of the internal heat gains of the system to reach the set point of the room. This was a cooling and dehumidification process.
3b	Off-coil conditions of the heating coil. This referred to a predefined constant value based on good engineering practices. It was the supply air condition introduced into the space. The hot air cooled down by means of the internal heat losses of the system to reach the set point of the room. This was a purely sensible process.
4	Room air conditions. These were the air conditions after the air inside the facility had changed temperature and moisture content.
4'	Return air condition. This air was recirculated to the mixing plenum that was mixed with the outside air ready to be cooled or heated.
X	Condensation rate caused by a difference in humidity ratio of conditions 3a and 2. The rate was driven by the supply air rate $\dot{m}_2 = \dot{m}_{SA}$
Y	Evaporation rate of growing tank water $\dot{m}_w$. The water, introduced into the environment by means of the tank water evaporation, increased the moisture content of the air. I.e., the humidity ratio and by extension the relative humidity of the facility increased over time.

The condensation rate was determined by Eq. (117) based on psychrometry theory:

$$\dot{m}_{w\,cond} = \dot{m}_{SA}(\omega_{3a} - \omega_2) \tag{117}$$

If $\dot{m}_{w\,cond} < 0$, water had condensed on the coil and a dehumidification process had occurred. If $\dot{m}_{w\,cond} > 0$, the dew point had not been reached and moisture had been introduced into the space. The moisture would have been introduced from the outside air due to ventilation requirements.

Determining the off-coil conditions is an elaborate process and required multiple calculations and readings from the psychrometric chart. This process had been made simple by incorporating a Python module name "Psychrolib". The module took conditions as an input and provided the corresponding result from the psychrometric chart. In this research, the usages of the module are referenced as $Psy(\dots)$ and by using the following notation.

$$Condition_n = Psy(Input_1, Input_2, \dots, Input_n)$$

How each condition point was calculated using energy balances and psychrometry are illustrated in Table 3.4 and Table 3.5 The calculations were performed when the system was in cooling mode and heating mode respectively.

Once all the condition points have been solved for an instantaneous time period the condensation rate can be determined, thus completing the water loop mass balance. The result was used to determine the stock variable "total water usage" in m^3.

Cooling

Table 3.4: *Determining the system psychrometric conditions during cooling mode*

Condition Point	Atmospheric pressure $[Pa]$	Dry bulb temperature $[°C]$	Relative Humidity [%]	Wet bulb temperature $[°C]$	Dew point $[°C]$	Humidity Ratio $\left[\frac{kg\ H_2O}{kg\ Air}\right]$	Enthalpy $\left[\frac{J}{kg}\right]$
1	$\tilde{P}_o$	$\tilde{T}_{db1}$	$\tilde{\emptyset}_1$	$T_{wb1} = Psy(\tilde{T}_{db1}; \tilde{\emptyset}_1; \tilde{P}_o)$	$T_{dew1} = Psy(\tilde{T}_{wb1}; \tilde{\emptyset}_1)$	$\omega_1 = Psy(\tilde{T}_{db1}; T_{wb1}; \tilde{P}_o)$	$h_1 = Psy(\tilde{T}_{db1}; \omega_1)$
2	$\tilde{P}_o$	$T_{db2} = Psy(h_2; \omega_2)$	$\emptyset_2 = Psy(T_{db2}; \omega_2; \tilde{P}_o)$	$T_{wb2} = Psy(T_{db2}; \omega_2; \tilde{P}_o$	$T_{dew2} = Psy(T_{wb2}; \emptyset_2)$	$\omega_2 = \frac{\dot{m}_1\omega_1 + \dot{m}_4\omega_4}{\dot{m}_1 + \dot{m}_4}$	$h_2 = \frac{\dot{m}_1 h_1 + \dot{m}_4 h_4}{\dot{m}_1 + \dot{m}_4}$
3a	$\tilde{P}_o$	T_{db3_a}	$\emptyset_{3a} = Psy(T_{db3_a}; T_{wb3_a}; \tilde{P}_o)$	T_{wb3_a}	$T_{dew3a} = Psy(T_{wb3_a}; \emptyset_{3b})$	$\omega_{3a} = Psy(T_{db3_a}; T_{wb3_a}; \tilde{P}_o)$	$h_{3a} = Psy(T_{db3_a}; \omega_{3a})$
3b	$\tilde{P}_o$	T_{db3_b}	$\emptyset_{3b} = Psy(T_{db3_b}; T_{wb3_b}; \tilde{P}_o)$	T_{wb3_b}	$T_{dew3b} = Psy(T_{wb3_b}; \emptyset_{3a})$	$\omega_{3b} = Psy(T_{db3_b}; T_{wb3_b}; \tilde{P}_o)$	$h_{3b} = Psy(T_{db3_b}; \omega_{3b})$
4	$\tilde{P}_o$	$T_{db4} = T_i$	$\emptyset_4 = Psy(T_{db4}; \omega_4; \tilde{P}_o)$	$T_{wb4} = Psy(T_{db4}; \omega_4; \tilde{P}_o)$	$T_{dew4} = Psy(T_{wb4}; \emptyset_4)$	$\omega_4 = Psy(h_4; T_{wb4})$	$h_4 = \frac{\dot{Q}_{RAS,room\ tot}}{\dot{m}_2} + h_3$

Heating

Table 3.5: *Determining the system psychrometric conditions during heating mode*

Condition Point	Atmospheric pressure $[Pa]$	Dry bulb temperature $[°C]$	Relative Humidity [%]	Wet bulb temperature $[°C]$	Dew point $[°C]$	Humidity Ratio $\left[\frac{kg\ H_2O}{kg\ Air}\right]$	Enthalpy $\left[\frac{J}{kg}\right]$
1	$\tilde{P}_o$	$\tilde{T}_{db1}$	$\tilde{\emptyset}_1$	$T_{wb1} = Psy(\tilde{T}_{db1}; \tilde{\emptyset}_1; \tilde{P}_o)$	$T_{dew1} = Psy(\tilde{T}_{wb1}; \tilde{\emptyset}_1)$	$\omega_1 = Psy(\tilde{T}_{db1}; T_{wb1}; \tilde{P}_o)$	$h_1 = Psy(\tilde{T}_{db1}; \omega_1)$
2	$\tilde{P}_o$	$T_{db2} = Psy(h_2; \omega_2)$	$\emptyset_2 = Psy(T_{db2}; \omega_2; \tilde{P}_o)$	$T_{wb2} = Psy(T_{db2}; \omega_2; \tilde{P}_o$	$T_{dew2} = Psy(T_{wb2}; \emptyset_2)$	$\omega_2 = \frac{\dot{m}_1\omega_1 + \dot{m}_4\omega_4}{\dot{m}_1 + \dot{m}_4}$	$h_2 = \frac{\dot{m}_1 h_1 + \dot{m}_4 h_4}{\dot{m}_1 + \dot{m}_4}$
3a	$\tilde{P}_o$	T_{db3_a}	$\emptyset_{3a} = \emptyset_{3a}$	T_{wb3_a}	$T_{dew3a} = Psy(T_{wb3_a}; \emptyset_{3b})$	$\omega_{3a} = Psy(T_{db3_a}; T_{wb3_a}; \tilde{P}_o)$	$h_{3a} = Psy(T_{db3_a}; \omega_{3a})$
3b	$\tilde{P}_o$	T_{db3_b}	$\emptyset_{3b} = \emptyset_{3b}$	T_{wb3_b}	$T_{dew3b} = Psy(T_{wb3_b}; \emptyset_{3a})$	$\omega_{3b} = Psy(T_{db3_b}; T_{wb3_b}; \tilde{P}_o)$	$h_{3b} = Psy(T_{db3_b}; \omega_{3b})$
4	$\tilde{P}_o$	$T_{db4} = T_i$	$\emptyset_4 = \emptyset_4$	$T_{wb4} = Psy(T_{db4}; \omega_4; \tilde{P}_o)$	$T_{dew4} = Psy(T_{wb4}; \emptyset_4)$	$\omega_4 = Psy(h_4; T_{wb4})$	$h_4 = \frac{\dot{Q}_{RAS,room\ tot}}{\dot{m}_2} + h_3$

3.3 Causal Loop Diagrams

The causal loop diagrams were developed using Microsoft Visio Professional 2019. They are used to describe basic causal mechanisms hypothesised to generate the reference mode of behaviour of the system over time. The system has been thoroughly discussed and described in the preceding sections. Therefore, all system boundaries and causal elements have been identified and described. The causal loop diagrams for the HP and RAS have been constructed based on the above-described system. The cause-and-effect relationships were identified and were formed for the variables in the system. The balancing and reinforcing feedback loops were also identified and indicated in each closed loop system.

The reference model, which was simulated over a year, consists of the investigation of the effects of local climatic conditions on system stocks such as energy and water consumption. Effects of global warming and climate change were then incorporated into the system via the causal loop diagrams. The effects of global warming and climate change were then simulated. The stocks were observed to see how the variables will react over a period of 80 years.

Important drivers to the changes of the system energy flow were elements that would cause increases or decreases of system energy over a period of time. The more energy a system required, the more electricity was required to be generated. The more electricity generated might lead to an increase in fossil fuel burning and thus leading to more CO_2 and soot emissions. These emissions could add to a rise in outside temperature, which would exert a significant impact on the system since the system is heavily influenced by the outside temperature. An increase in soot particles could lead to less solar radiation reaching the surface area of the system, which would also exert a significant impact on the system's energy usage. These factors provided an important feedback loop to the system and the effects were presented.

The cause and effect of the various system variables were indicated in the causal loop diagrams for the aquaculture facility and the hydroponic greenhouse, respectively. As described by the systems thinking and system dynamics modelling method, the "+" sign indicated a positive cause effect relationship, that is, if the one variable increased, the other variable would also increase or vice versa. The "-" sign indicated a negative cause effect relationship and if a variable increased the corresponding variable would decrease and vice versa. The closed loops of the cause-effect relationships were identified and indicated on the diagram using standard conventions. Balancing loops were indicated with a "B" and

reinforcing loops were indicated with an “R”. The identified closed loops were briefly summarised and discussed.

The causal loop diagrams shown in Figure 3.29 and Figure 3.30 for the aquaculture system and the hydroponic system were presented separately for ease of interpretation.

3.3.1 Closed Feedback Loops in the Aquaculture Facility

Biomass Loop B1

The relationship between the biomass, fish weight and how it affects the circulation flow rate is illustrated in Figure 3.16. The circulation mass flow rate increases as the biomass increases. The biomass is increased when the fish weight and fish feed increase. The fish weight increases since the fish growth rate increases when the feed rate increases. Fish will reach a certain weight causing the growth rate to saturate and the feed rate, and by extension the biomass, will decrease. Each component of the causal loop diagram in Figure 3.16 is driven by the mathematical expressions as discussed in section 3.2. The flow rate of the circulation pump, defined in Eq. (5), is the driving factor for the energy consumed by the pump as shown in Eq. (4). The hydraulic retention time also influences the flow rate as shown in Figure 3.16. The flow rate is influenced by the system biomass as defined in Eq. (7). Ultimately the system biomass is a function of biological processes, which are heavily driven by the fish weight, fish growth rate and the feed rate as defined in Eq. (10), Table 3.1 and Eq. (9) respectively.

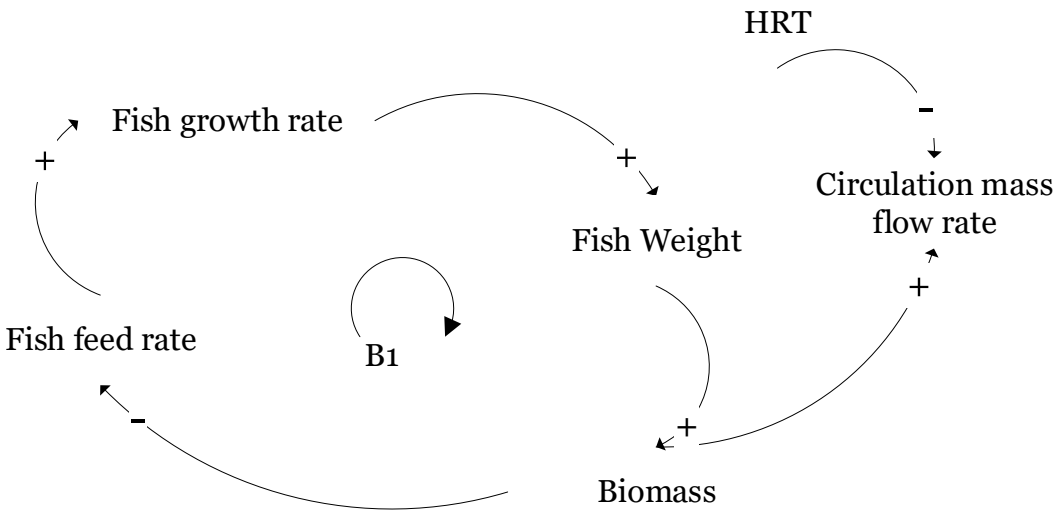

Figure 3.16: *Biomass balancing closed loop in the RAS facility*

The system flow rate, which is a function of time, is considered to be an inflow component to the total system energy usage, which is defined by Eq. (4).

Internal Humidity Loop B2

The inside humidity of the RAS facility, derived and expressed in Table 3.4, exerts an effect on the evaporation rate (Eq. (25)) of the tank water. The dynamics of the evaporation rate is a function of the density difference between the vapour mixture at the water surface and the environment as well as the mass transfer coefficient shown in Eq. (26). The higher the humidity, the more moisture is present in the air. The vapour density has a small gradient and the evaporation rate will decrease.

As the evaporation rate decreases so will the humidity for each hour as the space is being ventilated. This relationship is illustrated in Figure 3.17.

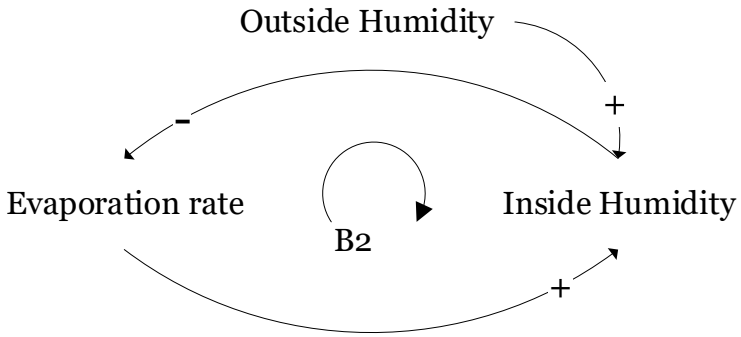

Figure 3.17: *Internal humidity balancing closed loop in the RAS facility*

The evaporation rate in Eq. (25) determined the heat loss to the environment shown as in Eq. (24), which will contribute to the cooling load required as in Eq. (20). Ultimately this component will influence the total system energy usage as described by Eq. (19).

Humidity Gradient Loop B3

The inside humidity is affected by the outside humidity. If the outside humidity is high, more moisture will be introduced into the system via the ventilation system. The inside water content in the air will then increase. The humidity gradient will therefore increase causing more water to be removed from the air due to dehumidification on the cooling coils. If the condensation rate (Eq. (117)) increases, the humidity levels will drop due to dehumidification. This relationship is illustrated in Figure 3.18.

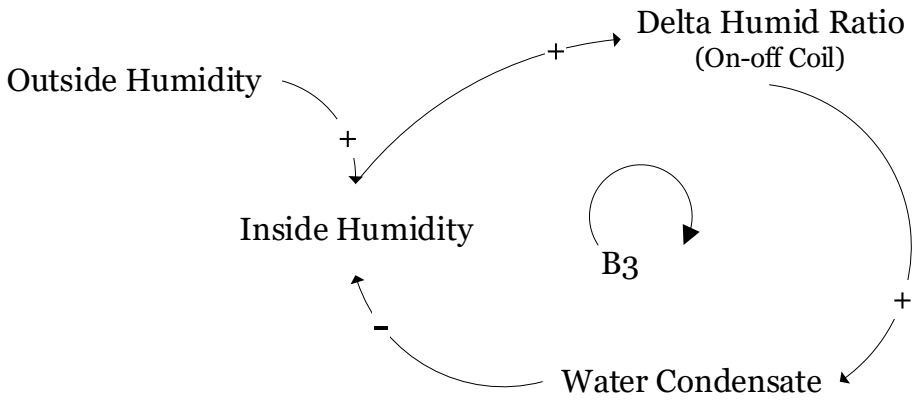

Figure 3.18: *Humidity gradient balancing closed loop in the RAS facility*

These system dynamics are driven by psychrometric processes that are read from the psychrometric chart. The air-vapour conditions are defined in Table 3.4 and Table 3.5. The condensation rate plays an important role in the net water usage in the system as defined by Eq. (116).

Incoming Solar Radiation Loop B4

The system will consume energy to maintain favourable conditions. Assuming that fossil fuels are the main source of electricity generation, this will lead to an increase in soot particles due to the burning process. Soot particles can absorb incoming solar radiation thus preventing the radiation from reaching the surface area of the RAS facility. The external heat gained by solar radiation is described by Eq. (52). Less solar radiation per square meter will reduce the thermal load on the facility as seen in Eq. (48) and Eq. (19). This relationship is shown in the causal loop diagram in Figure 3.19.

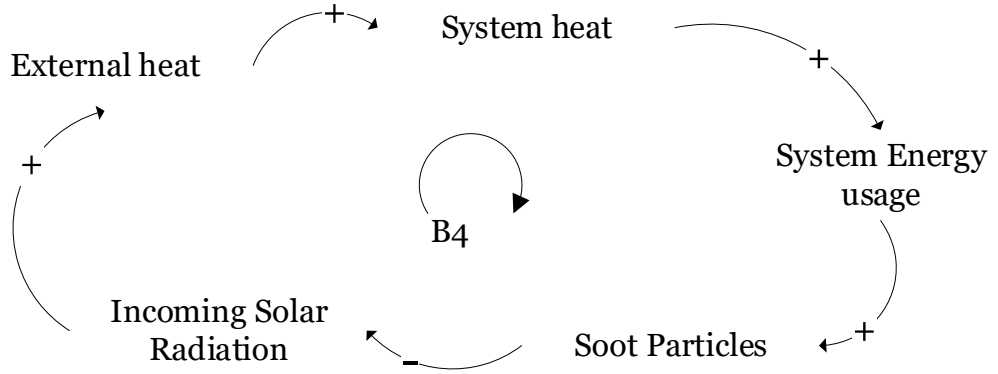

Figure 3.19: *Incoming solar radiation balancing closed loop in the RAS facility*

The causal loop diagram in Figure 3.19 is of particular interest in analysing the effects of dependence on fossil fuels for energy generation.

External Heat Loop R1

Burning of fossil fuel will also lead to an increase in CO_2 emissions. Over time, this could affect the temperature of a region due to climate change and global warming. With the increase of the outside air temperature, the external system heat will be affected as illustrated in Figure 3.20. The temperature difference between the inside and outside of the RAS is a major contributor to total system energy usage. Delta T, which is defined as the difference between the inside and outside temperatures, is represented in Eq. (49) and Eq. (56). A high delta T will have a significant effect on the total system energy usage, specifically the energy consumed by the HVAC system as shown in Eq. (19). As derived in section 3.2 the HVAC load will influence the total system energy as seen in Eq. (58), Eq. (60), Eq. (66) and Eq. (69).

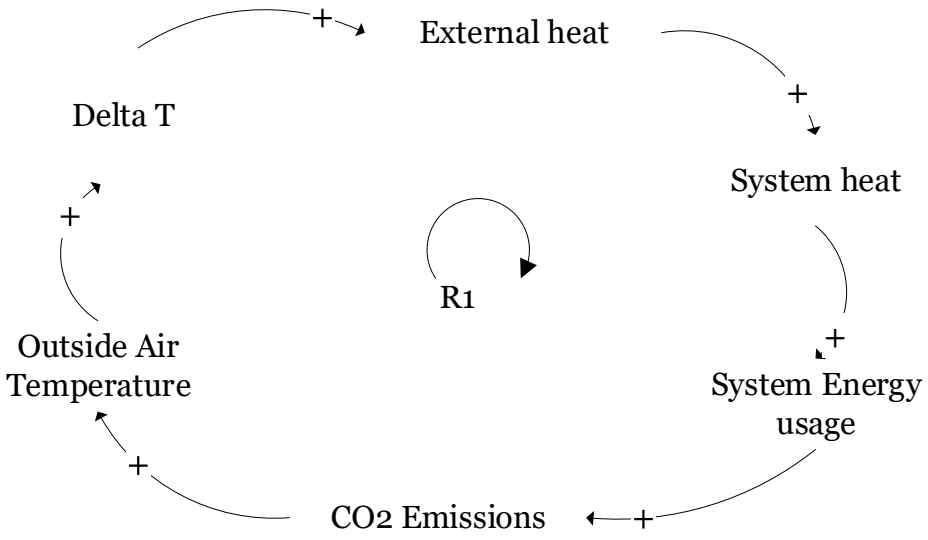

Figure 3.20: *External heat reinforcing closed loop in the RAS facility*

Ventilation Heat Loop R2

Similarly, the ventilation heat will be affected since there is a temperature difference in the governing equations such as Eq. (56).

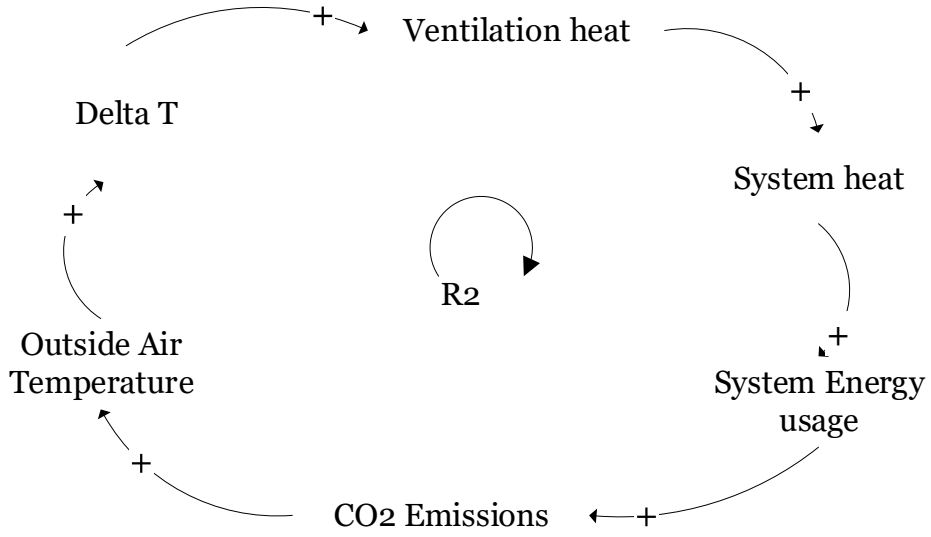

Figure 3.21: *Ventilation heat reinforcing closed loop in the RAS facility*

Internal Set point Loop R3

The setpoint temperature is controlled by means of the temperature gradient experienced, caused by the system heat flux as defined by Eq. (63). The system will react to maintain the desired set point by adjusting the current supply temperature of the air, as defined by Eq. (62).

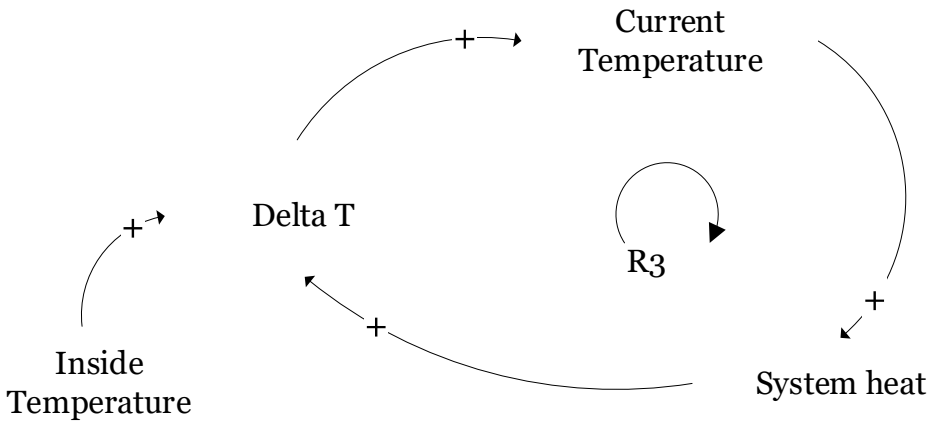

Figure 3.22: *Internal temperature set point reinforcing closed loop in the RAS facility*

System Heat Flux Loop R4

As the set point temperature changes, the temperature gradient will be affected and will cause the internal heat and tank heat losses to react as seen in the reinforcing loop illustrated in Figure 3.23.

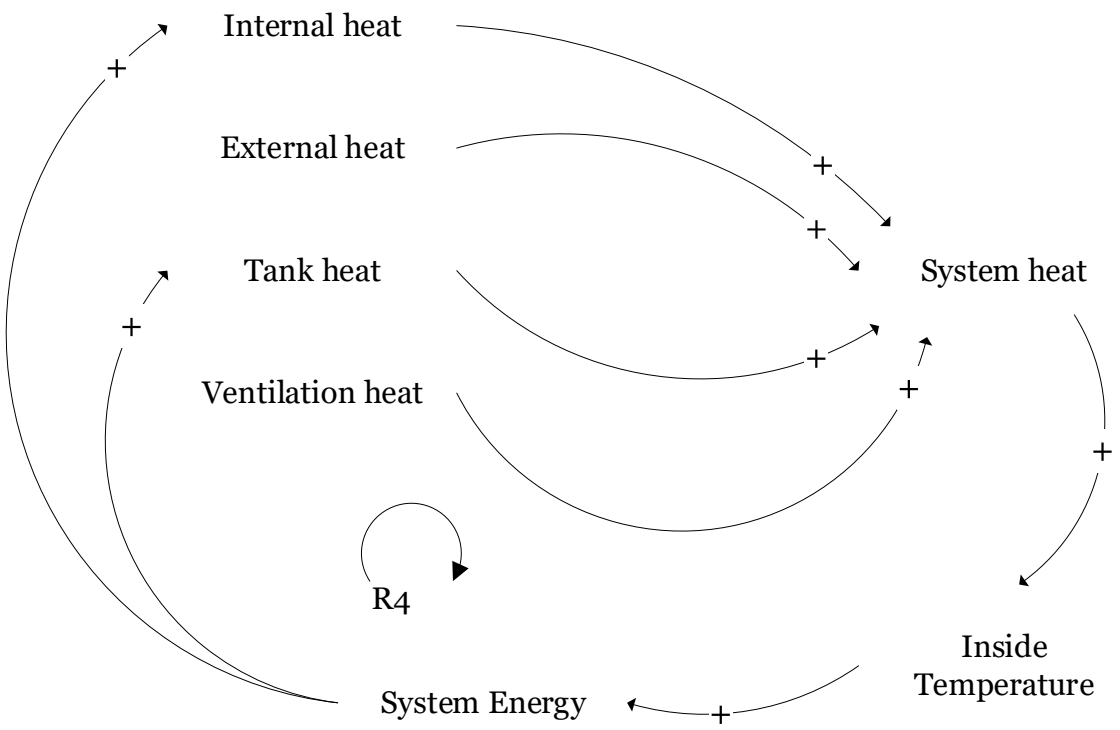

Figure 3.23: *System heat flux reinforcing closed loop in the RAS facility*

The system heat is described in Eq. (19) and each contributing component is described by Eq. (20), Eq. (43), Eq. (48), Eq. (56) and Eq. (57) respectively.

3.3.2 Closed Feedback Loops in the Hydroponic Greenhouse System

Internal Humidity Loop B1

The internal greenhouse humidity and evapotranspiration rate have a balancing cause-and-effect relationship. When the inside humidity increases the air will become saturated with moisture and the vapour density gradient will decrease. The smaller density gradient will cause the evapotranspiration rate to decrease, which will, in turn, decrease the humidity over a period of time as shown in Figure 3.24.

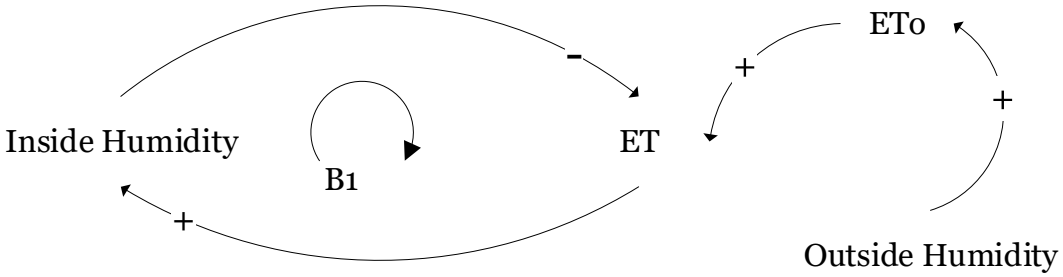

Figure 3.24: *Internal humidity balancing closed loop in the HP greenhouse*

The evapotranspiration rate is determined as derived in section 3.2. The evapotranspiration is described by Eq. (84) and is influenced by the reference evapotranspiration rate, which is a complex term influenced by a variety of factors, as seen in Eq. (86). Outside humidity, which is time varied, and will affect the reference evapotranspiration rate is related to the system. Ultimately the system energy defined in Eq. (75) is influenced by a latent energy component. The latent energy is driven by the evapotranspiration rate.

Incoming Solar Radiation Loops B2 and B3

Soot particles, which absorb incoming solar radiation, will prevent radiation from reaching the surface area of the greenhouse. Less solar radiation per square meter will reduce the thermal load on the greenhouse. This will have an effect on not only the solar heat gain per square meter but also the evapotranspiration rate and by extension the heat flux associated with evapotranspiration as shown in Figure 3.25.

The system energy (Eq. (75)) is heavily influenced by solar radiation since the greenhouse transmits a great deal of solar energy into the system. The incoming heat due to solar radiation is defined in Eq. (78) and will exhibit the relationship illustrated in the causal loop diagram. The reference evapotranspiration rate (Eq. (86)) is also heavily influenced by the incoming solar radiation, which affects the latent component in Eq. (75). The evapotranspiration rate also exerts an influence on the pump power as shown in Eq. (73) and Eq. (74) respectively.

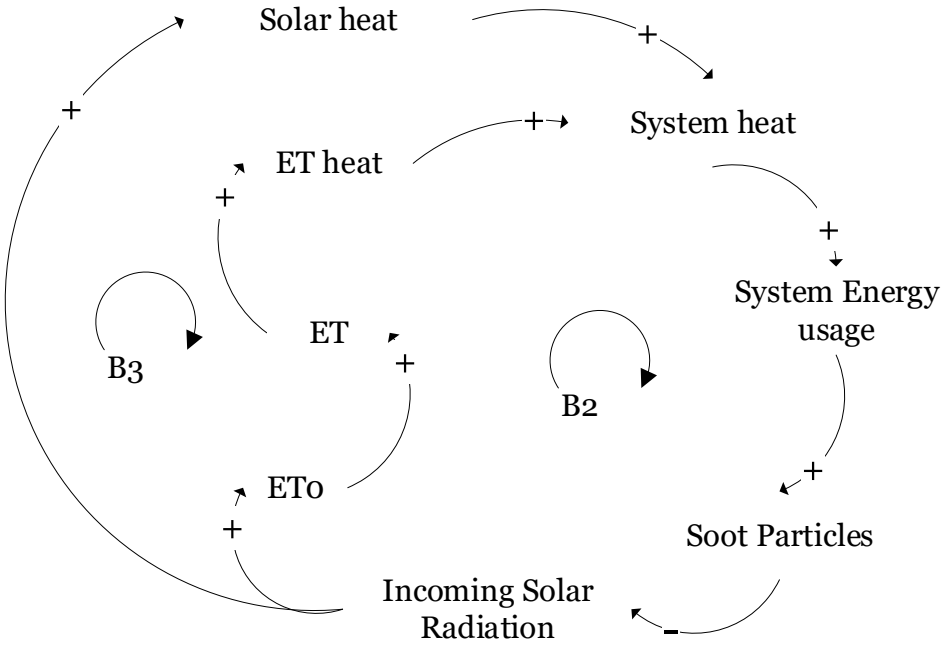

Figure 3.25: *Incoming solar radiation balancing closed loops in the HP greenhouse*

External Heat Loop R1, R4 & R5

The effects of CO_2 emissions during the burning of fossil fuels will influence the greenhouse energy balance. With an increase or decrease in external air temperature, heat flux terms with a temperature difference between inside and outside will be affected as seen in the reinforcing causal loop Figure 3.26.

It is hypothesised that the system energy (Eq. (75)) is heavily influenced by external factors such as external temperature. A variety of energy contributing factors are dependent on the external temperature. Eq. (79) describes the relationship between convective and conductive heat fluxes due to a temperature differential. The heat flux due to infiltration is governed by Eq. (105), which is dependent on the external temperature. Lastly, as the outside temperature increases the evapotranspiration rate (Eq. (84)) will also increase. Ultimately the system energy will be influenced by all these components.

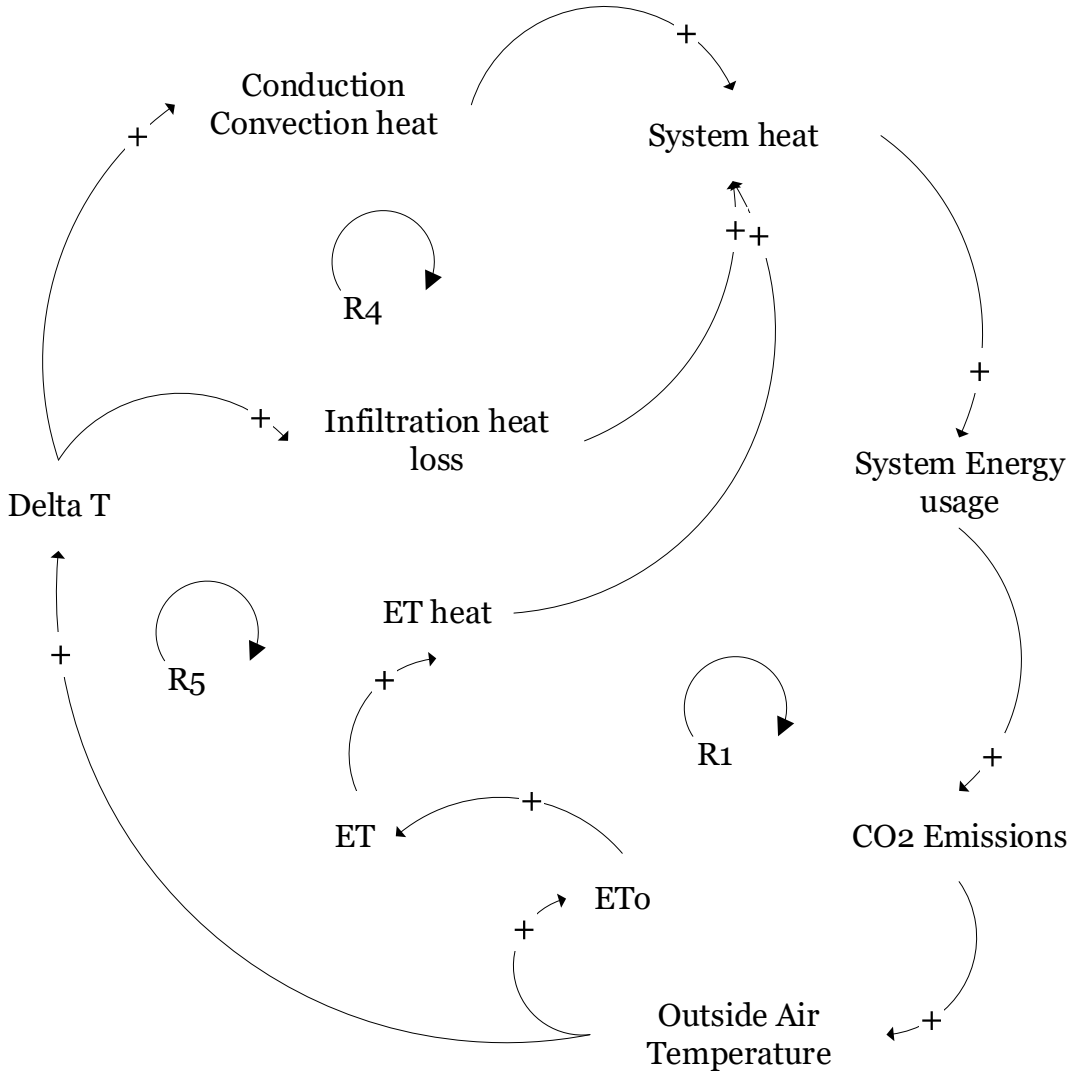

Figure 3.26: *External heat reinforcing closed loop in the HP greenhouse*

Internal Set point Loop R2

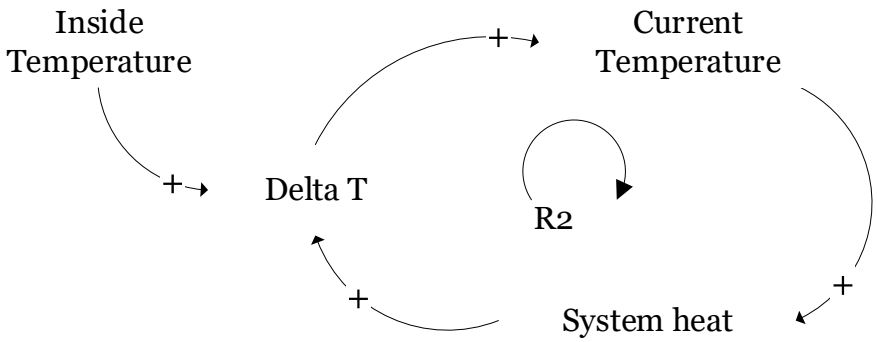

Figure 3.27: *Internal temperature set point reinforcing closed loop in the HP greenhouse*

The set point temperature is controlled by means of the temperature gradient caused by the system heat flux shown in Eq. (75). The system will react in order to maintain the desired set point by adjusting the current supply temperature of the air as described in Eq. (110) and Eq. (115). This cause-effect relationship is illustrated in Figure 3.27.

Ventilation Heat Loop R3

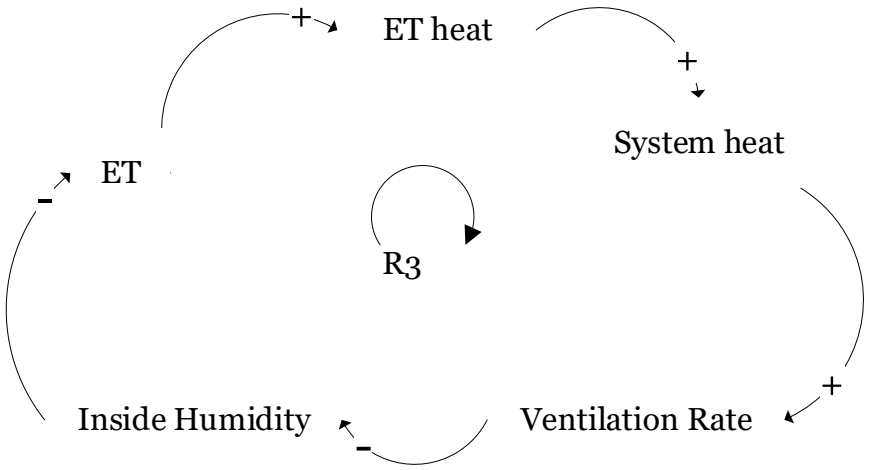

Figure 3.28: *Ventilation heat reinforcing closed loop in the HP greenhouse*

The ventilation rate, defined in Eq. (108), will affect the internal humidity. This will affect the evapotranspiration rate as illustrated in section 3.4. This will ultimately affect the evapotranspiration heat flux shown in Eq. (83) and therefore the system heat flux shown in Eq. (75). This relationship is illustrated in Figure 3.28.

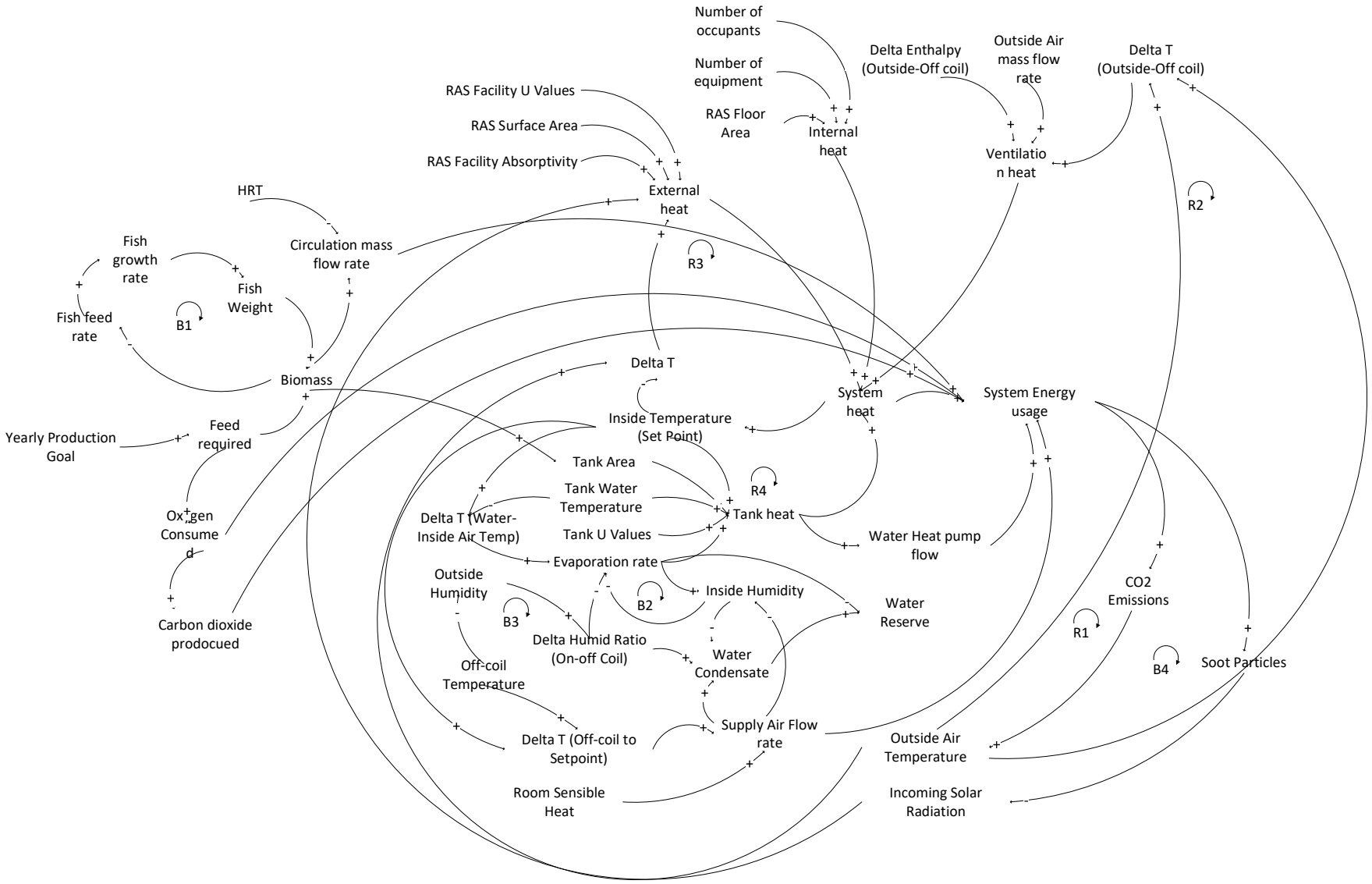

Figure 3.29: *Aquaculture facility causal loop diagram*

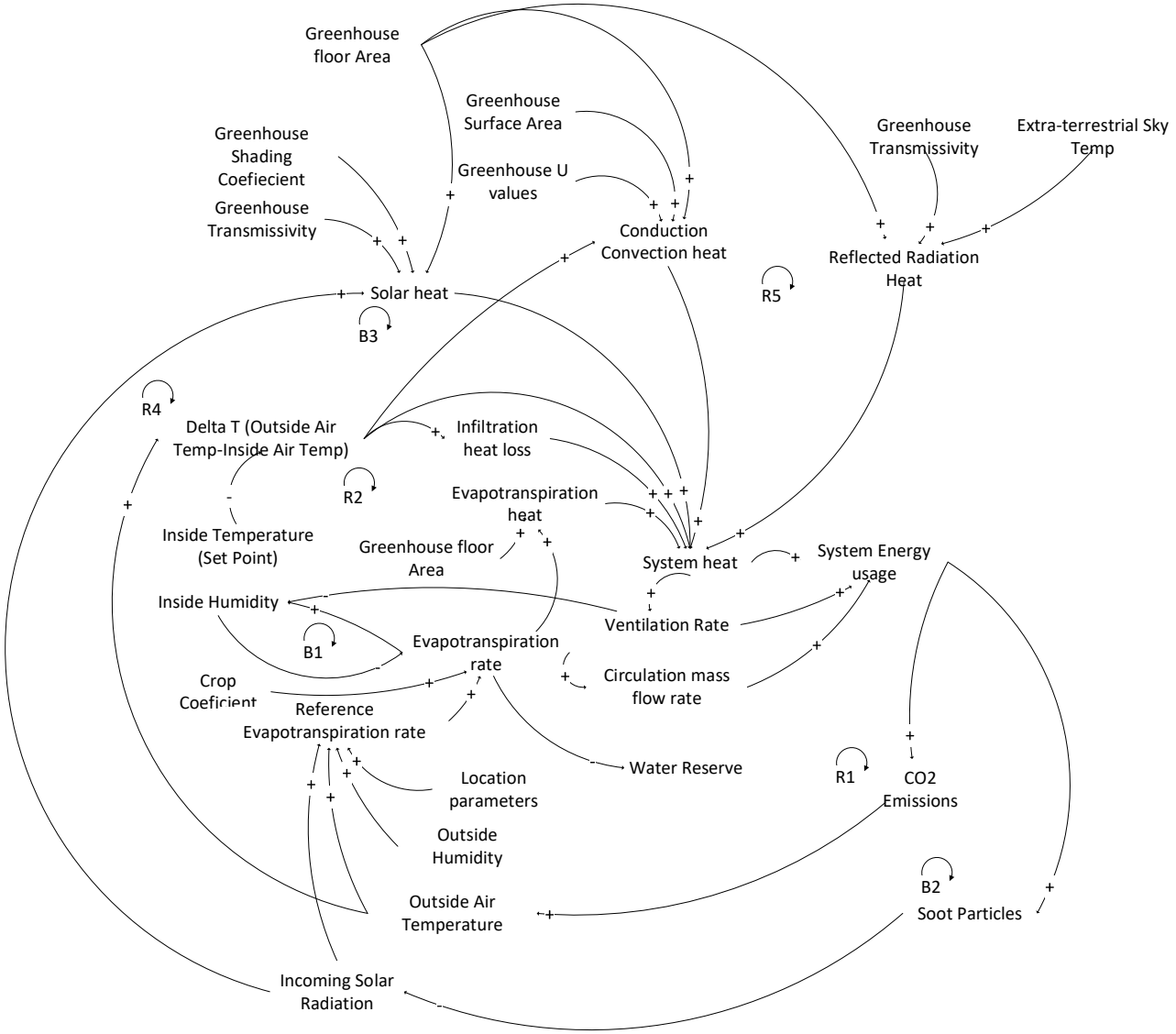

Figure 3.30: *Hydroponic greenhouse causal loop diagram*

3.4 Stock and Flow Diagrams

As discussed by Bala et al. (2017), causal loop diagrams do not properly capture the stock and flow of a system. Therefore, it is recommended to make use of flow diagrams to illustrate the relationship and to emphasise the loop structure of a system. First order differential equations represent the stock and flow of systems and are central to the system dynamics theory. Contained within the theory are feedback loops that are basic structural elements within the system boundary. The boundary separates the system from the surrounding environment as discussed by Bala et al. (2017). The dynamic behaviour of a system is simulated by the use of feedback loops. Essentially the feedback loop of the models acts as a path linking decisions, actions, system conditions and information to the path communicating with the decision point.

As previously stated, the most important stock variables were identified as total system energy consumption and total system water consumption. Secondary stock variables such as system humidity, total system biomass, CO_2 levels, O_2 levels and fish weight are also considered and modelled but are less predominant factors.

Flows of the system were essentially the per unit time variable, namely the heat flux measured in J/s and volumetric flow rates measured in m^3/s. The flows were the rate at which the energy and volume of fluids change over time.

All other parameters, dynamic variables and input data were defined as discussed in the previous sections and tables.

The dynamic behaviour of the systems is created by accumulations. Accumulations are mathematically represented by integration. Integration can occur naturally in systems of biological or physical nature. Equations representing the system stock can be represented by a first-order finite difference equation; it was expressed by the models as presented by Bala et al. (2017):

$$stock(t) = stock(t_0) + \int_{t_0}^{t} \big(inflow(t) - outflow(t)\big)dt \tag{118}$$

Eq. (118) can be written in the following differential equation:

$$\frac{d(stock)}{dt} = inflow(t) - ouflow(t) \tag{119}$$

The equations were then solved using numerical methods. The equations presented in section 3.2 assumed the format of Eq. 119 and served as input to the simulation software. The time parameter was selected in days and the simulations were executed for a single year in order to

compare the climatic effects of different locations with each other. The simulations were then executed for a period of 80 years to evaluate the effects of climate change the energy and water usage of the system. The system stock and flow diagrams were segmented for ease of presentation. The stock and flow diagrams were presented following the structure and sequence in which the system energy and water usage were described in section 3.2. The stock and flow diagrams were constructed in AnyLogic and are presented in Figure 3.31 to Figure 3.50. The components presented in Figure 3.31 to Figure 3.50 are interconnected in a large system to capture the system dynamics contained within the system boundaries as identified in section 3.2. The components are presented separately to fully explain the contribution of each component.

3.4.1 Recirculating Aquaculture System Facility

Lighting

The lighting in the aquaculture facility contributed to total system energy use, as illustrated in Figure 3.31. The flow variable is governed by Eq. (1) and the remaining dynamic variables and parameters are defined in Table 4.7. The biomass stock defined by Eq. (7) had an influence on the system floor area, and the lighting was dependent on floor area.

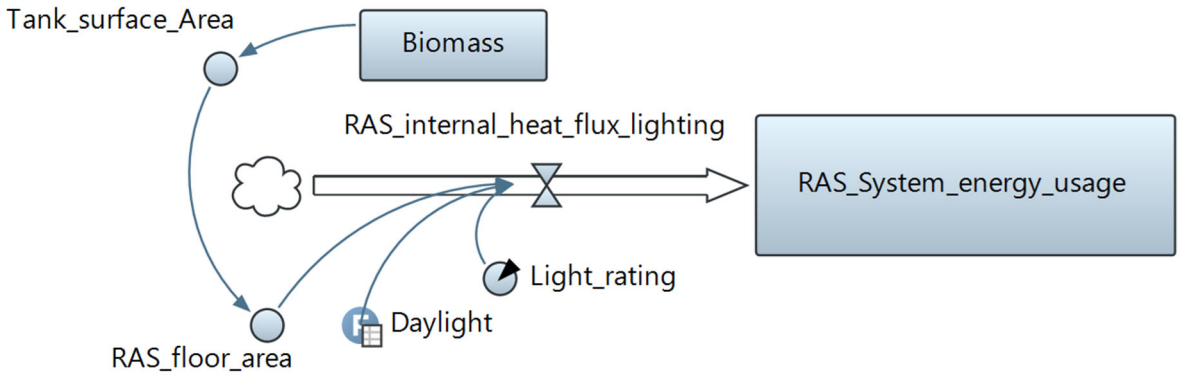

Figure 3.31: *Stock and flow diagram - RAS lighting*

Aeration Towers

The fans were required to strip the circulated water from CO_2. This component contributed to total system energy usage, as illustrated by Figure 3.32. The energy stock and flow, (Eq. (2)) is influenced by the CO_2 generation of the biomass as defined by Eq. (3) and Eq. (7). The remaining dynamic variables and parameters are defined in Table 4.7. A delay is introduced to simulate the harvesting of the fish and is denoted by 'Cycle purge'.

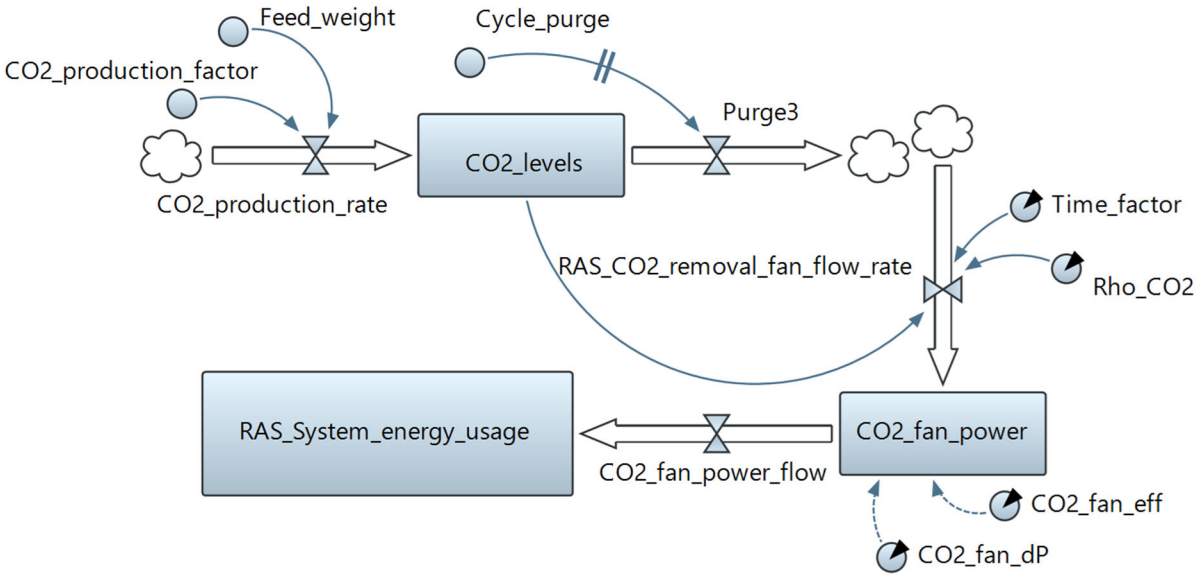

Figure 3.32: *Stock and flow diagram - Aeration towers*

Circulation Pumps

The energy stock and flow of the aquaculture circulation pump is illustrated in Figure 3.33. The energy flow is governed by Eq. (4) and is dependent on the volumetric flow rate defined by Eq. (5). The flow rate of circulation pump is dependent on the biomass (Eq. (7)) of the system. The dynamic variables and remaining parameters are defined in Table 4.7. Delays were introduced into the system to simulate the harvesting of fish.

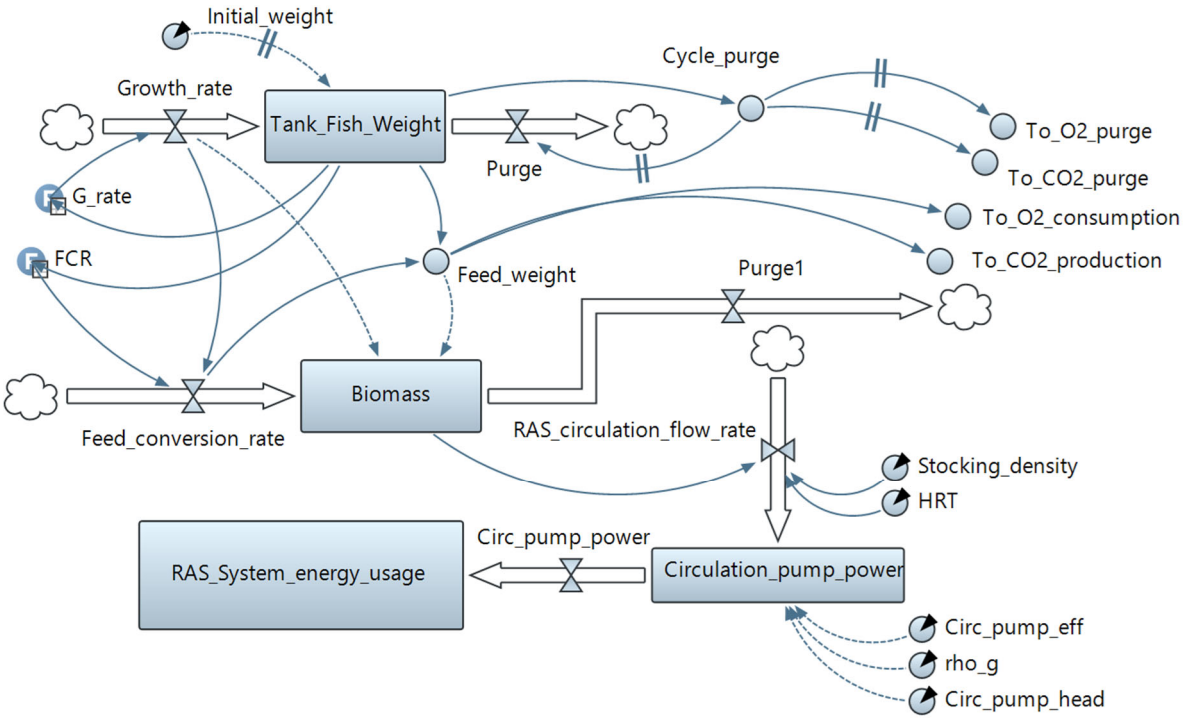

Figure 3.33: *Stock and flow diagram - RAS circulation pumps*

Ultra-Violet Disinfection

The energy flow variable due to UV disinfection is illustrated in Figure 3.34. The flow is defined by Eq. (12) and contributed to the total energy usage system stock. The remaining dynamic variables and parameters are defined in Table 4.7.

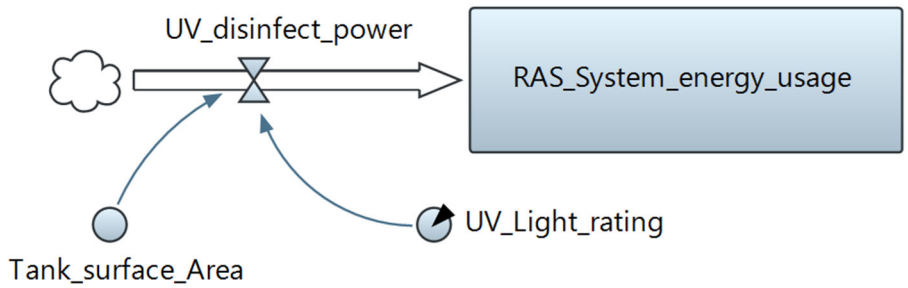

Figure 3.34: *Stock and flow diagram - RAS UV-disinfection*

Oxygen Generation

Oxygen compressors were required to replenish dissolved oxygen that was consumed by the biomass. This component contributed to total system energy usage, as illustrated by Figure 3.35. The energy stock and flow, (Eq. (13)) is influenced by the O_2 consumption of the biomass as defined by Eq. (14) and Eq. (7). The remaining dynamic variables and parameters are defined in Table 4.7. A delay is introduced to simulate the harvesting of the fish.

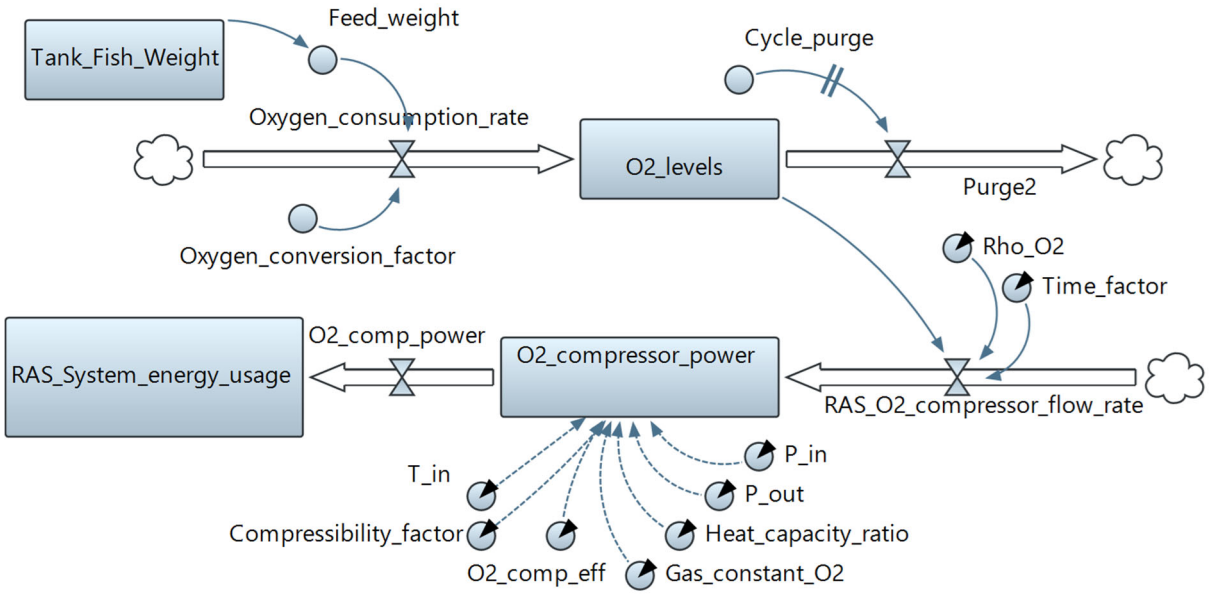

Figure 3.35: *Stock and flow diagram - Oxygen generation*

The relative humidity, within the aquaculture facility, influenced the energy and water flow in the system. Latent heat is a contributing factor to the heat balance as defined in Eq. (19). The heat balance ultimately determined the energy flow of the system as defined by Eq. (58) and Eq. (60). The relative humidity is also influenced by the evaporation rate of tank water due to a water vapor gradient as defined by Eq. (25). The relative humidity stock also influenced the water condensation rate on the cooling cools. This relationship is illustrated in Figure 3.37. Causal loop diagrams B2 and B3, shown in Figure 3.17, were used to construct the stock and flow diagram. The internal relative humidity was used to evaluate the psychrometric state of the system (Table 3.3) at each time step. The remaining dynamic variables and parameters are defined in Table 4.7.

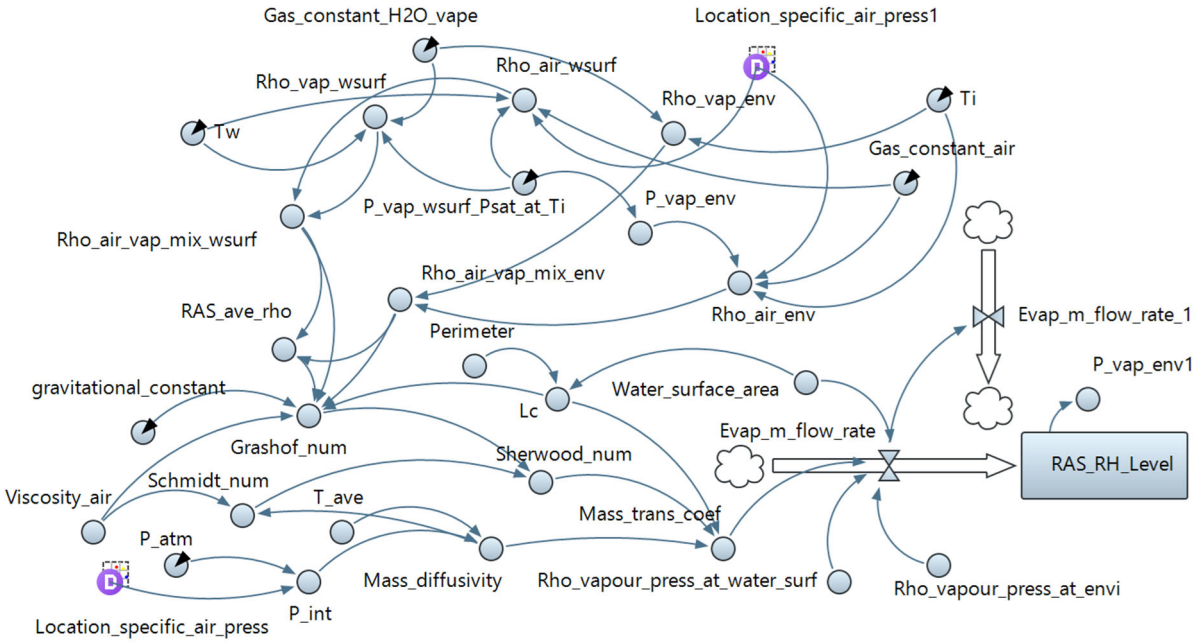

Figure 3.36: *Stock and flow diagram - Relative humidity of RAS facility*

The internal relative humidity was influenced by the ventilation flow rate as defined by Eq. (53). Water vapor was introduced into the system due to the ventilation requirements and influenced the ventilation heat as seen in Eq. (55). The ventilation heat is a contributing component to Eq. (19). The respective volumetric flow rates of the air system are illustrated in Figure 3.15. The influence of the respective volumetric flow rate on the system heat and water balance is illustrated in Figure 3.37.

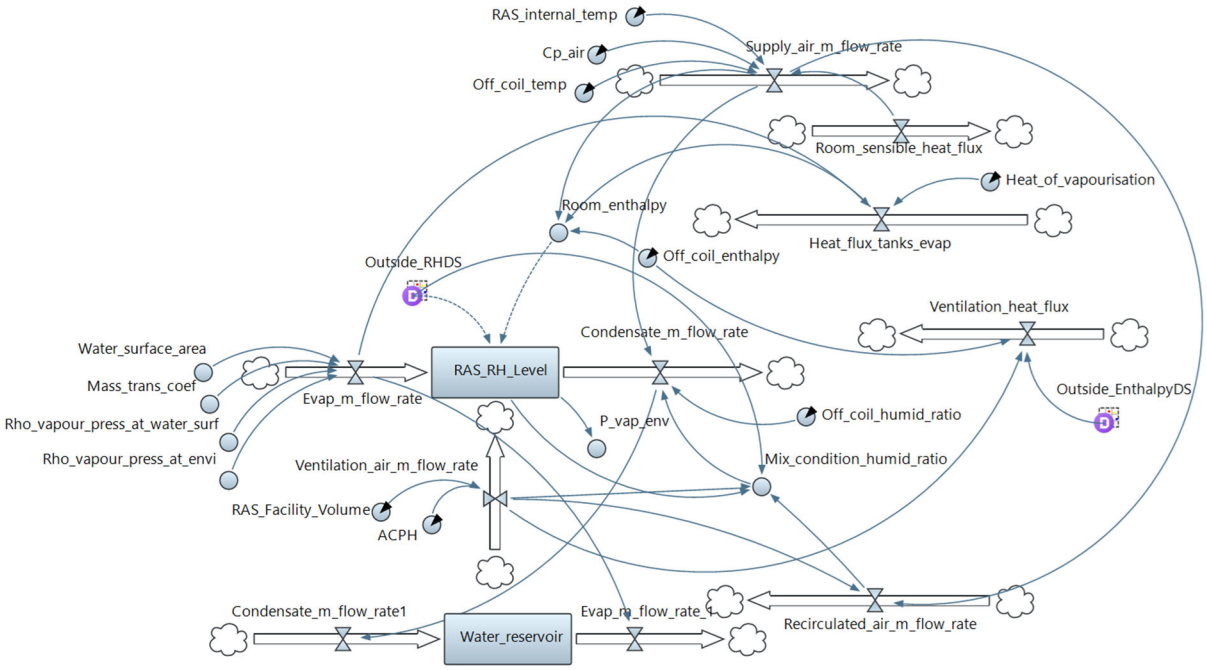

Figure 3.37: *Stock and flow diagram - Volumetric flow rates in RAS facility*

The respective heat fluxes in the aquaculture system were modelled as system flows and are illustrated in Figure 3.38. The heat flux components were modelled using the components in Eq. (19). The effects of external climatic conditions were incorporated into the model by using measured weather data. All the heat fluxes influenced the single system flow which determined the energy consumption of the HVAC system (Eq. (58), Eq. (59) and Eq. (64)) The remaining dynamic variables and parameters are defined in Table 4.7.

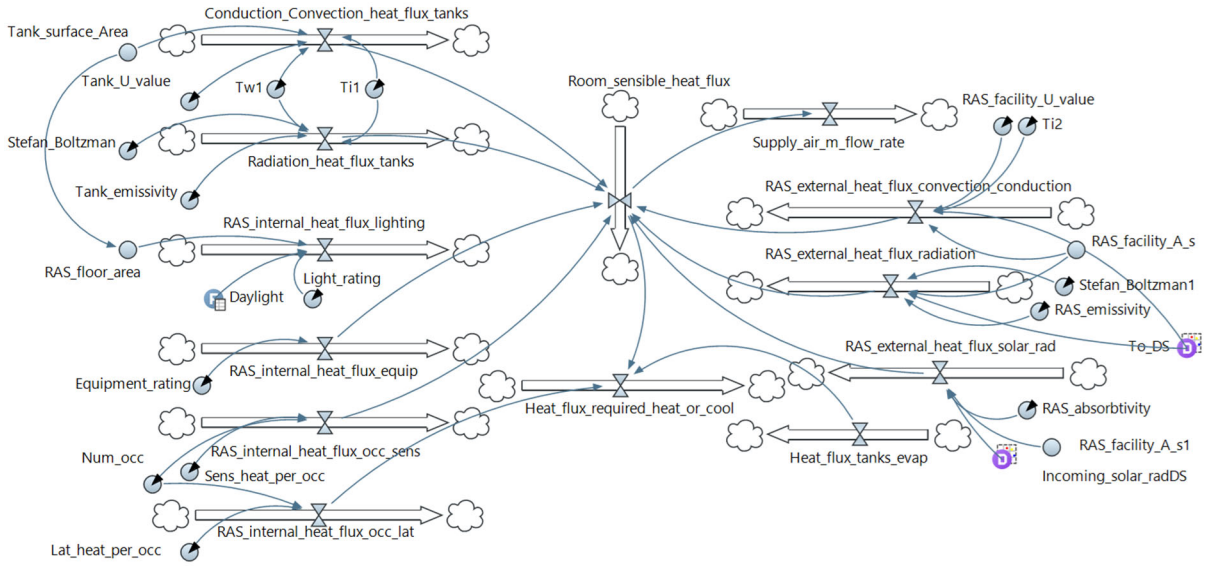

Figure 3.38: *Stock and flow diagram - Heat flux in RAS facility*

The HVAC pumps contributed to the system stock variable namely the total system energy usage as illustrated in Figure 3.39. The pump flow rate, Eq. (61), is a function of the heat required to maintain the desired conditions, Eq. (19). The pump contributed to the system energy usage at a rate defined by Eq. (59). The constant parameters are defined in Table 4.7.

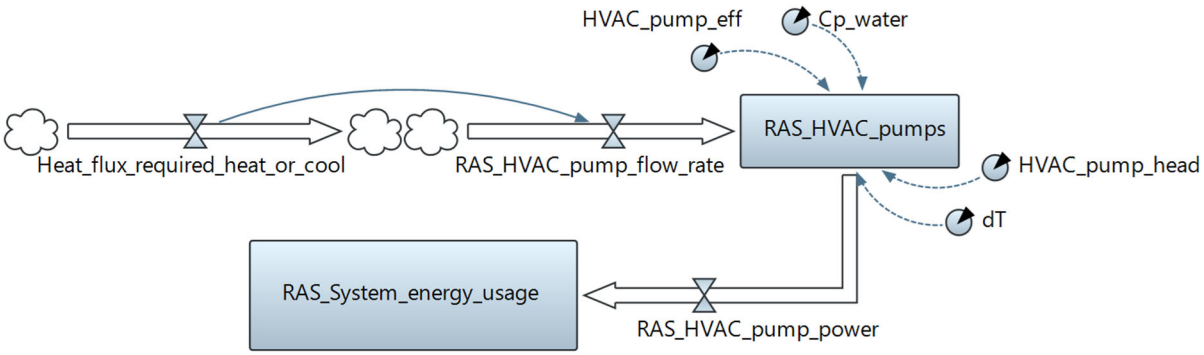

Figure 3.39: *Stock and flow diagram - Environmental control pumps*

The chiller and heat pump contributed to the total system energy stock variable as illustrated in Figure 3.40. The power consumption flow variable. in Eq. (58). was determined by the heat flow required to heat or cool the system shown in Eq. (19). The coefficients of performance are defined in Table 4.7.

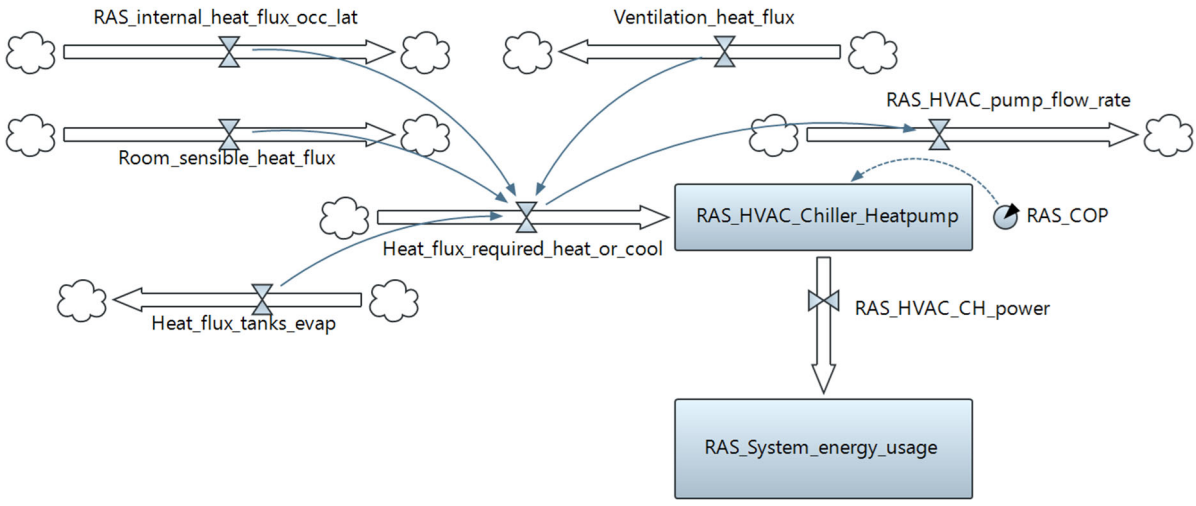

Figure 3.40: *Stock and flow diagram - Environmental control chiller and heat pump*

The air handling units required power to distribute the conditioned air into the space. The power requirement is governed by Eq. (64) and is a function of the supply air flow rate in Eq. (62). The energy flow variable contributed to the total system energy stock variable as illustrated in Figure 3.41. The system pressure drop and fan efficiencies are defined in Table 4.7.

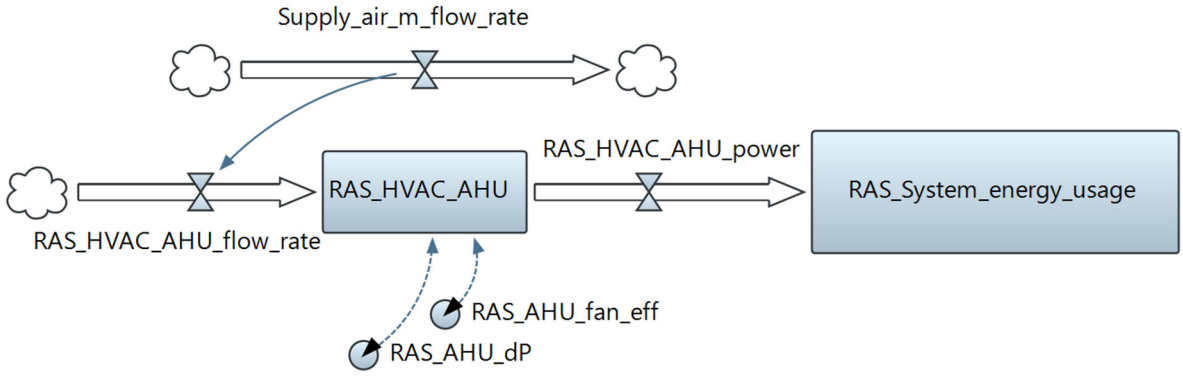

Figure 3.41: *Stock and flow diagram - Environmental control air handling equipment*

3.4.2 Hydroponic Greenhouse

Lighting

The lighting in the hydroponic greenhouse contributed to total system energy use, as illustrated in Figure 3.42. The flow variable is governed by Eq. (72) and the remaining dynamic variables and parameters are defined in Table 4.8. The system is heavily influenced by location dependent hourly daylight values. The values were modelled by using location specific weather data.

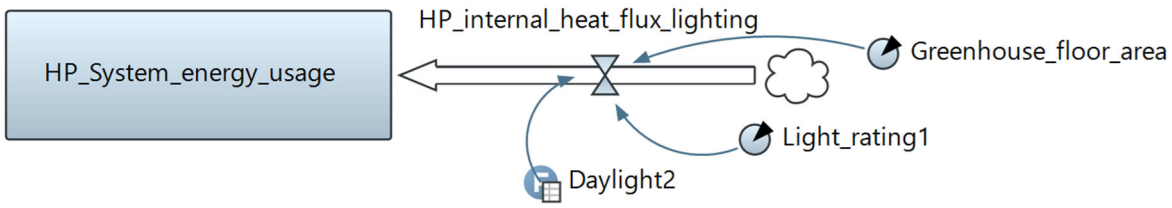

Figure 3.42: *Stock and flow diagram - HP lighting*

Circulation pumps

The energy stock and flow of the hydroponic greenhouse circulation pump is illustrated in Figure 3.43. The energy flow is governed by Eq. (73) and is dependent on the volumetric flow rate defined by Eq. (74). The flow rate of circulation pump is dependent on the

evapotranspiration rate of the crops defined by Eq. (84). The remaining parameters are defined in Table 4.8.

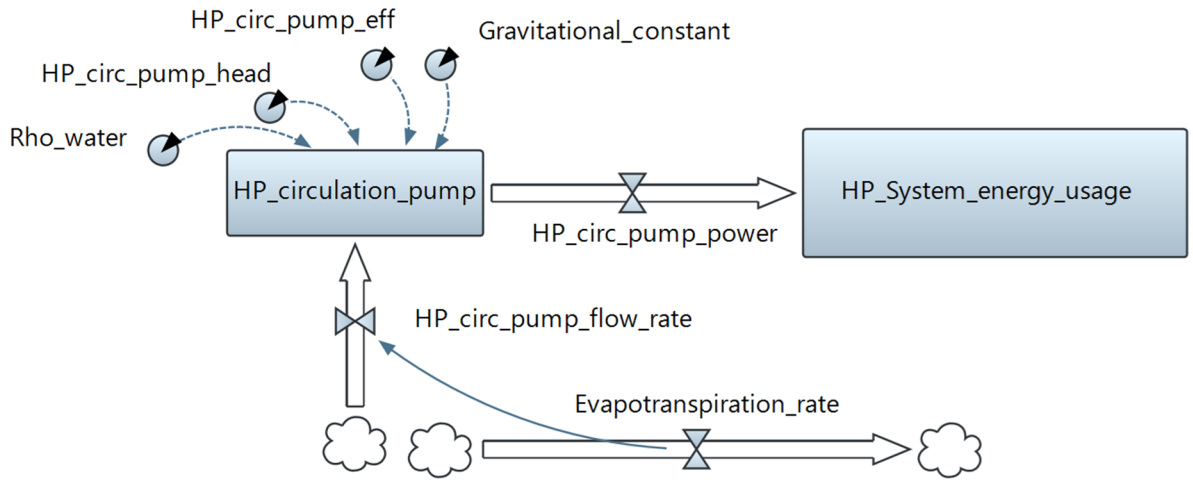

Figure 3.43: *Stock and flow diagram - HP circulation pumps*

Greenhouse Environmental Control

The flow variables in Figure 3.44 were contributing components that determined the heat required to heat or cool the greenhouse. Each flow variable is a component of the heat balance in Eq. (75). The effects of external climatic conditions were incorporated into the model by using measured weather data. The combined heat fluxes influenced the single system flow variable that determined the energy consumption of the HVAC system (Eq. (109), Eq. (111) and Eq. (114)) The remaining dynamic variables and parameters are defined in Table 4.8.

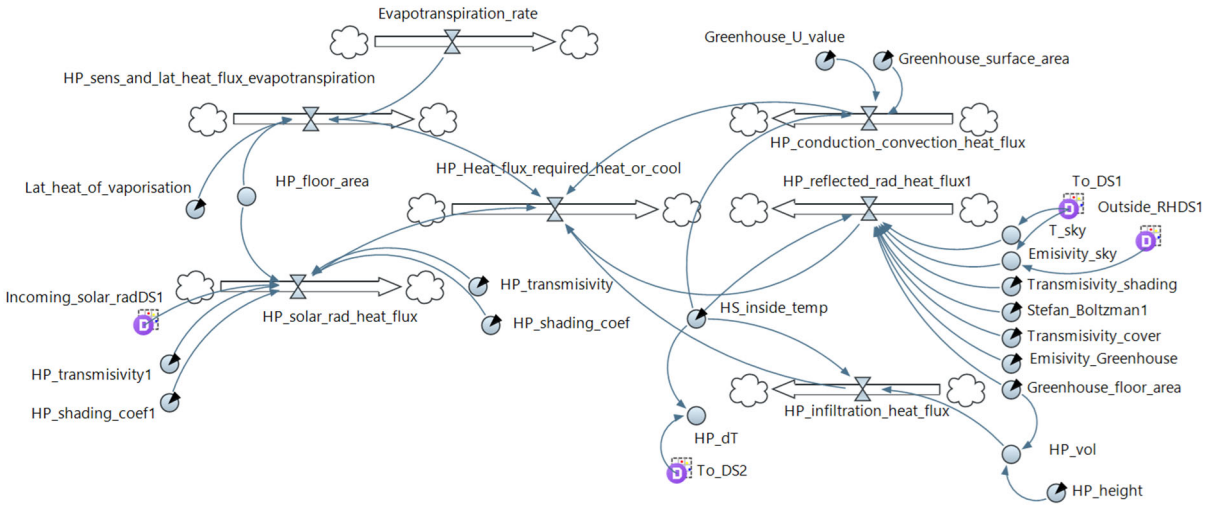

Figure 3.44: *Stock and flow diagram - Environmental control heat flux*

The evapotranspiration rate of the crops, defined by Eq. (84), played an important role in the system water and energy balance. The evapotranspiration rate determined the latent heat component in the system shown in Eq. (83). The evapotranspiration rate also influenced the mass balance as seen in Eq. (116) and in Figure 3.50. The evapotranspiration rate is influenced by the crop height stock variable which is a function of the crop type and growth cycles as defined by Eq. (85) and Table 3.2.

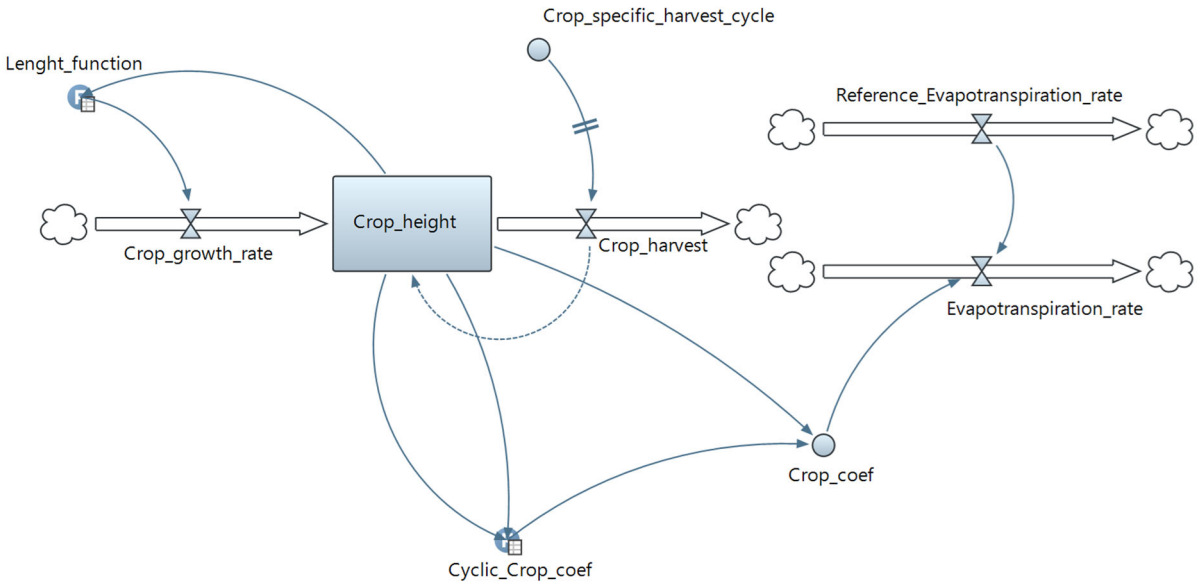

Figure 3.45: *Stock and flow diagram - Environmental control evapotranspiration rate*

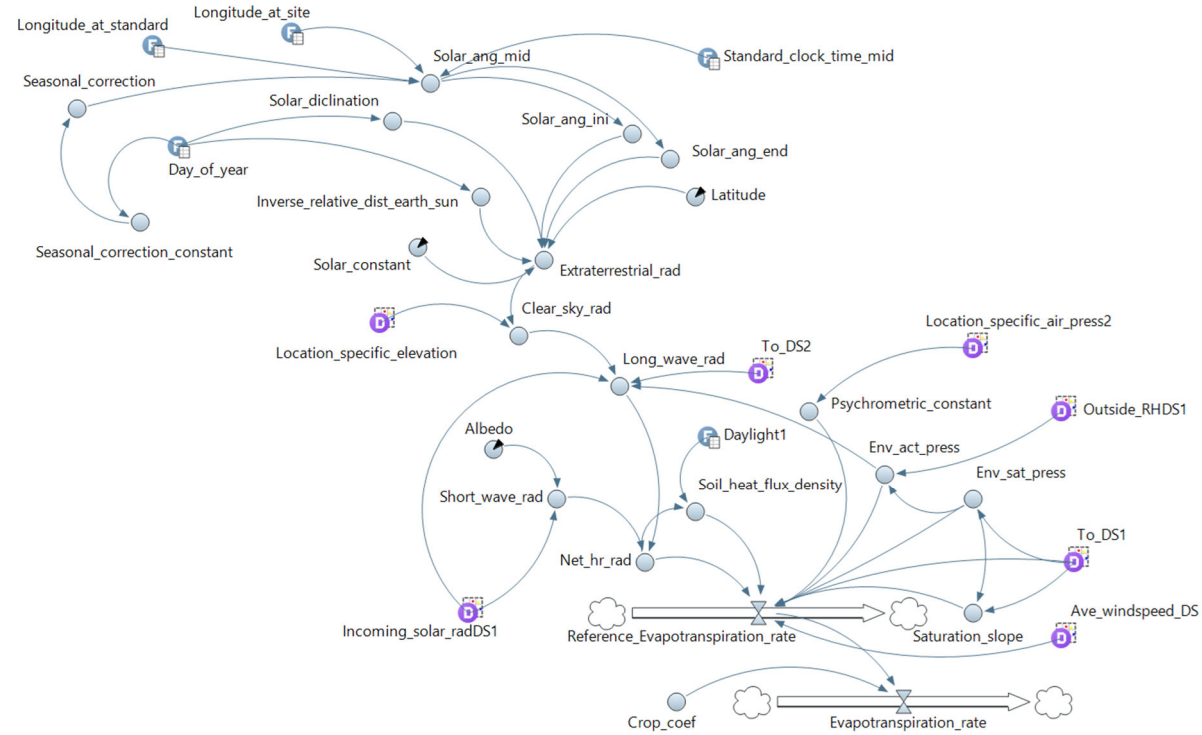

Figure 3.46: *Stock and flow diagram - Environmental control reference evapotranspiration rate*

The evapotranspiration rate is influenced by the *reference* evapotranspiration rate as defined by Eq. (86). This flow variable is a complicated element in the model and were described by the dynamic variables and parameters shown in Figure 3.46. The flow variable is heavily influenced by external weather conditions.

The HVAC pumps contributed to the system stock variable namely the total system energy usage as illustrated in Figure 3.47. The pump flow rate, Eq. (113), is a function of the heat required to maintain the desired conditions, Eq. (75). The pump contributed to the system energy usage at a rate defined by Eq. (112). The constant parameters are defined in Table 4.8.

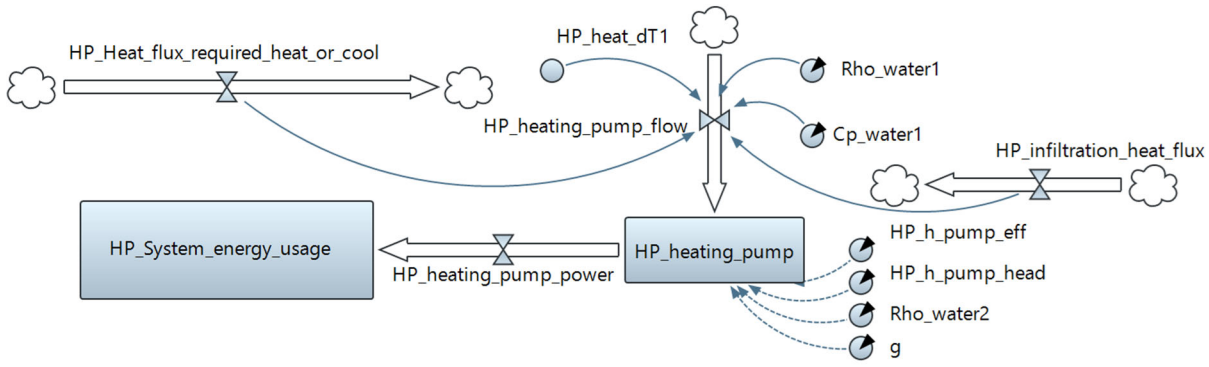

Figure 3.47: *Stock and flow diagram - HP environmental control pumps*

The heat pump contributed to the total system energy stock variable as illustrated in Figure 3.48. The power consumption flow variable, in Eq. (111), was determined by the heat flow required to heat the system shown in Eq. (75). The coefficients of performance are defined in Table 4.8.

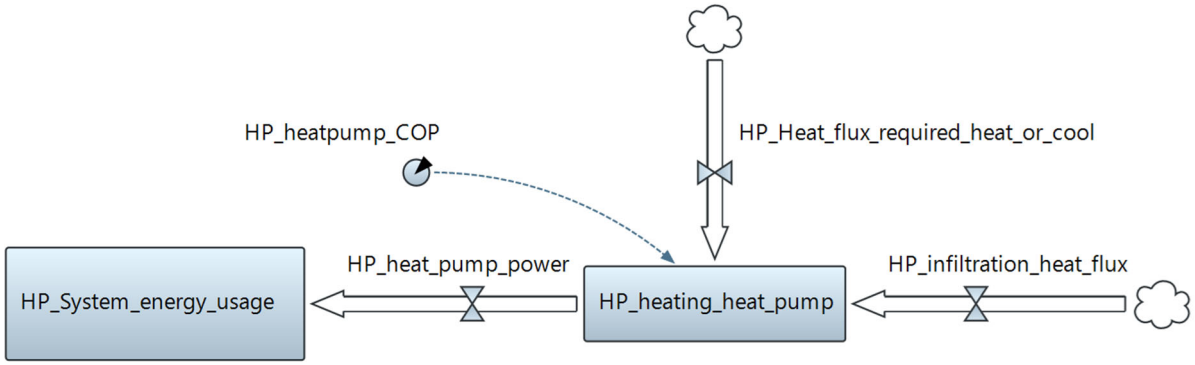

Figure 3.48: *Stock and flow diagram - HP environmental control heat pump*

The air handling units required power to distribute the conditioned air into the space as illustrated in Figure 3.49. The power required to ventilate the system is defined by Eq. (107). The cooling flow variable is a function of the heat balance in Eq. (75) and the internal-external temperature difference. The heating energy flow variable was determined by the heat balance

in Eq. (75) and the internal-external temperature difference. The remaining dynamic variables and constant parameters are defined in Table 4.8.

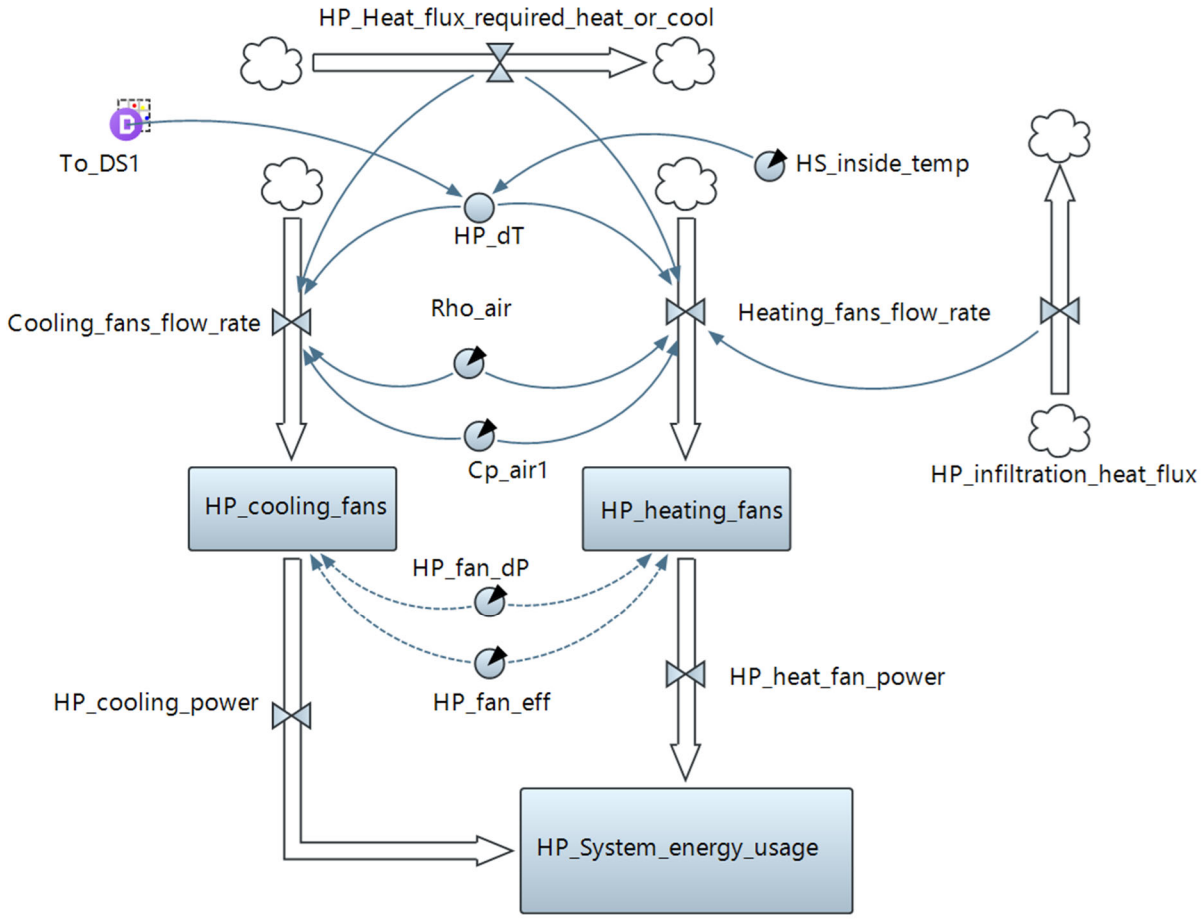

Figure 3.49: *Stock and flow diagram - HP environmental control air handling equipment*

3.4.3 Water Loop

The system water balance is defined by Eq. (116) and was modelled as illustrated in Figure 3.50. It served as a link between the aquaculture facility and the hydroponic greenhouse. The water usage was monitored via the defined stock variable. The respective flow variables were discussed in the previous sections and are illustrated in Figure 3.37 and Figure 3.46.

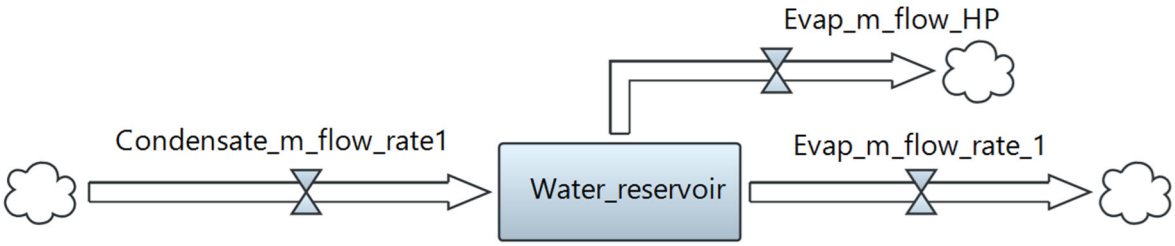

Figure 3.50: *Stock and flow diagram - Decoupled system water balance*

3.5 Simulation Approach

The decoupled system model was firstly described by using causal loop diagrams. This model was used to construct stock and flow diagrams. The stock and flow diagrams were modelled in the software package known as AnyLogic. To properly illustrate the theory applied during the process of creating the system dynamics model, AnyLogic was used. Since AnyLogic has built-in functions specifically used in system dynamics modelling, this software was chosen to construct the stock and flow diagrams. Python was used to handle the large amount of weather data that were fed into the model for all the simulations. The weather data was extracted from location specific weather files containing each location's hourly meteorological data including hourly air temperature, hourly humidity, hourly incoming solar radiation, elevation, hourly wind speeds, cloud coverage, hourly precipitation. Ultimately, 8760 data points were processed by the model for each location simulated. A full discussion and presentation of the data is presented in Chapter Four. Python is suited for this specific model since multiple locations were observed at the same time and advanced mathematical and loop functions were required.

3.6 Concluding Remarks

This chapter presented a full description of the modelled aquaponic system. The climatic and geographical factors of a specific location and the effects of these factors on stock variables such as energy and water usage were explained. The decoupled system was described and illustrated by explaining the theoretical principles that govern the dynamics of the system. The causal loop diagrams were constructed and an illustration of the feedback loops of the systems was presented. The stock and flow diagrams were constructed. An illustration of how the flows (volumetric flow rate and heat flux) contribute to the stocks (energy and water usage) of the system was presented. The effects of local climatic factors can be observed throughout all discussed theory. The following chapter will be dedicated to describing the results obtained from the model and will be discussed in detail.

CHAPTER FOUR

Data Presentation, Results and Discussions

4.1 Chapter Overview

This chapter presents and discusses the results obtained from the models as described in Chapter Three. The climate of the respective regions was discussed and visually presented using weather plots. The constant input parameters for the aquaculture facility and hydroponic greenhouse were presented. The time response plots illustrating the energy usage that is location dependent and location independent were presented and discussed. The total system energy and total system water usage time responses were presented and discussed. These plots are the core results of this research. The best performing regions with regard to energy and water consumption across the world were identified. The best performing regions in South Africa were compared with other prime performing regions to compare the suitability of aquaponic operations in South Africa. Finally, the feedback effects of increasing CO_2 concentrations in the atmosphere on energy usage were presented to emphasise sustainable resource utilisation.

4.2 Period of Analysis

The models presented in Chapter Three describe the rate of energy usage and total energy usage over a defined period. The operation was analysed for a yearly period of 365 days a year. During a yearly period, fish can be harvested three times since the fish have a growth cycle of 120 days. After 120 days the system is purged, cleaned and new fingerlings are added. The greenhouse produces lettuce and has a growth cycle of 100 days. The greenhouse produces three harvests a year and energy is required to sustain half a harvest cycle, which will be harvested the following year.

4.3 Data Presentation

4.3.1 Locational and Climatic Factors

In part, this research aims to determine whether South Africa would be a suitable location to operate and maintain economically thriving commercial aquaponic systems. Therefore, local climatic factors played an important role in determining the energy and water usage of the systems.

Equations describing the system indicate where climatic parameters play a role in determining the energy usage and water usage of the system. Essentially, a higher temperature differential (between inside and outside) and a higher humidity differential will indicate higher energy and water usage throughout a given year. A variety of other location specific parameters such as incoming solar radiation, daylight duration, local air pressure and elevations also play a role in determining system energy usage and water usage.

Climate change and global warming can also have a significant effect on a system. Such factors were incorporated into the proposed models in order to determine the effects of the temperature rise. The system dynamics model can indicate of the effects of global warming and climate change in the coming years in order to make more sustainable policies and decisions.

Weather files were extracted from the database Climate.OneBuilding., (2021). The weather files contain weather data gathered from locations specific weather stations. The data served as input to the system dynamic model. The information was used to simulate hourly responses of the system given the specific weather condition. The following weather parameters were used in the model:

- Hourly outside air temperature
- Hourly outside average humidity
- Elevation
- Pressure
- Incoming solar radiation
- Hourly average wind speeds
- Hourly daylight intensity
- Longitudinal and Latitudinal coordinates.

Domestic Locations

South Africa has a diverse climate and ranges from humid coastal regions to semi-arid regions. Therefore, it is important to compare a variety of locations within South Africa to determine where the most suitable location could be. Major cities and economically developed urban areas were considered, given that these locations will be most suitable from an economical, logistical and infrastructural point of view. The locations were further categorised into coastal regions and inland regions for ease of comparison. Table 4.1 provides a list of the locations that were used in the model. The tables also present a brief locational data summary.

Table 4.1: *Geographic and climatic summary of domestic simulated locations in South Africa*

Location	Region	Weather Station Coordinates	Elevation above sea level [m]	Average yearly ATM [kPa]	Köppen-Geiger climate classification
Cape Town	Coastal	33.97 S, 18.60 E	46	101.0	Mediterranean climate
Durban	Coastal	29.62 S, 31.13 E	127	99.9	Humid subtropical climate
Johannesburg	In-land	26.15 S, 28.00 E	1626	83.9	Oceanic subtropical highland climate
Kimberley	In-land	28.80 S, 24.77 E	1204	88.1	Hot semi-arid climate
Mokopane	In-land	24.2 S, 29.00 E	1097	89.3	Hot semi-arid climate
Nelspruit	In-land	25.43 S, 30.98 E	883	92.1	Subtropical highland climate
Port Elizabeth	Coastal	33.99 S, 25.62 E	68.9	100.7	Humid subtropical climate
Pretoria	In-land	25.92 S, 28.22 E	1500	85.2	Monsoon-influenced humid subtropical climate
Welkom	In-land	28.0 S, 26.67 E	1342	86.7	Cold semi-arid climate

Figure 4.1 to Figure 4.9 present summaries of the three major input parameters to the model namely, hourly outside air temperature, hourly relative humidity and hourly global incoming solar radiation. The data were extracted from the weather file of each location and plotted for each hour of the day for an entire year. A colour scale is applied to indicate the magnitude of each data value. This representation is a quick way to illustrate and summarise the climate and weather patterns of a location. It is presented as an alternative to providing the tabulated weather data of each location.

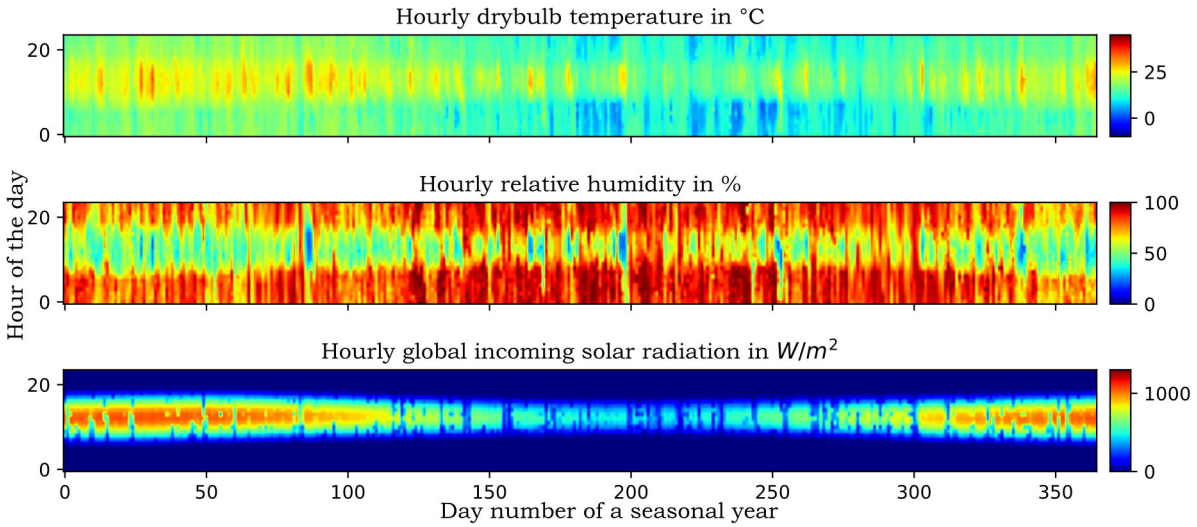

Figure 4.1: *Weather data summary for Cape Town, SA*

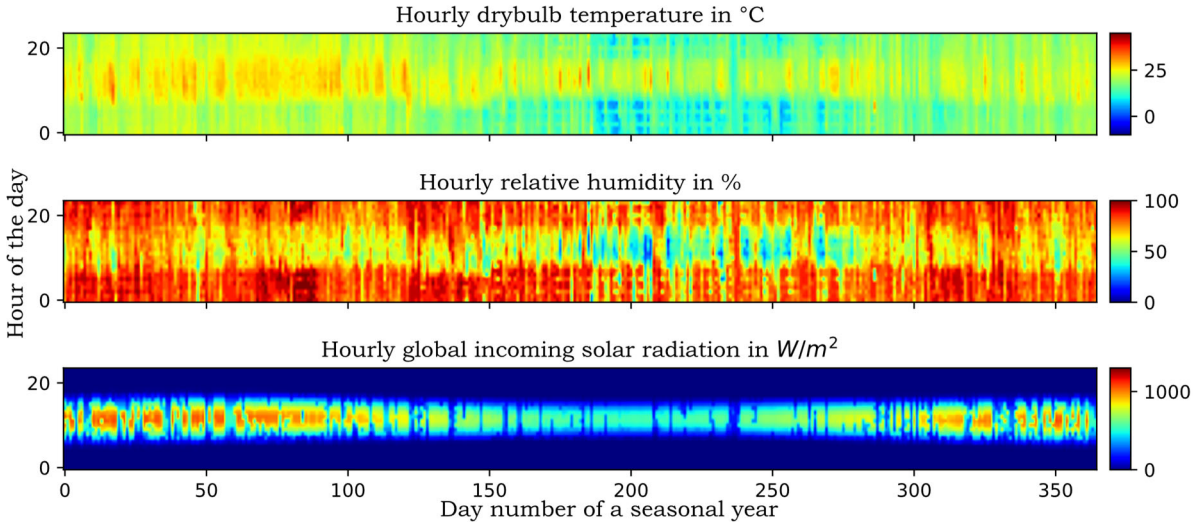

Figure 4.2: *Weather data summary for Durban, SA*

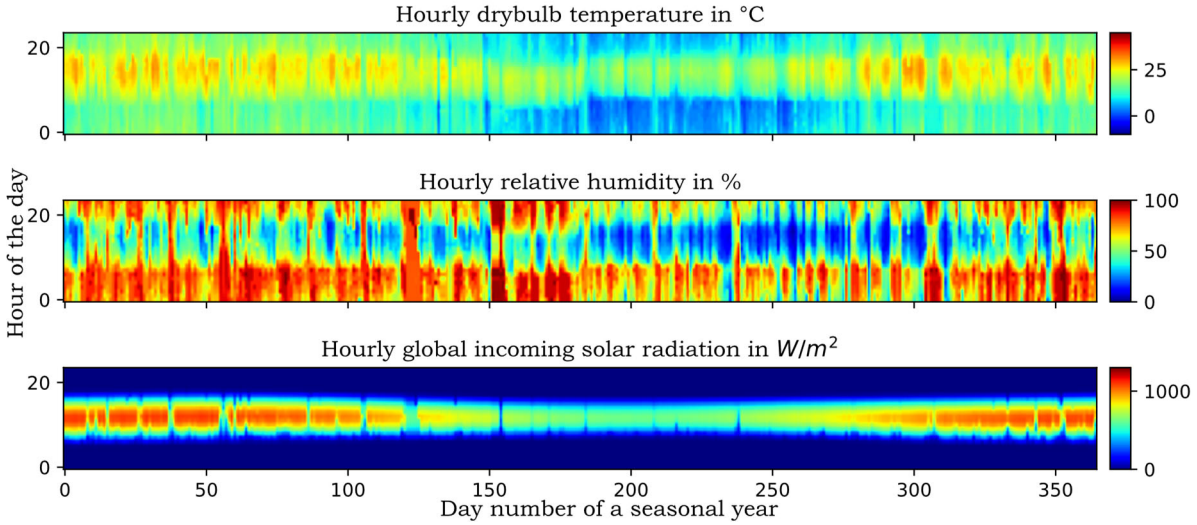

Figure 4.3: *Weather data summary for Johannesburg, SA*

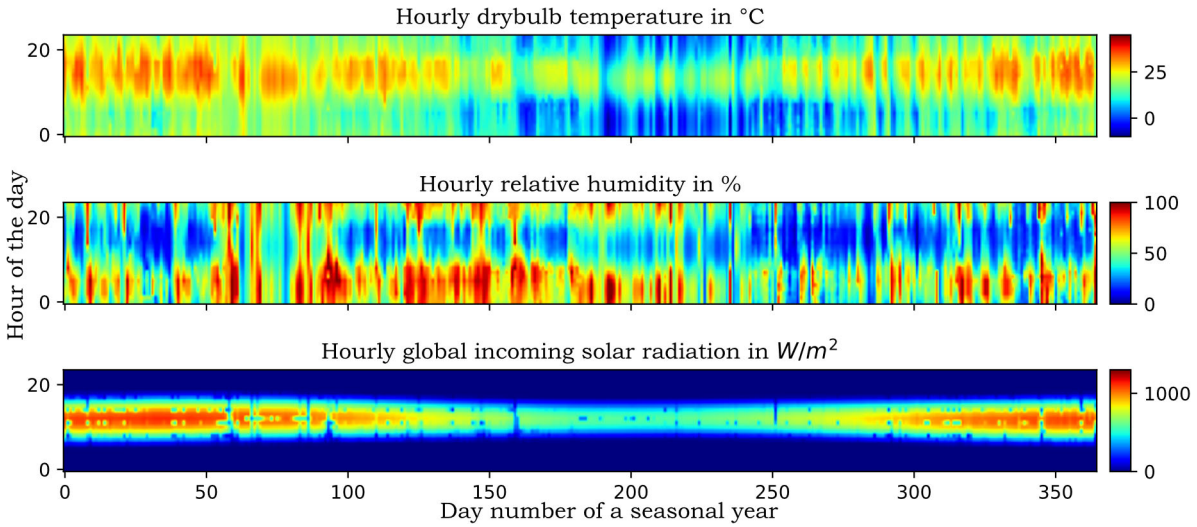

Figure 4.4: *Weather data summary for Kimberley, SA*

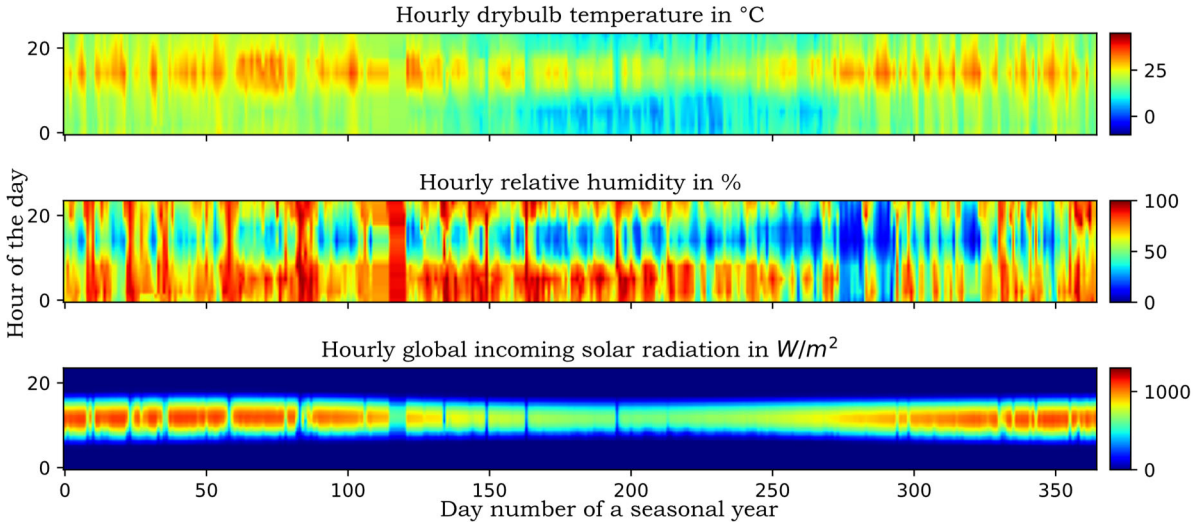

Figure 4.5: *Weather data summary for Mokopane, SA*

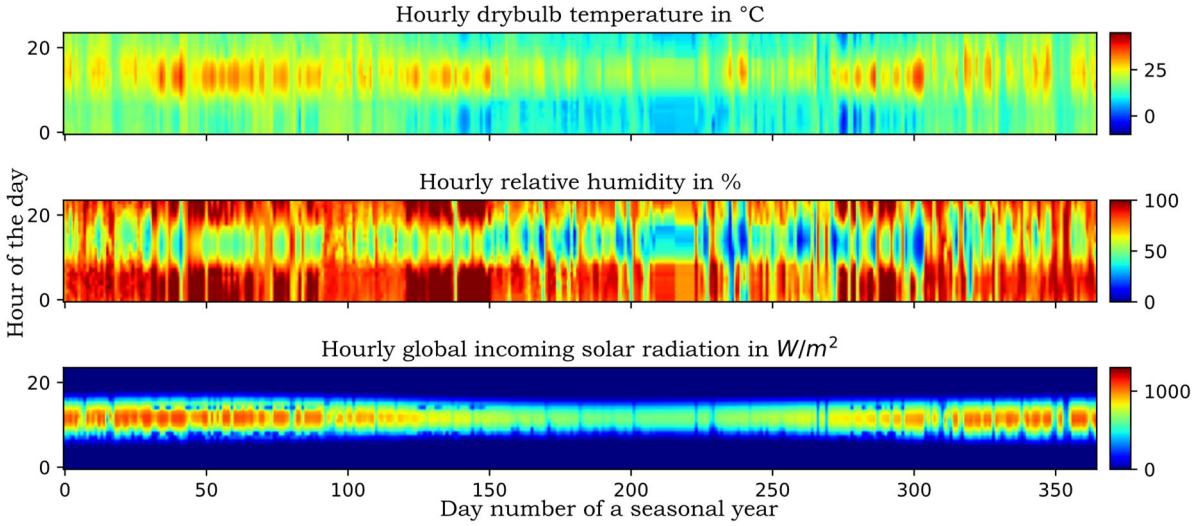

Figure 4.6: *Weather data summary for Nelspruit, SA*

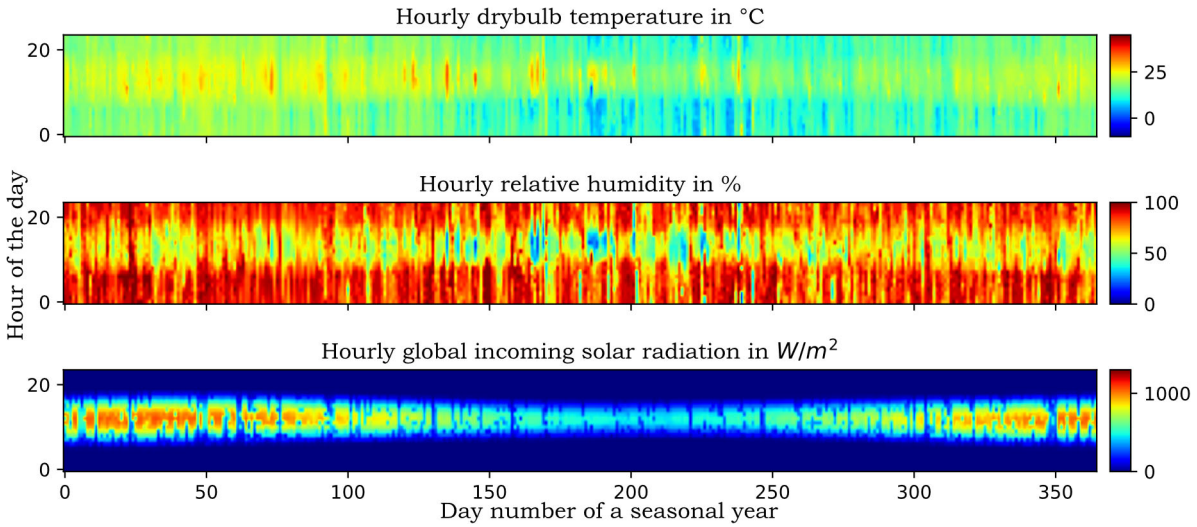

Figure 4.7: *Weather data summary for Port Elizabeth, SA*

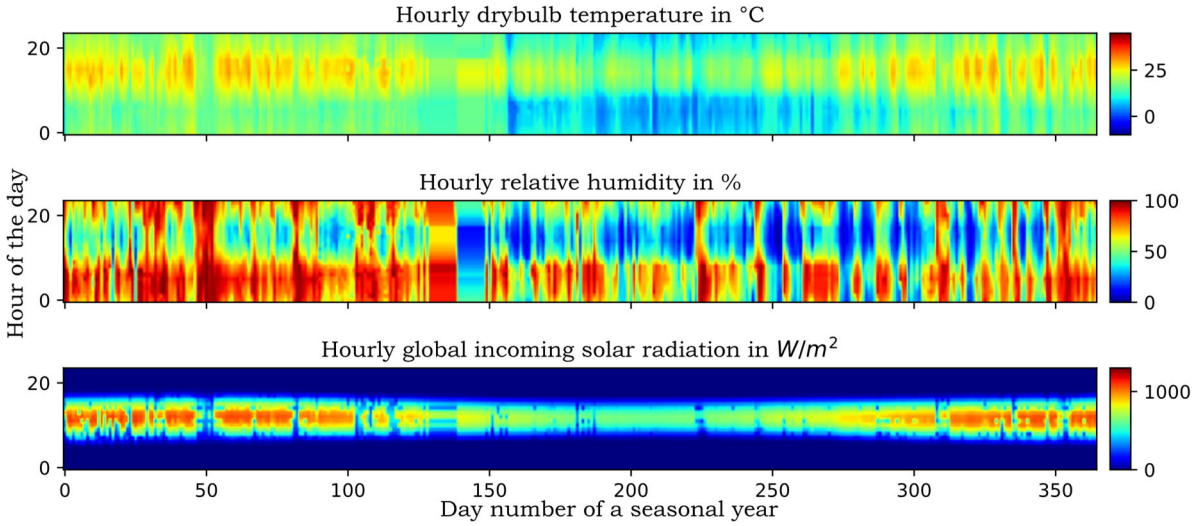

Figure 4.8: *Weather data summary for Pretoria, SA*

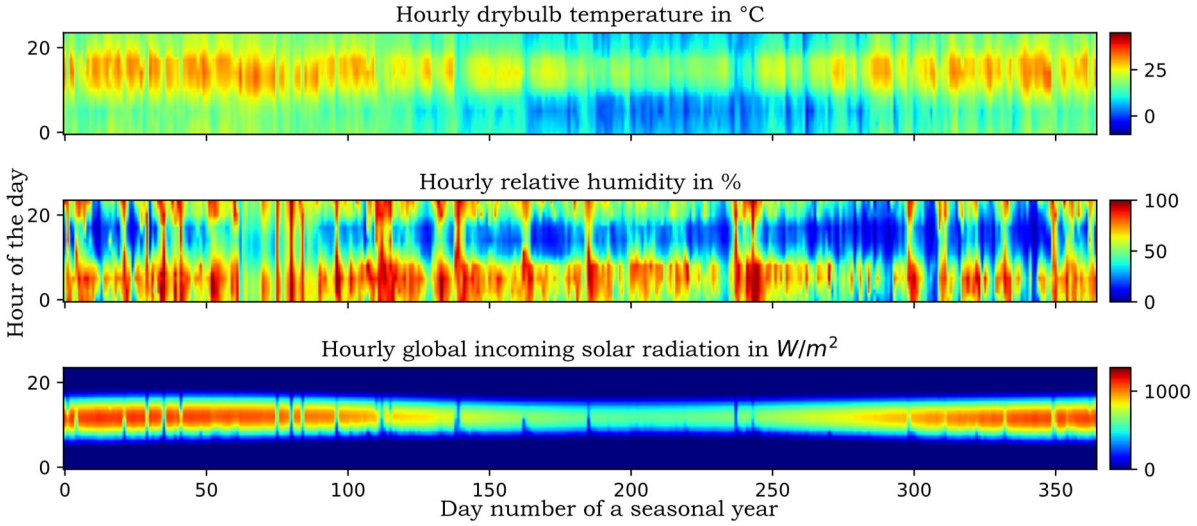

Figure 4.9: *Weather data summary for Welkom, SA*

International Locations

International locations were identified based on where current systems such as cage aquaculture systems are being operated as discussed in Chapter Two. There are several locations around the world where fish are being grown on a commercial scale. These locations are suitable for aquaculture operations in terms of the climate and environment. These locations serve as an appropriate reference to evaluate how well a similar system will perform from an energy and water consumption point of view. However, there are multiple countries globally that operate aquaculture systems and therefore an initial simulation was performed to identify the best performing countries on each continent. This was done to reduce the locations that were presented in this research.

Each global location was categorised based on the continent. Each continent could have a variety of countries where aquaculture and hydroponics are being implemented. The two countries on each continent, that consumed the least energy and water during a year, were identified and eventually, these best performing locations could be compared on a global scale. System performance was evaluated based on the locations response to energy and water usage. High energy and water usage indicated low system performance and low energy and water usage indicated high system performance. The Australia-Oceania area was excluded due to the stringent policies regarding invasive species. Antarctica was excluded due to extremely undesirable conditions. Table 4.2 to Table 4.6 provide a list of the international locations, categorised based on continental location. The tables also provide a brief locational data summary. The climate summary plots are presented. Only the plots of the best performing countries were presented.

Africa

Table 4.2: *Geographic and climatic summary of simulated locations in Africa*

Location	Region	Weather Station Coordinates	Elevation above sea level [m]	Average yearly ATM [kPa]	Köppen-Geiger climate classification
Tanta	Egypt	30.78 N, 31.0 E	12	101.2	Tropical and subtropical desert climate
Abuja	Nigeria	9.25 N, 7.0 E	344	97.4	Tropical savanna climate
Tororo	Uganda	0.68 N, 34.17 E	1171	88.6	Tropical rainforest climate
Lusaka	Zambia	15.33 S, 28.45 E	1152	88.7	Monsoon-influenced humid subtropical climate

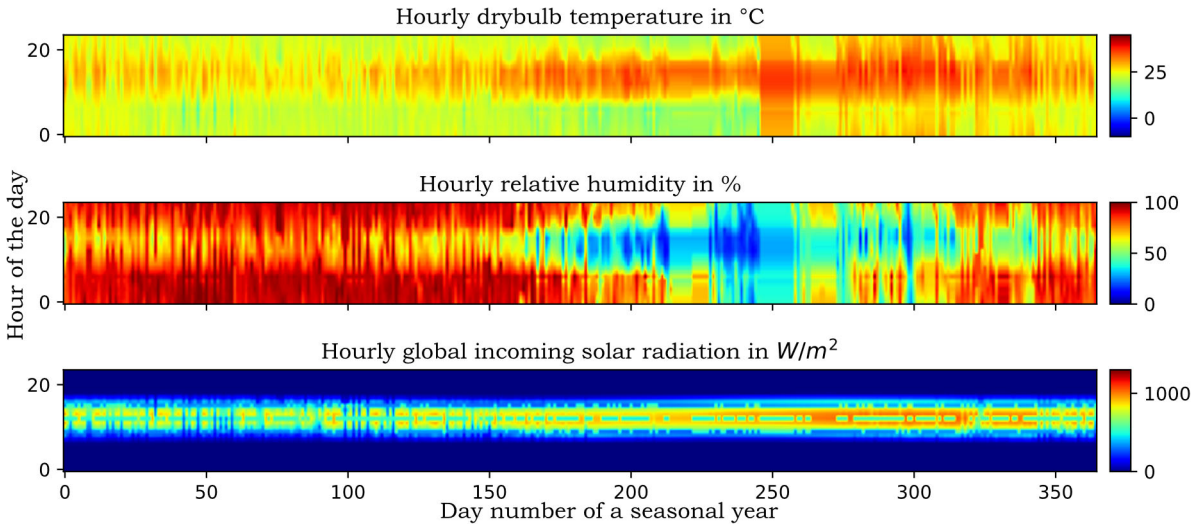

Figure 4.10: *Weather data summary for Abuja, Nigeria*

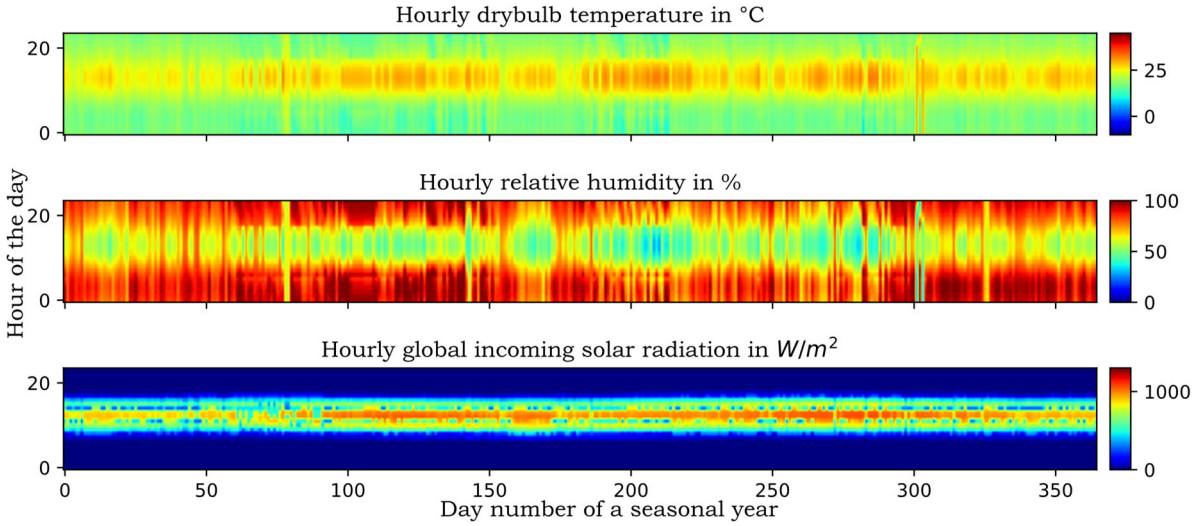

Figure 4.11: *Weather data summary for Tororo, Uganda*

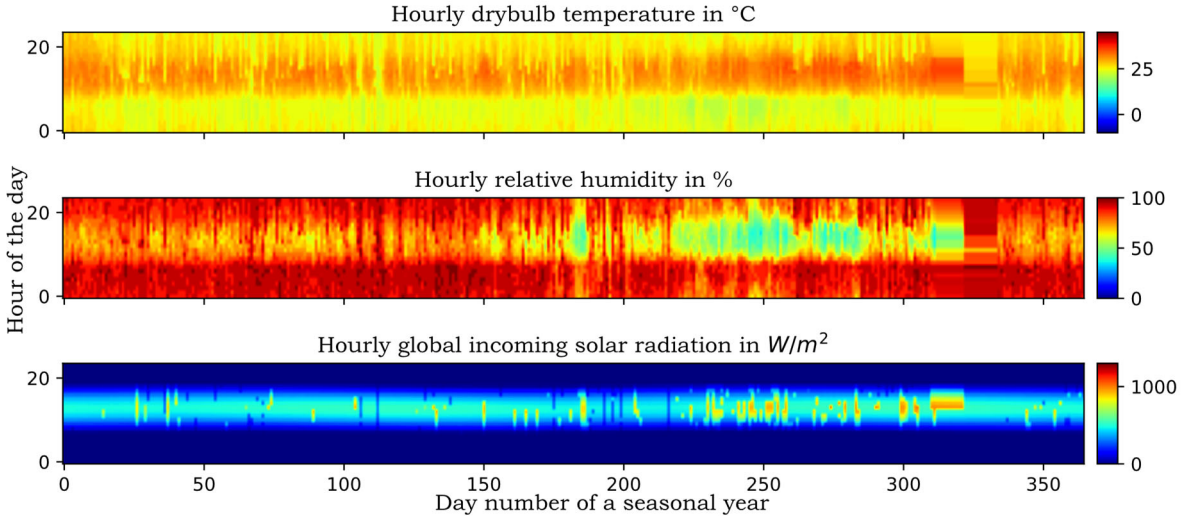

Figure 4.12: *Weather data summary for Alor Setar, Malaysia*

Asia

Table 4.3: *Geographic and climatic summary of simulated locations in Asia*

Location	Region	Weather Station Coordinates	Elevation above sea level [m]	Average yearly ATM [kPa]	Köppen-Geiger climate classification
Tangail	Bangladesh	24.25 N, 89.93 E	14	100.6	Tropical savanna
Guangzhou	China	23.17 N, 113.33 E	41	100.8	Humid subtropical climate
Bandar Aceh	Indonesia	5.52 N, 95.42 E	19.8	100.7	Tropical rainforest
Vientiane	Laos	17.99 N, 102.56 E	171.9	99.2	Tropical savanna climate
Alor Setar	Malaysia	6.2 N, 100.4 E	5	101.3	Tropical monsoon climate
Myitkyina	Myanmar	25.36 N, 97.4 E	147	99.3	Humid subtropical climate
Vigan-Mindoro	Philippines	17.55 N, 120.36 E	4.9	101.0	Tropical savanna
Taipei	Taiwan	25.07 N, 121.55 E	6	101.4	Humid subtropical climate
Phichit Agromet	Thailand	16.33 N, 100.37 E	39.4	100.4	Tropical savanna
Can Tho	Vietnam	10.08 N, 105.72 E	3.1	101.3	Tropical savanna

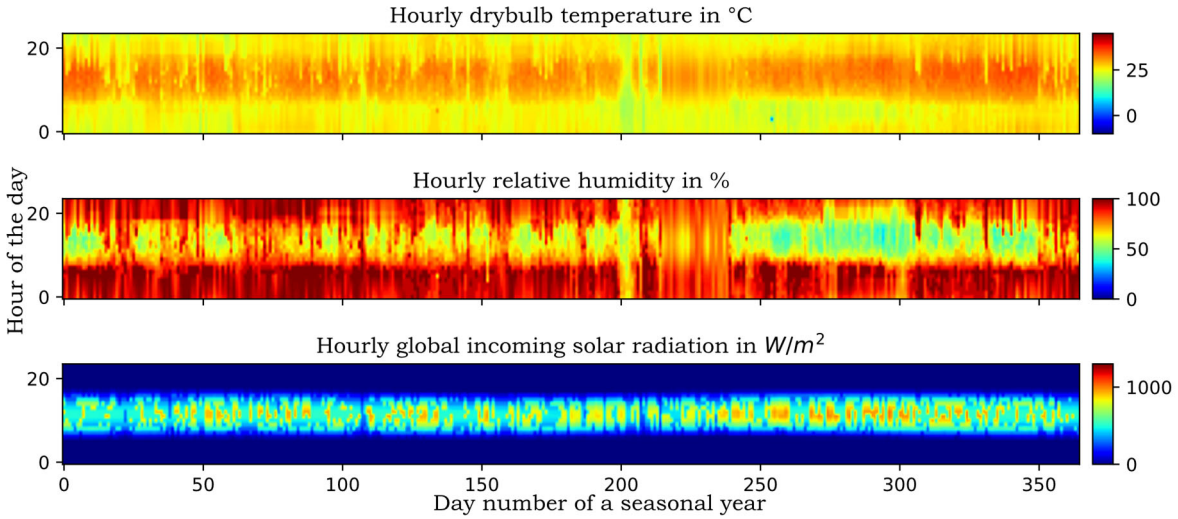

Figure 4.13: *Weather data summary for Can Tho, Vietnam*

Europe

Table 4.4: *Geographic and climatic summary of simulated locations in Europe*

Location	Region	Weather Station Coordinates	Elevation above sea level [m]	Average yearly ATM [kPa]	Köppen-Geiger climate classification
Berlin	Germany	52.47 N, 13.4 E	49	100.9	Marine West coast climate
Groningen	Netherlands	53.13 N, 6.58 E	4	101.5	Marine West coast climate
Lisbon	Portugal	38.73 N, 9.15 W	71	100.4	Subtropical-Mediterranean climate
Madrid	Spain	40.45 N, 3.55 W	582	95.1	Semi-arid climate
Glasgow	United-Kingdoms	55.86 N, 4.267 W	17	101.0	Marine West coast climate
Berlin	Germany	52.47 N, 13.4 E	49	100.9	Marine West coast climate

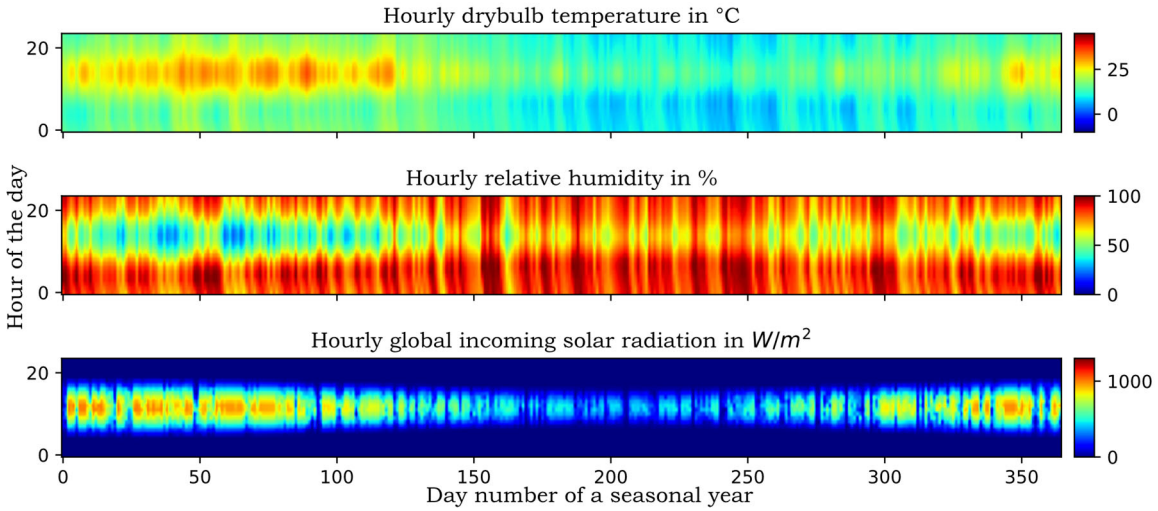

Figure 4.14: *Weather data summary for Lisbon, Portugal*

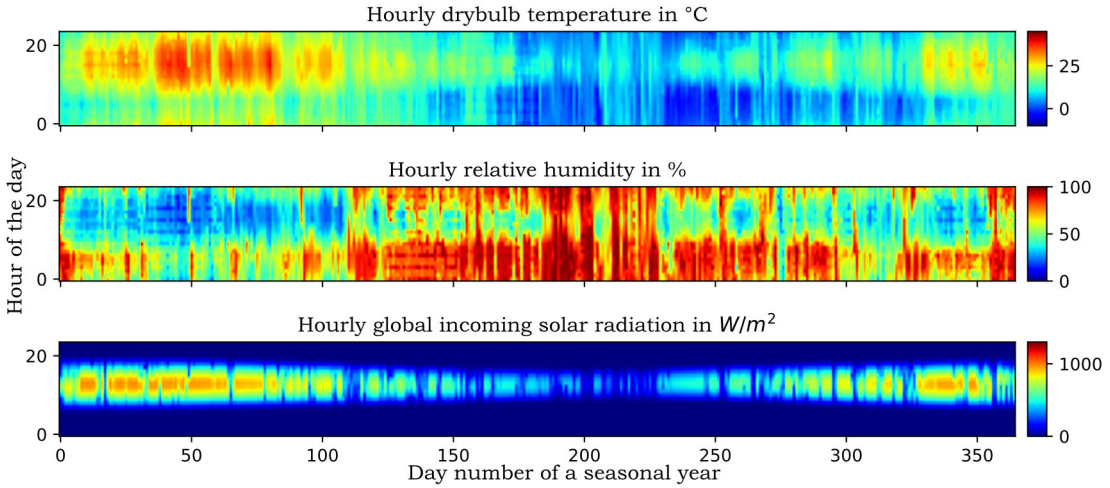

Figure 4.15: *Weather data summary for Madrid, Spain*

North America

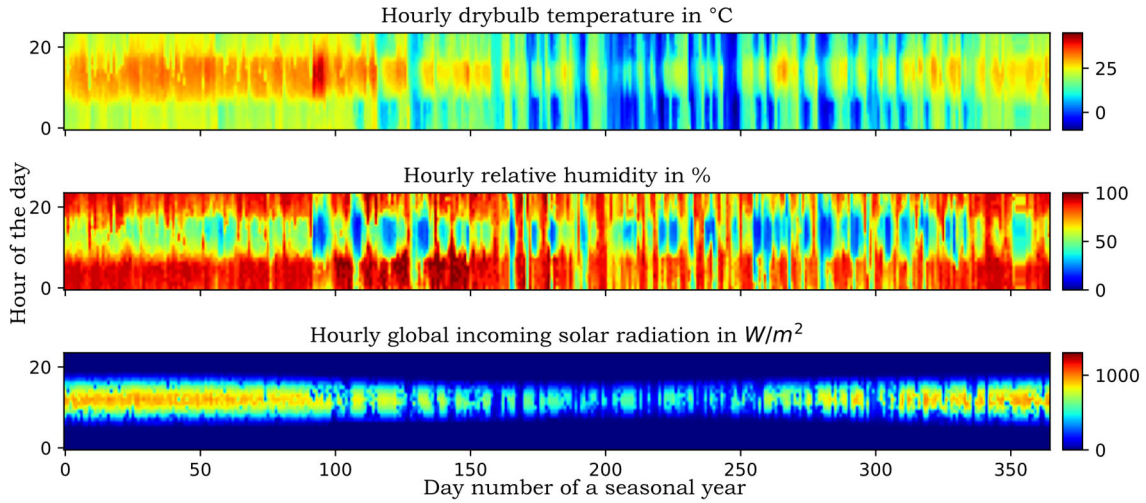

Figure 4.16: *Weather data summary for Texas, USA*

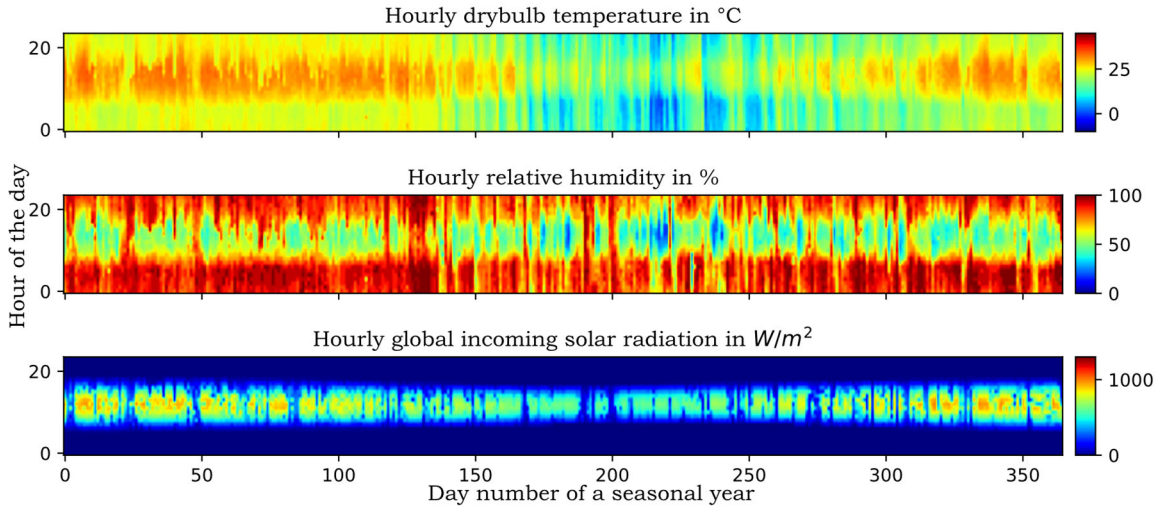

Figure 4.17:*Weather data summary for Florida, USA*

Table 4.5: *Geographic and climatic summary of simulated locations in North America*

Location	Region	Weather Station Coordinates	Elevation above sea level [m]	Average yearly ATM [kPa]	Köppen-Geiger climate classification
Phoenix	USA (AZ)	33.45 N, 112.0 W	337	97.4	Tropical and subtropical desert climate
San Francisco	USA (CA)	37.62 N, 122.4 W	2	101.7	Mediterranean climate
Orlando	USA (FL)	28.55 N, 81.33 W	33	101.4	Humid subtropical climate
Boone	USA (IA)	42.05 N, 93.85 W	354	97.1	Marine West coast climate
Chicago	USA (IL)	41.78 N, 87.75 W	186	99.4	Hot-summer humid continental climate
New York	USA (NY)	40.78 N, 73.97 W	40	101.7	Humid subtropical climate
Columbus	USA (OH)	40.0 N, 82.88 W	247	98.8	Hot-summer humid continental climate
Jackson	USA (TN)	35.6 N, 88.92 W	132	100.1	Humid subtropical climate
Nacogdoches	USA (TX)	31.58 N, 94.72 W	108	100.0	Humid subtropical climate
Montpelier	USA (VT)	44.2 N, 72.6 W	343	97.4	Mediterranean climate

South America

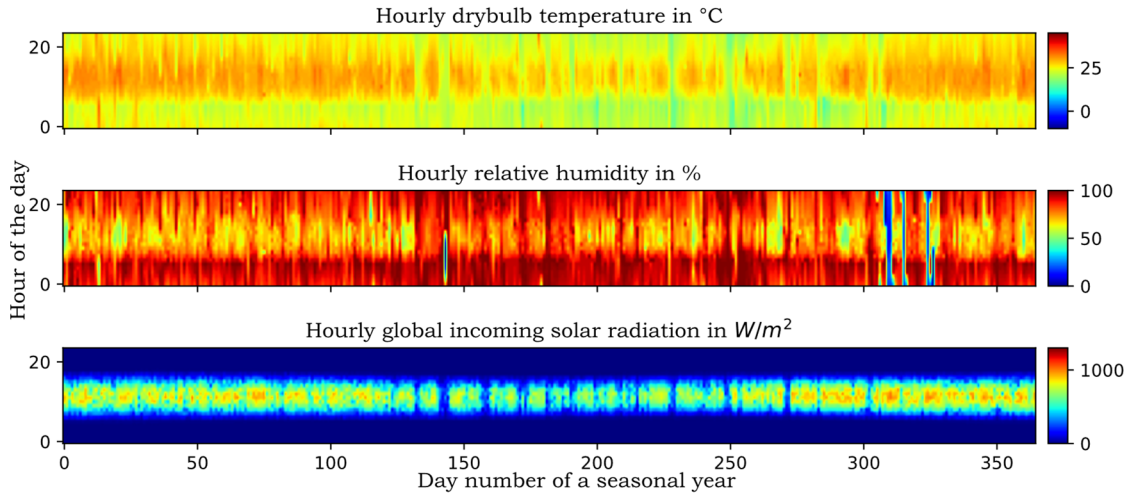

Figure 4.18: *Weather data summary for Tela, Honduras*

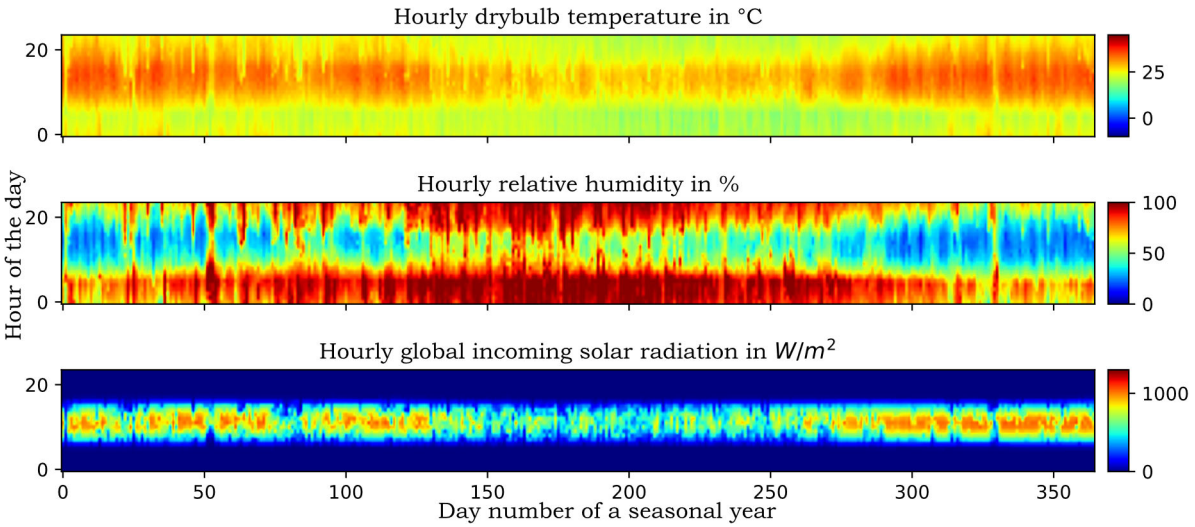

Figure 4.19: *Weather data summary for Floresta, Brazil*

Table 4.6: *Geographic and climatic summary of simulated locations in South America*

Location	Region	Weather Station Coordinates	Elevation above sea level [m]	Average yearly ATM [kPa]	Köppen-Geiger climate classification
Floresta	Brazil	8.61 S, 38.59 W	329	97.5	Tropical wet
Neiva	Colombia	2.95 N, 75.29 W	446.2	96.2	Tropical climate
Nicoya	Costa Rica	10.15 N, 85.45 W	120	99.8	Tropical wet
Salinas-Paez	Ecuador	2.21 S, 81.0 W	5.5	101.2	Hot semi-arid climate
Tela	Honduras	15.72 N, 87.48 W	3	101.2	Tropical rainforest climate

4.3.2 Data Validity

It should be mentioned that not all weather files contain data from the most recent years. As far as possible, the most recent and relevant data were used to obtain the most accurate output from the models. If data for a specific location were unreasonably outdated, a different location was considered. For the purpose of this research, it is more important to view general climatic trends rather than complete data accuracy during a specific year of measurement.

4.3.3 Comparability

Certain locations are situated in the northern hemisphere while others are situated in the southern hemisphere. In order to ensure comparability between these locations with regard to seasonal trends, the model considered and simulated a seasonal year rather than a standard calendar year, that is, at the start of summer to the end of spring rather than 1 January to 31 December.

Locations where aquaculture and aquaponics are currently implemented, experience conditions that are often so favourable that there is no need for water recirculation or growing facilities as proposed by this research. Asian countries, for example, make use of outside cage farming since water is abundant and the climate is very mild. These types of operations require a minimal amount of resources and energy and therefore more profit can be made. To ensure comparability, a generic system was constructed. The generic system was defined by a fixed set of parameters such as facility size, yield goals, physical system components configuration, water quality and construction materials. Therefore, only the effects of local climatic factors on aspects such as energy and water usage were evaluated.

Data smoothing techniques were applied to better visualise the results. This research is not focused on the accuracy of each individual measured data point but rather the general trend and shape of the time series. General trends and moving averages can indicate how regional climates would generally affect the parameters that are being observed. Comparisons can easily be drawn using these techniques.

4.3.4 Constant Input Parameters for the Recirculating Aquaculture System

In describing the generic notional model, certain parameters were independent of location. Table 4.7 includes a summary of all constant input parameters to the aquaculture facility that did not change based on the location. Descriptions of all symbols are noted in the list of nomenclature.

Table 4.7: *Constant input parameters for the RAS facility*

Parameter	Value	Unit
$\boldsymbol{Fish\ Species}$	*Nile Tilapia*	–
$\boldsymbol{K_o}$	3.125	g
$\boldsymbol{K_F}$	250	g
$\boldsymbol{G_f}$	1000	t
$\boldsymbol{d_{gc}}$	120	$days$
$\boldsymbol{d}$	100	kg_{fish}/m^3
$\boldsymbol{HRT}$	3600	s
$\boldsymbol{h_t}$	1.8	m
$\boldsymbol{r_t}$	7	m
$\boldsymbol{\eta_{RAS,cp}}$	80	%
$\boldsymbol{H_{RAS,circ\ pump}}$	20	m
$\boldsymbol{\rho_{water}}$	999	kg/m^3
$\boldsymbol{g}$	9.81	m/s^2
$\boldsymbol{O_2C}$	0.6	kg_{O_2}/kg_{feed}
$\boldsymbol{\rho_{O_2}}$	1.331	kg/m^3
$\boldsymbol{R_{O_2}}$	0.2598	$J.mol^{-1}.K^{-1}$
$\boldsymbol{k}$	1.395	–
$\boldsymbol{Z_c}$	1	–
$\boldsymbol{P_{O_2,1}}$	200×10^3	Pa
$\boldsymbol{P_{O_2,2}}$	20×10^6	Pa
$\boldsymbol{T_{O_2,1}}$	299	K
$\boldsymbol{\eta_{RAS,O_2\ comp}}$	80	%
$\boldsymbol{CO_2P}$	1.4	kg_{CO_2}/kg_{O_2}
$\boldsymbol{\eta_{RAS,CO_2\ fan}}$	60	%
$\boldsymbol{\Delta P_{RAS,CO_2\ fan}}$	250	Pa
$\boldsymbol{P_{RAS,light}}$	2	W/m^2
$\boldsymbol{D_v}$	18	$hours$
$\boldsymbol{P_{RAS,UV}}$	0.05	W/m^2
$\boldsymbol{T_w}$	28	℃
$\boldsymbol{T_{RAS,i}}$	26	℃
$\boldsymbol{U_{RAS,tanks}}$	2	W/m^2K
$\boldsymbol{\varepsilon_{tank}}$	0.7	–

Parameter	Value	Unit
$\boldsymbol{P_{atm}}$	101.3	kPa
$\boldsymbol{\emptyset_n}$	50	%
$\boldsymbol{\omega_n}$	10.5	g_{H_2O}/kg_{air}
$\boldsymbol{A_{fRAS}}$	10,000	m^2
$\boldsymbol{h_{RAS}}$	8	m
$\boldsymbol{N_{Occ}}$	50	–
$\boldsymbol{Q_{sens}}$	70.3	$W/person$
$\boldsymbol{Q_{lat}}$	149	$W/person$
$\boldsymbol{\dot{Q}_{RAS,i\ equip}}$	2	W/m^2
$\boldsymbol{U_{RAS}}$	0.5	W/m^2K
$\boldsymbol{AC}$	2	$1/hr$
$\boldsymbol{h_{fg}}$	2434.56	kJ/kg
$\boldsymbol{\alpha_{RAS}}$	0.3	–
$\boldsymbol{T_{db3a}}$	15	℃
$\boldsymbol{T_{wb3a}}$	14	℃
$\boldsymbol{T_{db3b}}$	38	℃
$\boldsymbol{T_{wb3b}}$	31	℃
$\boldsymbol{\Delta T_{cool}}$	6	℃
$\boldsymbol{COP_{RAS,chiller}}$	10	–
$\boldsymbol{\Delta T_{heat}}$	5	℃
$\boldsymbol{COP_{RAS,heatpump}}$	12	–
$\boldsymbol{C_{p,water}}$	4186	J/kgK
$\boldsymbol{\eta_{RAS,HVAC\ cool\ p}}$	80	%
$\boldsymbol{\eta_{RAS,HVAC\ heat\ p}}$	80	%
$\boldsymbol{H_{RAS,HVAC\ pump\ cool}}$	30	m
$\boldsymbol{H_{RAS,HVAC\ pump\ heat}}$	30	m
$\boldsymbol{C_{p,air}}$	1000	J/kgK
$\boldsymbol{\eta_{RAS,AHU\ cool\ fan}}$	60	%
$\boldsymbol{\eta_{RAS,AHU\ heat\ fan}}$	60	%
$\boldsymbol{\Delta P_{RAS,AHU\ Cool}}$	500	Pa
$\boldsymbol{\Delta P_{RAS,AHU\ Heat}}$	500	Pa

4.3.5 Constant Input Parameters for the Hydroponic Greenhouse

As part of the generic notional model, the hydroponic greenhouse had the following constant input parameters (Table 4.8):

Table 4.8: *Constant input parameters for the HP Greenhouse*

Parameter	Value	Unit
$\boldsymbol{Crop\ type}$	*Lettuce*	–
$\boldsymbol{A_{fHP}}$	2500	m^2
$\boldsymbol{SC}$	1.02	–
$\boldsymbol{\tau_c}$	0.76	–
$\boldsymbol{\lambda}$	2410	kJ/kg
$\boldsymbol{U_{HP}}$	2.73	W/m^2K
$\boldsymbol{A_{cHP}}$	3397.5	m^2
$\boldsymbol{T_{iHP}}$	26	℃
$\boldsymbol{\sigma}$	5.67×10^{-8}	W/m^2K^4
$\boldsymbol{\tau_{tc}}$	0.76	–
$\boldsymbol{\tau_{os}}$	0.7	–

Parameter	Value	Unit
$\boldsymbol{\varepsilon_{iHP}}$	0.9	–
$\boldsymbol{\rho_{air}}$	1.2	kg/m^3
$\boldsymbol{C_{p,air}}$	1000	J/kgK
$\boldsymbol{\eta_{HP,f}}$	60	%
$\boldsymbol{\Delta P_{HP,fan}}$	500	Pa
$\boldsymbol{h_{HP}}$	10	m
$\boldsymbol{P_{HP,light}}$	0.5	W/m^2
$\boldsymbol{H_{HP,pump}}$	20	m
$\boldsymbol{\eta_{HP,p}}$	75	%
$\boldsymbol{COP_{HP}}$	12	–

4.4 Results and Discussion

4.4.1 Location Independent Energy Time Response

Certain components, which require energy in the system, did not change based on the location. Certain components were process driven rather than influenced by the external environment. These components included the RAS circulation pumps, described by Eq. (4), O_2 generation described by Eq. (13), CO_2 degassing described by Eq. (2), RAS lighting described by Eq. (1) and UV-disinfection described by Eq. (12). The system biomass drives the energy usage of these components and since a constant internal environment was maintained throughout the year, the energy time series was the same for each location. The above-mentioned components are in the same order of magnitude and are presented on a single plot for comparison purposes (Figure 4.20).

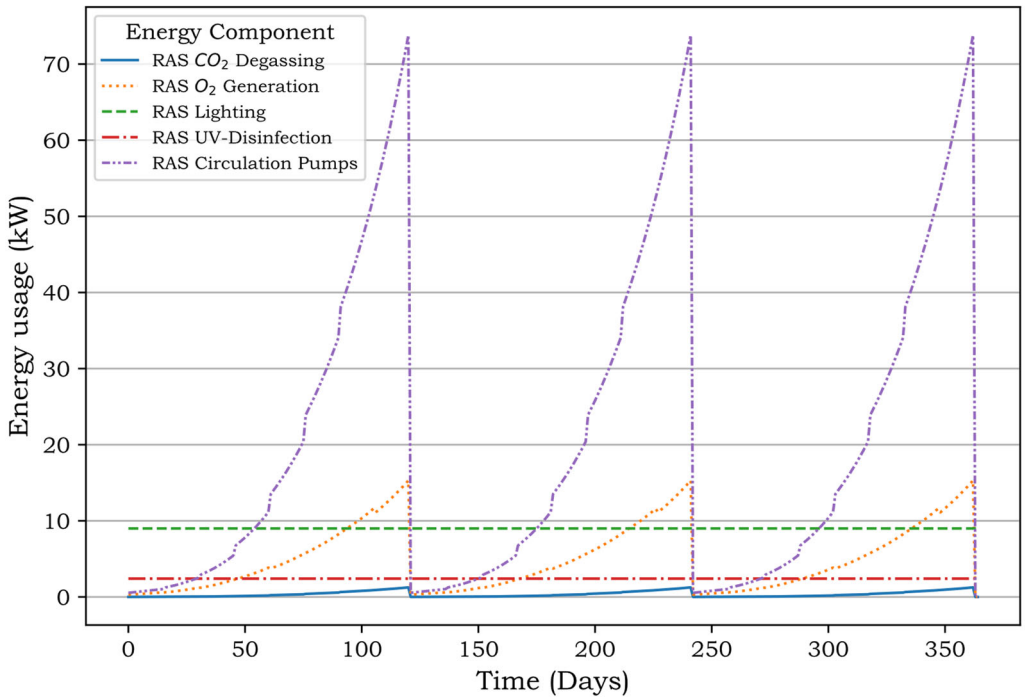

Figure 4.20: *Total energy time response by location independent energy input components for the generic decoupled system.*

The energy required by the lighting and UV-disinfection of the aquaculture facility yielded a constant value for the entire year. The UV-disinfection was required at a constant rate since the operation is continuous and it is vital that water quality is maintained throughout the life cycle of the fish. Lighting was subjected to a constant hourly schedule and therefore the hourly sum of each day was constant throughout the year. Based on the model described in Chapter Three,

lighting was determined at 9 kW per day and the UV-disinfection consumed 3 kW per day for 365 days of the year. The RAS lighting and UV-disinfection responses in Figure 4.20 are the result of the stock and flow diagrams presented in Figure 3.31 and Figure 3.34 respectively.

The energy required to operate the RAS circulation pumps, O_2 generation and CO_2 degassing was driven by the system biomass. Under the favourable conditions, which were maintained throughout the year, the fish had an exponential growth rate that influenced the feed rate and excretions. These factors caused the total system biomass to increase exponentially until harvest. With the exponential increase in system biomass, biological processes such as CO_2 generation and O_2 consumption followed the same trend. With a constant hydraulic retention time, the system required an increased system flow to ensure proper water quality. With the exponential increase in CO_2 generation, O_2 consumption and system flow rate, the energy associated with CO_2 stripping, O_2 replenishment and increased flow rate therefore also followed an exponential increase in energy usage throughout the harvest cycle. The energy increased exponentially until the fish were harvested and the system was purged. The energy usage was reduced to a minimum as the fingerlings are introduced into the growing tanks and the growth cycle started from the beginning. Since the fish were harvested three times a year, the energy usage followed a cyclic exponential time response. The exponential system responses caused by the system biomass are illustrated by the stock and flow diagrams in Figure 3.33 for the circulation pumps, Figure 3.35 for the O_2 generation and Figure 3.32 for the CO_2 degassing. The output of the respective stock and flow diagrams is shown in Figure 4.20.

The peak energy usage occurred just before harvest at the point where the system biomass was the greatest. The highest energy consumers were the circulation pumps with a peak demand of 75 kW per day. The O_2 generators required 15 kW per day at peak demand and the CO_2 degassing required 2 kW per day. The CO_2 degassing was the least energy intensive consumer in the system.

The energy components presented in Figure 4.20 had a minimal contribution to the total system energy usage and do not significantly influence the trend.

4.4.2 Location Dependent Energy Time Response

The remaining energy consuming components were heavily affected by external conditions and are therefore location dependent. The remaining components were classified as low and high energy consumers respectively. Low energy consumers included lighting required for the hydroponic greenhouse and HP circulation pumps. High energy consumers were components

required to maintain the year-round internal conditions of the respective systems, that is, the HVAC systems.

Low Energy Consumers

Lighting in the HP is required to maintain light intensity throughout the year which will stimulate the crops to produce optimal yields. The lighting schedule was subjected to an hourly schedule and the available daylight for a certain season and region. The energy equation, which describes the time response, was determined by Eq. (72). The flow rate of the circulation pump is a function of the evapotranspiration rate of the crop and therefore varied based on the external conditions. The energy equation, which determined the energy times response of the circulation pump, was given by Eq. (73). The Energy-Time response of the circulation pumps and lighting are illustrated in Figure 4.21 to Figure 4.30 for each respective location. These figures are the output results of the described stock and flow diagrams and are based on the time varying external weather data. The HP circulation pump system energy response is a result of the model in Figure 3.43. The HP lighting energy response is the result of the model described in Figure 3.42.

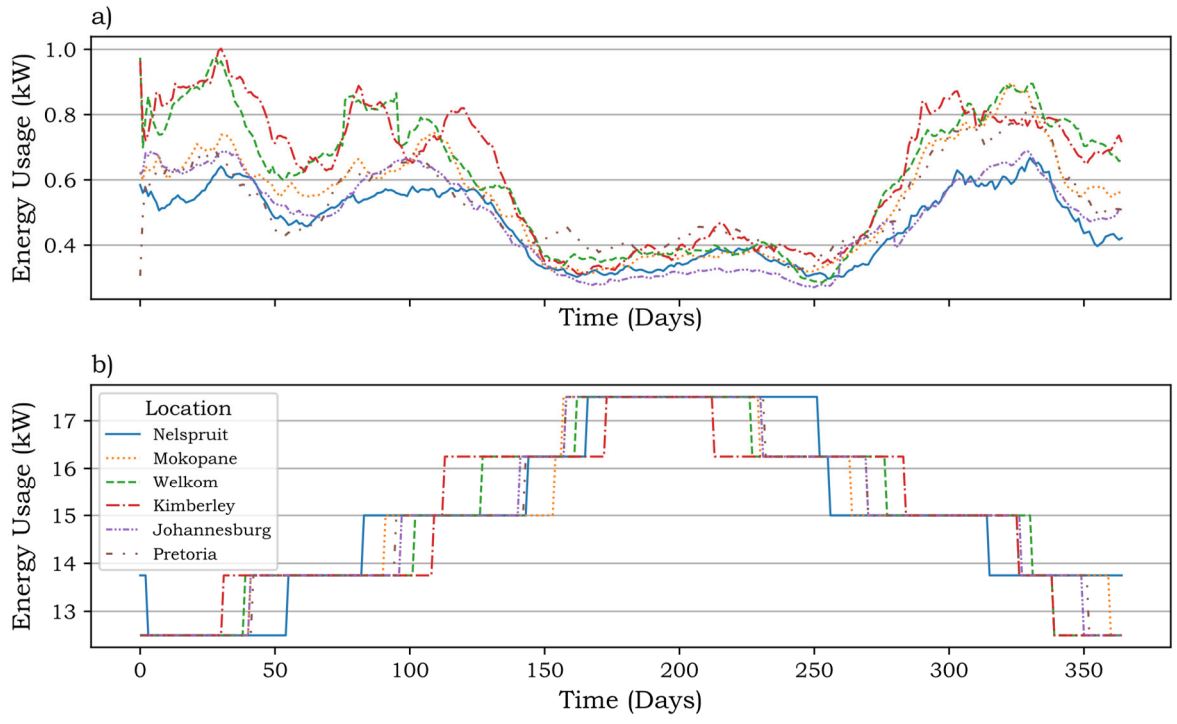

Figure 4.21: *Yearly energy time response for (a) circulation pumps and (b) lighting for the HP for inland regions of SA.*

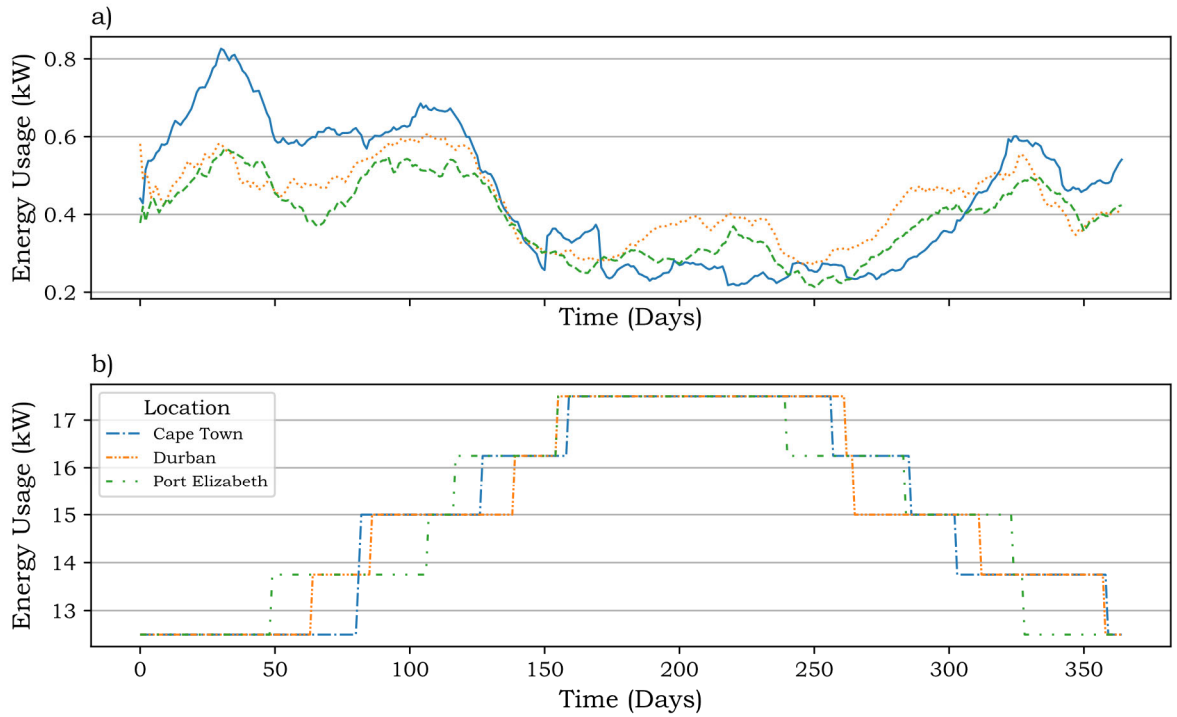

Figure 4.22: *Yearly energy time response for (a) circulation pumps and (b) lighting for the HP for coastal regions of SA.*

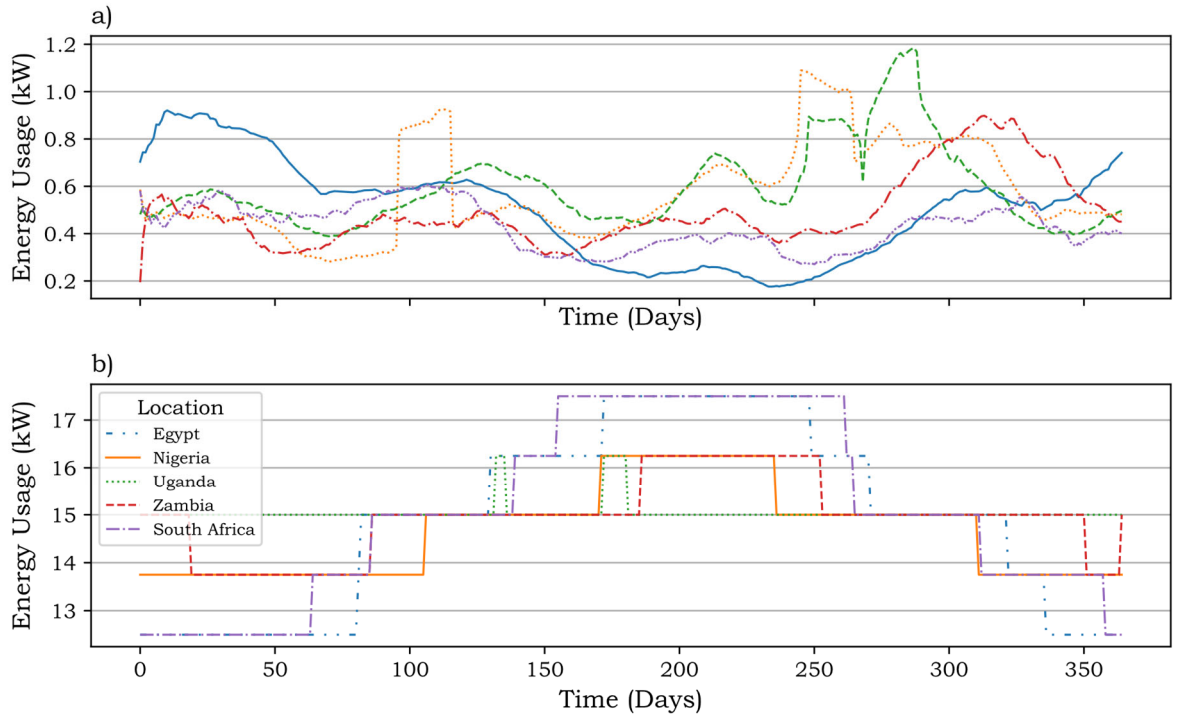

Figure 4.23: *Yearly energy time response for (a) circulation pumps and (b) lighting for the HP for countries in Africa.*

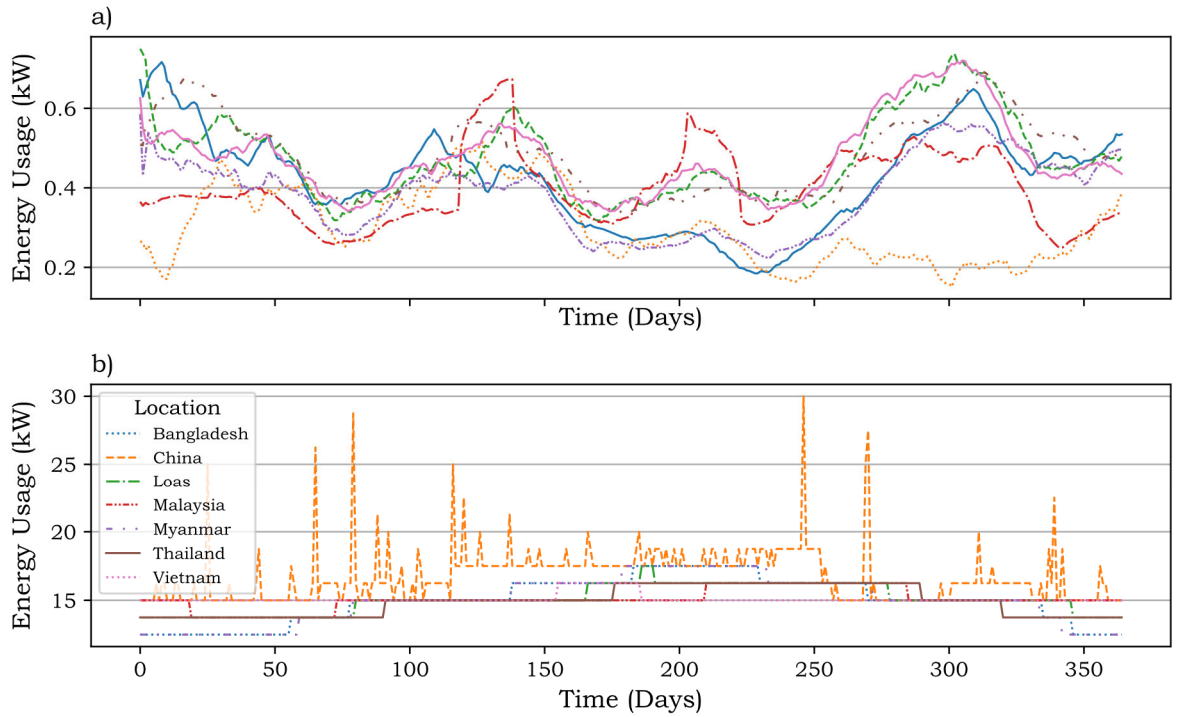

Figure 4.24: *Yearly energy time response for (a) circulation pumps and (b) lighting for the HP for mainland regions of Asia.*

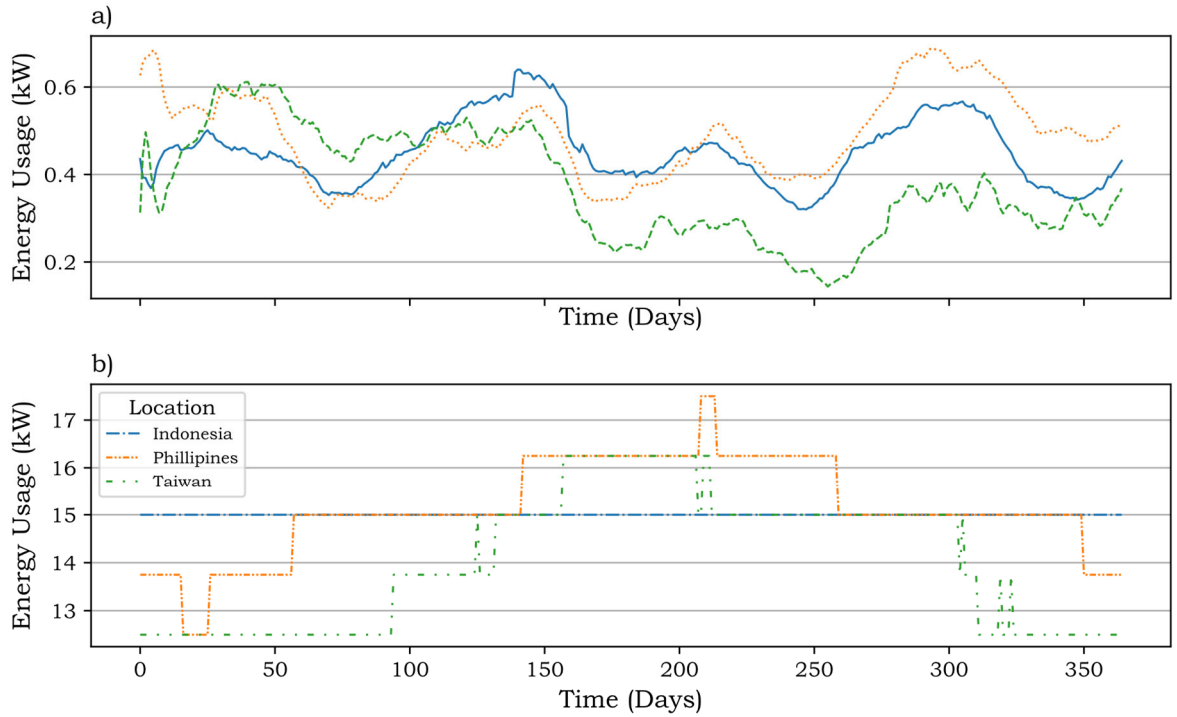

Figure 4.25: *Yearly energy time response for (a) circulation pumps and (b) lighting for the HP for island regions of Asia.*

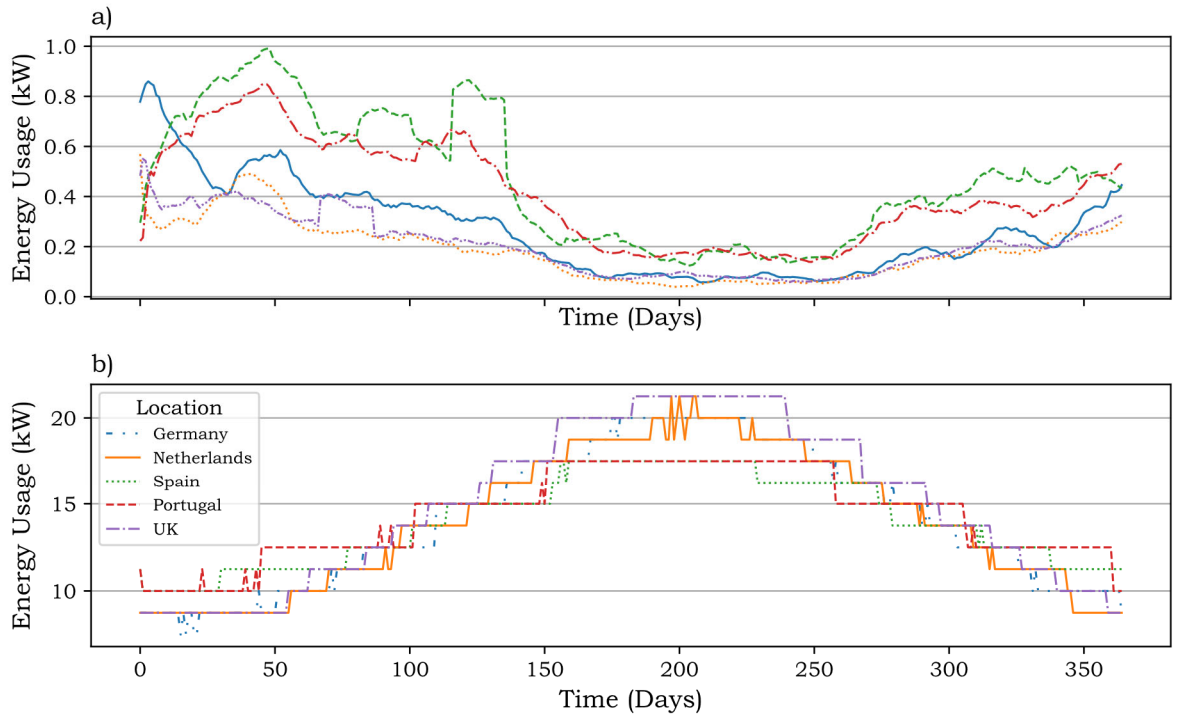

Figure 4.26: *Yearly energy time response for (a) circulation pumps and (b) lighting for the HP for countries in Europe.*

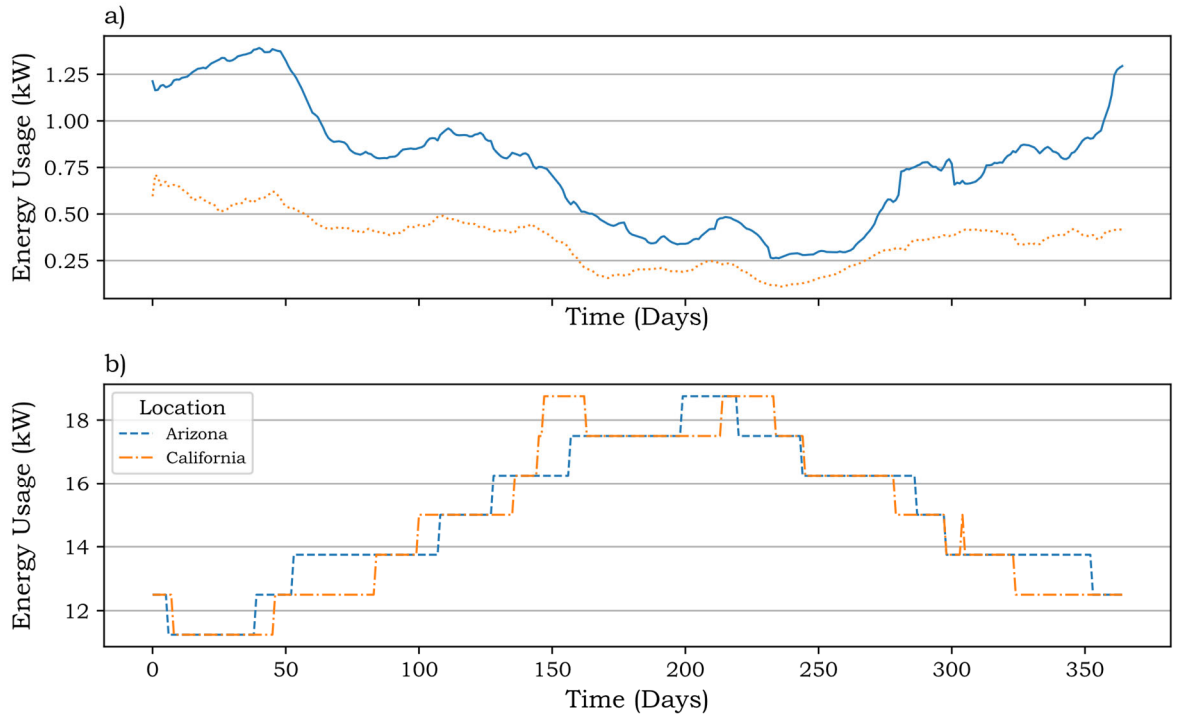

Figure 4.27: *Yearly energy time response for (a) circulation pumps and (b) lighting for the HP for Western States of the USA.*

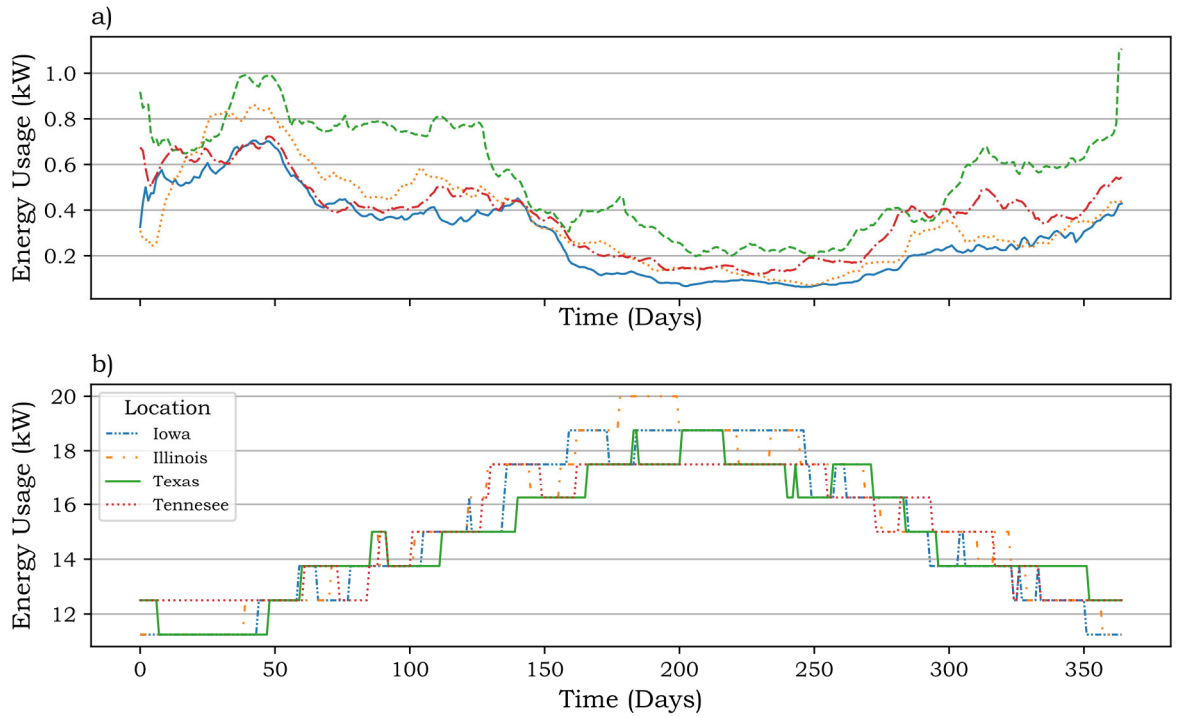

Figure 4.28: *Yearly energy time response for (a) circulation pumps and (b) lighting for the HP for Central States of the USA.*

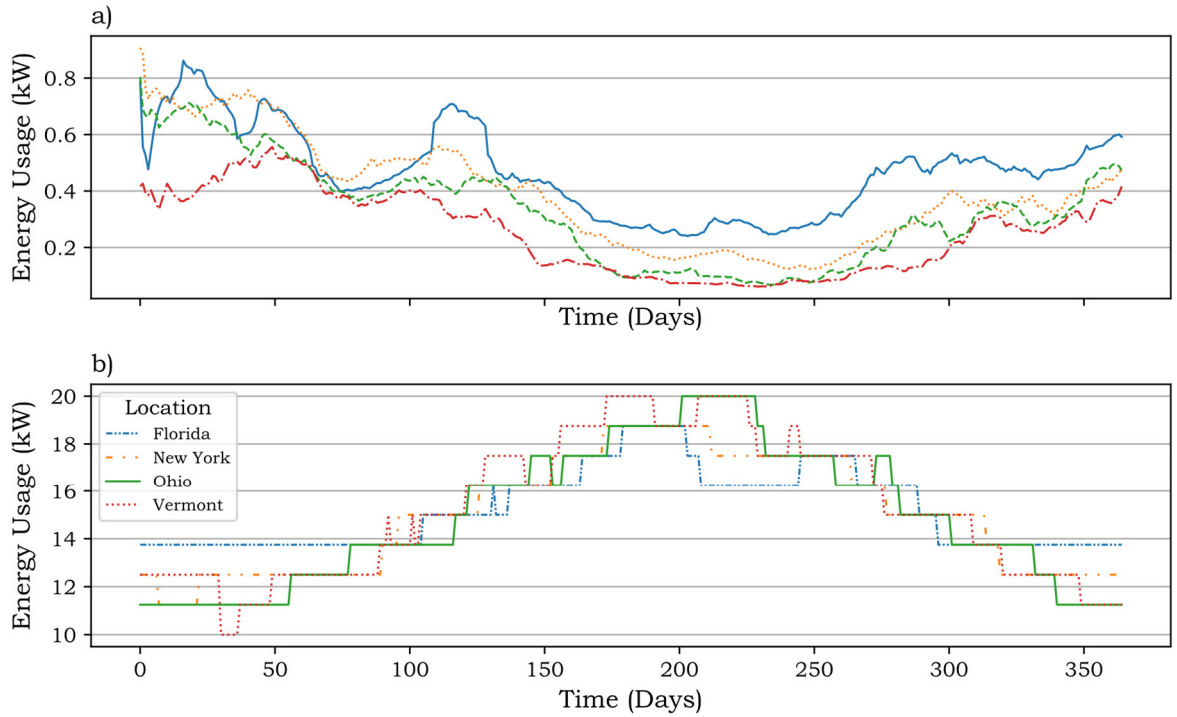

Figure 4.29 *Yearly energy time response for (a) circulation pumps and (b) lighting for the HP for Eastern States of the USA.*

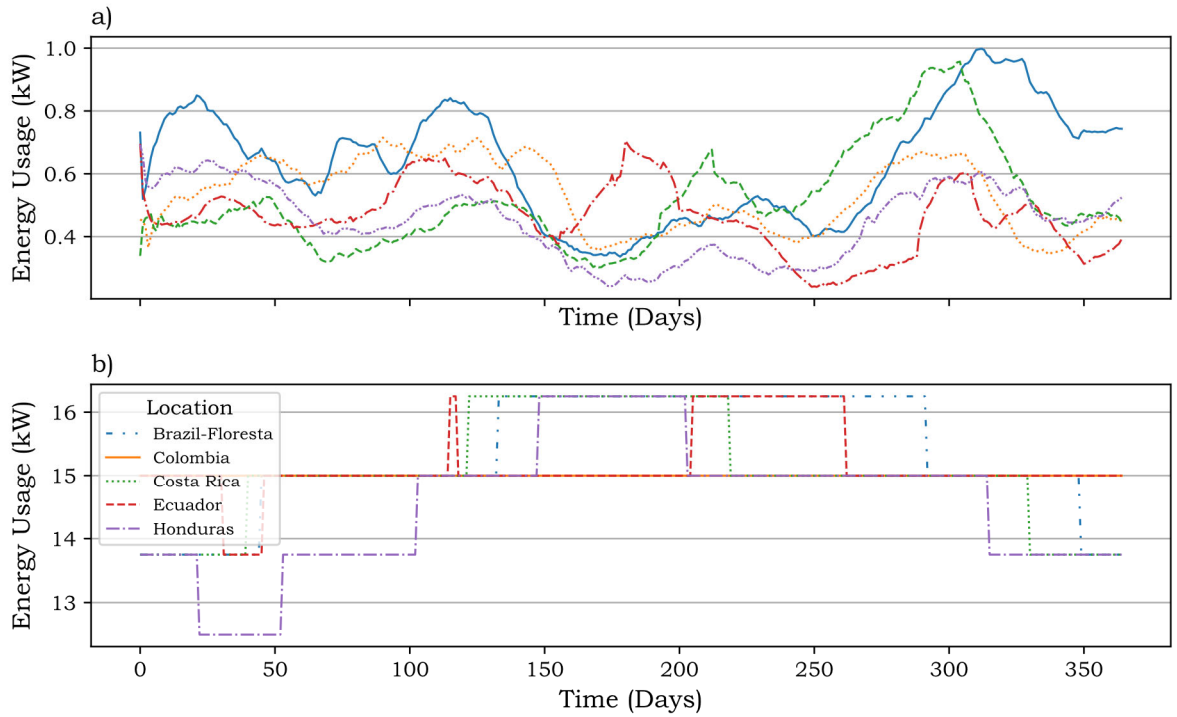

Figure 4.30: *Yearly energy time response for (a) circulation pumps and (b) lighting for the HP for countries in South America.*

Both the lighting and HP circulation pumps demanded energy in the order of 10^3 Watts, which indicated that the requirements are an order of magnitude thousand times less than the biggest contributor to energy usage, namely the HVAC system. This result is similar to the results obtained by the location independent energy consumers. Since the lighting and circulation pump did not have a significant impact on the total energy usage trend, the figures were not discussed in detail. Each variation and peak demand were not discussed but rather, the general shape of the results.

Generally, most regions exhibited a similar trend with regard to the energy usage of the circulation pumps. During summer, a higher circulation demand was experienced due to water loss via evapotranspiration. During the colder winter seasons, the temperature differential was less, and less water was lost via evapotranspiration. The circulation was normalised and more constant during the colder seasons. It was noted that hot humid regions such as South America and Asian countries showed a more uniform trend throughout the year compared to countries where the seasons differ drastically. The general trend was a seasonal response where energy demand was high in the high temperature months and low in the low temperature months. The system imitated an undampened system response for a yearly period. Without a drastic change in temperature, the system should follow the same trend annually.

The lighting was subjected to season. Countries close to the equator will experience similar daylight conditions throughout the year whereas countries located further away will experience more extreme variations in duration in the summer and winter seasons. This was evident in the results figures for the Asian and South American countries, which are situated close to the equator, showing little variation in energy demands throughout the year. Countries such as South Africa and the USA, showed moderate variation where European countries showed extreme variations due to long daylight hours in summer and short daylight hours in winter. It was evident that daylight is heavily influenced by location and therefore the requirement for supplementation by artificial lighting occurred during certain times of the year. Since lighting was not a major contributor to the total energy usage, the effects were not significant when considering the entire system.

High Energy Consumers

The major contributors to the total system energy usage were the HVAC systems serving the hydroponic greenhouse and aquaculture facility. The energy demand was in the order of magnitude 10^6 Watts. The energy required to heat and/or cool the systems to maintain favourable conditions was intensive. The HVAC systems were the most expensive energy consumer in the entire system.

The energy equation, which governs the energy time response for the environmental control of the RAS facility is given by Eq. (19). The energy equation, which governs the energy time response for the environmental control of the hydroponic greenhouse was given by Eq. (75). The heating and cooling demands were determined by these equations. The total energy required for cooling and heating the respective systems is the sum of the three main components that contribute to the heating and cooling energy required. These components are the chiller, heat pump, pumps and fans respectively. The cooling energy required for the RAS facility is the sum of Eq. (58), Eq. (59) and Eq. (64). The heating energy required for the RAS facility is the sum of Eq. (66), Eq. (67) and Eq. (70). The cooling energy required for the hydroponic greenhouse is merely Eq. (109), since cooling is achieved by means of ventilation only. The heating energy required for the hydroponic greenhouse is the sum of Eq. (111), Eq. (112) and Eq. (114).

High temperature differential fluctuations throughout the year influenced and drove the energy demands as presented in Figure 4.31 to Figure 4.40. Since the energy demand of the HVAC systems was so large, this component heavily affected the trend of the total system energy usage. The contribution of energy usage by the HVAC systems ultimately determined

the peak energy demands and general trends of the entire system. Since local climate factors greatly influenced the energy response of the system, it is important to describe the system response for each region. The output results presented in Figure 4.31 to Figure 4.40 were the product of the stock and flow diagrams as presented in section 3.4. The stock and flow diagrams presented in Figure 3.36 to Figure 3.41 were the models that produced the results for the heating and cooling of the aquaculture facility. The stock and flow diagrams presented in Figure 3.44 to Figure 3.49 were the models that produced the results for the heating and cooling of the hydroponic greenhouse.

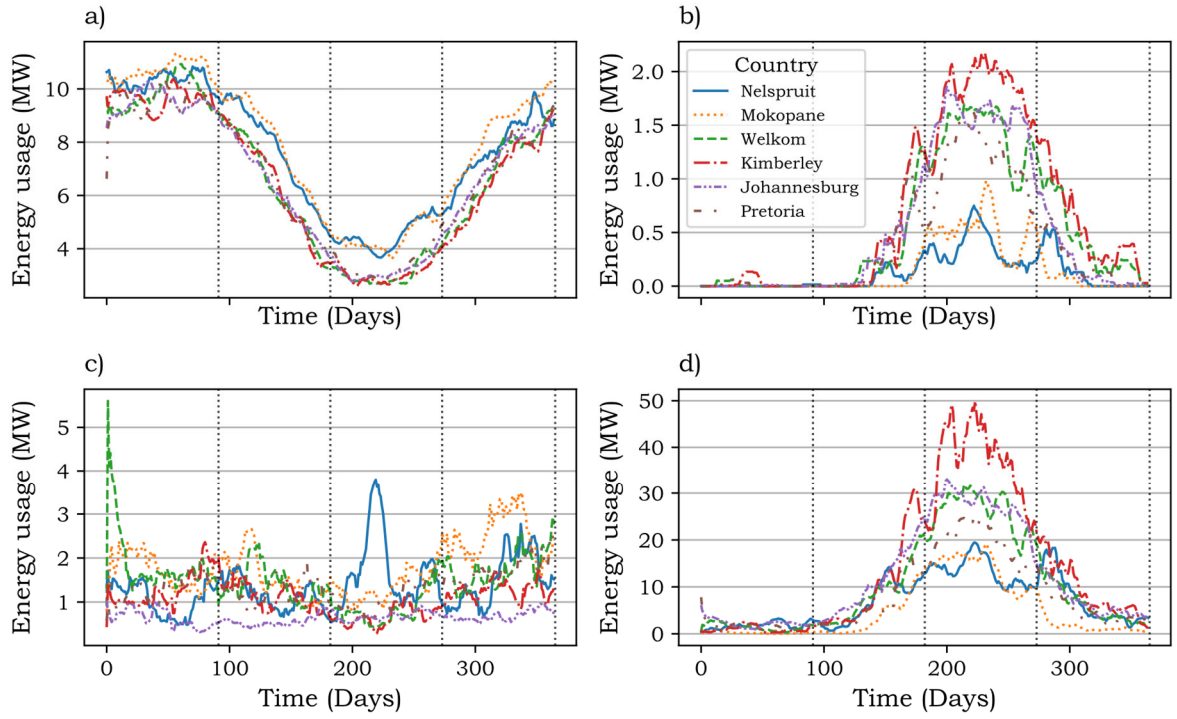

Figure 4.31: *Yearly energy time response for (a) cooling of the RAS, (b) heating of the RAS, (c) cooling of the HP and (d) heating of the HP for inland regions of South Africa.*

Energy was required to cool the RAS facility throughout the year for all the inland regions of South Africa (Figure 4.31). All the locations followed a seasonal trend which indicated an undamped system response. Given South Africa's hot climate, more energy was required to cool the facility during summer compared to winter. The peak cooling demand was comparable for all locations and ranged between 10.1 MW and 11.3 MW. The inland locations had a large seasonal variation in cooling which indicated the temperature differences between summer and winter was significantly large. Nelspruit and Mokopane were the only two locations where cooling energy contributed the most towards the total system energy usage, with 44.0% and 53.2% respectively.

During the summer, little to no heating was required in the RAS facility. Arid climates where cold nights are experienced, for example, Kimberly and Welkom indicated a heating requirement in summer. The peak heating demand for all locations occurred in mid-winter. Generally, the heating energy demand was far less than the cooling demand owing to the hot climate experienced in South Africa. This is evident by the low percentage contribution to total energy usage in the system which was 3% for the worst performing location, Kimberley. A summary of the output results is shown in Table 4.9. The table contains information regarding the respective subsystem's energy usage for heating and cooling.

Table 4.9: *HVAC data summary for the RAS & HP for inland regions in South Africa*

Region	Energy Component	Peak Energy Usage [MW]	Season Variation [MW]	Percentage Contribution to Total Energy [%]
Nelspruit	RAS HVAC Cooling Total	10.8	7.0	46.1
	RAS HVAC Heating Total	0.7	0.7	0.8
	HP HVAC Heating Total	18.6	17.8	44.0
	HP HVAC Cooling Total	3.2	2.8	8.2
Mokopane	RAS HVAC Cooling Total	11.3	7.5	53.2
	RAS HVAC Heating Total	0.8	0.8	1.0
	HP HVAC Heating Total	17.7	17.7	32.7
	HP HVAC Cooling Total	3.5	3.1	12.6
Welkom	RAS HVAC Cooling Total	10.8	8.1	34.3
	RAS HVAC Heating Total	1.7	1.7	2.7
	HP HVAC Heating Total	31.9	31.5	54.6
	HP HVAC Cooling Total	3.2	2.8	7.6
Kimberley	RAS HVAC Cooling Total	10.1	7.5	28.3
	RAS HVAC Heating Total	2.1	2.1	3.0
	HP HVAC Heating Total	48.3	48.0	63.3
	HP HVAC Cooling Total	2.1	1.7	4.8
Johannesburg	RAS HVAC Cooling Total	10.6	7.8	33.7
	RAS HVAC Heating Total	1.8	1.8	2.6
	HP HVAC Heating Total	33.1	32.4	59.7
	HP HVAC Cooling Total	1.2	0.8	3.3
Pretoria	RAS HVAC Cooling Total	10.9	8.0	39.9
	RAS HVAC Heating Total	1.6	1.6	2.4
	HP HVAC Heating Total	25.1	24.2	48.5
	HP HVAC Cooling Total	2.4	2	8.3

The location that required the most heating during the winter was Kimberley with 2.1 MW heating required; this was due to the cold weather experienced due to the arid climate. The least amount of heating energy was required by Nelspruit with 0.7 MW.

The energy required to heat the greenhouse during winter was the most energy intensive component for all locations. The heating demand by the HP in winter outweighed the cooling demand in summer by the RAS facility. Kimberley required 48.3 MW of heating in the winter, which was the worst performing region. The heating contributed 63.3% to the total system energy usage. Nelspruit was the best performing region and requires 18.6 MW of heating in winter and contributed 46.1% to the total energy usage.

The ventilation required in the greenhouse followed a less seasonal trend since the driver was the evapotranspiration rate. South Africa experiences high day temperatures, even in winter, and will cause the response to be normalised over a yearly period. There was still a smaller requirement for ventilation during winter, but the variation was less. Johannesburg required the least amount of energy for HP cooling with 1.2 MW. Mokopane required the most energy for ventilation with 3.5 MW required.

External climatic factors had an extreme influence on the energy demand of the system throughout the year. The two major contributors to energy demand for the inland regions of South Africa were the cooling required by the RAS facility and the heating required by the HP greenhouse. More energy was required for heating the HP greenhouse than for cooling the RAS facility.

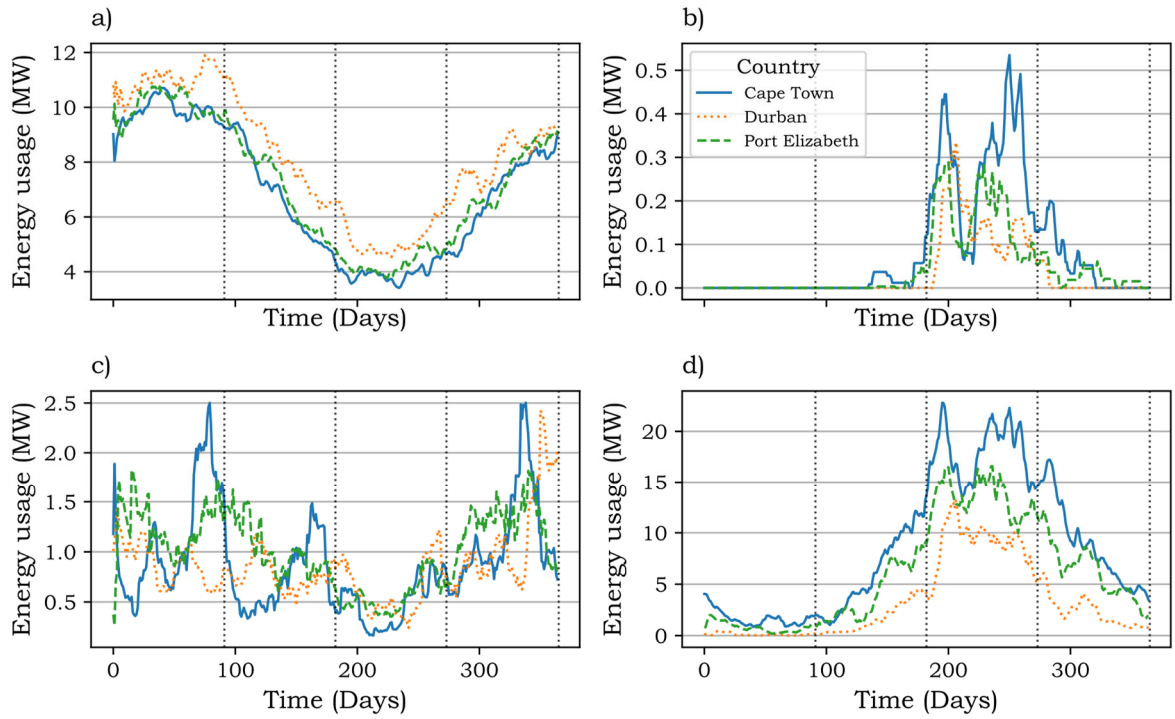

Figure 4.32: *Yearly energy time response for (a) cooling of the RAS, (b) heating of the RAS, (c) cooling of the HP and (d) heating of the HP for coastal regions of South Africa.*

The cooling demands for the RAS facility for coastal regions (Figure 4.32) were similar to the inland regions and ranged between 10.6 MW and 12.9 MW. The same seasonal trend was observed in the coastal regions as in the inland regions.

Durban required the most cooling during the summer with 12.9 MW of cooling, this was due to the hot humid climate of this region. The cooling demands in Durban and Port Elizabeth were the largest contributors to total system energy usage with 65.5% and 49.3% respectively.

The peak heating demands were experienced as the season became colder in winter. The worst performing location, Cape Town, had the highest heating demand of 0.4 MW. This is 0.3 MW less than the best performing inland region, Nelspruit. Given the humidity and warmer winters of the coastal regions, less heating was required. Heating of the RAS facility was the smallest contributor to the total system energy usage for all the regions, with only 0.5% contribution by the worst performing region, Cape Town.

The biggest contributor to energy was once again the heating required by the HP greenhouse during the winter. Generally, less energy was required by the coastal regions compared to the inland regions of South Africa. This is due to warmer winters and humidity in the coastal regions. Durban was the best performing region with 12.9 MW required for heating. This value was much less than the best performing inland region, Nelspruit, with a heating demand of 18.6 MW. Cape Town was the only coastal region where heating of the HP greenhouse had the biggest contribution to total system energy with 51.8%. The other coastal regions had bigger RAS facility cooling demands.

The ventilation followed a similar trend as the inland regions with a minor dip in energy demand in winter, with the rest of the year showing small seasonal variations. Port Elizabeth was the best performing region with a 1.7 MW demand.

All three coastal regions performed well compared with one another. The results indicated that the coastal regions outperform the inland regions with regard to HVAC energy usage. The HVAC energy contributed roughly 99% to the total energy usage in the system. A summary of the HVAC energy is presented in Table 4.10 for the coastal regions of South Africa.

Table 4.10: *HVAC data summary for the RAS & HP for coastal regions in South Africa*

Region	Energy Component	Peak Energy Usage [MW]	Season Variation [MW]	Percentage Contribution to Total Energy [%]
Cape Town	RAS HVAC Cooling Total	11.1	7.6	41.6
	RAS HVAC Heating Total	0.4	0.4	0.5
	HP HVAC Heating Total	22.3	21.6	51.8
	HP HVAC Cooling Total	2.3	2.1	5.1
Durban	RAS HVAC Cooling Total	12.3	7.8	65.5
	RAS HVAC Heating Total	0.3	0.3	0.3
	HP HVAC Heating Total	12.9	12.9	26.3
	HP HVAC Cooling Total	2.2	1.9	6.8
Port Elizabeth	RAS HVAC Cooling Total	10.6	6.8	49.3
	RAS HVAC Heating Total	0.3	0.3	0.3
	HP HVAC Heating Total	16.4	16.1	42.5
	HP HVAC Cooling Total	1.7	1.4	6.9

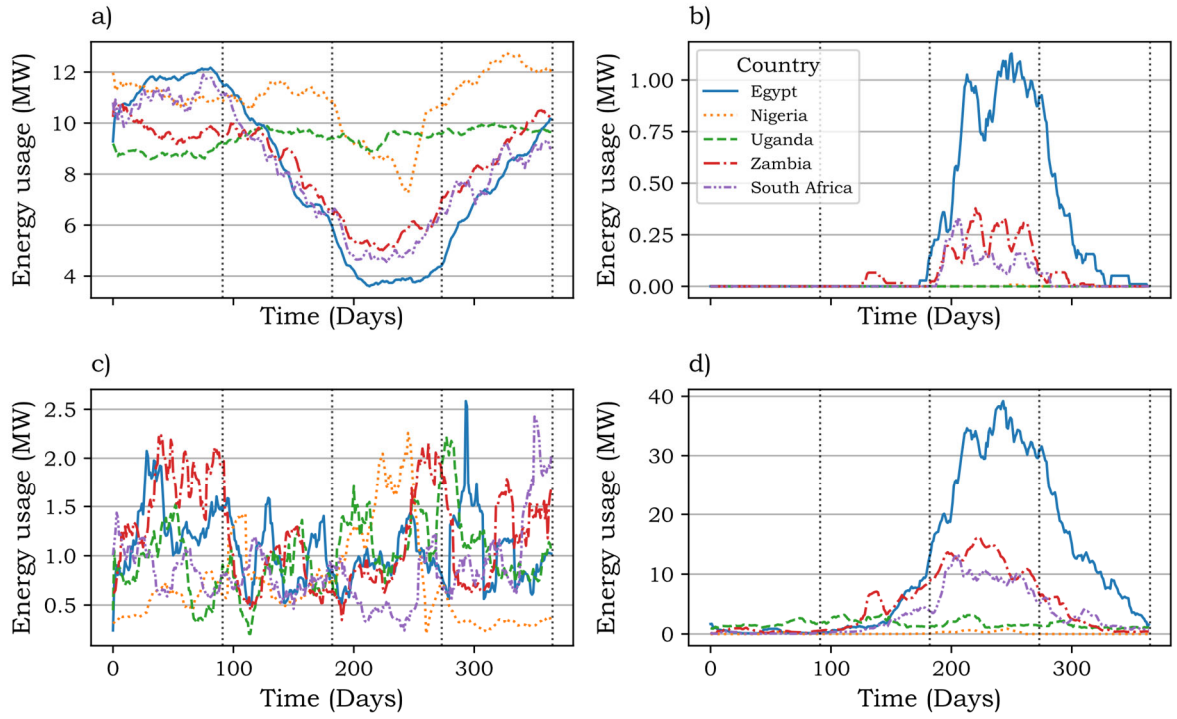

Figure 4.33: *Yearly energy time response for (a) cooling of the RAS, (b) heating of the RAS, (c) cooling of the HP and (d) heating of the HP for countries in Africa.*

The RAS cooling demand (Figure 4.33) of Egypt and Zambia followed a similar trend as Durban, South Africa. A seasonal trend was observed with a smaller cooling demand in winter, but cooling was still required throughout the year. Egypt had the greatest variation in cooling demand due to the extreme temperature differences between summer and winter. The temperature differences were due to the arid climate experienced in Egypt. Uganda and Nigeria followed a less seasonal trend and by comparing the weather data of these countries, it was

observed that the day temperatures are quite constant throughout the year. The cooling demand varied between 9.9 MW and 12.6 MW. This was comparable to that of South Africa. The RAS cooling energy of Nigeria, Uganda and Zambia was the major contributor to total system energy usage, with 91.5%, 77.3% and 57.3% respectively. This indicated hot climates throughout the year.

Uganda and Nigeria effectively required no heating energy in the RAS facility throughout the year. Given the arid climate of Egypt, cold temperatures were experienced at night and in winter, therefore Egypt was the country with the highest heating demand in the RAS facility compared to the other African countries, with 1.2 MW peak heating demand in winter.

Uganda and Nigeria required the least amount of heating for the HP greenhouse compared to the other African countries. The demand was more constant throughout the year due to the constant day temperature during summer and winter. This was evident by the small seasonal variation. Egypt and Zambia followed a trend similar to the South African regions and experienced peak heating demands of 38.7 MW and 15.7 MW respectively. Egypt was the worst performing country and the HP heating was the largest contributor to total system energy usage with a value of 54.4%.

The ventilation demands for all the countries were comparable and the peak demands fell in the range of 2.4 MW and 2.0 MW. Given the high day temperature experienced by all the countries, the ventilation demand exhibited a small seasonal variation.

Table 4.11: *HVAC data summary for the RAS & HP for countries in Africa*

Region	Energy Component	Peak Energy Usage [MW]	Season Variation [MW]	Percentage Contribution to Total Energy [%]
Egypt	RAS HVAC Cooling Total	12.1	8.4	38.5
	RAS HVAC Heating Total	1.1	1.1	1.2
	HP HVAC Heating Total	38.7	38.6	54.4
	HP HVAC Cooling Total	2.0	1.5	5.2
Nigeria	RAS HVAC Cooling Total	12.6	5.1	91.5
	RAS HVAC Heating Total	0.01	0.01	0.0
	HP HVAC Heating Total	0.8	0.8	0.9
	HP HVAC Cooling Total	2.3	2.0	6.3
Uganda	RAS HVAC Cooling Total	9.9	1.3	77.3
	RAS HVAC Heating Total	0.0	0.0	0.0
	HP HVAC Heating Total	3.4	2.8	13.3
	HP HVAC Cooling Total	2.0	1.6	8.1
Zambia	RAS HVAC Cooling Total	10.5	5.5	57.3
	RAS HVAC Heating Total	0.3	0.3	0.4
	HP HVAC Heating Total	15.7	15.5	32.8
	HP HVAC Cooling Total	2.4	1.9	8.5

Uganda and Nigeria were the best overall performing countries with regard to energy usage due to the constant high temperature throughout the year. The hot humid conditions ensured that heat was not lost during the night, which reduced heating demands. The largest contributor to energy usage was cooling of the RAS facility. A summary of the HVAC energy usage of the respective regions is presented in Table 4.11.

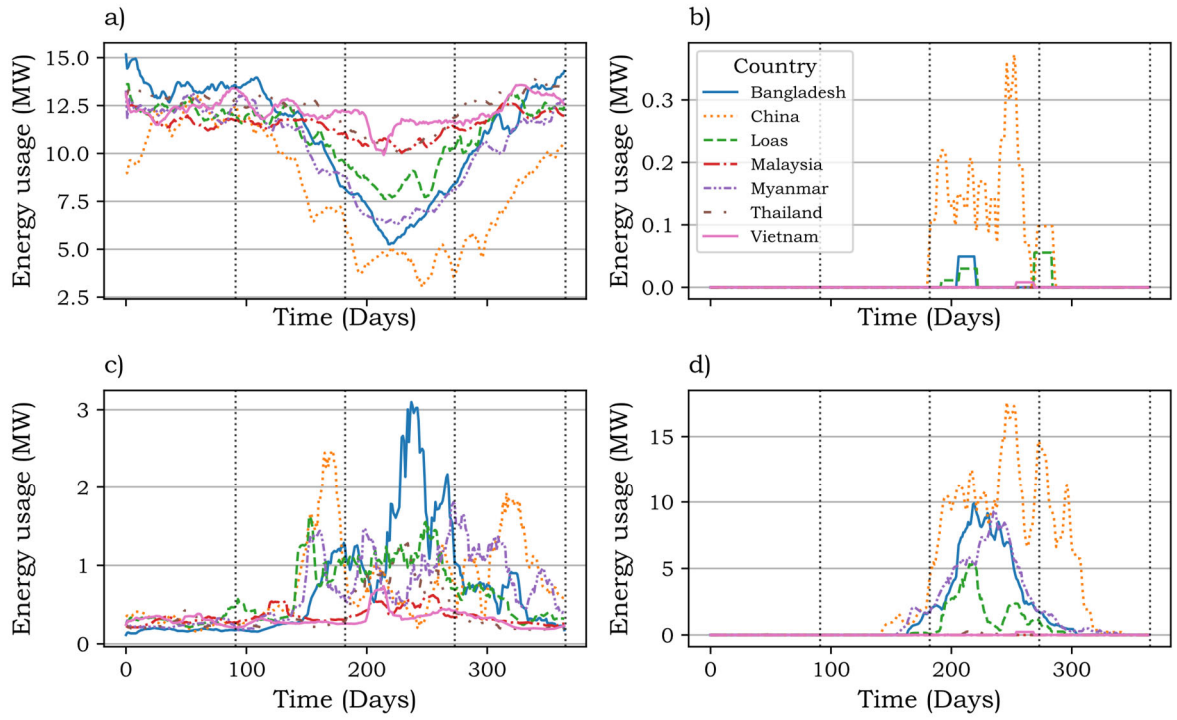

Figure 4.34: *Yearly energy time response for (a) cooling of the RAS, (b) heating of the RAS, (c) cooling of the HP and (d) heating of the HP for mainland regions in Asia.*

Generally, the Asian countries (Figure 4.34) that were compared showed high cooling demand and low heating demand throughout the year. The countries that were compared experience hot humid conditions and temperatures were mostly the same throughout the year. Cooling demands were higher for the Asian countries compared to the African countries, including South Africa. The cooling demands for the RAS facility ranged from 12.6 MW to 14.7 MW. The best performing region, Malaysia, with RAS cooling demand of 12.6 MW, was the same as the worst performing country in Africa, Egypt. It was observed that for all mainland Asian countries, the greatest contributor to total system energy usage was RAS cooling, with contributions as high as 96.3% for Vietnam. This indicated that cooling outweighs heating which meant that even during winter, these regions can produce crops and fish and still be energy efficient.

Bangladesh, China and Laos were the only countries that required RAS heating during the colder months. The highest heating demand was experienced by China with a value of 0.4

MW. Malaysia, Myanmar, Thailand and Vietnam require no heating during the year for the RAS facility and the response yielded a constant plot.

Malaysia required no heating of the HP greenhouse throughout the year. China had the biggest heating demand of 17 MW. The remaining countries required heating during the colder months of the year. The energy usage during winter was less than the RAS cooling, which indicated that extreme temperature differences were not experienced during the winter. Ventilation was required throughout the year for all the countries and made a more significant contribution to total system energy usage than RAS heating did.

Given the hot humid conditions experienced throughout the year in these countries, ventilation was required to maintain favourable conditions inside the HP greenhouse. Malaysia appeared to be the best performing country with regard to HVAC energy usage, as evident in the Table 4.12 summary of the HVAC energy usage for the respective regions.

Table 4.12: *HVAC data summary for the RAS & HP for mainland regions in Asia*

Region	Energy Component	Peak Energy Usage [MW]	Season Variation [MW]	Percentage Contribution to Total Energy [%]
Bangladesh	RAS HVAC Cooling Total	14.7	10.4	82.3
	RAS HVAC Heating Total	0.03	0.03	0.0
	HP HVAC Heating Total	11.9	11.9	11.1
	HP HVAC Cooling Total	3.0	2.9	5.4
China	RAS HVAC Cooling Total	12.9	9.5	62.7
	RAS HVAC Heating Total	0.6	0.6	0.4
	HP HVAC Heating Total	22.3	22.3	30.1
	HP HVAC Cooling Total	2.3	2.1	5.6
Laos	RAS HVAC Cooling Total	13.0	6.0	89.6
	RAS HVAC Heating Total	0.04	0.04	0.02
	HP HVAC Heating Total	4.7	4.7	3.7
	HP HVAC Cooling Total	2.2	1.9	5.4
Malaysia	RAS HVAC Cooling Total	12.6	2.6	95.8
	RAS HVAC Heating Total	0.0	0.0	0.0
	HP HVAC Heating Total	0.0	0.0	0.0
	HP HVAC Cooling Total	0.6	0.4	2.9
Myanmar	RAS HVAC Cooling Total	12.9	7.2	81.3
	RAS HVAC Heating Total	0.0	0.0	0.0
	HP HVAC Heating Total	9.1	9.1	12.2
	HP HVAC Cooling Total	1.6	1.4	5.3
Thailand	RAS HVAC Cooling Total	13.8	4.0	95.6
	RAS HVAC Heating Total	0.0	0.0	0.0
	HP HVAC Heating Total	0.2	0.2	0.1
	HP HVAC Cooling Total	1.3	1.2	3.1
Vietnam	RAS HVAC Cooling Total	13.5	6.0	96.3
	RAS HVAC Heating Total	0.01	0.01	0.0
	HP HVAC Heating Total	0.2	0.2	0.07
	HP HVAC Cooling Total	1.0	0.8	2.4

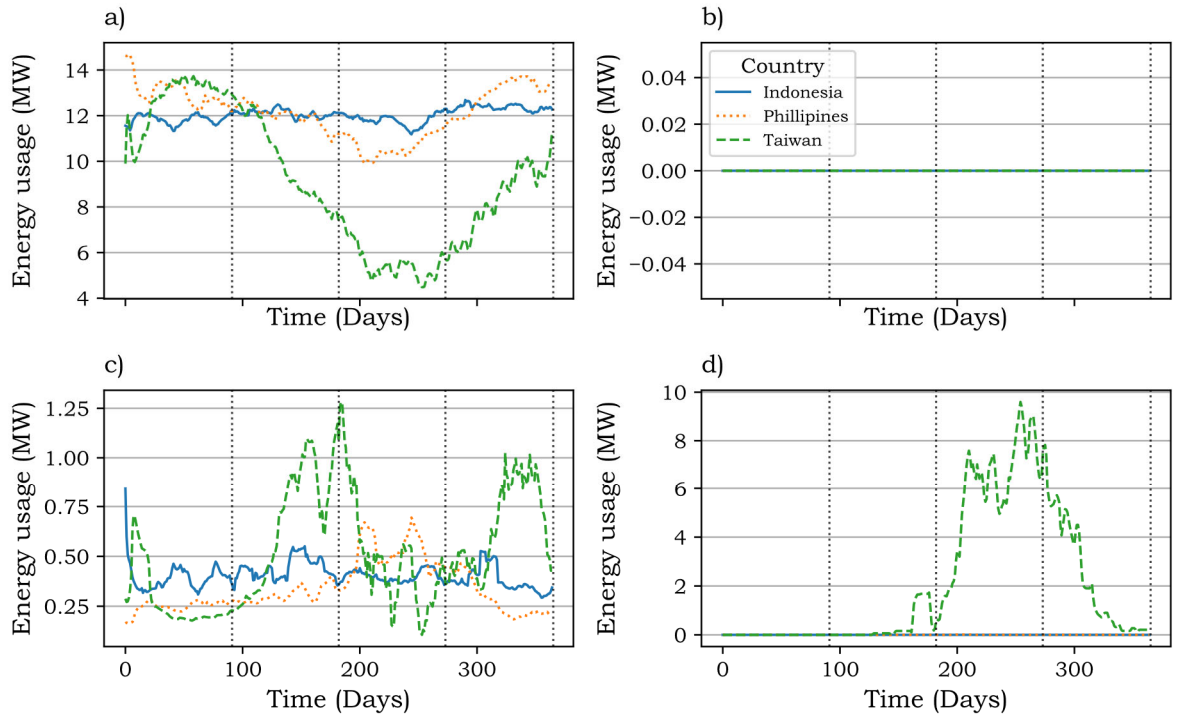

Figure 4.35: *Yearly energy time response for (a) cooling of the RAS, (b) heating of the RAS, (c) cooling of the HP and (d) heating of the HP for island regions in Asia.*

The island Asian countries (Figure 4.35) performed very similarly to the mainland Asian countries. The biggest contributor to total system energy usage was RAS cooling. Indonesia, Philippines and Taiwan made 95.6%, 96.1% and 77.0% contributions to total system energy respectively. This meant that the RAS cooling was the dominant component and would ultimately affect the total energy usage curve the most. The Philippines had the highest RAS cooling demand of 13.9 MW. The best performing Asian island was Indonesia with 12.6 MW cooling demand. Taiwan had a bigger reduction in cooling energy in winter, which meant it is a colder region. Indonesia and the Philippines both showed a seasonal response but had a smaller seasonal variation and was more constant throughout the year. This indicated that the temperatures remain high throughout the year and therefore the cooling demand remained high.

All three countries had a constant response of zero heating demand throughout the year for the RAS facility. This meant no energy was required for RAS heating and the external conditions would not affect the internal environment due to colder temperatures.

Indonesia and the Philippines also did not require any heating in the HP greenhouse to maintain internal conditions throughout the year. The lack of a heating requirement greatly assisted in energy efficiency since heating can be a very energy intensive process. Taiwan required heating during the colder months and had a peak heating demand of 9.3 MW. The ventilation required showed small seasonal variations for Indonesia and the Philippines.

Taiwan required higher ventilation rates and was the worst performing country compared to Indonesia and the Philippines. Table 4.13 is a summary of the HVAC energy for the respective regions.

Table 4.13: *HVAC data summary for the RAS & HP for island regions in Asia*

Region	Energy Component	Peak Energy Usage [MW]	Season Variation [MW]	Percentage Contribution to Total Energy [%]
Indonesia	RAS HVAC Cooling Total	12.6	1.2	95.6
	RAS HVAC Heating Total	0.0	0.0	0.0
	HP HVAC Heating Total	0.0	0.0	0.0
	HP HVAC Cooling Total	0.5	0.2	3.2
Philippines	RAS HVAC Cooling Total	13.9	3.9	96.1
	RAS HVAC Heating Total	0.0	0.0	0.0
	HP HVAC Heating Total	0.0	0.0	0.0
	HP HVAC Cooling Total	0.7	0.5	2.7
Taiwan	RAS HVAC Cooling Total	13.7	9.1	77.0
	RAS HVAC Heating Total	0.0	0.0	0.0
	HP HVAC Heating Total	9.3	9.3	17.5
	HP HVAC Cooling Total	1.1	1.0	4.3

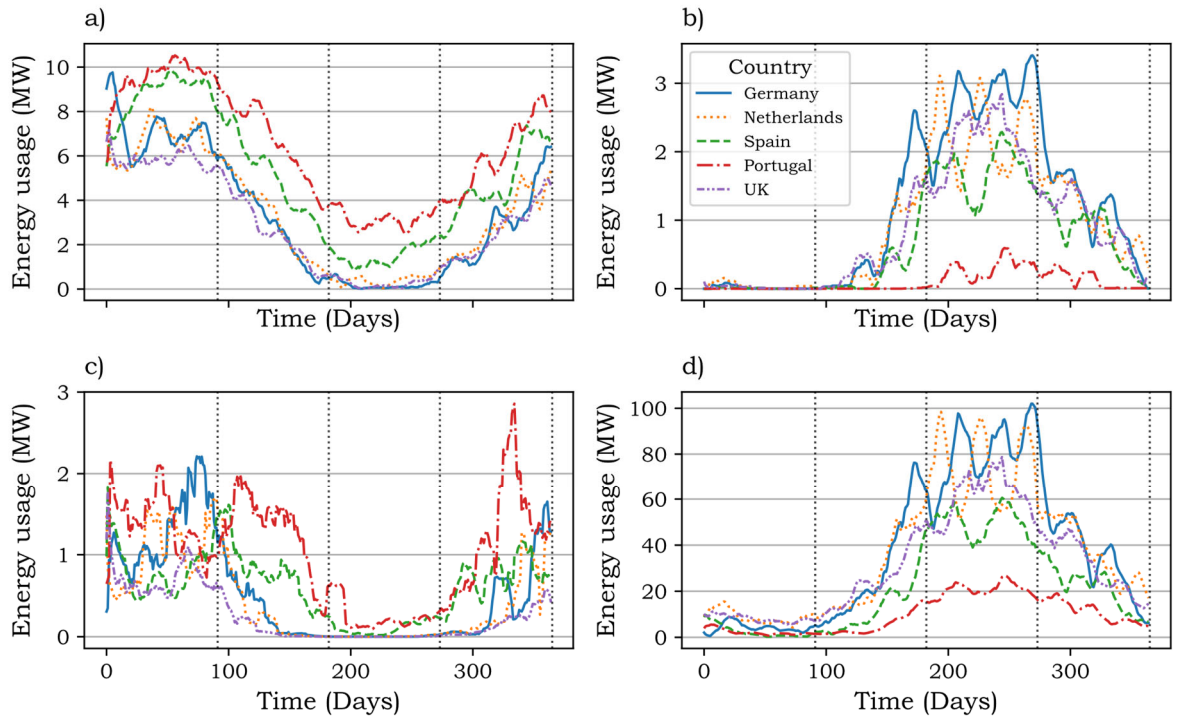

Figure 4.36: *Yearly energy time response for (a) cooling of the RAS, (b) heating of the RAS, (c) cooling of the HP and (d) heating of the HP for countries in Europe.*

The seasonal response of the European countries (Figure 4.36) followed the same trend throughout the year. The RAS cooling peak demands were experienced in summer and the lowest demands were experienced in winter.

The peak cooling demands ranged from 10.4 MW for Portugal to 6.3 MW for the UK. The peak cooling demand was less compared to Asian and African countries; this was due to the cold weather experienced in Europe. Colder European countries such as Germany, Netherlands and the UK made RAS cooling contributions to the total system energy of 7.6%, 7.6% and 8.0% respectively. Warmer countries such as Spain and Portugal made a bigger cooling contribution to the total system energy usage of 18.1% and 36.7% respectively. This was significantly higher due to the warmer climate.

The RAS heating was required for much longer periods of the year for European countries compared to Asian and African countries. The worst performing country was the Netherlands with peak heating demands of 3.7 MW. The best performing country was Portugal with a peak heating demand of 0.5 MW. Given winters that often reach temperatures below zero as experienced by European countries, heating was the most energy intensive contributor to total system energy usage.

The greatest contributor to total system energy usage was HP heating. Since greenhouses are poorly insulated and heat loss occurs at a rapid rate, a large amount of energy was required to maintain internal conditions. A seasonal trend was observed with large peaks observed in winter. Colder countries such as Germany, the Netherlands and the UK had HP heating demands that contributed 88.0%, 88.6% and 88.4% to the total energy usage of the system. Spain and Portugal made smaller contributions of 76.6% and 55.9% but was still the leading contributor to total system energy usage and ultimately determined the system energy trend. The best performing country, Portugal, had a heating demand of 24.6 MW which was worse than the best performing region in South Africa, Durban, with a heating demand of 12.9 MW.

Ventilation produced a seasonal response with the peak demand in the hotter months. Portugal had the highest peak demand of 2.6 MW and the UK had the lowest peak demand of 1.0 MW. Table 4.14 presents a summary of the HVAC energy usage. Seasonal variations for all four energy components were large compared to the other countries and regions. This was due to the extreme variation in summer and winter temperatures.

Table 4.14: *HVAC data summary for the RAS & HP for countries in Europe*

Region	Energy Component	Peak Energy Usage [MW]	Season Variation [MW]	Percentage Contribution to Total Energy [%]
Germany	RAS HVAC Cooling Total	7.5	7.5	7.6
	RAS HVAC Heating Total	3.3	3.3	2.7
	HP HVAC Heating Total	96.7	94.1	88.0
	HP HVAC Cooling Total	2.1	2.1	1.2
Netherlands	RAS HVAC Cooling Total	7.7	7.7	7.6
	RAS HVAC Heating Total	3.7	3.7	2.3
	HP HVAC Heating Total	120.2	114.3	88.6
	HP HVAC Cooling Total	1.6	1.6	1.0
Spain	RAS HVAC Cooling Total	9.7	8.8	18.1
	RAS HVAC Heating Total	2.2	2.2	2.5
	HP HVAC Heating Total	60.7	60.4	76.7
	HP HVAC Cooling Total	1.5	1.5	2.2
Portugal	RAS HVAC Cooling Total	10.4	7.7	36.7
	RAS HVAC Heating Total	0.5	0.5	0.5
	HP HVAC Heating Total	24.6	23.4	55.9
	HP HVAC Cooling Total	2.6	2.5	6.0
UK	RAS HVAC Cooling Total	6.3	6.2	8.0
	RAS HVAC Heating Total	2.7	2.7	2.5
	HP HVAC Heating Total	75.7	69.9	88.4
	HP HVAC Cooling Total	1.0	1.0	0.7

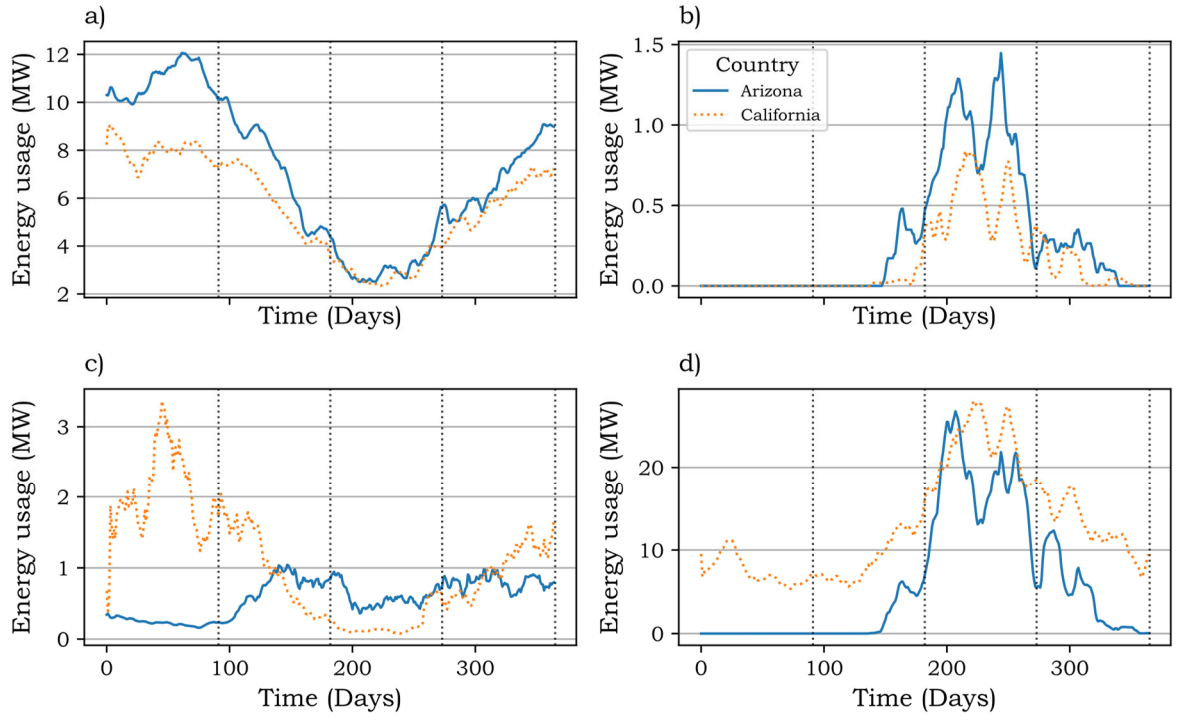

Figure 4.37: *Yearly energy time response for (a) cooling of the RAS, (b) heating of the RAS, (c) cooling of the HP and (d) heating of the HP for Western regions of USA.*

The western regions of the USA (Figure 4.37) required RAS cooling throughout the year. Both regions had a seasonal response large seasonal variation. The regions had a large cooling demand in summer months and small cooling demand in winter. Arizona had a peak demand of 12.0 MW and California had a peak demand of 8.3 MW. Arizona's RAS cooling component contributed to 51.1% of the total system energy. California's RAS cooling component contributed 28.1% and was not the dominant contributor.

Arizona experiences hot dry climate conditions but experiences colder winters and therefore heating was required. Arizona experienced large seasonal variations and required more heating in the winter for the RAS facility. A peak heating demand of 1.3 MW was observed. California experiences fewer extreme temperatures and is more humid, a peak heating demand of 1.0 MW was observed for this region. The peak demand occurred in winter and no heating was required during the hot summer months.

Heating required for the HP greenhouse was a big contributor to the total system energy usage. California had a dominant HP heating contribution to the total system energy usage of 65.0%. Although Arizona showed a high HP heating contribution of 41.5% the RAS, cooling was still dominant. Heating was required throughout the year for California and had a peak demand of 29.3 MW. Arizona had a peak demand of 25.7 MW.

To cope with the high day temperatures experienced by both regions, ventilation was required throughout the year. California had a smaller seasonal variation given the higher humidity and Arizona experienced large peaks in summer. California had a peak demand of 3.1 MW and Arizona had a peak demand of 1.0 MW. constitutes a summary of the HVAC energy usage for the respective regions.

Table 4.15 constitutes a summary of the HVAC energy usage for the respective regions.

Table 4.15: *HVAC data summary for the RAS & HP for Western regions of USA*

Region	Energy Component	Peak Energy Usage [MW]	Season Variation [MW]	Percentage Contribution to Total Energy [%]
Arizona	RAS HVAC Cooling Total	12.0	9.6	51.1
	RAS HVAC Heating Total	1.3	1.3	2.0
	HP HVAC Heating Total	25.7	25.7	41.5
	HP HVAC Cooling Total	1.0	0.9	4.3
California	RAS HVAC Cooling Total	8.3	6.1	28.1
	RAS HVAC Heating Total	1.0	1.0	0.8
	HP HVAC Heating Total	29.3	23.8	65.0
	HP HVAC Cooling Total	3.1	3.0	5.3

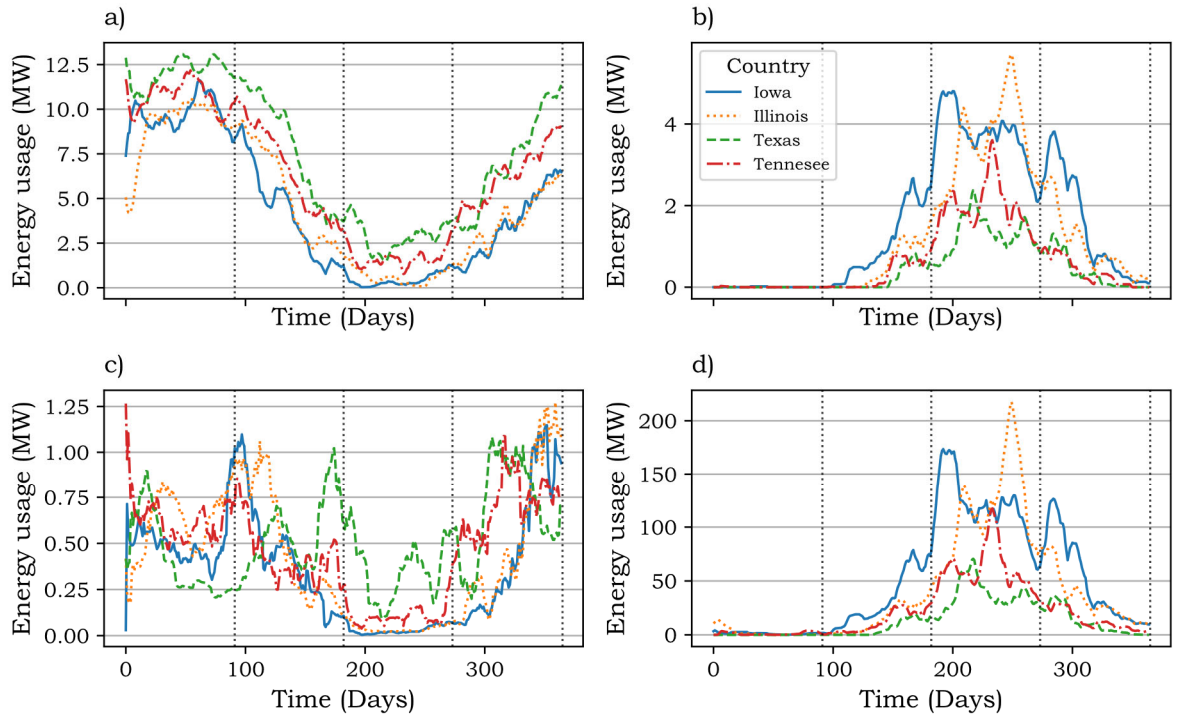

Figure 4.38: *Yearly energy time response for (a) cooling of the RAS, (b) heating of the RAS, (c) cooling of the HP and (d) heating of the HP for Central regions of USA.*

The central regions of the USA (Figure 4.38) had a seasonal response with large seasonal variations. The peak RAS cooling demand was experienced in summer and minimal energy was required in winter. The peak RAS cooling demands ranged from 10.5 MW for Illinois to 12.9 MW for Texas. The cooling was a minor contributor to the total system energy usages with the best performing region, Illinois, contributing 10.1% to the total system energy usage. Texas contributed 33.6% to the total system energy which indicated that the most cooling was required for this region since this region had experienced the highest temperatures.

The RAS heating was required for the colder months for all regions. Texas, the hottest region, required the least amount of heating and had a peak heating demand of 3.1 MW. Iowa was the coldest region and had a peak heating demand of 5.7 MW. The response showed a peak energy demand during the coldest part of the year and no heating was required during summer. The best performing region, Texas, had a peak heating demand that was 10 times the heating demand of the best performing region in South Africa, Durban.

The HP heating had a similar response as the RAS heating. HP heating was the greatest contributor to the total system energy usage for all the regions. The HP heating in Iowa was 88.9% of the total system energy, in Illinois at 86.0%, Texas at 61.3% and Tennessee at 73.7%. These large contributions heavily affected the trend of the total system energy. The best performing region for HP peak heating demand was Texas with 81.1 MW of heating required.

The worst performing region was Iowa with 231.6 MW heating required. Texas had a peak heating demand that was 6 times larger than the peak demand of Durban, South Africa.

Ventilation was required throughout the year to maintain internal conditions. Large seasonal variations were noted, much like the European countries. The most ventilation was required in summer and ventilation demands were smaller in winter during the colder months. Table 4.16 constitutes a summary of the HVAC energy usage for the respective regions.

Table 4.16: *HVAC data summary for the RAS & HP for Central regions of USA*

Region	Energy Component	Peak Energy Usage [MW]	Season Variation [MW]	Percentage Contribution to Total Energy [%]
Iowa	RAS HVAC Cooling Total	11.2	11.2	7.5
	RAS HVAC Heating Total	5.7	5.7	2.7
	HP HVAC Heating Total	231.6	231.4	88.9
	HP HVAC Cooling Total	1.1	1.1	0.6
Illinois	RAS HVAC Cooling Total	10.5	10.4	10.1
	RAS HVAC Heating Total	5.4	5.4	2.6
	HP HVAC Heating Total	199.4	199.3	86.0
	HP HVAC Cooling Total	1.2	1.2	0.9
Texas	RAS HVAC Cooling Total	12.9	12.2	33.6
	RAS HVAC Heating Total	3.1	3.1	2.1
	HP HVAC Heating Total	81.1	81.1	61.3
	HP HVAC Cooling Total	1.1	1.0	2.3
Tennessee	RAS HVAC Cooling Total	11.9	10.7	22.0
	RAS HVAC Heating Total	2.9	2.9	2.1
	HP HVAC Heating Total	95.4	95.3	73.7
	HP HVAC Cooling Total	0.9	0.9	1.6

The eastern regions of USA (Figure 4.39) had a seasonal system response with regard to RAS cooling. The highest demands were experienced in the hot summer months with an energy reduction in the colder winter months. Florida, which is a hot humid region, followed the same trend as New York, Ohio and Vermont but there was a significant off set that indicated an increased cooling demand throughout the year. Florida had a peak cooling demand of 12.5 MW and was the best performing region with regard to RAS cooling was Vermont with a peak demand of 8.5 MW. Florida was the only region where the RAS cooling response was the largest contributor to the total system energy usage with a value of 61.9%. The total energy usage in the remaining regions was overwhelmingly driven by HP heating.

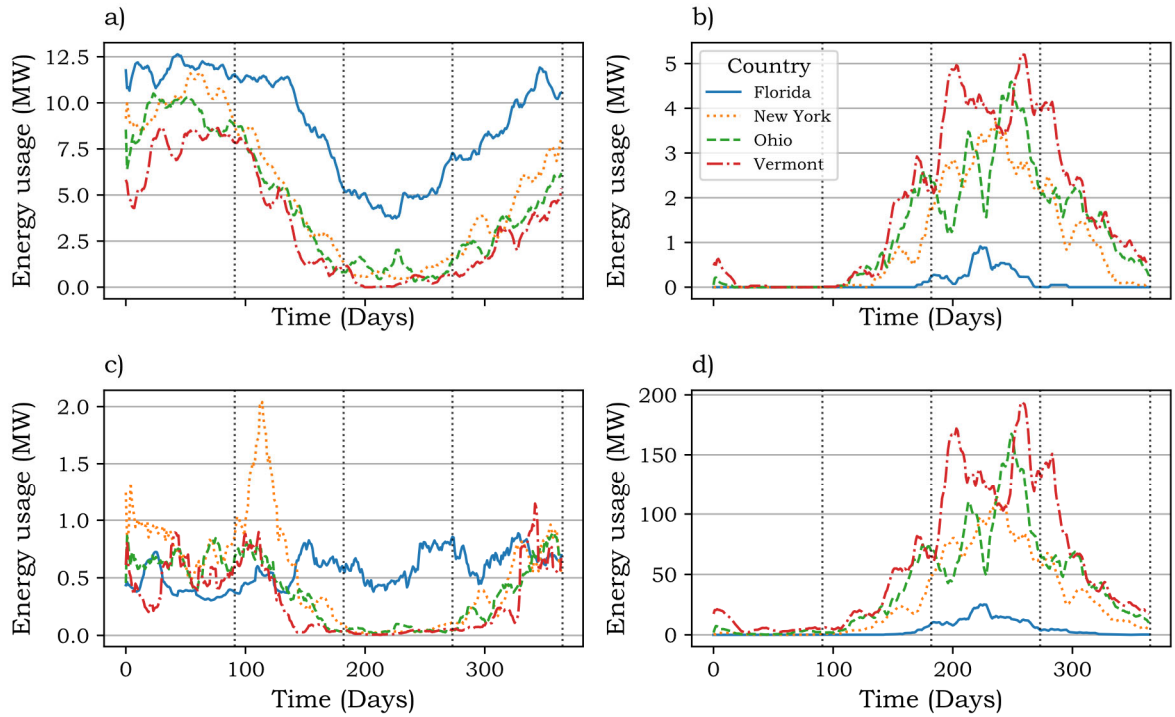

Figure 4.39: *Yearly energy time response for (a) cooling of the RAS, (b) heating of the RAS, (c) cooling of the HP and (d) heating of the HP for Eastern regions of USA.*

The RAS heating had a minimal demand during summer, with the peak demands occurring in winter. Florida showed significantly fewer heating requirements than the other four states. Florida had a peak heating demand of 1.9 MW. The worst performing region, Vermont, had a peak heating demand of 5.1 MW.

The HP heating was the biggest contributor to the total system energy usage for New York, Ohio and Vermont, with values of 81.7%, 85.9% and 90.9% for the respective regions. Florida was the best performing region with an HP heating demand of 42.8 MW. The worst performing region was Vermont with a heating requirement of 175.2 MW. The peak heating demands were experienced in the colder winter months. Florida is a hot and humid region that required more cooling than heating throughout the year. The other regions experienced extreme winters and high energy demands are the result of this.

Florida showed small seasonal variation with regard to ventilation demands. The response was constant throughout the year in order to deal with the high day temperatures. The other three states showed bigger seasonal variation due to the cold winters. The output results are summarised in Table 4.17.

Table 4.17: *HVAC data summary for the RAS & HP for Eastern regions of USA*

Region	Energy Component	Peak Energy Usage [MW]	Season Variation [MW]	Percentage Contribution to Total Energy [%]
Florida	RAS HVAC Cooling Total	12.5	10.6	61.9
	RAS HVAC Heating Total	1.9	1.9	0.9
	HP HVAC Heating Total	42.8	42.8	32.2
	HP HVAC Cooling Total	0.9	0.7	3.9
New York	RAS HVAC Cooling Total	11.5	11.1	13.7
	RAS HVAC Heating Total	3.7	3.7	2.7
	HP HVAC Heating Total	112.6	112.5	81.7
	HP HVAC Cooling Total	1.8	1.8	1.4
Ohio	RAS HVAC Cooling Total	10.4	10.1	10.3
	RAS HVAC Heating Total	4.6	4.6	2.7
	HP HVAC Heating Total	164.3	163.9	85.9
	HP HVAC Cooling Total	0.9	0.9	0.9
Vermont	RAS HVAC Cooling Total	8.5	8.5	5.5
	RAS HVAC Heating Total	5.1	5.1	2.8
	HP HVAC Heating Total	175.2	172.3	90.9
	HP HVAC Cooling Total	1.0	1.0	0.5

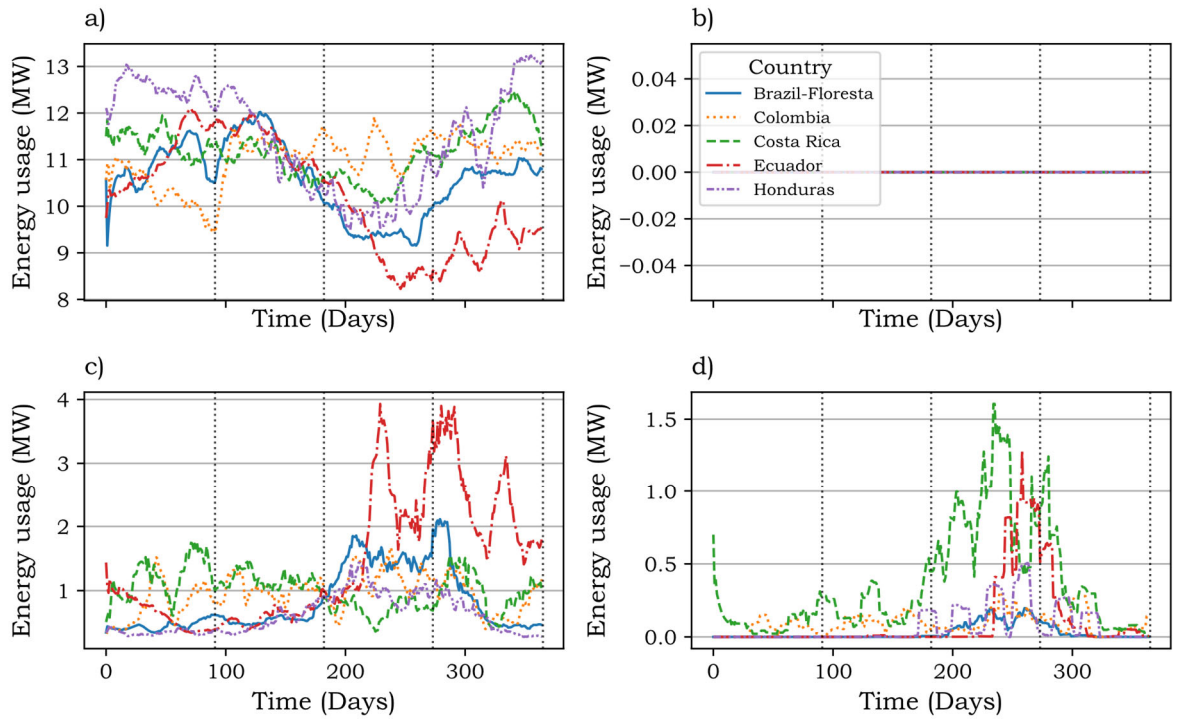

Figure 4.40: *Yearly energy time response for (a) cooling of the RAS, (b) heating of the RAS, (c) cooling of the HP and (d) heating of the HP for countries in South America.*

All the countries in South America (Figure 4.40) had small seasonal variations, which indicated that there were small variations between the winter and summer temperatures. There was a reduction in RAS cooling demand for winter but not as drastic as the African, European and North American countries. Honduras had the highest peak RAS cooling demand of 13.2 MW.

Floresta Brazil and Ecuador had the smallest peak RAS cooling demand of 12.0 MW. All the countries indicated that the highest contributor to the total system energy use was RAS cooling with values above 85%.

All the countries indicated that there was no demand for RAS heating during any time of the year. A constant response of 0 MW was produced by the model. Given the small seasonal variations and that all these regions experience tropical, hot and humid climates there was no demand for heating during winter.

The HP heating was required during the colder periods of the year but was minimal compared to the other countries. Costa Rica had the highest HP heating demand with a value of 1.5 MW.

Ventilation demands for Floresta Brazil, Colombia, Costa Rica and Honduras had small seasonal variations. Ventilation demands did not drastically change for winter and summer given the hot humid climate. Ventilation demands made a greater contribution to the total system energy usage than heating did. This was not the case for other regions around the world. The HVAC energy usage is summarised in Table 4.18.

Table 4.18: *HVAC data summary for the RAS & HP for countries in South America*

Region	Energy Component	Peak Energy Usage [MW]	Season Variation [MW]	Percentage Contribution to Total Energy [%]
Brazil	RAS HVAC Cooling Total	12.0	2.8	91.3
	RAS HVAC Heating Total	0.0	0.0	0.0
	HP HVAC Heating Total	0.2	0.2	0.3
	HP HVAC Cooling Total	2.0	1.7	7.1
Colombia	RAS HVAC Cooling Total	12.7	3.2	90.2
	RAS HVAC Heating Total	0.0	0.0	0.0
	HP HVAC Heating Total	0.2	0.2	0.8
	HP HVAC Cooling Total	1.5	1.4	7.8
Costa Rica	RAS HVAC Cooling Total	12.4	2.4	88.1
	RAS HVAC Heating Total	0.0	0.0	0.0
	HP HVAC Heating Total	1.5	1.5	2.7
	HP HVAC Cooling Total	1.8	1.4	8.0
Ecuador	RAS HVAC Cooling Total	12.0	3.6	85.8
	RAS HVAC Heating Total	0.0	0.0	0.0
	HP HVAC Heating Total	1.0	1.0	0.9
	HP HVAC Cooling Total	3.8	3.4	12.0
Honduras	RAS HVAC Cooling Total	13.2	3.7	93.4
	RAS HVAC Heating Total	0.0	0.0	0.0
	HP HVAC Heating Total	0.4	0.4	0.6
	HP HVAC Cooling Total	1.4	1.1	4.8

4.4.3 Total System Energy Usage

It was observed that the major contributors to the total system energy usage were RAS cooling and HP heating. Other components exerted a minor influence on the system response and the RAS cooling, and the HP heating components ultimately determined the final energy demand trend. With this information and an initial comparison of the results for each region, the number of regions used in the comparison was reduced. Only the top performing regions of each continent were considered and compared. The total energy usage of the system was determined by adding the individual components that require energy. These components included RAS circulation pumps from Eq. (4), RAS lighting from Eq. (1), RAS UV-disinfection from Eq. (12), RAS O_2 generation from Eq. (13), RAS CO_2 degassing from Eq. (2), RAS HVAC from Eq. (58), Eq. (59), Eq. (64), Eq. (66), Eq. (67) and Eq. (70), HP circulation pumps from Eq. (73), HP lighting from Eq. (72), and lastly, HP HVAC from Eq. (109), Eq. (111), Eq. (112), and Eq. (114). The cumulative yearly energy was the time integral of the sum of each energy contributing component in the system. The results obtained from the models were plotted and are presented in Figure 4.41 to Figure 4.46.

The energy usage for the top performing regions of each continent is illustrated in Figure 4.47 and was compared with the performance of South Africa. The first figure is the time response for the rate at which energy is used throughout the year in Mega Watts (MW). This is the result of the flow component (rate) for the total system energy usage. The second plot is the stock component (accumulation) of the energy in the system.

The total system energy response for the two top performing regions in South Africa, namely Durban and Port Elizabeth, is illustrated in Figure 4.41. Both regions are coastal regions with high humidity levels throughout the year and where winters are not extremely cold. Durban indicated higher levels of incoming solar radiation compared to Port Elizabeth. The weather data summaries are evident in Figure 4.2 and Figure 4.7.

The regions had similar time responses during summer. Although a similar trend was observed for winter, Durban showed less energy usage during this period. This meant less heating was required compared to Port Elizabeth. It was observed that the system energy demand spiked halfway through autumn when colder temperatures were experienced. The system required heating which was much more energy intensive than the cooling required as illustrated in Figure 4.41. Energy was accumulated at a linear increasing rate for both regions. As soon as the system required heating, there was a sudden increase in energy. Port Elizabeth showed a greater increasing slope compared to Durban.

The yearly cumulative energy for Durban was 4550 MW and 5324 MW for Port Elizabeth. Durban had a peak energy demand of 18.4 MW and Port Elizabeth had a value of 21.1 MW. Ultimately the total energy consumed by the system was less for Durban than for Port Elizabeth owing to higher winter temperatures and incoming solar radiation.

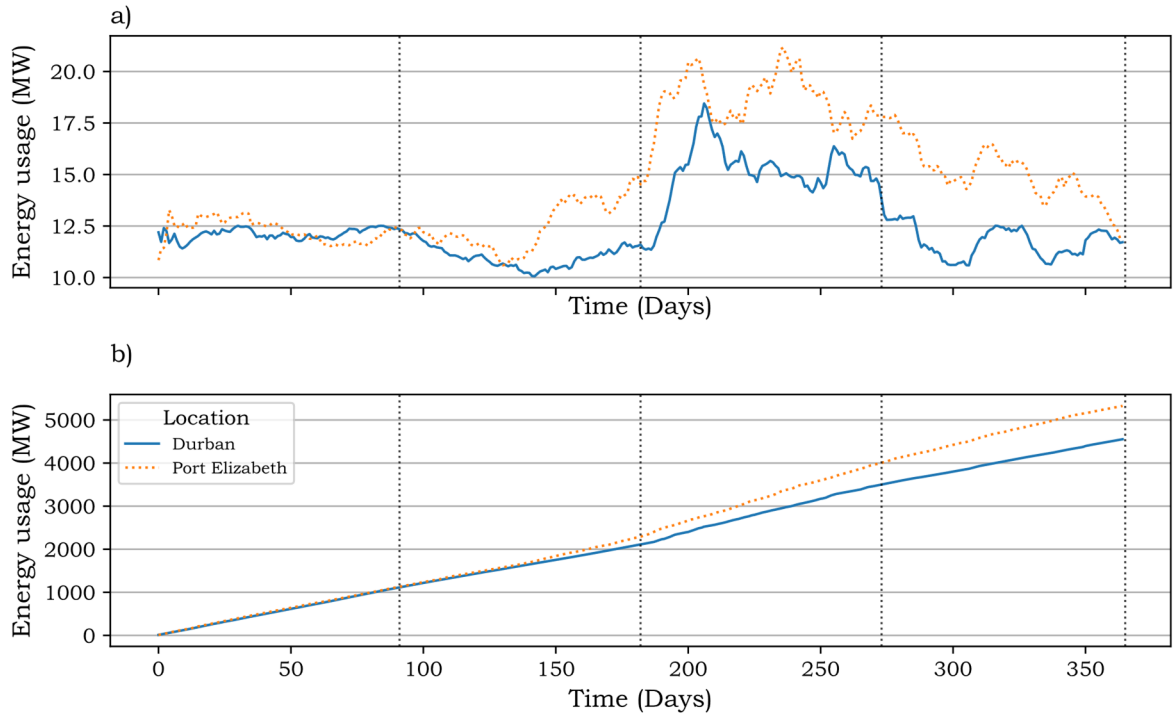

Figure 4.41: *(a) Total system energy time response and (b) Total cumulative energy usage for top performing regions in South Africa.*

Figure 4.42. Both regions exhibited high humidity levels throughout the year. The yearly temperatures of the two regions did not change drastically during the year and the winters are moderate.

Uganda had higher levels of incoming solar radiation compared to Nigeria. The weather data summaries are displayed in Figure 4.10 and Figure 4.11.

During summer, Nigeria had a higher energy demand due to higher temperatures and the demand for cooling. During the autumn and winter months, Uganda had a higher energy demand owing to heating requirements. This was due to colder winters and colder temperatures during the night compared to Nigeria. Both system responses were similar when comparing the energy accumulation. The rate of accumulation was linear for the year. However, the gradient for Nigeria was lower and therefore this indicated that less energy was consumed during the year. Nigeria experienced higher temperatures for longer periods of the year. The humidity was also higher for longer periods of the year which aided in heat loss. This caused energy usage to be more efficient in Nigeria as less heating was required.

The yearly cumulative energy for Nigeria was 4330 MW and for Uganda, 4473 MW. Nigeria had a peak energy demand of 13.1 MW and Uganda had a value of 13.7 MW. Ultimately, the total energy consumed by the system was less for Nigeria than for Uganda owing to higher humidity and longer periods of high temperatures.

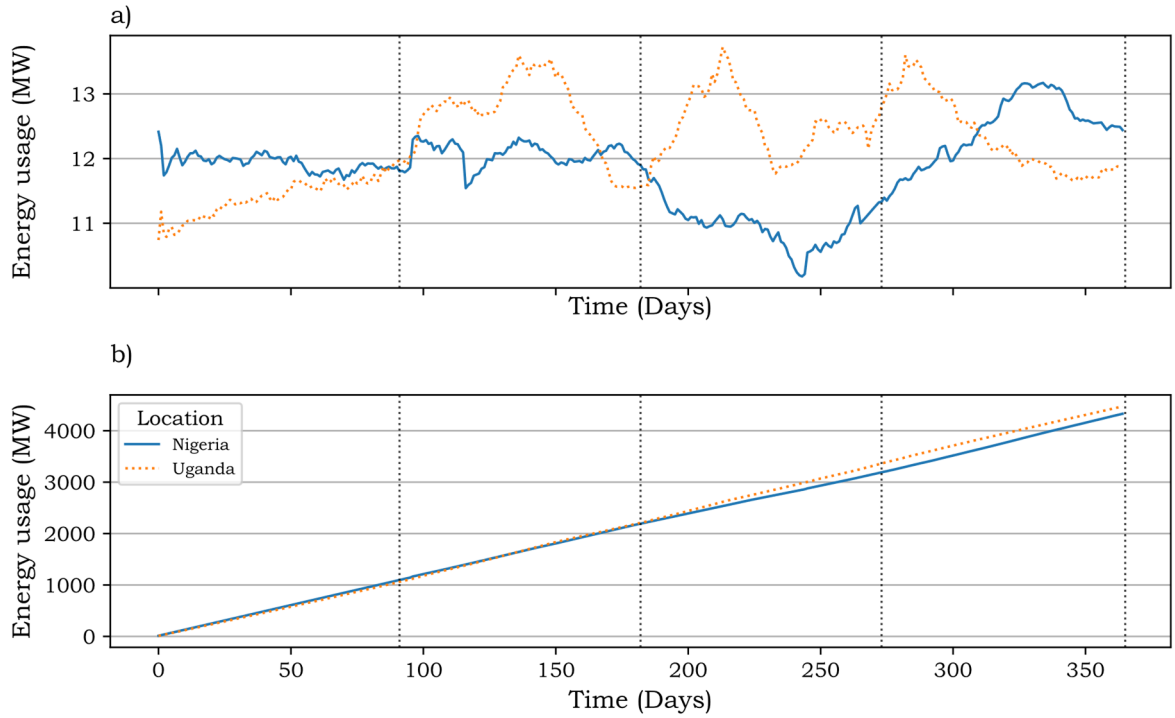

Figure 4.42: *(a) Total system energy time response and (b) Total cumulative energy usage for top performing regions in Africa.*

The total system energy response for the two top performing regions in Asia, namely Alor Setar, Malaysia, and Can Tho, Vietnam, is illustrated in Figure 4.43. Both regions have extremely high humidity levels throughout the year. The yearly temperatures of the two regions did not change drastically during the year and there was almost no differentiation between summer and winter. Vietnam had higher levels of incoming solar radiation compared to Malaysia. The weather data summaries are presented in Figure 4.12 and Figure 4.13.

Both regions had a similar time response, with Vietnam exhibiting a higher energy demand throughout the year compared to Malaysia. During summer, Vietnam had a higher energy demand owing to higher temperatures and the demand for cooling. During autumn and winter, Vietnam had a higher energy demand due to heating requirements. Both system responses were similar when comparing the energy accumulation. The rate of accumulation was linear for the year. However, the slope for Malaysia was less steep and therefore, this indicated that less energy was consumed during the year. For both systems, the dominant

contributor was cooling demand rather than heating demand. This was due to the constant high temperature experienced throughout the year and the absence of a colder season.

The yearly cumulative energy for Malaysia was 4372 MW and 4621 MW for Vietnam. Malaysia had a peak energy demand of 13.1 MW and Vietnam had a value of 13.9 MW. Ultimately the total energy consumed by the system was less for Malaysia than Vietnam by slight margins. Humidity and air temperature were the biggest contributors to efficient energy usage since the incoming solar radiation for the regions was less compared to that of African countries.

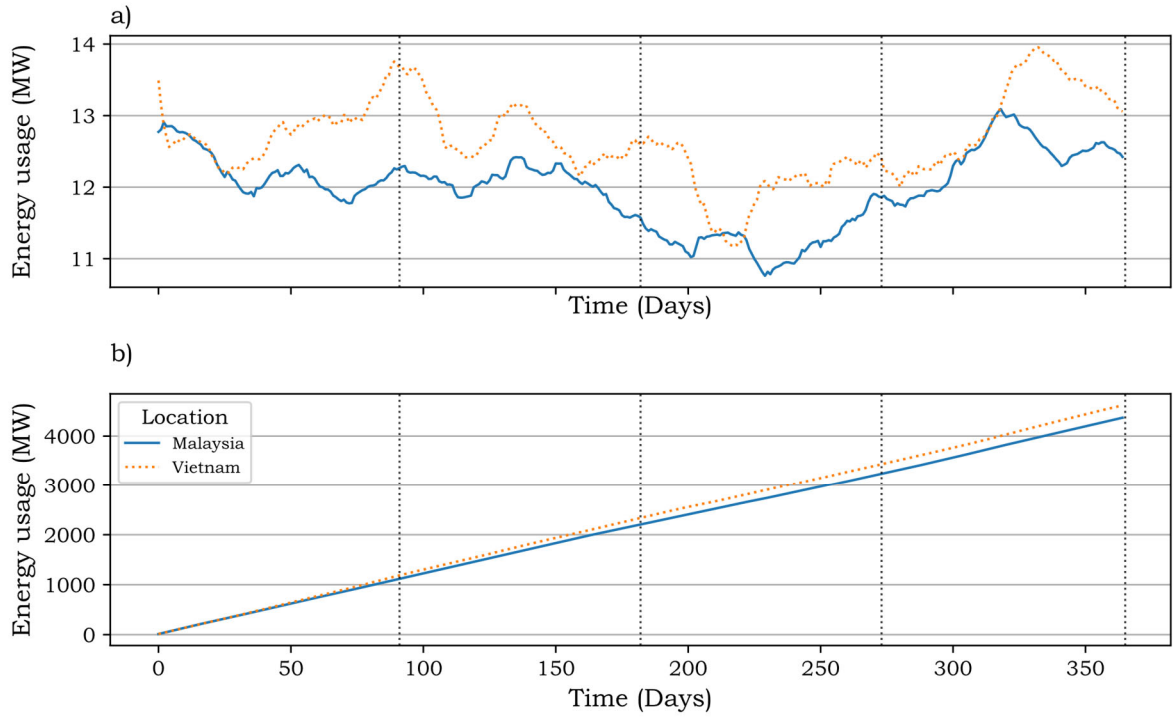

Figure 4.43: *(a) Total system energy time response and (b) Total cumulative energy usage for top performing regions in Asia.*

The total system energy response for the two top performing regions in Europe, namely Lisbon, Portugal and Madrid, Spain, is Illustrated in Figure 4.44. These regions are warmer compared to the rest of Western Europe. Portugal has high humidity levels throughout the year and winters are milder compared to Spain. Portugal has higher levels of incoming solar radiation compared to Spain. The weather data summaries are displayed in Figure 4.14 and Figure 4.15. The regions have similar time responses during summer. Although a similar trend is observed for winter, Portugal shows less energy usage during this period. This means that less heating is required compared to Spain. It is observed that the system energy demand spikes halfway through autumn when colder temperatures are experienced. The system requires heating, which

is much more energy intensive than the cooling required, as illustrated in Figure 4.44. Energy is accumulated at a constant increasing rate for both regions. As soon as the system requires heating, there is a sudden increase in energy. Spain shows a steeper increasing slope compared to Portugal.

The yearly cumulative energy for Portugal was 6370 MW and 10250 MW for Spain. Portugal has a peak energy demand of 28.1 MW and Spain has a value of 65.2 MW. Ultimately, the total energy consumed by the system is less for Portugal than Spain owing to a more constant temperature variation between summer and winter and higher humidity.

The trends are similar to the South African regions, but the colder winters cause the systems to consume more energy compared to Durban and Port Elizabeth.

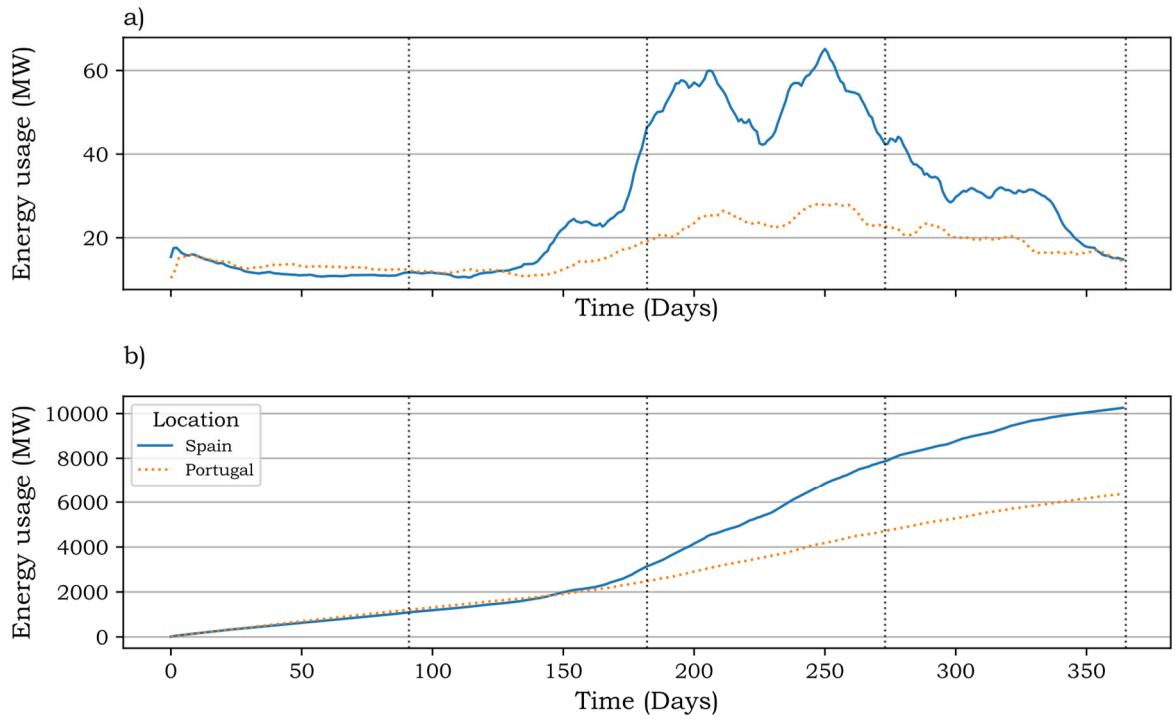

Figure 4.44: *(a) Total system energy time response and (b) Total cumulative energy usage for top performing regions in Europe.*

The total system energy response for the two top performing regions in North America, namely Orlando, Florida, USA and Dallas, Texas, USA, is illustrated in Figure 4.45. Both regions experienced high levels of humidity throughout the year with high levels of incoming solar radiation. Texas had colder winters compared to Florida and higher temperatures were experienced by Florida for longer periods of the day. The weather data summaries are displayed in Figure 4.16 and Figure 4.17.

The regions had similar time responses during summer. Although a similar trend was observed for winter, Florida showed less energy usage during this period. This meant that less heating was required compared to Texas.

It was observed that the system energy demand spiked halfway through autumn when colder temperatures were experienced. The system required heating, which is much more energy intensive than the cooling required (Figure 4.45). Energy was accumulated at a constant increasing rate for both regions. As soon as the system required heating there was a sudden increase in energy. Texas showed a much steeper increased slope compared to Florida.

The yearly cumulative energy for Florida was 5240 MW and 8100 MW for Texas. Florida had a peak energy demand of 27.9 MW and Texas had a value of 67.4 MW. Ultimately, the total energy consumed by the system was less for Florida than Texas owing to less extreme temperature differences in winter.

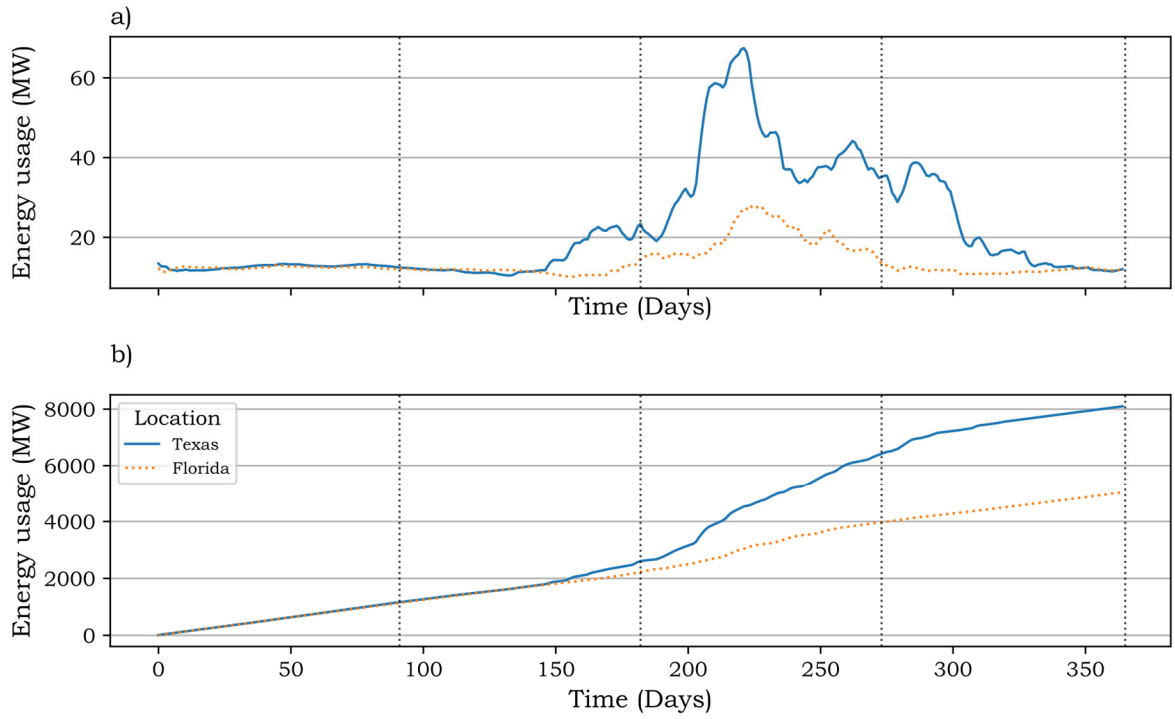

Figure 4.45: *(a) Total system energy time response and (b) Total cumulative energy usage for top performing regions in North America.*

The total system energy response for the two top performing regions in South America, namely Floresta, Brazil and Tela, Honduras, is illustrated in Figure 4.46. Both regions had extremely high humidity levels throughout the year. The yearly temperatures of the two regions did not change drastically throughout the year and there was almost no differentiation between summer and winter. Floresta Brazil had higher levels of incoming solar radiation compared to Honduras. The weather data summaries are displayed in Figure 4.19 and Figure 4.18.

Both regions had a similar response with the Honduras exhibiting a higher energy demand throughout the year compared to Floresta Brazil. During summer, Honduras had a higher energy demand due to higher temperatures and the demand for cooling. During autumn and winter, the heating demands of both regions followed the same trend and magnitudes. Both system responses were similar when comparing the energy accumulation. The rate of accumulation was linear for the year. However, Floresta, Brazil had a lesser slope and therefore, this indicated that less energy was consumed during the year.

For both systems, the dominant contributor was cooling demand rather than heating demand. This was due to the constant high temperature experienced during the year and the absence of a colder season.

The yearly cumulative energy for Brazil was 4239 MW and 4505 MW for Honduras. Brazil had a peak energy demand of 12.6 MW and Honduras had a value of 13.7 MW. Ultimately, the total energy consumed by the system was less for Brazil than Honduras by slight margins. Humidity and air temperature were the biggest contributors to efficient energy usage since the incoming solar radiation for the regions was smaller compared to African countries.

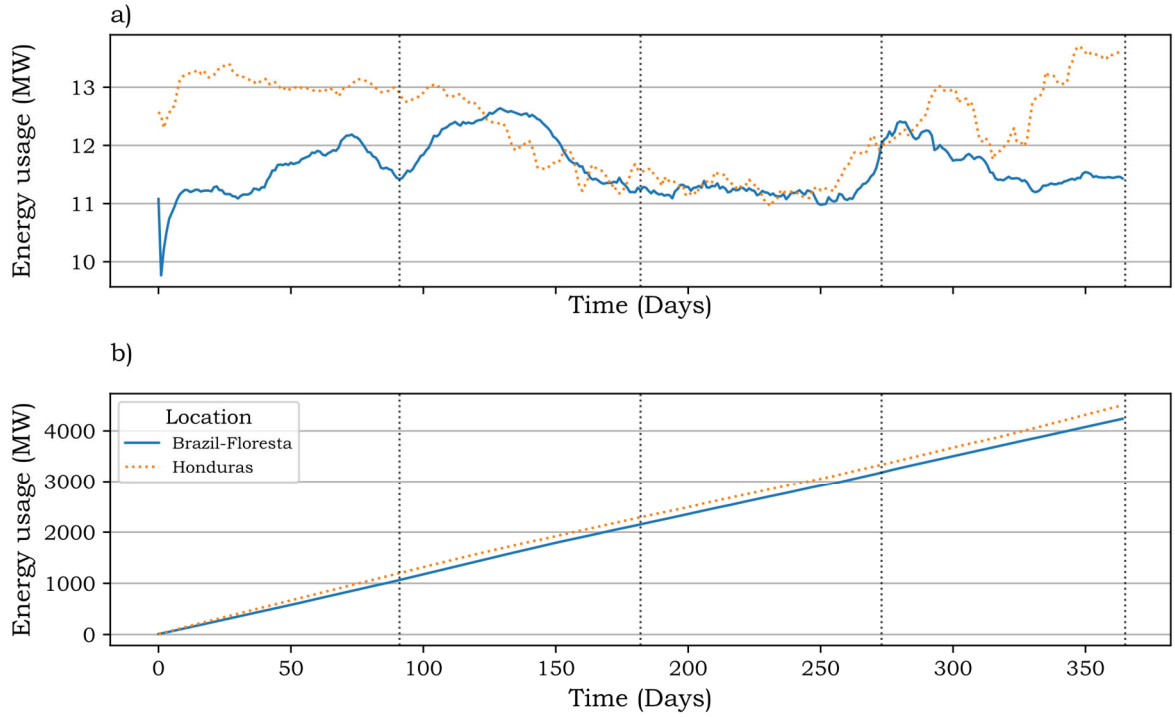

Figure 4.46: *(a) Total system energy time response and (b) Total cumulative energy usage for top performing regions in South America.*

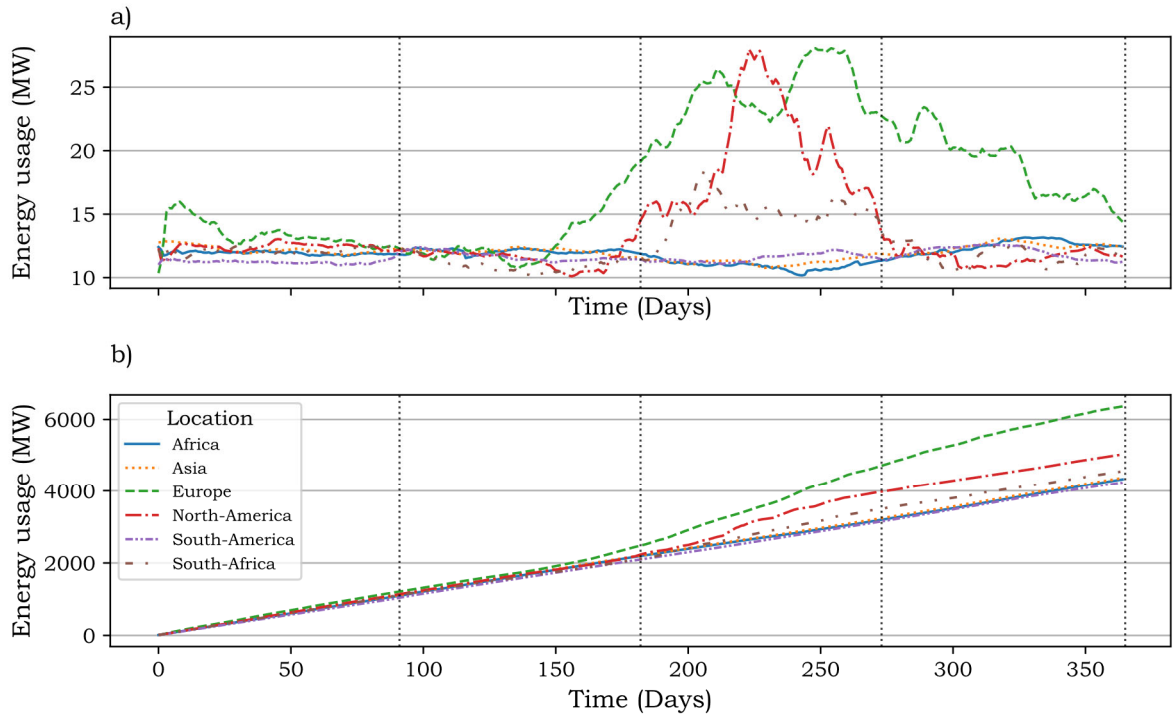

Figure 4.47: *(a) Total system energy time response and (b) Total cumulative energy usage for top performing regions around the World.*

The results of the top performing region for each continent are summarised in Table 4.19.

Table 4.19: *Performance indicators for top energy performing countries around the World.*

Region	Rank	Peak Energy Demand [MW]	Cumulative Energy Consumption [MW]	Percentage underperforming. [%]
Floresta Brazil South America	1	12.6	4239	0
Abuja Nigeria Africa	2	13.1	4330	2.1
Alor Setar Malaysia Asia	3	13.1	4372	3.1
Durban South Arica	4	18.4	4550	7.3
Orlando Florida North America	5	27.9	5240	23.6
Lisbon Portugal Europe	6	28.1	6370	50.3

The results revealed that Floresta Brazil, South America, was the most energy efficient country in which to operate a system as described in the research, followed by Abuja, Nigeria, in Africa and Alor Setar, Malaysia, in Asia. The stock and flow diagrams as presented in Figure 3.31 to Figure 3.49 produced the output result illustrated in Figure 4.47. All the flow variable components in the model contributed to the stock variable namely total system energy consumption.

The top three locations in terms of energy performance have hot, humid climates where a minimal amount of heating was required during the year. Cooling demands were the dominant

contributor to the total system energy usage. The low performing locations such as Orlando, Florida, USA and Lisbon, Portugal, had higher energy consumption of 23.6% and 50.3% respectively for a year compared to the top performing country. Although these locations have humid and hotter climates, the duration for which these conditions were experienced was not long enough to exhibit energy efficiency. Cold winters caused heating demands, which were very energy intensive, as evident by the results.

Durban, South Africa, had a 7.3% higher cumulative energy compared to the best performing region. Even though the energy usage was higher throughout the year, it was still a good performing region. The cooling demands during summer were comparable with the top three performing countries, and closely followed the same trend and slope as the countries that were more energy efficient. There was a short period of three months during winter where energy demands spiked which caused a peak demand of 18.4 MW. Given the humid and hot climate in the Durban region, the results showed that Durban offers favourable climatic conditions when compared to global operations. The region provides competitive energy efficiency, given the climate. Other regions in South Africa could still be suitable for operating aquaponic systems on a large scale; however, they might be less energy efficient.

4.4.4 Total System Water Usage

The yearly water consumption in the system and the cumulative water consumption for a yearly period are illustrated in Figure 4.48 to Figure 4.58. The output results presented in this section is the result of the stock and flow diagram presented in Figure 3.50. According to the mass balance presented in Eq. (116), a negative value indicates a water deficit and that the system is consuming water. A positive value indicates that there was a water surplus, which was stored in a tank and used in the process in the future. Regional humidity and air temperature played a major role in driving the water usage. The higher the humidity, the lower the evapotranspiration rate and the less water will be lost. However, the higher the air temperature, the higher the evapotranspiration rate and more water will be lost. The higher the external humidity, the higher the condensation rate and the higher the water gain in the system. The cumulative water usage is the time integral of Eq. (116), which yields the total net water consumption for the year.

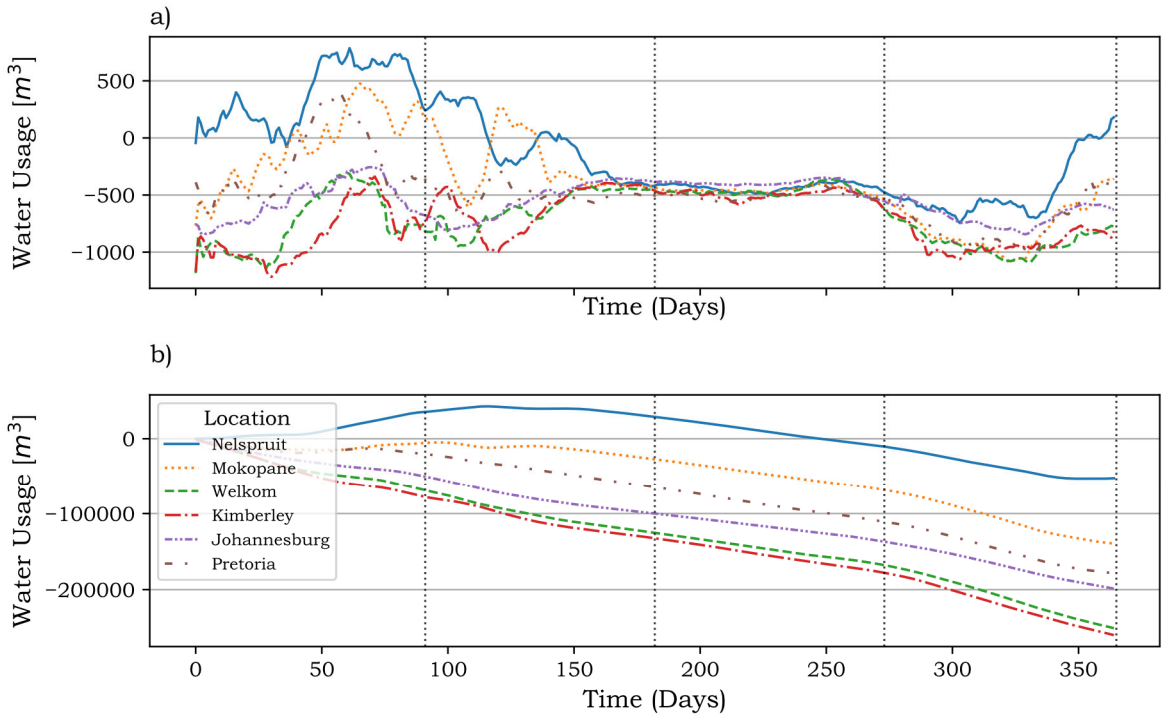

Figure 4.48: *Total system water usage (a) and Total cumulative water usage (b) for inland regions of South Africa*

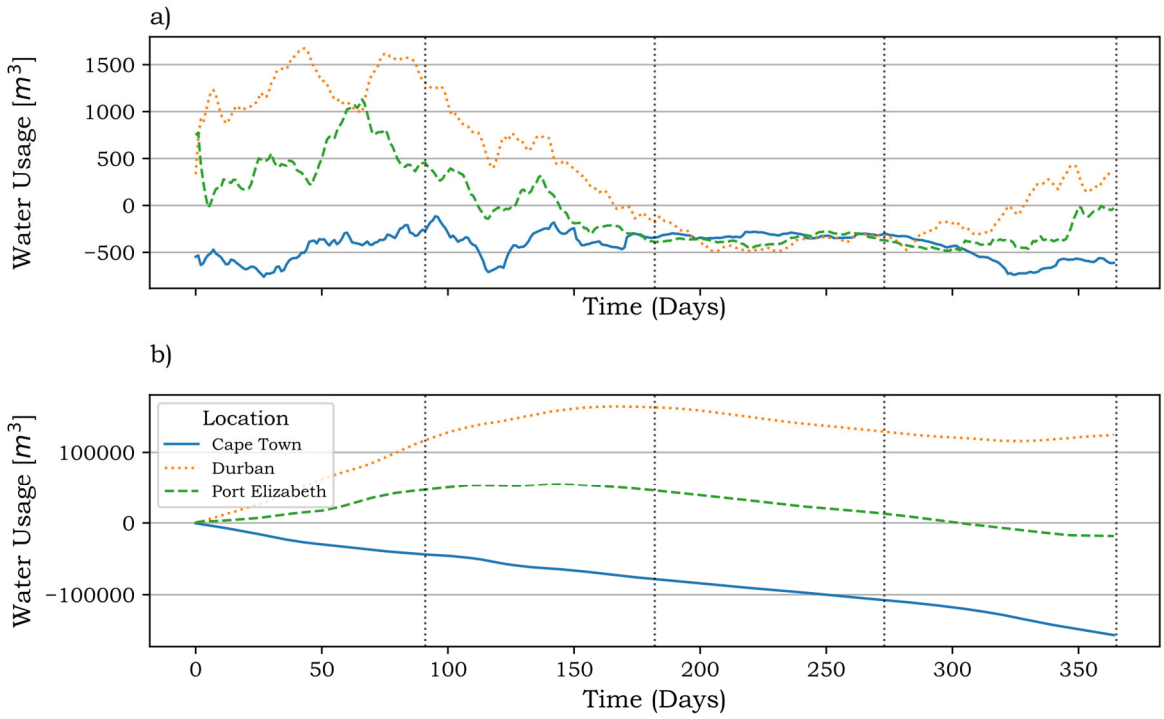

Figure 4.49: *Total system water usage (a) and Total cumulative water usage (b) for coastal regions of South Africa*

All the regions in South Africa (Figure 4.48 and Figure 4.49) consumed water during winter and a constant water consumption response was observed.

Durban was the only region in South Africa that had a water surplus at the end of the year. All the other regions had a net water consumption during the year.

Nelspruit and Port Elizabeth showed positive water returns during summer when the humidity was high. The rate of water consumption was greater than the water production and at the end of the seasonal year, both regions had a negative net water usage. The inland regions, excluding Nelspruit, consumed water throughout the year and had a net water usage. These regions had drier climates compared to the humid coastal regions.

Table 4.20: *Net water usage or return for regions in South Africa*

Rank	Region	Water Usage [$10^3 m^3$]	Rank	Region	Water Usage [$10^3 m^3$]
1	Durban	124.8	**6**	Pretoria	-178.5
2	Port Elizabeth	-18.2	**7**	Johannesburg	-198.6
3	Nelspruit	-52.4	**8**	Welkom	-250.6
4	Mokopane	-139.5	**9**	Kimberley	-259.7
5	Cape Town	-156.3			

Durban was the top water performing region in South Africa (Table 4.20) with a net water surplus of 124.8x10^3 m^3. Since South Africa is considered to be a water scarce country, water usage efficiency is an extremely important factor to consider. The models showed that most regions in South Africa will consume water given their dry climates.

The models revealed that the African regions performed well with regard to water usage and water efficiency (Figure 4.50). Nigeria, Zambia, and Uganda yielded a net water return in a yearly cycle. These regions experience hot humid conditions, which favour water usage during the year. Moisture saturated air reduced the rate of water loss in crops and increased the rate of condensation, which contributed to the positive water return.

Table 4.21: *Net water usage or return for regions in Africa*

Rank	Region	Water Usage [$10^3 m^3$]	Rank	Region	Water Usage [$10^3 m^3$]
1	Nigeria	556.9	**3**	Uganda	55.2
2	Zambia	57.3	**4**	Egypt	-29.7

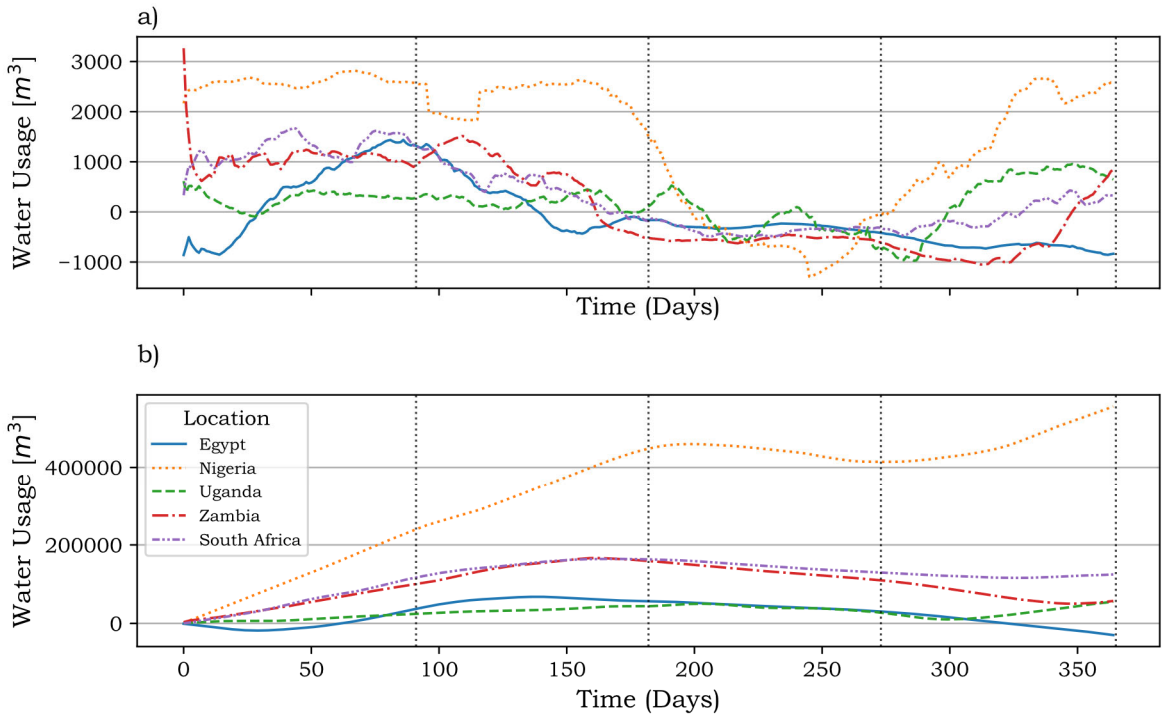

Figure 4.50: *Total system water usage (a) and Total cumulative water usage (b) for countries in Africa*

Nigeria was the top water performing region in Africa (Table 4.21) with a net water surplus of 556.9x10^3 m^3. Egypt, which has a dry arid climate, was the worst water performing region in Africa with a net water usage of -29.7x10^3 m^3 for a yearly cycle.

Table 4.22: *Net water usage or return for regions in Asia*

Rank	Region	Water Usage [$10^3 m^3$]	Rank	Region	Water Usage [$10^3 m^3$]
1	Malaysia	1209.1	**6**	Bangladesh	831.5
2	Vietnam	1129.7	**7**	Laos	742.6
3	Indonesia	1081.2	**8**	Myanmar	706.6
4	Thailand	1061.2	**9**	China	612.6
5	Philippines	1035.4	**10**	Taiwan	595.3

All the regions in Asia had a net positive water return for the year (Figure 4.51 and Figure 4.52). These regions experience humid conditions, which drive water return in the system. The worst performing region, Taiwan, still produced more water than the best performing region in Africa. Malaysia was the top water performing region in Asia (Table 4.22) with a net water surplus of 1209.1 x10^3 m^3. The models showed that the Asian countries are very suitable for aquaponics since they provide water efficient conditions. All the regions had a constant water

return rate during summer. There was a slight reduction in water production when winter started, which dampened the system. After winter, the rate of water production increased.

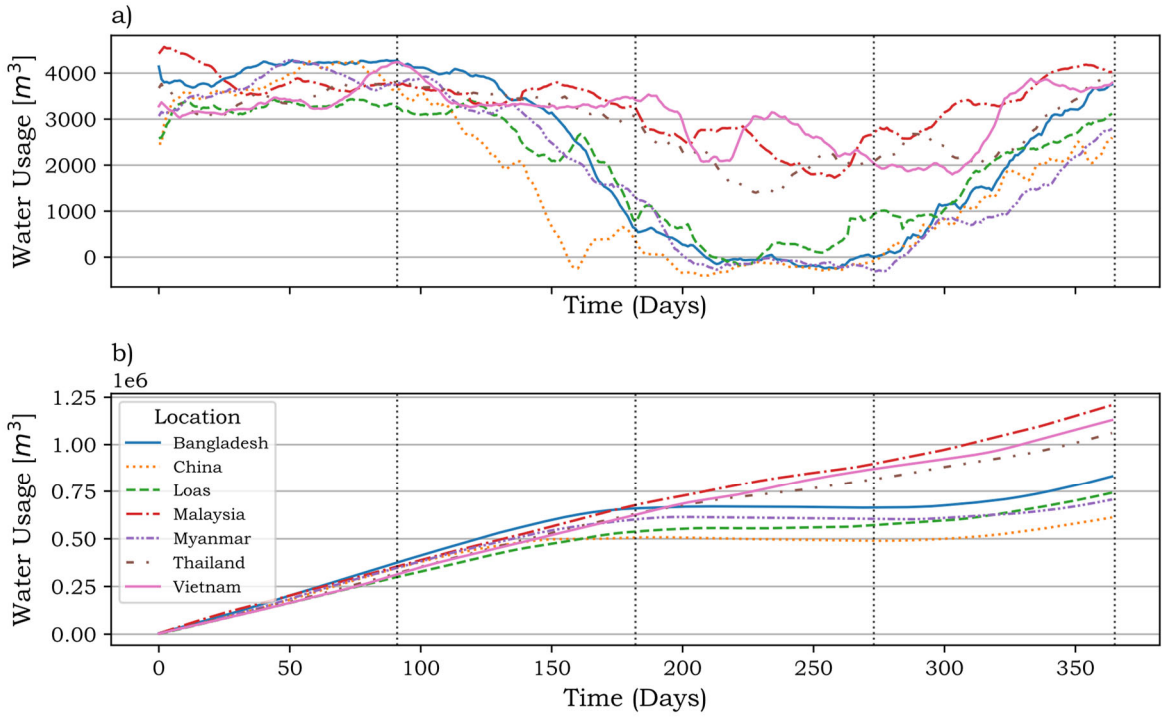

Figure 4.51: *Total system water usage (a) and Total cumulative water usage (b) for mainland countries in Asia*

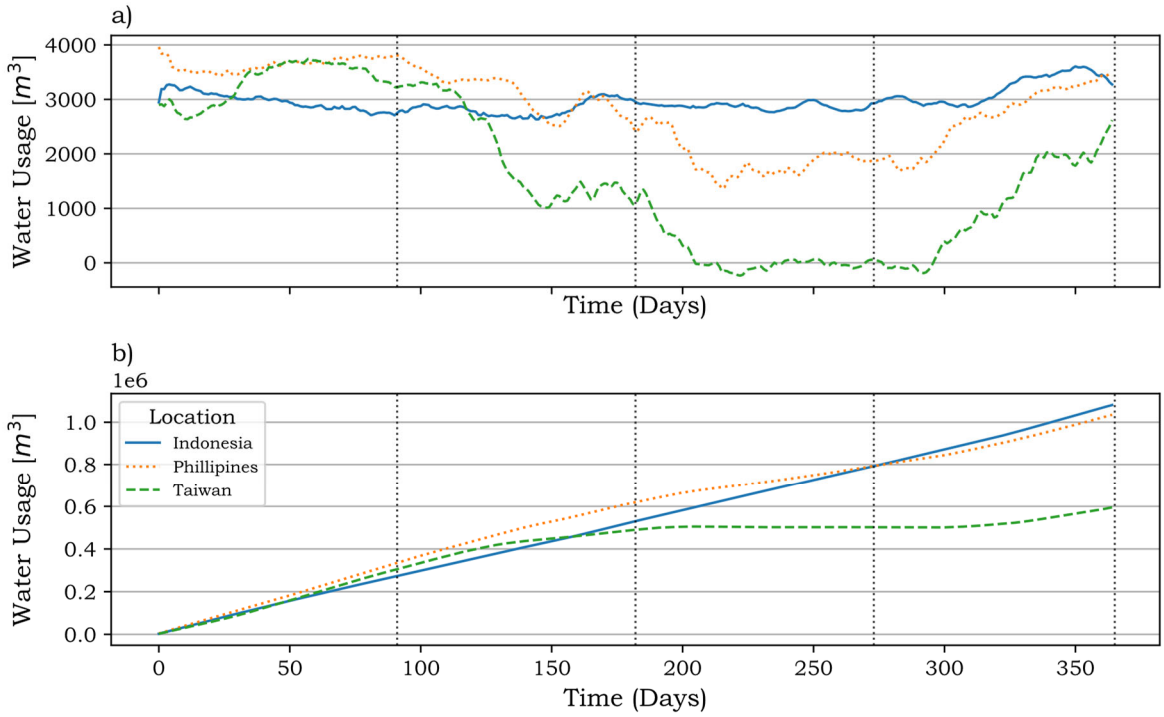

Figure 4.52: *Total system water usage (a) and Total cumulative water usage (b) for island countries in Asia*

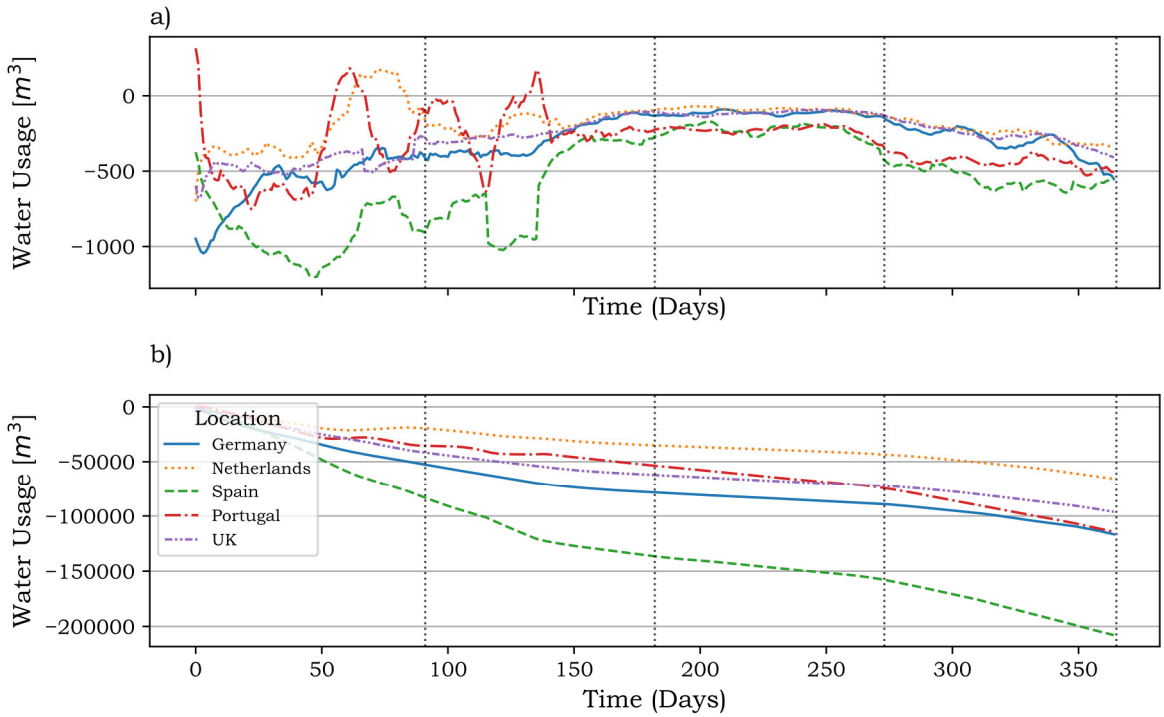

Figure 4.53: *Total system water usage (a) and Total cumulative water usage (b) for countries in Europe*

The European countries showed no water return throughout the year (Figure 4.53). During summer, Portugal and the Netherlands showed a slight water return to the system. The cumulative water usage for all the European regions was negative for the year. The colder regions require less cooling and never reached the dew point on the cooling coil; therefore, no condensation occurred.

Table 4.23: *Net water usage or return for regions in Europe*

Rank	Region	Water Usage [$10^3 m^3$]
1	Netherlands	-65.7
2	UK	-96.3
3	Portugal	-114.3
4	Germany	-116.6
5	Spain	-207.8

The Netherlands was the top water performing region in Europe (Table 4.23) with a net water consumption of 65.7x10^3 m^3.

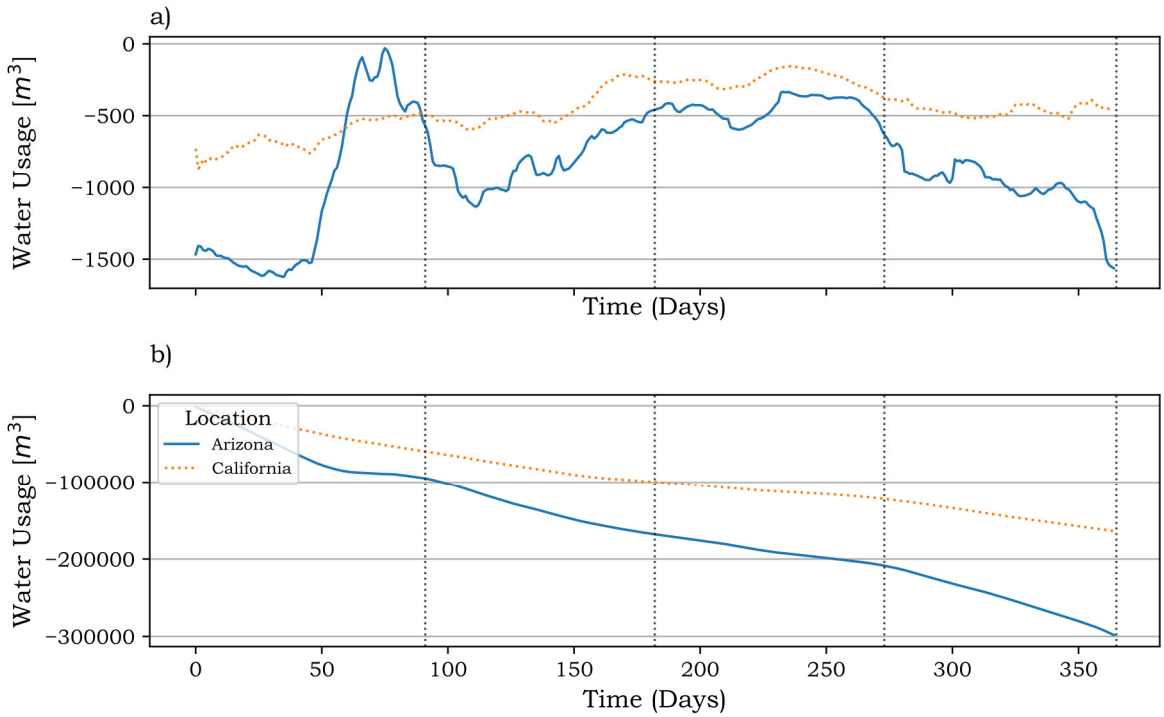

Figure 4.54: *Total system water usage (a) and Total cumulative water usage (b) for Western regions of North America*

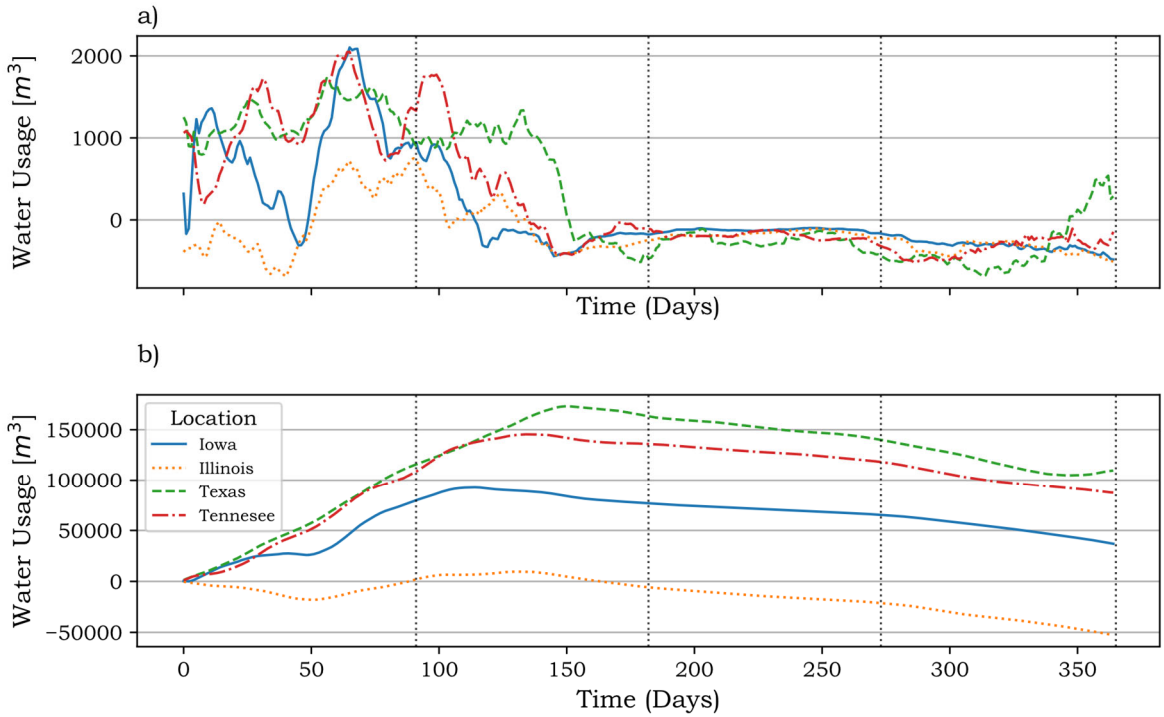

Figure 4.55: *Total system water usage (a) and Total cumulative water usage (b) for Central regions of North America*

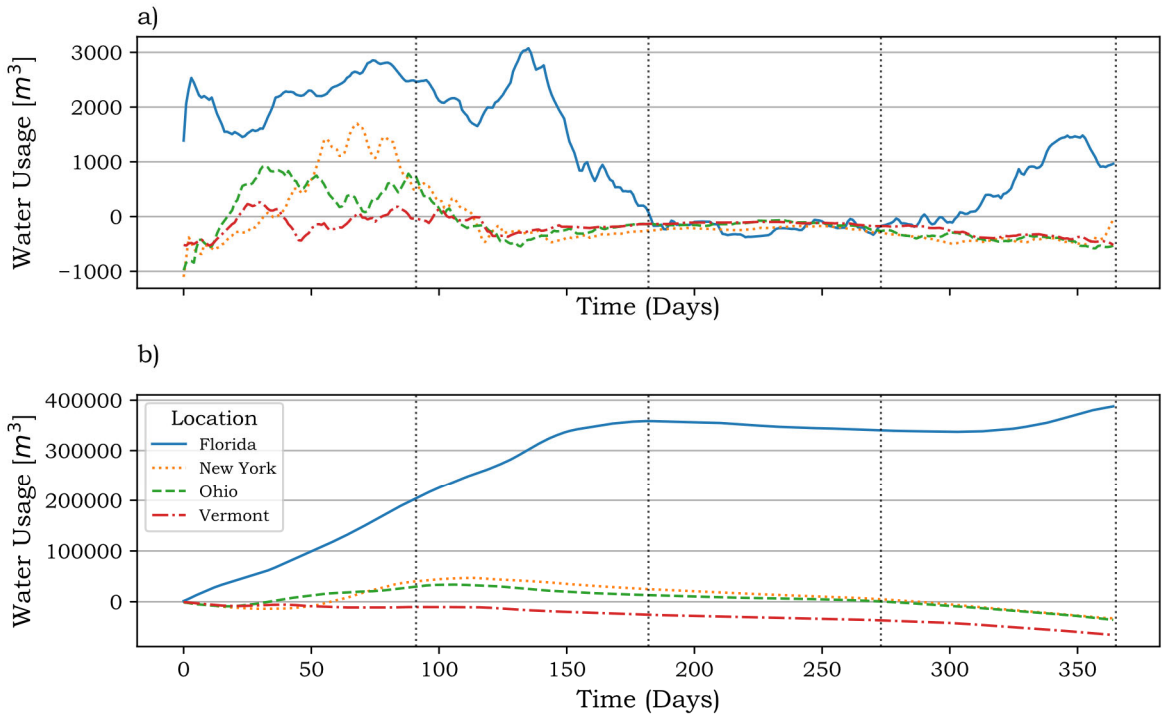

Figure 4.56: *Total system water usage (a) and Total cumulative water usage (b) for Eastern regions of North America*

Once again, the hot humid regions yielded a net positive water return during the year (Figure 4.56). Florida, which has a high humidity and air temperatures throughout the year, produced the most water. The central and western regions (Figure 4.54 and Figure 4.55), which required less cooling during the year, had less water returns compared to the hot eastern regions.

Table 4.24: *Net water usage or return for regions in North America*

Rank	Region	Water Usage [$10^3 m^3$]	Rank	Region	Water Usage [$10^3 m^3$]
1	Florida	387.9	**6**	Ohio	-35.7
2	Texas	109.7	**7**	Illinois	-52.7
3	Tennessee	87.2	**8**	Vermont	-65.6
4	Iowa	36.9	**9**	California	-163.7
5	New York	-32.4	**10**	Arizona	-298.2

Orlando Florida was the top water performing region in North America with a net water surplus of 387.9x10^3 m^3 as seen in Table 4.24.

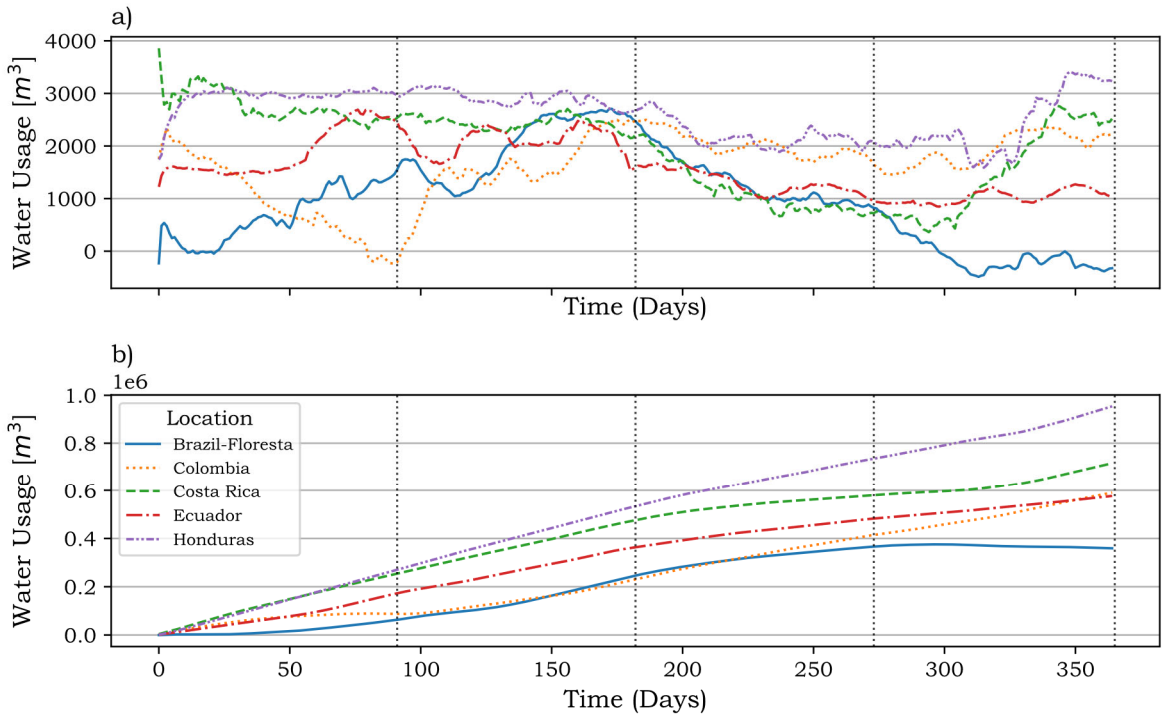

Figure 4.57: *Total system water usage (a) and Total cumulative water usage (b) for countries in South America*

All the regions in South America had a net positive water return for the year (Figure 4.57). These regions experience humid conditions which drive water return in the system.

The models showed that the South American countries were very suitable for aquaponics since they provide water efficient conditions. All the regions had a constant water return rate during the summer. There was a slight reduction in water production when winter started, which dampened the system. After winter, the rate of water production increased.

Table 4.25: *Net water usage or return for regions in South America*

Rank	Region	Water Usage [$10^3 m^3$]
1	Honduras	953.9
2	Costa Rica	716.1
3	Colombia	590.4
4	Ecuador	576.5
5	Brazil	359.2

Honduras was the top water performing region in South America with a net water surplus of 953.9x10^3 m^3 (Table 4.25).

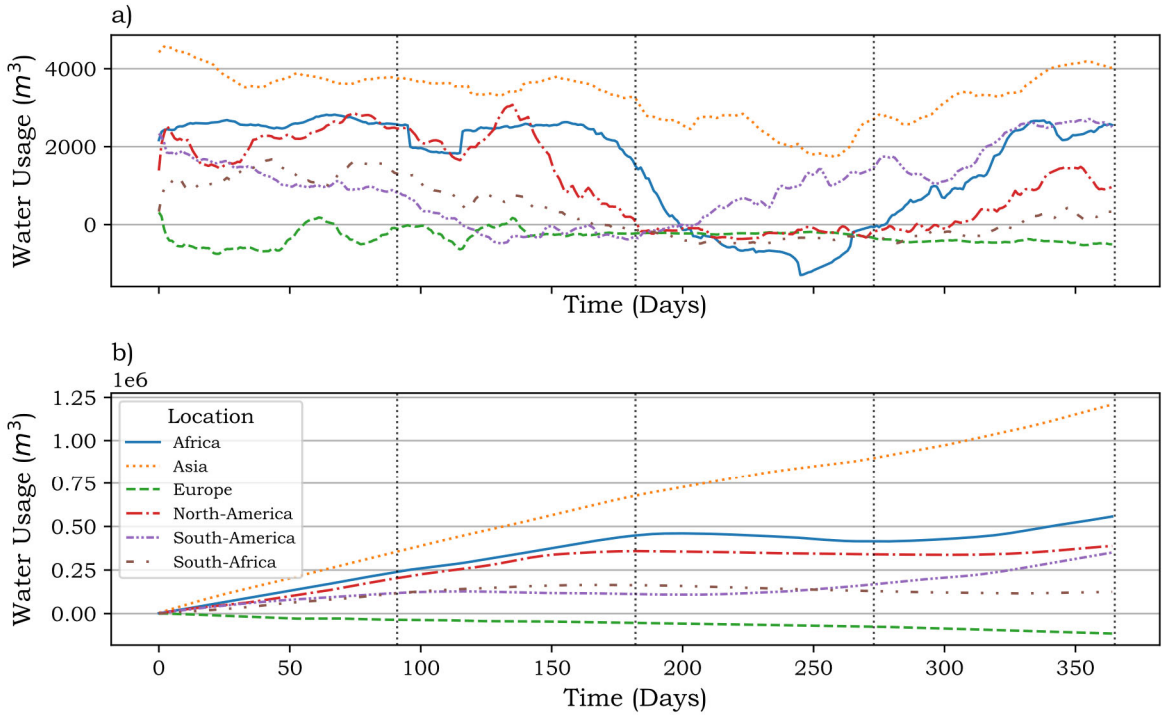

Figure 4.58: *Total system water usage (a) and Total cumulative water usage (b) for best performing countries around the World*

Table 4.26 presents a summary of the top water performing countries around the world. Malaysia was the top performing country with 1209.1 x10^3 m^3 of water return. This value was more than double the yield of the closest competitor, Nigeria, with a water surplus of 556.9 x10^3 m^3. The top performing region in South Africa, Durban, ranked second to last in performance globally with a net water return of 124.8 x10^3 m^3. This was 89.7% less water return compared to Malaysia. South Africa had 65.3% less water return than the region that was ranked fourth (Floresta Brazil) with a water return of 359.2 x10^3 m^3. This indicated that although Durban has a hot and humid climate throughout the year, it still performed poorly compared to global locations. This was due to the fact that South Africa is a water scarce country and even within the humid climate, water usage should be carefully managed.

Table 4.26: *Net water usage or return for best performing regions around the World*

Region	Rank	Water Usage [$10^3 m^3$]	Percentage Underperforming [%]
Malaysia (Asia)	1	1209.1	0
Nigeria (Africa)	2	556.9	53.9
Florida (North America)	3	387.9	67.9
Brazil (South America)	4	359.2	70.3
Durban (South Africa)	5	124.8	89.7
Portugal (Europe)	6	-114.3	109.5

4.4.5 System Dynamic Response Due to Increased Levels of CO_2

The models indicated that Durban was the most suitable location in South Africa to operate a commercial scale aquaponic system. The climate of this region provides favourable external conditions, which maximised energy and water efficiency. Given the strain on natural resources and the environment, it is important that resources are managed and unutilised responsibly and sustainably. South Africa is heavily reliant on coal for electricity generation. The burning of coal is an unsustainable and environmentally unfriendly source of energy. The burning of coal contributes to CO_2 emissions into the atmosphere, which increases the concentration of CO_2 in the atmosphere. A Representative Concentration Pathway (RCP) is a greenhouse gas concentration trajectory adopted by the IPCC. The RCPs are labelled after a possible range of radiative forcing values in the year 2100 (2.6, 4.5, 6, and 8.5 W/m^2, respectively). Based on these projections, the rise in temperature and radiative forcing were determined. The effects of the rise in temperatures and radiative forcing were incorporated into the model to investigate the effects on the system energy for the next 80 years. Only the Durban region was investigated since it was the best performing region with regard to energy usage. All four possible projection paths were investigated. The result of the increased levels of CO_2 on the system energy is presented in Figure 4.59.

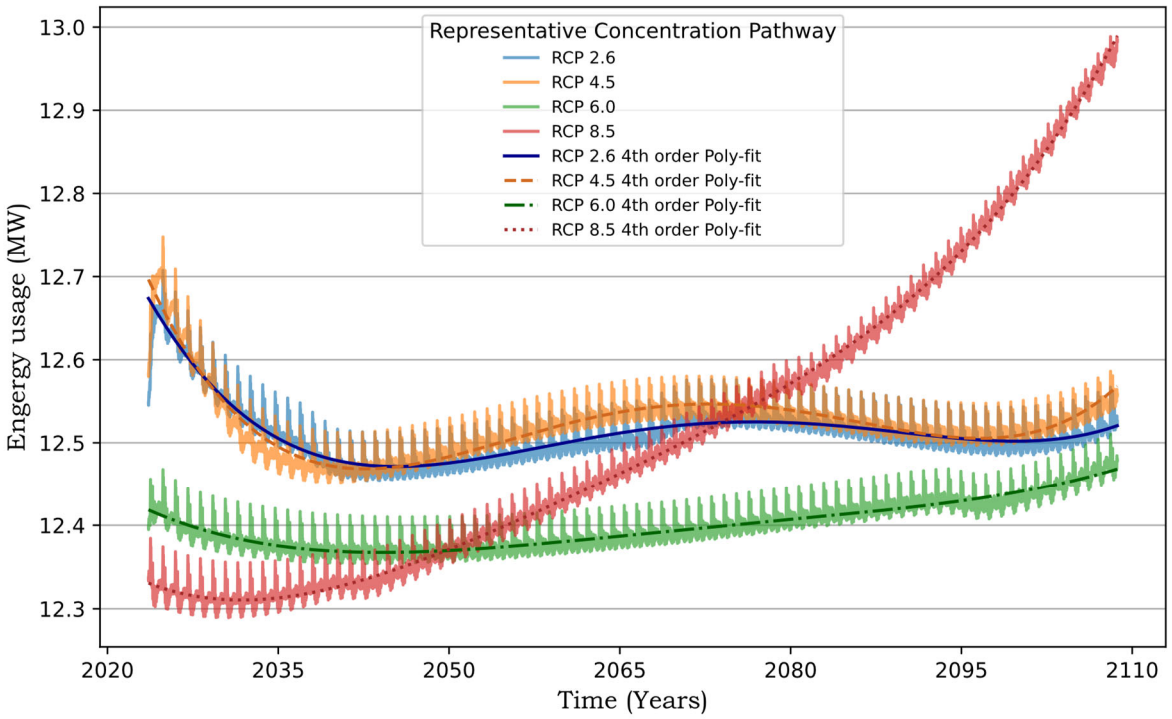

Figure 4.59: *Effects of CO_2 concentrations in the atmosphere on energy usage for the best performing energy region in South Africa, Durban*

The model produced a cyclic trend for each year, with the cycle continuing along the respective RCP projection line. According to the projections, with the increase in CO_2 concentrations in the atmosphere, the temperature rose along the same curve. The increased temperatures and radiative forcing caused higher cooling demand in the systems during hot periods of the year.

The trend of the RCP lines on energy response was heavily influenced by system heating. Increased temperatures reduced the temperature differential during cold winter months, which meant less heating was required. Since heating is such an energy intensive component, the drastic rise in temperature aided in reducing the overall system energy consumption. This is seen by the initial value of RCP 8.5 being the lowest compared to the other RCPs. The RCP 8.5 soon becomes exponentially worse since the cooling demands, caused by higher temperatures in summer, outweighed the benefit of less heating required in winter.

The RCP 6.0 had a small initial value due to the reduction in heating demand caused by the rapid rise in temperature. The energy usage continued to drop until 2050 where the rise in temperatures and radiative forcing caused the cooling demands to dominate. With the rise in temperature, energy usage will ultimately keep increasing beyond 2100.

The RCPs 4.5 and 2.6 closely followed the same trend. Policies, which are prescribed to achieve RCPs 4.5 and 2.6, will cause limited concentration of CO_2 in the atmosphere and therefore will cause a slower rate or a rate reduction of temperature increases. Because temperatures will remain low, the initial energy consumption will be high due to high heating demands in winter. This will normalise and cooling demand will be the dominant factor causing higher energy usage in the future.

4.5 Concluding Remarks

This chapter presented a detailed dataset and analyses in respect of the aquaponic system. Furthermore, a comprehensive set of simulation results emanating from the proposed models were presented and discussed. Locations specific climates were discussed, and weather data were presented. The time response plots from the system dynamics models were presented, interpreted and discussed. The total energy and water usage responses of the system were the focal point of the presented results.

CHAPTER FIVE

Conclusions and Recommendations

5.1 Chapter Overview

This chapter includes a final conclusion based on the obtained results. Recommendations are made on the outcome of the research and the benefit of the research is discussed. The research objectives and questions are discussed, and comments are made on the contribution of this research. Possible future expansion and improvement on the research are discussed.

5.2 Research Findings

The models provided valuable insights into the effects of local climatic conditions on a generically defined decoupled aquaponic system. The system was defined with certain constant input parameters such as internal environment set point conditions, construction materials and operation specific components such as duration and harvest cycles. The external conditions were varied for a variety of locations around the world and the effects on the system dynamics such as energy and water consumption were captured and illustrated on a time series plot.

The results revealed that environmental control is the most energy intensive component of the defined aquaponic system. Between 98% and 99% of the total system energy is used to maintain favourable internal conditions for year-round operation. The environmental control is heavily affected by external weather conditions since the external air temperature, humidity, and incoming solar radiation of a region determine how much energy is required to heat or cool the aquaponic system to maintain favourable conditions. This result is supported by the work of Ginzburg et al. (2016). The results revealed that ultimately the dominant energy contributor (heating or cooling demands) will determine the overall system response.

Energy saving strategies and alternative, location specific, system configurations were not considered during this research. Basic strategies such as lowering internal temperature set points during colder seasons, considering better material properties that are region specific, and finding optimum off-coil conditions, would aid in reducing energy demands during peak conditions. Other policies such as eliminating heating requirements during mid-winter by reducing harvest frequency can be adopted to save energy during colder months.

It was observed that regions that experience cold weather such as North America, Europe and parts of South Africa, had significantly higher energy demands throughout the year due to heating requirements. This result is further supported by Hong et al. (2013) which

observed that the weather impact was greater for buildings in colder climates compared to warmer climates. The energy required for heating outweighed the energy required for cooling in these regions. Cold regions required 20% or more energy throughout the year compared to the best performing region. These cold regions often experienced temperatures below zero. This caused rapid heat loss due to the high temperature differential that led to high energy demands.

The results revealed that regions that experienced high temperatures and high humidity for prolonged periods throughout the year had the best energy performance. Countries close to the equator such as Malaysia, Floresta Brazil and Nigeria exhibited little difference in temperature and humidity experienced throughout the year. The constant high temperatures and humidity caused more uniform energy demand profiles throughout the year. Minimal heating was required for these regions and cooling was the dominant energy contributor. It can be concluded that regions that experience tropical climates are the most suited for aquaponic systems with regard to energy usage. Durban is the most tropical region that was considered for local comparison; hence, this conclusion is confirmed by the fact that Durban was the best performing region in South Africa.

It was observed that regions with high temperatures and humidity had the best performance with regard to water usage. Regions that had high cooling demands were the regions where the most water was returned to the system. Cooling allowed for dehumidification of the air by means of condensation on the cooling coils. This occurred when the supply air temperature reached levels below the dew point, which caused the moisture to be removed from the humid air. Since humid conditions were experienced throughout the year in regions such as Malaysia, Nigeria, Florida and Floresta Brazil and that these regions required continuous cooling, water was captured during the dehumidification process. Of all the regions that were compared in South Africa, Durban's climate resembled the best performing regions. Hence, Durban was the best performing region in South Africa with regard to water usage with a total water surplus of 124.8 $x10^3$ m^3.

It is noted that the top performing regions provide such favourable conditions that aquaculture and aquaponics systems can operate without environmental control. This is evident by the current operations in these regions, as discussed in Chapter Two. To provide environmental control to these regions would in some cases be redundant and impractically expensive. However, as explained by El-Sayed and Kawanna (2008), the traditional, inland-based culture systems for tilapia, such as earthen ponds and concrete tanks, are encountering some problems that make their sustainability unwarranted. These include environmental

concerns about the ejection of the effluent from land-based aquaculture facilities, the shortage of freshwater together with the competition for it with other activities, the increasing land costs and climatic changes. Therefore, tilapia culture in re-circulating systems could be an ideal option for other land-based systems, especially in areas that face freshwater shortages and/or rough climatic conditions. This serves as a motivation and recommendation for exploring RAS and decouples aquaponic configurations in a country like South Africa, given the limited water resources.

5.3 Research Outcome

System dynamics modelling and systems thinking methodology were applied to represent a generic decoupled aquaponic system. This method aided in capturing the system dynamics with regard to energy usage and water usage in a large complex system where there are a many variables and complex system dynamics. The research objectives were successfully achieved to effectively satisfy the research questions posed in Chapter One.

A generic reference decoupled aquaponic system was conceptualised and constructed using systems thinking and a system modelling approach as discussed in detail in sections 3.2 to 3.5. Differential equations were derived that represented the dynamic nature of the proposed system. This concluded the first research objective posed in section 1.4.2. The second research objective in section 1.4.2 addressed the effects of local climatic factors on the energy and water usage of a system. The varying effects were modelled, and the results were captured. A sensitivity analysis was conducted by varying the external location parameters and investigating the effects on the system stock and flow variables (Chapter Four). The data inputs, which were used to perform the sensitivity analysis, were presented in section 4.3 and the results were presented in section 4.4. In order to investigate the effects of increased CO_2 levels in the atmosphere due to the energy required to operate the aquaponic system, a simulation was run for 80 years. This simulation was carried out to achieve the final research objective of section 1.4.2. The results were discussed in terms of RCP projections in section 4.4.5.

The method used to describe and model the proposed system serves as outcome to the first research question posed in section 1.5. The outcome of the second research question (section 1.5) indicated that local climatic factors such as ambient air temperature, relative humidity and incoming solar radiation play a major role in system stock variables such as energy and water usage. This was demonstrated by the fact that environmental control (section 4.4.2), which was heavily affected by external conditions, contributed 99% to the energy usage

of the total system (section 4.4.3). Furthermore, it was shown that regions with high temperatures and high humidity produce significantly more water than colder climates with large seasonal variation as discussed in section 4.4.4. The models produced in this research showed that the top performing regions in South Africa compare relatively well to international locations with regard to energy (section 4.4.3) and water usage (section 4.4.4). In the context of the defined system and conditions described in this research, commercial aquaponic systems in South Africa could have relatively good energy and water efficiency compared globally. This fact addresses the third research question posed in section 1.5. The results motivate that the best region in which to operate such systems would be tropical climates as experienced in the eastern coastal regions of South Africa (Durban), where high humidity and temperatures are experienced. This addressed the fourth research question posed in section 1.5. Mchunu et al. (2018) revealed that currently, most hobby scale systems were situated in KwaZulu-Natal while commercial systems were mostly located in the Gauteng and Western Cape provinces as discussed in section 2.2.5. Given South Africa's current dependence on coal, energy required for the system will increase CO_2 released into the atmosphere due to the burning of fossil fuels. The increased level of CO_2 influences the global temperature. The total energy will eventually increase significantly due to the rise in temperature and the system's response to keep up with the cooling demands, which in turn will create more CO_2 emissions as presented and discussed in section 4.4.5. The final research question was hereby addressed and the demand for sustainable energy sources was fully emphasised by this research.

The aim of the research (section 1.4.1) was achieved, and a working system dynamics model of a generic reference decoupled aquaponics system was developed to investigate and evaluate a range of variables such as energy and water usage. This model can serve as a decision-making tool for sustainable policy development with regard to aquaponics systems in South-Africa. This research could be used to ensure a positive outcome during the conceptualisation phase of projects and or policy design of aquaponic systems. This research could aid stakeholders such as engineers, government and investors in coming up with the best solution without initial expensive experimentation and trial and error methodologies.

5.4 Future Work

Current research that focuses on system dynamics rarely explores the energy and water efficiency of the systems in detail. System dynamics modelling is used on a component level rather than a high, overall level. This research can be extended to explore a variety of energy

related aspects of aquaponic systems. Durban was identified as the most suited region with regard to energy and water. Even though this region proved to be the best performing region, other regions could still provide successful operations. This research does not comment on the success of a commercial scale aquaponic system based on location but rather investigated where it will operate the most efficiently. The results produced a recommended region but does not provide insight into the extent of regional change. The location can be further narrowed down to an optimal location within the region of Durban. It is recommended that the results of this research are tested and verified using experiments on at least small-scale operations. It is also recommended that more weather data that could be used to increase the accuracy of the produced models should be captured. With more data obtained from a variety of weather stations, the estimation error can be reduced and the results will be more reliable. Currently, there is a lack of reliable data in South Africa, which could exert a negative impact on the results. It is therefore important to gather dependable data to draw better conclusions.

This research can be extended by investigating the effects of energy-improving strategies on the total system energy usage. Given a selected location where the basic weather data trend is known, other parameters could be varied, and the system response could be observed. Parameters such as internal environment set points could be altered to investigate the optimal internal environmental conditions. Material properties could be varied to determine location specific optimal material selections.

Other energy improving strategies could also be incorporated into the model and the effects of the strategies could be investigated. These strategies could be the incorporation of system heating by means of process waste heat, or thermal storage techniques and evaporative cooling technology. The different strategies could be compared to determine the best solutions. The system dynamics model could be altered to account for all the changes in the system due to the energy improving techniques. This could add a delay element to the system and valuable observation could be produced.

5.5 Research Conclusion

This chapter contained detailed conclusions and recommendations on the outcome of this research. The conclusions and recommendations were presented in discussion form and the vital elements of the research were commented on.

The effects of external local driving factors on system stock and flow variables were clearly accentuated and it was concluded that the local external factors of a decoupled

aquaponic system greatly affect the energy and water usage of the systems. It was concluded that regions that experience prolonged periods of high temperatures and humidity provide the most favourable conditions in which to operate energy and water efficient systems.

The recommendation was made that tropical regions should be considered when planning and deciding on sites for such operations. It was concluded that based on the comparison of the local locations mentioned in this study, Durban had the most suitable climate regarding energy and water efficiency. Recommendations were made that the continuous use of fossil fuel dependent energy sources would lead to a rise in energy consumption owing to an increase in energy demand created by a rise in the global temperature. It was concluded that these current practices are not sustainable for the next 80 years.

The research questions, objectives, and aim were addressed and fully discussed. System dynamics modelling was successfully used to conduct simulations that serve as a valuable decision-making tool for stakeholders who wish to explore the feasibility of aquaponics in South Africa. Since aquaponics provides abundant benefits such as food security, job creation and more sustainable aquacultural and agricultural practices, it is a worthwhile endeavour to consider.

The final recommendation is made on possible future work that could spawn from the current research. This research could be expanded to incorporate a variety of additional factors or configurations to investigate the effects on the system. Comments were made on the importance of complete and accurate data to ensure that the model provides similarly accurate results.

References

Abdel-Ghany, A., & Kozai, T. (2006). Dynamic modeling of the environment in a naturally ventilated, fog-cooled greenhouse. *Renewable Energy*, *31*(10), 1521-1539.

Africa, S. S. (2017). *Poverty trends in South Africa. An examination of absolute poverty between 2006 and 2015*. Pretoria: Statistics South Africa Report No. 03-10-062015.

Ahmed, N., & Turchini, G. M. (2021). Recirculating aquaculture systems (RAS): Environmental solution and climate change adaptation. *Journal of Cleaner Production*, *297*, 126604.

Akrami, M., Salah, A. H., Javadi, A. A., Fath, H. E. S., Hassanein, M. J., Farmani, R., Dibaj, M., & Negm, A. (2020). Towards a sustainable greenhouse: Review of trends and emerging practices in analysing greenhouse ventilation requirements to sustain maximum agricultural yield. *Sustainability*, *12*(7), 2794.

Al-Helal, I. (1998). *A computational fluid dynamics study of natural ventilation in arid region greenhouses.*, The Ohio State University. Columbus, OH: Ph.D. Thesis.

Al-Hafedh, Y. S., Alam, A., & Beltagi, M. S. (2008). Food production and water conservation in a recirculating aquaponic system in Saudi Arabia at different ratios of fish feed to plants. *Journal of the world aquaculture society*, *39*(4), 510-520.

Alkhalidi, A., Khawaja, M. K., & Abusubaih, D. (2020). Energy efficient cooling and heating of aquaponics facilities based on regional climate. *International Journal of Low-Carbon Technologies*, *15*, 287-298.

Allen, R., Pereira, L., Raes, D., & Smith, M. (1998). *Crop evapotranspiration - Guidelines for computing crop water requirements. FAO Irrigation and drainage paper 56 ed*. Rome: FAO - Food and Agriculture Organization of the United Nations.

Andersen, P., & Lorch, R. (1998). Food security and sustainable use of natural resources: a 2020 Vision. *Ecological Economics, 72*, 1-10.

Arbel, A., Barak, M., & Shklyar, A. (2003). Combination of forced ventilation and fogging systems for cooling greenhouses. *Biosystems Engineering*, *84*(1), 45-55.

Arnfield, A. J. (2020, November 11). *Köppen climate classification*. Encyclopedia Britannica. https://www.britannica.com/science/Koppen-climate-classification,

ASHRAE. (2013). *ASHRAE Standard 169-2013*, Weather Data for Building Design Standards. American Society of Heating, Refrigerating and Air-Conditioning Engineers, Atlanta, Georgia.

Babatunde, R.O., Omotesho, O.A., & Sholotan, O.S. (2007). Factors influencing food security status of rural farming households in North Central Nigeria. *Agricultural Journal, 2*, 351-357.

Badiola, M., Basurko, O. C., Gabina, G., & Mendiola, D. (2017). Integration of energy audits in the life cycle assessment methodology to improve the environmental performance assessment of recirculating aquaculture systems. *Journal of Cleaner Production*, *157*, 155-166.

Badiola, M., Basurko, O. C., Piedrahita, R. H., & Hundley, P. (2018). Energy use in recirculating aquaculture systems (RAS): A review. *Aquacultural Engineering, 81,* 57-70.

Badiola, M., Mendiola, D., & Bostock, J. (2012). Recirculating aquaculture systems (RAS) analysis: Main issues on management and future challenges. *Aquacultural Engineering*, *51*, 26-35.

Baille, M., Baille, A., & Laury, J. (1994). A simplified model for predicting evapotranspiration rate of nine ornamental species vs. climate factors and leaf area. *Scientia Horticulturae*, *59*, 217-232.

Bala, B. K., Arshad, F. M., & Noh, K. M. (2017). Chapter 9: Modelling of Hilsa Fish (Tenualosa ilisha) Population in Bangladesh, *System Dynamics Modelling and Simulation*. (179-189). Springer.

Bala, B., Arshad, F., & Noh, K. (2017). *System Dynamics Modelling and Simulations*. Springer.

Bartzanas, T. (2005). Influence of the heating method on greenhouse microclimate and energy consumption. *Biosystems Engineering*, *91*(4), 487-499.

Battersby, J. (2011). Urban food insecurity in Cape Town, South Africa: An alternative approach to food access. *Development South Africa, 28*, 545-561.

Boulard, T., & Baille, A. (1993). A simple greenhouse climate control model incorporating effects of ventilation and evaporative cooling. *Agricultural and Forest Meteorology*, *65*(3-4), 145-157.

Boulard, T., Draoui, B. (1995). Natural ventilation of a greenhouse with continuous roof vents: measurements and data analysis. *Journal of Agricultural Engineering Research*, *61*(1), 27-36.

Boulard, T., Haxaire, R., Lamrani, M. A., Roy, J. C., & Jaffrin, A. (1999). Characterization and modelling of the air fluxes induced by natural ventilation in a greenhouse. *Journal of Agricultural Engineering Research*, *74*(2), 135-144.

Boulard, T., & Wang, S. (2000). Greenhouse crop transpiration simulation from external climate conditions. *Agricultural and Forest Meteorology*, *100*(1), 25-34.

Bremner, J. (2012). Population and food security: Africa's challenge. *Population Reference Bureau Policy Brief*.

Cengel, Y., & Ghajar, A. (2014). *Heat and Mass Transfer: Fundamentals and Applications*. 4th ed. McGraw-Hill Professional.

Chakona, G., & Shackleton, C. (2019). Food insecurity in South Africa: To what extent can social grants and consumption of wild foods eradicate hunger?. *World Developement Perspectives*, *13*, 87-94.

Chervinski, J. (1982). Environmental physiology of tilapias. In *The Biology and Culture of Tilapia. Proceedings of the 7th ICLARM Conference, Manila, Philippines: International Center for Livin,* 119-128.

Clarke, L., Eom, J., Marten, E. H., Horowitz, R., Kyle, P., Link, R., Mignone, B. K., Mundra, A., & Zhou, Y. (2018). Effects of long-term climate change on global building energy expenditures. *Energy Economics*, *72*, 667-677.

Climate.OneBuilding. (2021, February 12). *Climate.OneBuilding.Org: Climate/Weather Data Sources*. http://climate.onebuilding.org/sources/default.html

Cnaani, A., Gall, G. A.. & Hulata, G. (2000). Cold tolerance of tilapia species and hybrids. *Aquaculture International, 8*, 289-298.

Davison, A. (2018). *Recirculating Aquaculture Systems A Guide to farm design & operations.* Farmfish LLC.

Dayan, J., Dayan, E., Strassberg, Y., & Presnov, E. (2004). Simulation and control of ventilation rates in greenhouses. *Mathematics and Computers in Simulation*, *65*(1-2), 3-17.

de Jong, T. (1990). *Natural ventilation of large multi-span greenhouses*., Wageningen Agricultural University. The Netherlands, Wageningen: Ph.D. Thesis.

Effendi, H., Utomo, B. A., Darmawangsa, G. M., & Sulaeman, N. (2015). Combination of water spinach (Ipomeaaquatica) and bacteria for freshwater cryfish red claw (Cherax quadricarinatus) culture wastewater treatment in aquaponic system. *Journal of Advance Chemistry., 6*, 1072-1078.

El-Sayed, A.-F. M., & Kawanna, M. (2008). Optimum water temperature boosts the growth performance of Nile tilapia (Oreochromis niloticus) fry reared in a recycling system. *Aquaculture Research, 39(6)*, 670-672.

El-Sayed, A.-F. M. (2013). On-farm feed management practices for Nile tilapia (Oreochromis niloticus) in Egypt. *FAO Fisheries and Aquaculture, 583*, 101-129.

European Commission. (2021). *EU aquaculture report: sales value goes up while volume remains steady*. EU Science Hub - European Commission. https://ec.europa.eu/jrc/en/news/eu-aquaculture-report-2020

Fanzo, J. (2012). *The nutrition challenge in sub-Saharan Africa* (No. 2012-012). United Nations Development Programme, Regional Bureau for Africa.

FAO, (2010). *The state of food insecurity in the World- Addressing food insecurity in protracted crises.* Food and Agriculture Organization of the United Nations.

FAO, (2020). *The state of world fisheries and aquaculture.* Food and Agriculture Organization of the United Nations.

Faridi, R., & Wadood, S. N. (2010). An econometric assessment of household food security in Bangladesh. *The Bangladesh Development Studies, 33(3)* 97-111.

Fitz-Rodriguez, E., Kubota, C., Giacomelli, G., Tignor, M. E., Wilson, S. B., & McMahon, M. (2010). Dynamic modeling and simulation of greenhouse environments under several scenarios: A web-based application. *Computers and Electronics in Agriculture, 70*, 105-116.

Fitzsimmons, K. (2000). Future trends of tilapia aquaculture in the Americas. In B.A. Costa-Pierce and J.E. Rakocy, (Eds). *Tilapia Aquaculture in the Americas, Vol. 2*. The World Aquaculture Society.

Fitzsimmons, K. (2006). Prospect and potential for global production. *Tilapia: Biology, Culture, and Nutrition, 5(12)*, 51-72.

Giaglaras, P., Lykas, C., & Kittas, C. (1998). Dynamic simulation of nutrient solution composition in a closed hydroponics system. *IFAC Proceedings Volumes*, *31*(12), 219-224.

Ginzburg, A. S., Reshetar, O. A., & Belova, I. N. (2016). Impact of climatic factors on energy consumption during the heating season. *Thermal Engineering*, *63*(9), 621-627.

Goddek, S., Delaide, B., Mankasingh, U., Ragnarsdottir, K. V., Jijakli, H., & Thorarinsdottir, R. (2015). Challenges of sustainable and commercial aquaponics. *Sustainability*, *7*(4), 4199-4224.

Goddek, S., Espinal, C. A., Delaide, B., Jijakli, M. H., Schmautz, Z., Wuertz, S., & Keesman, K. J. (2016). Navigating towards decoupled aquaponic systems: a system dynamics design approach. *Water*, *8*(7), 303.

Goddek, S., Joyce, A., Kotzen, B., & Dos-Santos, M. (2019). Aquaponics and global food challenges. In *Aquaponics Food Production Systems* (3-17). Springer.

Goddek, S., & Körner, O. (2019). A fully integrated simulation model of multi-loop aquaponics: A case study for system sizing in different environments. *Agricultural Systems*, *171*, 143-154.

Graber, A., & Junge, R. (2009). Aquaponic Systems: Nutrient recycling from fish wastewater by vegetable production. *Desalination*, *246*(1-3), 147-156.

Hofer, S. C., & Watts, S. A. (2002). Cold tolerance in genetically male tilapia (GMT registered). Oreochromis niloticus. *World Aquaculture*, *33*, 19-21.

Hong, T., Chang, W. K., & Lin, H. W. (2013). A fresh look at weather impact on peak electricity demand and energy use of buildings using 30-year actual weather data. *Applied energy*, *111*, 333-350.

Idso, S. B. (1981). A set of equations for full spectrum and 8- to 14-μm and 10.5-to 12.5-μm thermal radiation from cloudless skies. *Water Resources Research*, *17*(2), 295-304.

IFOAM, (2006). *Basic Standards for Organic Production and Processing (IFOAM)*, BC, Canada: Technology Analysis & Strategic Management..

Jensen, M. H. (2001). Controlled Environment agriculture in deserts, tropics and temperate regions-A World Review. In *International Symposium on Design and Environmental Control of Tropical and Subtropical Greenhouses, 578*, 19-25.

Jijakli, M. H., Delaide, B., & Gott, J. (2016) *Plant Production Capacity and Nutrient Mass Balance in the PAFF Box, an Urban Aquaponics Module: Preliminary Findings*; Geography and Environment University of Southampton.

Jones, J. W., Dayan, E., Van Keulen, H., & Challa, H. (1988). Modeling tomato growth for optimizing greenhouse temperatures and carbon dioxide concentrations. *Acta Hortic*. *248*, 285-294

Jones, P., Jones, J. W., & Hwang, Y. (1990). Simulation for determining greenhouse temperature setpoints. *Transactions of the ASAE*, *33*(5), 1-1728.

Karimanzira, D., Keesman, K. J., Kloas, W., Baganz, D., & Rauschenbach, T. (2016). Dynamic modeling of the INAPRO aquaponic system. *Aquacultural Engineering*, *75*, 29-45.

Kempkes, F. L. K., Van de Braak, N. J., & Bakker, J. C. (2000). Effect of heating system position on vertical distribution of crop temperature and transpiration in greenhouse tomatoes. *Journal of agricultural engineering research*, *75*(1), 57-64.

Kindelan, M. (1980). Dynamic Modeling of Greenhouse Environment. *Transactions of the ASABE, 23*, 1232-1239.

Körner, O., Aaslyng, J. M., Andreassen, A. U., & Holst, N. (2007). Microclimate prediction for dynamic greenhouse climate control. *HortScience*, *42*(2), 272-279.

Lastiri, D. R., Geelen, C., Cappon, H. J., Rijnaarts, H. H., Baganz, D., Kloas, W., Karimanzira, D., & Keesman, K. J. (2018). Model-based management strategy for resource efficient design and operation of an aquaponic system. *Aquacultural Engineering*, *83*, 27-39.

Li, M., Shi, J., Cao, J., Fang, X., Wang, M., & Wang, X. (2020). Climate change impacts on extreme energy consumption of office buildings in different climate zones of China. *Theoretical and Applied Climatology*, *140*(3), 1291-1298.

Maharjan, K. L., & Joshi, N. P. (2011). Determinants of household food security in Nepal: A binary logistic regression analysis. *Journal of Mountain Science*, *8*(3), 403-413.

Mchunu, N., Lagerwall, G., & Senzanje, A. (2017). Food sovereignty for food security, aquaponics system as a potential method: A review. *Journal of Aquaculture Research and Development, 8*, 1-9.

Mchunu, N., Lagerwall, G., & Senzanje, A. (2018). Aquaponics in South Africa: Results of a national survey. *Aquaculture Reports*, *12*, 12-19.

Nichols, M. A., & Savidov, N. A. (2012, May). Aquaponics: a nutrient and water efficient production system. In *II International Symposium on Soilless Culture and Hydroponics 947,* 129-132.

Pahl-Wostl, C., Tàbara, D., Bouwen, R., Craps, M., Dewulf, A., Mostert, E., Ridder, D & Taillieu, T. (2008). The importance of social learning and culture for sustainable water management. *Ecological economics*, *64*(3), 484-495.

Rahman, M.L., Shchjahan, M., Ahmed, N. (2021) Tilapia farming in Bangladesh: Adaptation to climate Change. *Sustainability*, *13*, 7657.

Rakocy, J. E. (1990). Tank culture of Tilapia. *Leaflet/Texas Agricultural Extension Service; no. 2409.*

Rakocy, J., Masser, M. P., & Losordo, T. (2016). Recirculating aquaculture tank production systems: aquaponics-integrating fish and plant culture. *SRAC Publication*, *454*.

Robadue Jr, D. D., & del Moral Simanek, R. (2007, July). A system dynamics perspective on a global fishing enterprise: The case of tuna ranching in Mexico. In *Proceedings of the 25th International Conference of the System Dynamics Society*, *29*, 1-30.

Rothwell, A., Ridoutt, B., Page, G., & Bellotti, W. (2015). Feeding and housing the urban population: Environmental impacts at the peri-urban interface under different land-use scenarios. *Land Use Policy*, *48*, 377-388.

Sampantamit, T., Ho, L., Lachat, C., Sutummawong, N., Sorgeloos, P., & Goethals, P. (2020). Aquaculture production and its environmental sustainability in Thailand: Challenges and potential solutions. *Sustainability*, *12*(5), 2010.

Sharma, N., Acharya, S., Kumar, K., Singh, N., & Chaurasia, O. P. (2018). Hydroponics as an advanced technique for vegetable production: An overview. *Journal of Soil and Water Conservation*, *17*(4), 364-371.

Sikwela, M. M. (2008). *Determinants of Household Food security in the semi-arid areas of Zimbabwe: A case study of irrigation and non-irrigation farmers in Lupane and Hwange Districts* [Doctoral dissertation, University of Fort Hare].

Standard, A. S. H. R. A. E. (1973). STANDARD 62-1973. *Standards for natural and mechanical ventilation.* The American Society of Heating, Refrigerating, and Air Conditioning Engineers. Inc. New York.

Takakura, T., Jordan, K. A., & Boyd, L. L. (1971). Dynamic simulation of plant growth and environment in the greenhouse. *Transactions of the ASAE*, *14*(5), 964-0971.

Tian, Y., Akamine, T., & Suda, M. (2004). Modeling the influence of oceanic-climatic changes on the dynamics of Pacific saury in the northwestern Pacific using a life cycle model. *Fisheries Oceanography*, *13*, 125-137.

Veras, G. C., Murgas, L. D. S., Rosa, P. V., Zangeronimo, M. G., Ferreira, M. S. D. S., & Leon, J. A. S. D. (2013). Effect of photoperiod on locomotor activity, growth, feed efficiency and gonadal development of Nile tilapia. *Revista Brasileira de Zootecnia*, *42*, 844-849.

Von Zabeltitz, C. (2011). Greenhouse structures. In *Integrated Greenhouse Systems for Mild Climates* (pp. 59-135). Springer.

Vox, G., Teitel, M., Pardossi, A., Minuto, A., Tinivella, F., & Schettini, E. (2010). Chapter 1: Sustainable Greenhouse Systems. In A. Salazar & I. Rios (Eds), *Sustainable Agriculture: Technology, Planning and Management (1-79)*, Nova Science Publishers, Inc. NY USA.

Walker , J. (1965). Predicting temperatures in ventilated greenhouses. *Transactions of the ASAE*, *8*(3), 445-448.

Willits, D. H. (2003). Cooling fan-ventilated greenhouses: a modelling study. *Biosystems Engineering*, *84*(3), 315-329.

Yogev, U., Barnes, A., & Gross, A. (2016). Nutrients and energy balance analysis for a conceptual model of a three loops off grid, aquaponics. *Water*, *8(12)*, 589.